C-SRC CHEMICAL RESCUE: CONTRIBUTION TO THE C-SRC PHOSPHOPROTEOME AND THE ELUCIDATION OF THE MECHANISM OF ACTIVATION OF C3G

by

Maria Isabel Martinez Ferrando

A thesis submitted to Johns Hopkins University in conformity with the requirements for the degree of Doctor of Philosophy

Baltimore, Maryland

July, 2012

ABSTRACT

The cellular proto-oncogene c-Src is a non-receptor tyrosine kinase involved in cell growth and cytoskeletal regulation. Despite being dysregulated in a variety of human cancers, its precise functions are not fully understood. Identification of c-Src's substrates remains a major challenge, as there is no simple way to directly stimulate its activity. Here we combine the chemical rescue of mutant c-Src and global quantitative phosphoproteomics to obtain the first high-resolution snapshot of the range of tyrosine phosphorylation events that occur in the cell immediately after specific c-Src stimulation. After enrichment by anti-phosphotyrosine antibodies, we identified 28 potential novel c-Src substrate proteins. Tyrosine phosphopeptide mapping allowed the identification of 382 non-redundant tyrosine phosphopeptides on 213 phosphoproteins. SILAC- based quantitation allowed the detection of 97 non-redundant tyrosine phosphopeptides whose level of phosphorylation is increased by c-Src. A large number of previously uncharacterized c-Src putative protein targets and phosphorylation sites are presented here, a majority of which play key roles in signaling and cytoskeletal networks, particularly in cell adhesion. Integrin signaling and focal adhesion kinase (FAK) signaling pathway are two of the most altered pathways upon c-Src activation through chemical rescue. In this context, our study revealed the temporal connection between c-Src activation and the GTPase Rap1, known to stimulate integrin-dependent adhesion. Chemical rescue of c-Src provided a tool to dissect the spatiotemporal mechanism of activation of the Rap1 guanine exchange factor (Rap1GEF), C3G, one of the identified

potential c-Src substrates that plays a role in focal adhesion signaling. Phosphorylation of C3G on tyrosine 514 is known to increase activation of C3G. Translocation of C3G to the membrane by the adaptor protein Crk brings C3G to close proximity to its effector Rap1. Chemical rescue of c-Src allowed clarification of the timing and connection between both events as well as the identification of Crk phosphorylation as the possible event that lead to the observed C3G-Crk disassembly. In addition to unveiling the role of c-Src in the cell and, specifically, in the Crk-C3G-Rap1 pathway, these results exemplify a strategy for obtaining a comprehensive understanding of the functions of non-receptor tyrosine kinases with high specificity and kinetic resolution.

Advisor: Philip A. Cole

Dissertation readers: Philip A. Cole, Jun Liu, and Peter Maloney

DISSERTATION REFEREES

GRADUATE ADVISOR: **PHILIP A. COLE, M.D., PH.D.**

DIRECTOR AND E.K. MARSHALL AND THOMAS H. MAREN PROFESSOR

DEPARTMENT OF PHARMACOLOGY AND MOLECULAR SCIENCES

DISSERTATION READER: **JUN O. LIU, PH.D.**

PROFESSOR

DEPARTMENT OF PHARMACOLOGY AND MOLECULAR SCIENCES

ACKNOWLEDGEMENTS

The totality of this thesis work would not have been accomplished without the knowledge, advice, encouragement and insight of many persons with whom I have worked, collaborated and interacted during my PhD.

First of all, I would like to recognize my advisor, Philip Cole. He gave me the opportunity to join his group and participate in the research being done in his laboratory. I was able to learn some of the many techniques and approaches to scientific discovery. This breadth of methodologies to tackle scientific questions is one of the aspects that made me become interested in his laboratory and I can say that I have been privileged to gain a variety of unique skills and an open attitude to learn whatever strategy or methodology necessary to better approach a scientific question. He has definitively fostered my sense of scientific autonomy and I strongly believe this has contributed to my development as a scientist.

As part of the Cole laboratory, I had the pleasure to interact with and learn from many very talented and inspiring group members, who shared scientific knowledge and insight as well as support and encouragement. When I first joined the lab I had the privilege of being trained and continuing the work of Yingfeng Qiao, an extremely talented scientist who introduced me to her project and has continued offering suggestions and advice from her current position during the course of my PhD. Dirk Schwarzer and Ron Bose also had an enormous impact in the first stages of my PhD. They trained me in some essential techniques such as cloning or mammalian tissue

culture. They also helped me developed a high level of scientific integrity and rigor and for that I am extremely thankful.

I would also like to thank Marc Holbert with whom I shared my bay for several years. He is an extremely talented scientist and great human being who helped me endure through some of the most difficult times of my PhD. I would like to mention many other members of the laboratory with whom I have interacted all these years and from whom I have learn about different ways to perceive and approach the challenges or research: Mary Katherine Connacher Tarrant, Zhihong Wang, YouSang Wang, David Meyers, Young Hoon Young and many others who I have met during the course of my PhD. Beverley and Blair Dancy have been an enormous support both as colleagues and good friends who have been there when I have needed them.

One of the best experiences from being at Johns Hopkins School of Medicine was the possibility to become exposed and collaborate with excellent researchers. As a result of the progress of my research, we took a direction towards proteomics. Consequently, I collaborated with the laboratory of Akhilesh Pandey. Dr. Pandey is a very enthusiastic scientist and an innovator who inspires his students and collaborators. His laboratory is involved in multiple collaborations and the members of his lab are extremely well trained and excel at their research. In his laboratory, I met wonderful individuals with whom I worked at different stages of the project. Henrik Molina introduced me to the field of mass spectrometry and became a good friend too. Raghothama Chaerkady is a very knowledgeable and efficient collaborator who never stopped impressing me with his ability to be involved simultaneously in multiple projects and perform them with impeccable rigor, dedication and thoroughness. Jun Zhong is a collaborator and friend

who trained me in the SILAC methodology. They all patiently listened to my scientific concerns and inquiries and helped me reach the level of expertise to perform high quality proteomic research that I am particularly proud and confident of. Harrys Kishore helped me with my experiments during that period and also during a later stage in my PhD. He became a good friend too. I must also thank Robert Cole and Robert O´Meally for spending a significant amount of time to obtain high quality mass spectrometry data in the proteomic section of my thesis.

I also had the privilege to collaborate Jin Zhang's laboratory. It has been a delightful experience to interact with both Dr. Zhang and her lab members. In particular, I would like to thank Katie Herbst who, during a conference suggested the possibility to collaborate with her and who then spent a generous part of her time helping me perform the experiment, which led to a significant improvement in my project. I must also mention the microscopy facility, especially Scot C. Kuo, Michael Delannoy, and Barbara Smith, for introducing me to the field of confocal microscopy and for their continuous advice and help during the C3G localization studies.

I would also like to thank my thesis committee members, including Philip Cole, Akhilesh Pandey, Jun Liu, Robert Siliciano, Robert Cotter, and James Stivers for their helpful advice during the meetings and for their encouragement. I would like to specially thank Jun Liu for being the second reader of my thesis, for his continuous support and guidance and the long hours spent advising me during difficult times.

I would like to also thank Craig Townsend, Jun Liu, and Robert Siliciano who gave me the opportunity to join their laboratory for my research rotations during the first

year of my PhD. The quality of the training I obtained in their laboratories still inspires me and serves as a reference in my research.

I would like to dedicate a special mention to Peter Maloney, the associate dean for graduate student affairs. Simply put, he is an extraordinary human being who has had a crucial impact in the completion of my PhD. He has spent a generous amount of time and dedication to help me in difficult times. He has protected me, provided me with advice and encouragement when I needed it the most and for that I am extremely grateful. He also has been a reader of the Appendix 1 in this thesis.

I also wish to recognize other professors who, at some point during my PhD have provided me their insightful advice or have provided resources and support. I wish to thank Ron Schnaar, Tom August, Caren Feel Meyers, Jef Boeke, Carolyn Machamer for their support. I must also mention the staff in the Department of Pharmacology, including Robin Hart, Frank Williams, Amy Paronto, Brenda Figueroa, Paula Mattingly, and Mimi Guercio for keeping all of us on track logistically and administratively.

Of course, I would not have been able to endure these years without a large group of people who are not always close to me but they are part of my life and therefore part of me. I have been lucky enough to meet wonderful friends in my life. Some of them are my friends since I was six to eight years old like Sonia, Emma, Ana, Myriam, Davina, Nuria. They are my “sisters” for life and I have their constant support whenever I need them. We have share years of friendship that I consider indestructible. During my undergraduate studies I met another exceptional group of friends who had closer interest to mines and we also have actively continued our friendship until now. I would like to

thank Asun, Eva, Angela, Marian, Laura, Bea, Alvaro, Fernando, Julio, Jesús, and Santi for continuously supporting me and cheering me up in person and from a distance.

I have also been very lucky to grow up surrounded by many cousins with similar ages to mine who have become really good friends, including Maria José, Margarita, Cristina, Miguel, Juan, Guillermo, Sandra, Jaime, Beatriz, Javier, Ana, Marta, and Pepe. I would like to thank Maito, for having shared beautiful years with me and tried to help me succeed in so many occasions. I have him in high esteem and I want to acknowledge the difficult times we faced in the past.

It is not surprising that having all these friends and family I have an enormous source of happiness and encouragement that I took for granted before but makes me now realize how lucky and loved I am. I have also met wonderful friends in the United States, including Jerome Salmon, Pablo López, Michael Freeman, Faisal Karmali, Thuy-Co Hoang, Abhishek Gupta, Duane Sanchez, Genaro Ramirez, Eva Andrés Mateo, Rebeca Mejías Estevez, Vedangi Sample, Meritxell Rovira, Matt Feldman, Anabella Palandri, Iliana Lorenzini, Michelle Reilly, Dana Brenner, and William Cooper Gilbert who have filled my days with happiness along these years. I would like to dedicate a special acknowledgement to a person who is very special for me, David Zuckerman. He has always been a loyal friend who I knew I could count on, who has made possible the impossible, and who has made me happy and continues making me happy with his larger-than-life personality, authenticity and idealism.

I would also like to thank my advisor during my project thesis at Escuela Técnica Superior de Montes, Universidad Politécnica of Madrid, Luis Gómez Fernandez. He gave me the opportunity to work in his laboratory without having any previous experience in

biochemistry and he gave me an exceptional training that I am still benefiting from. He also supported me and adviced me in my desire to come to the United States to conduct graduate studies. Other professors were also extremely supportive and always encouraged me to accomplish my desire to start a career in scientific research. I would like to mention Cipriano Aragoncillo, Antonio Notario, Carlos Morla, Alfonso SanMiguel Ayanz, Pedro Cifuentes, and Luis Gil.

I want to dedicate the final paragraphs to what I consider the most precious in my life, which is my family. I have had the privilege to have the most loving, intelligent, and joyful grandparents one could imagine. I felt really loved by them. They made me feel I could do whatever I wanted to do if I worked hard, if I acted with integrity, respect and kindness to others, and mostly, if I was passionate. They gave me the happiest memories of my life and I want to send hugs and kisses to Natividad Monserrat, Guillermo Ferrando, Germán Martínez wherever they are. My grandmother Concha lives in Madrid and I will see her soon to celebrate my thesis completion.

I am extremely proud and grateful to two young men, Germán and Guillermo, who are my wonderful brothers. They are successful professionals and have created a beautiful life around them. Germán and his wife Anahí just had a wonderful baby girl, Olivia. Guillermo lives with Bea and they are really happy together. However, what makes me prouder about them is that they are genuinely good-hearted people and I thank them for inspiring me.

Lastly, I would like to thank the two people I love the most in the world, my parents. My father is one of the most intelligent and knowledgeable persons I know. He was a great student and continues to be because one of the most amazing aspects of his

personality is that he has a very young spirit and is always willing to explore and to learn. Nothing seems impossible for him, as long as it is done with conscientiousness and integrity. He definitively transmitted these values to me during years of playing and working together. My mother is the perfect combination of sweetness and strength. I have seen my mother go through the hardest times without wasting a tear and I have seen her feel compassion for the weak and done whatever was in her hand to help. She is gorgeous, creative and good-hearted. I have to thank her for having given up on her promising career as an artist to make sure we had the best childhood one could imagine. I have to thank her for having listened to my concerns, doubts, and fears in so many occasions. She is an angel to me. My parents made sure that they were fair and generous to us. They gave us all. We lived in a wonderful city and they made sure we enjoyed and appreciate nature during the weekends and summers. They gave as a magnific education and they made sure we learned languages and skills, even if it meant supporting internships in international schools during the summers. They introduced us to different cultures, arts, disciplines, books, etc. They showed us how to be kind to others, how to strive and behave during difficult situations. They were the best example. I could not have chosen a better family if I had been able to. They showed us how to enjoy life and be happy and that is the best gift I have ever received.

I adore my family and I thank them for all the goodness they have done to me.

COPYRIGHT DISCLAIMER

Figures and text in this document arereproduced in part or in whole from the following manuscript, courtesy of the American Society of Biochemistry and Molecular Biology:

Martinez-Ferrando, I, Chaerkady R, Zhong J, Molina H, Kishore H, Herbst-Robinson K, Dancy BM, Katju V, Bose R, Zhang J, Pandey A, Cole PA. ***Identification of targets of c-Src tyrosine kinase by chemical complementation and phophoproteomics.*** Mol. Cell. Proteomics. 2012 Apr 12. [Epub ahead of print] PMID: 22499769

TABLE OF CONTENTS

Abstract ..... **ii**
Dissertation Referees ..... **iv**
Acknowledgements ..... **v**
Copyright Disclaimer ..... **xii**
Table of contents ..... **xiii**
List of Tables ..... **xvii**
List of Figures ..... **xviii**
List of Appendix Figures ..... **xxi**
List of Appendix Tables **23**
CHAPTER 1 – INTRODUCTION **1**
1. Signaling networks 1
1.1. Components of signaling networks 1
1.1.1. Receptors and ion channels 1
1.1.2. Second messengers 2
1.1.3. Intracellular signaling peptides and proteins 5
1.2. Signaling domains 8
1.3. Cell signaling in space and time 9
1.3.1. Signal-dependent formation of signaling complexes 9
1.3.2. Signal processing through preassembled multiprotein complexes 11
1.3.3. Signal regulation by subcellular localization 11
1.3.4. Temporal control of signal transduction 12
2. Tyrosine kinases 12
2.1. Introduction 12
2.2. Structure of protein tyrosine kinases 13
2.3. Regulation of protein tyrosine kinases 16
3. Src 17
3.1. Introduction 17
3.2. Domains of Src 18
3.3. Crystal structure of Src 22
3.4. The Role of Src in the cell: v-Src 22
3.4.1. Induced signaling in v-Src transformed cells 24
3.4.2. v-Src and adhesion 24
3.4.2.1. Stress fiber disorganization 24
3.4.2.2. Focal adhesion disruption 26
3.4.2.2.1. v-Src-induced proteolysis of FAK 26
3.4.2.2.2. v-Src effects on integrin function 26

3.4.2.3. Disruption of adherens junctions 28
3.4.2.4. Disruption of Gap junctions 28
3.4.2.5. v-Src and FAK induced expression of MMPs (matrix metalloproteinases) 29
3.5. c-Src 29
3.5.1. Localization of c-Src in the cell 31
3.5.2. Regulation of Src activity in the cell 31
3.5.2.1. Phosphorylation on C-terminal tyrosine (Tyr-527) 31
3.5.2.2. Interaction with binding partners 32
3.5.2.3. Receptor-mediated activation of Src 32
3.5.3. c-Src in signaling pathways 33
3.5.3.1. Src-FAK complex 33
3.5.3.2. Src targets in adhesion, motility and invasion 35
3.5.3.3. Src and the Ras/ MAPK pathway 36
3.5.3.4. Induction of DNA synthesis 37
3.5.3.5. Degradation of Src 38
4. Methods for identification of tyrosine kinase substrates 38
4.1 Classical methods 38
4.1.1. Genetic methods 39
4.1.2 Biochemical Fractionation 39
4.1.3. In vitro identification of kinase substrate 39
4.1.3.1. Solid phase phosphorylation screening of phage expression libraries 39
4.1.3.2. Oriented peptide library screen of optimal substrate motifs 40
4.1.4. *In vivo* identification of kinase substrates 40
4.1.4.1. Two- dimensional gels 40
4.1.4.2. Protein chips 41
4.1.4.3. Kinase-substrate crosslinking 41
4.1.4.4. ATP analog and mutant kinase pair 42
4.1.4.5. Phospho-motif specific antibodies 42
4.1.4.6. Chemical Rescue 42
5. Chemical Rescue 43
5.1. Introduction of chemical rescue 43
5.2. Chemical rescue and signaling 45
5.3. Chemical rescue of Src 46

Chapter 2. Identification and Characterization of Novel Substrates of Src Using Proteomics 53

1. Introduction 53
1.1. Proteomics Methods 54
1.2. Applying proteomics to signaling networks: detection of phosphorylation 58
1.2.1. Phosphospecific antibodies 60
1.2.2. IMAC 60
1.2. Src proteomics 62
1.3.1. v-Src proteomics 62
1.3.2. Proteomics using constitutively active c-Src mutants 64
1.3.3. c-Src proteomics 65
2. Methods 67
2.1. Cell Culture and SILAC 67

2.2. Cell treatment 68
2.3. SILAC experiment at the protein level 69
2.3.1. Tyrosine phosphoprotein enrichment and quantitative analysis 71
2.4. SILAC experiment at the peptide level 72
2.4.1. Peptide preparation 76
2.4.2. Immunoaffinity purification of tyrosine phosphopeptides 76
2.4.3. LC-MS/MS analysis of tyrosine phosphorylated peptides 78
2.4.4. Data analysis 79
2.5. Network Modeling and Literature Curation 80
2.6. Immunobloting and Immunoprecipitations 82
3. Results 85
3. 1. c-Src chemical rescue optimization 85
3.2. Phosphoprotein identification and quantitation 89
3.3. Confirmation of c-Src targets by immunoprecipitation-Western blot analysis 96
3.4. Phosphosite mapping by chemical rescue of mutant c-Src 99
Discussion 109

Chapter 3: The role of c-Src in the phosphorylation and activation of C3G 114

1. Introduction 114
1.1. C3G 114
1.2. p130cas 114
1.3. Crk 116
1.4. Rap1 120
1.5. THE SRC-CRK-C3G-RAP1 PATHWAY 120
1.6. C3G activation 121
1.6.1. C3G- Crk binding and membrane recruitment 121
1.6.2. C3G phosphorylation 124
1.6.3. C3G binding to p130Cas 129
2. Methods 129
2.1. Cell treatment and lysate preparation 129
2.2. Immunobloting and Immunoprecipitations 130
2.3. Immunofluorescence and Confocal Microscopy 132
2.4. FRET Microscopy 133
3. Results 137
3.1. c-Src chemical rescue leads to Rap-1 activation 137
3.2. Effects of c-Src activation on C3G phosphorylation 139
3.3. Effects of c-Src activation on C3G-Crk binding 143
3.4. Tyr-221 Crk phosphorylation and Crk-C3G complex dissociation 147
3.5. Effects of c-Src activation on C3G subcellular localization 150
4. Discussion 150
Tables 164

Appendix 1- Validation of Matrin through immunoprecipitation and Western blot 225

1. Summary 225
2. Methods 230
3. Results 233
3.1. First attempt 234

3.2. Three following unsuccessful attempts 238
3.3. Final attempt- R390A/ SYF cells 239
3.3.1. Matrin 3 loading control (R390A/ SYF cells) 239
3.3.2. Anti-phosphotyrosine Western blot before the sandwich reaction.....244
3.3.3. Anti-phosphotyrosine Western blot after the first sandwich reaction 244
3.3.4. Anti-phosphotyrosine Western blot after the first sandwich reaction. Second exposure.....255
3.3.5. Anti-phosphotyrosine Western blot after the first sandwich reaction. After washing and developing again.....261
3.3.6. Anti-phosphotyrosine Western blot after the second sandwich reaction. First exposure.....269
3.3.7. Anti-phosphotyrosine Western blot after the second sandwich reaction. Second exposure.....276
3.3.8. Anti-phosphotyrosine Western blot after the second sandwich reaction. Third exposure.....287
3.4. Final attempt- D398N/ SYF cells. Anti-matrin 3 Western blot and anti-phosphotyrosine Western blot 294
Discussion.....298

References 320

CURRICULUM VITAE 337

LIST OF TABLES

Table 1. Stable isotopic amino acids used in SILAC media 164
Table 2. List of identified proteins from the SILAC experiment at the protein level. Phenylphosphate elution. 165
Table 3. List of identified proteins from the SILAC experiment at the protein level. Boiled beads elution. 168
Table 4. List of identified proteins from the SILAC experiment at the protein level. Phenylphosphate and Boiled beads elutions combined. 173
Table 5. Simplified list of identified proteins from the SILAC experiment at the protein level. Phenylphosphate and Boiled beads elutions combined. 197
Table 6. Complete set of tyrosine phosphorylated peptides quantitated by SILAC at the peptide level. 202
Table 7. Set of c-Src- induced tyrosine phosphorylated peptides quantitated by SILAC at the peptide level. 217
Table 8. Combined list of Src substrates (140) from prior proteomics studies. 220

LIST OF FIGURES

Figure 1: Mechanism of activation of second messenger signaling 4
Figure 2. Schematic of two types of adaptor proteins: Scaffold proteins and anchoring proteins 7
Figure 3. Domain organization for a variety of RTKs 14
Figure 4. Domain organization for a variety of NRTK 15
Figure 5. Schematics of c-Src domains 19
Figure 6. Photomicrographs showing the v-Src phenotype 23
Figure 7. Schematics of the mechanism of v-Src –induced proteolysis of FAK 27
Figure 8. Schematics of the interactions of Src, FAK, p130Cas and paxillin in focal adhesions 34
Figure 9. Position of the catalytc Arg-388 of Src- family kinases as compared to other tyrosine kinases 47
Figure 10. Time course of tyrosine phosphorylation induced by imidazole treatment of Src R388A/Y527F in SYF cells (8A7F) and Src D386N/Y527F in SYF cells (6N7F cells) 49
Figure 11. Src autophosphorylation (Y416) induced by imidazole treatment of Src R388A/Y527F in SYF cells (8A7F) and Src D386N/Y527F in SYF cells (6N7F cells) 50
Figure 12. Reversible Src autophosphorylation (Y416) in R388A/Y527F in SYF cells (8A7F cells) after imidazole washout 52
Figure 13. Schematics of MudPIT (multidimensional LC-MS/MS) or 'bottom up' shotgun proteomics 56
Figure 14. Peptide labeling with isotopically labeled amino acids 59
Figure 15. Schematics of IMAC (immobilized metal affinity chromatography) 61
Figure 16. Identification and quantitation of tyrosine phosphorylated proteins by SILAC and LC-MS/MS. Anti-phosphotyrosine immunoblot revealing chemical rescue. SDS-Page and colloidal Coomassie stained gels of immunoprecipitated eluates. 70
Figure 17. Site-specific mapping and quantification. Control 1 73

Figure 18. Site-specific mapping and quantification. Control 2 74
Figure 19. Site-specific mapping and quantification. Control 3 75
Figure 20. Site-specific mapping and quantification. Control 4 77
Figure 21. Flow-chart representing the complete data analysis process corresponding to the phosphopeptide enrichment by SILAC and LC-MS/MS 81
Figure 22. Western blot experiment to optimize c-Src rescue conditions 87
Figure 23. Western blot experiment showing c-Src chemical rescue in R390A/ SYF cells but not in D388N/ SYF cells 88
Figure 24. Control Western blot experiment showing no effects of c-Src chemical rescue in SYF MEF and MEF cells 90
Figure 25. Scheme of the experimental design of SILAC-based quantitative phosphoproteomic approach. Protein level 92
Figure 26. Graph showing the distribution of identified and quantified phosphoproteins 94
Figure 27. Validation of protein phosphorylation of known Src substrates Fak and paxillin upon c-Src rescue 97
Figure 28. Validation of six identified potential novel c-Src substrates 98
Figure 29. Scheme of the experimental design of SILAC-based quantitative phosphoproteomic approach. Peptide level 100
Figure 30. Overview of identified phosphopeptides with upregulated tyrosine phosphorylation upon c-Src rescue in R390A c-Src SYF MEF cells 104
Figure 31. Ingenuity Pathway analysis of the c-Src upregulated phosphoproteome 105
Figure 32. Role of c-Src in focal adhesion signaling 107
Figure 33. C3G domain structure 115
Figure 34. Crk domain structure 117
Figure 35. Crk negative regulation by phosphorylation on Tyr-221 by c-Abl 119
Figure 36. The Src-Crk-C3G-Rap1 pathway 122
Figure 38. C3G and pTyr-514-C3G increased localization at the cell periphery after c-Src rescue 134
Figure 39. Schematic representation of the Raichu-Rap1 reporter bound to GDP or GTP 136

Figure 40. Detection of the effect of c-Src activation on C3G's ability to activate Rap1 138
Figure 41. Detection of the effect of c-Src activation on C3G's phosphorylation on Tyr-514 140
Figure 42. Biological replicates for the experiment to detect the effect of c-Src activation on C3G's phosphorylation on Tyr-514 141
Figure 43. Detection of the effect of c-Src activation on C3G- Crk binding 144
Figure 44. Biological replicates for the experiment to detect the effect of c-Src activation on C3G- Crk binding 145
Figure 45. Detection of the effect of c-Src activation on Crk's phosphorylation on Tyr-221 148
Figure 46. Biological replicates for the experiment to detect the effect of c-Src activation on Crk's phosphorylation on Tyr-221 149
Figure 47. Detection of the effect of c-Src activation on C3G's subcellular localization 151
Figure 48. Hypothetical parallelism between the phosphorylation of the RasGEF Sos and the adaptor protein Crk as events for the regulation of the Raf/MEF/ERK cascade 155
Figure 49. Novel tyrosine phosphorylation site in C3G (Tyr-571) as evidenced by MS/MS 158
Figure 50. Schematics of a hypothetical C3G-Crk interaction based on Tyr-571 phosphorylation 160
Figure 51. Schematics of the observations made on the Crk-C3G-Rap1 pathway 162

LIST OF APPENDIX FIGURES

Appendix 1 Figure 1. MS/MS spectrum showing the identified peptide (LAEPYGK) from matrin 3. 226

Appendix 1 Figure 2. MS spectrum showing the increase in intensity between the "light" and the "heavy" (isotopically labeled) forms of the peptide (LAEPYGK) from matrin 3. 228

Appendix 1 Figure 3. Repeats of the immunoprecipitation- Western blot experiments to validate the mass spectrometry results that revealed matrin 3 as a potential c-Src substrate. 236

Appendix 1 Figure 4. Workflow of the process to obtained the different blots in the last attempt to detect matrin 3 phosphorylation 240

Appendix 1 Figure 5. Matrin 3 loading control of the final experimental repeat in the rescuable cell line R390A/SYF. 241

Appendix 1 Figure 6. IP-WB experiment to validate matrin 3 as a potential c-Src substrate. R390A/ SYF cells. Anti-phosphotyrosine Western blots before first sandwich reaction 245

Appendix 1 Figure 7.1. IP-WB experiment to validate matrin 3 as a potential c-Src substrate. R390A/ SYF cells. Anti-phosphotyrosine Western blots after the first sandwich reaction. 246

Appendix 1 Figure 7.2. IP-WB experiment to validate matrin 3 as a potential c-Src substrate. R390A/ SYF cells. Anti-phosphotyrosine Western blots after the first sandwich reaction (cont.) 248

Appendix 1 Figure 8.1. IP-WB experiment to validate matrin 3 as a potential c-Src substrate. R390A/ SYF cells. Anti-phosphotyrosine Western blots after the first sandwich reaction. Second exposure. 256

Appendix 1 Figure 8.2. IP-WB experiment to validate matrin 3 as a potential c-Src substrate. R390A/ SYF cells. Anti-phosphotyrosine Western blots after the first sandwich reaction. Second exposure (cont). 258

Appendix 1 Figure 9.1. IP-WB experiment to validate matrin 3 as a potential c-Src substrate. R390A/ SYF cells. Anti-phosphotyrosine Western blots after washing and redeveloping. 262

Appendix 1 Figure 9.2. IP-WB experiment to validate matrin 3 as a potential c-Src substrate. R390A/ SYF cells. Anti-phosphotyrosine Western blots after washing and redeveloping (cont). 264
Appendix 1 Figure 10.1. IP-WB experiment to validate matrin 3 as a potential c-Src substrate. R390A/ SYF cells. Anti-phosphotyrosine Western blots after second sandwich reaction. First exposure. 271
Appendix 1 Figure 10.2. IP-WB experiment to validate matrin 3 as a potential c-Src substrate. R390A/ SYF cells. Anti-phosphotyrosine Western blots after second sandwich reaction. First exposure (cont). 273
Appendix 1 Figure 11.1. IP-WB experiment to validate matrin 3 as a potential c-Src substrate. R390A/ SYF cells. Anti-phosphotyrosine Western blots after second sandwich reaction. Second exposure. 277
Appendix 1 Figure 11.2. IP-WB experiment to validate matrin 3 as a potential c-Src substrate. R390A/ SYF cells. Anti-phosphotyrosine Western blots after second sandwich reaction. Second exposure (cont). 279
Appendix 1 Figure 11.3. Change in phosphorylation of matrin 3 upon c-Src when using the quantitation from the image obtained from the translucent scan of the blot obtained after the second sandwich reaction (second exposure) and the translucent scans of the matrin 3 loading control. 286
Appendix 1 Figure 12.1. IP-WB experiment to validate matrin 3 as a potential c-Src substrate. R390A/ SYF cells. Anti-phosphotyrosine Western blots after second sandwich reaction. Third exposure. 288
Appendix 1 Figure 12.2. IP-WB experiment to validate matrin 3 as a potential c-Src substrate. R390A/ SYF cells. Anti-phosphotyrosine Western blots after second sandwich reaction. Third exposure (cont). 290
Appendix 1 Figure 13. Matrin 3 loading control of the final experimental repeat in the non-rescuable cell line D388N/SYF. 296

LIST OF APPENDIX TABLES

Appendix 1 Table 1. List of Proteins identified with 95% confidence by Scaffold …317

Appendix 1 Table 2. List of Proteins identified with 85% confidence by Scaffold…319

CHAPTER 1 – INTRODUCTION

1. Signaling networks

Cells have the ability to communicate with the external environment through dynamic signaling pathways. These pathways receive signals from the external environment and from different regions of the cell. Signaling pathways generally interconnect to form signaling networks. This complex dynamic spatial organization results in a higher level of cellular coordination with the environment and other cells (1).

1.1. Components of signaling networks

1.1.1. Receptors and ion channels

Cells receive external stimuli through cell surface molecules such as receptor proteins and ion channels. Receptors can be extracellular and intracellular. Extracellular receptors are integral transmembrane proteins that, upon ligand binding, change their intracellular conformation leading to a cascade of signaling events.

An example of extracellular receptors is the G protein-coupled receptor (GPCR). The GPCRs are a large family of receptor proteins, which consist of seven transmembrane domains. These GPCRs interact with a heterotrimetric G protein and, when activated, lead to signaling events to several downstream effector proteins.

Receptor tyrosine kinases (RTKs), such as growth factor receptors (i.e. insulin receptor) are characterized by an intracellular kinase domain. Upon ligand binding, RTKs form dimers in the plasma membrane (2), which leads to autophosphorylation of tyrosines in opposite monomers. The resulting conformational change leads to kinase activation and a consequent signaling cascade.

Integrin receptors (integrins) play a major role in cell attachment, both with other cells and with the extracellular matrix (ECM), as well as in the signaling resulting from ECM components such as fibronectin and collagen. After ligand binding, integrins undergo conformational changes that lead to clustering of integrin molecules at the membrane. Integrins do not have kinase activity. Instead, downstream signaling occurs through protein kinases and adaptors coordinated by integrin-linked kinase (3). Other relevant extracellular receptors include Toll-like receptors (TLRs) and ligand-gated ion channels.

Intracellular receptors can be categorized as nuclear receptors, with the subclass of steroid receptors and the subclass of the retinoic acid receptors, and cytoplasmic receptors, such as the recently identified NOD-like receptors (NLRs) (4).

1.1.2. Second messengers

Second messengers are molecules that transmit signals from receptors to target molecules inside the cell. Enzymes can synthesize, activate and break down secondary messenger networks (i.e. cyclases synthesize cyclic nucleotides). When ion channels open, they can also allow the influx of metal ions like Ca^{2+}, which can be stored in

certain organelles and released at specific moments. The input and output of second messengers can be localized, allowing spatial and temporal compartmentalization of the signaling activity within the cell. Second messengers bind and activate other proteins continuing the signaling cascade. They are able to significantly amplify the strength of the extracellular signal.

A common mechanism of secondary messenger systems is the following: A neurotransmitter (first messenger) binds to a receptor protein. This binding leads to a conformational change that exposes a binding site for a G-protein (transducer). Upon binding to the receptor, the G-protein exchanges a GDP (guanosine diphosphate) for a GTP (guanosine triphosphate). The G-protein alpha subunit detaches from the beta and gamma subunits, and moves along the inner membrane, where it will eventually contact another protein bound to the membrane (primary effector). The primary effector produces a signal (second messenger), which is diffused in the cell and will eventually activate the secondary effector **(Figure 1).**

Second messengers can be classified in three major groups: Hydrophobic molecules, such as diaglycerol and phosphatidylinositols, that diffuse from the plasma membrane into the intermembrane, where they bind and regulate effector proteins that are associated to the membrane. Hydrophilic molecules locate in the cytosol, such as cAMP, cGMP, IP_3, and Ca^{2+}. Gases, such as nitric oxide (NO), a well-established signaling molecule, and perhaps carbon monoxide (CO) and hydrogen sulfide (H_2S), can diffuse through the cytosol and across cellular membranes to transmit information. A few representative second messengers, which play a key role in intracellular signal

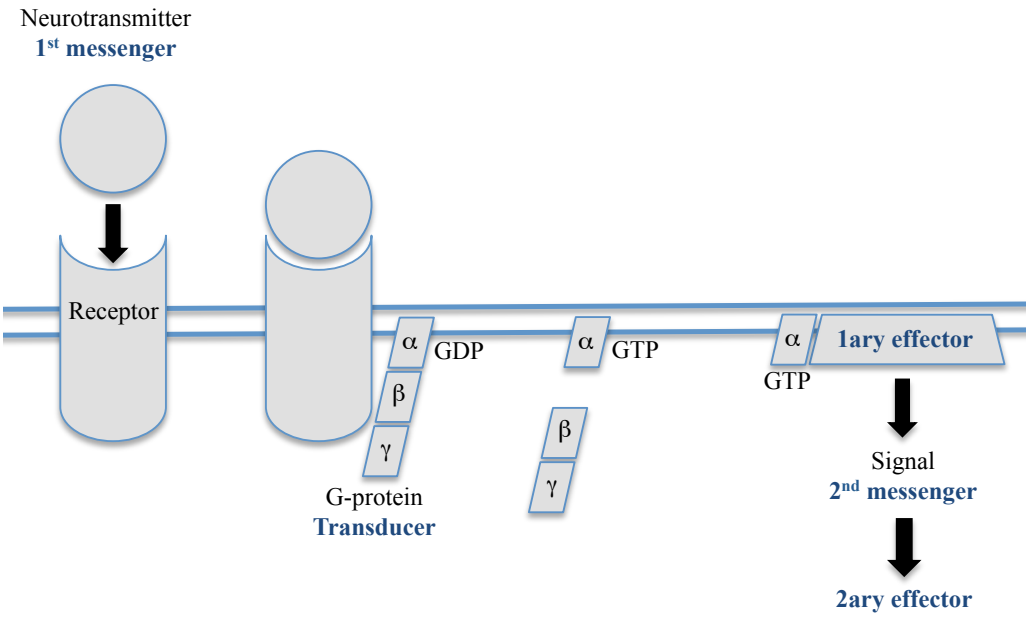

Figure 1: Mechanism of activation of second messenger signaling

Representation of a common mechanism of secondary messenger signaling activation: The first messenger binds the receptor that will undergo a conformational change and expose a G-protein binding site. The G-protein will bind the receptor and exchange a GDP for a GTP. The alpha subunit will detach from the beta and gamma subunits. The alpha subunit will contact the primary effector that will lead to the transmission of a signal (second messenger) that will activate the secondary effector.

transduction, are analyzed in more detail. Calcium is involved in many biological processes from muscle contraction to cell migration. There are three main pathways that result in calcium activation: GPCR pathways, RTK pathways and gated ion channels. Calcium is released from the endoplasmic reticulum to the cytosol. There, it binds and activates signaling proteins, like calmodulin. Calcium is sequestered afterwards in the smooth endoplasmic reticulum and the mitochondria.

Lipophilic second messengers are formed when enzymes stimulated by activated receptors modify lipids from cellular membranes. Ceramide and diacylglycerol are such examples. Nitric oxide (NO) is synthesized by the NO synthase from arginine and oxygen. NO affects the biology of cells through different mechanisms such as oxidation of iron-containing proteins, activation of soluble guanylyl cyclase, ADP ribosylation of proteins, protein sulfhydryl group nitrosylation, or iron regulatory factor activation (5). NO can diffuse through the plasma membrane and affect surrounding cells.

1.1.3. Intracellular signaling peptides and proteins

These signaling components are found in the cytoplasm and transmit extracellular signals to intracellular effectors and regulate the activity of transcription factors. Signaling enzymes are proteins that catalyze chemical reactions and serve a broad variety of functions in living organisms as diverse as active transport (ATPases that constitute ion pumps in the cell membrane) or generation of movement (Myosin ATPases that contribute to muscle contraction). Enzymes are indispensable for signal transduction and cell regulation, often via post-translational modifications of proteins. Through these

modifications, cells can regulate post-translationally key cellular pathways. Among these post-translational modifications are phosphorylation (kinases and phosphatases), acetylation (acetyltransferase and deacetylases), methylation (methyltransferases and demethylases), ubiquitinylation, ADP-ribosylation and sumoylation (6).

Considering the type of signal modulation that the signaling enzyme is responsible for within the signaling cascade, they can be classified as amplifiers or coincidence detectors. Amplifiers tend to increase the signal by producing large amounts of small intracellular second messengers or by activating a variety of downstream signaling proteins. Coincidence detectors are signaling enzymes that are only activated when several signals occur together. As an example, cAMP-generating adenylyl (adenylate) cyclases are modulated by G-proteins, forskolin, Ca2+/calmodulin, and other class-specific substrates.

Adaptor proteins are non-catalytic multivalent binding proteins that serve as platforms for the assembly of signaling molecules **(Figure 2)** (7). Kinase-phosphatase signaling complexes modulate the phosphorylation state of their substrates. Signaling complexes related to tyrosine phosphorylation were identified first. Many tyrosine kinases and phosphatases function through adaptor proteins. These proteins contain SH2 domains, which bind to certain phosphorylated tyrosines as part of the signaling process, and SH3 domains that bind to PXXP motifs in other signaling proteins including cytoskeletal components and small G-proteins (8). Signaling complexes of serine/threonine kinases form through two different types of adaptor proteins. Scaffold proteins simultaneously associate with several kinases of a signaling pathway in a way that allows sequential activation of each kinase. Anchoring proteins are targeted to

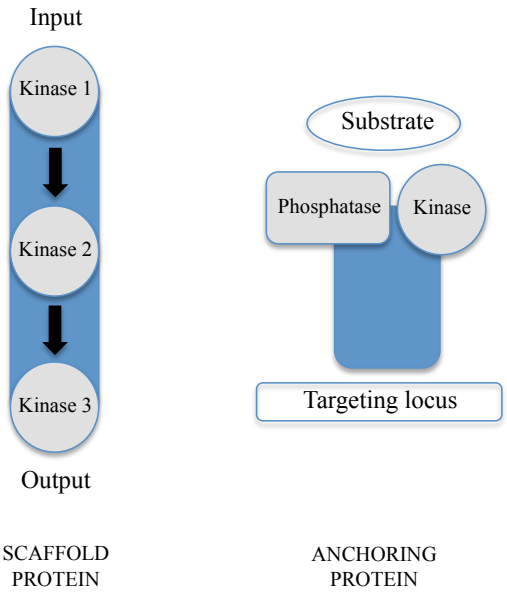

Adapted from Scott JD *et al*., Cell 1996

Figure 2. Schematic of two types of adaptor proteins: Scaffold proteins and anchoring proteins

Adaptor proteins: scaffold proteins serve as a dock for several kinases that are sequentially activated as part of a signaling pathway. Anchoring proteins localize proteins near specific areas in the cell where they induce signaling responses.

specific regions of the cell, and localize their bound proteins close to their site of action, providing a spatial dimension to signaling.

1.2. Signaling domains

Signaling proteins often have a modular organization formed by catalytic domains separated by regions that serve as docking or substrate sites for other signaling molecules. The Src homology 2 (SH2) domain is a compact domain of about 100 amino acids that bind phosphotyrosine-containing peptide motifs (9,10). Most proteins containing SH2 domains are recruited to sites of tyrosine phosphorylation to help in the coordinated assembly of molecular machines (11). SH2 domains can also influence enzymatic activity in different ways. The SH2 domain of human FES cytoplasmic kinase stabilizes its activity since the kinase is only fully active when the SH2 domain is bound to a primed substrate (12). In other contexts, SH2 domains can also suppress tyrosine kinase activity, as in enzymes like Abl, Src, Lyn, and Fyn (13,14).

The smaller Src homology 3 (SH3) domain contains about 60 amino acids and binds proline-containing sequences capable of forming a polyproline type II helix (15).

Pleckstrin homology (PH) domains bind to phosphatidylinositol lipids that have been phosphorylated at particular positions on the head group. In this manner, PH domain-containing proteins can be recruited to activate signaling complexes at the membrane through interactions with phosphorylated PtdIns lipids (15).

Many other types of domains have been identified, like EF hand domains or PDZ domains. There are specialized domains found in cell-surface adhesion and inflammatory

responses. Some of them are: cadherin repeats, carbohydrate-recognition domain (CRD), caspase recruiting domains, CARD domains, C-lectin domain (CTLD), death domain (DD), death effector domain (DED), Ffas-Associated Death domain (FADD), and zinc finger DNA binding domains.

1.3. Cell signaling in space and time

The components of signaling pathways are organized in sophisticated regulatory mechanisms to ensure that signaling enzymes find their intracellular substrates in the correct place and time. Several mechanisms have emerged to ensure the accurate coordination of events in space and time.

1.3.1. Signal-dependent formation of signaling complexes

The flow of information commonly requires the dynamic formation of protein complexes, and this process can be initiated by posttranslational modifications or protein oligomerization that can generate pockets of increased enzyme activity. Different covalent modifications can be used by the cell to facilitate signal-dependent recruitment of proteins.

In the case of tyrosine phosphorylation signaling, the building block of these units is usually a complex of adaptor proteins that recognize the activated receptor (through their SH2 domain in case of upstream RTKs) and bind other proteins through their other binding domains, such as SH3 domains. Adaptor proteins such as Grb2 (SH3-SH2-SH3)

or Nck (SH3-SH3-SH3-SH2) are examples of this strategy (16). As described in the previous section, SH2 domains can also stabilize or suppress tyrosine kinase activity. Other modular domains regulate serine or threonine phosphorylation events. Specifically these protein interactions occur through pThr and pSer binding molecules like WW and FHA (Forkhead homology-asociated) domains and 14-3-3 proteins (17) (18). Sometimes the assembly or disassembly of signaling complexes occurs in specific subcellular compartments. Certain domains have their ability to target the protein to certain subcellular regions through the recognition of phosphoinositides in particular membranes. As an example, protein kinase B (PKB) / Akt protein kinase and its regulator phosphoinositide-dependent protein kinase 1 (PDK1) both have PH domains that are selective for $PI(3,4,5)P_3$ or $PtdIns(3,4)P_2$ that recruit the kinase and its regulator to the membrane when PI3K is activated (16).

Ubiquitination of lysine residues is another posttranslational modification that aids in the formation of protein complexes (19). While polyubiquitination often leads to degradation of target proteins by the 26S proteasome, mono-ubiquitination and di-ubiquitination also mediate other cellular functions. Ubiquitin-binding domains (UBDs) bind ubiquitin in a similar manner than in phosphotyrosine signaling (20) but with micromolar affinities (21). As a result UBD proteins usually control transient cellular processes.

Lysines can also be acetylated. This posttranslational modification is usually associated with changes in the activity of histones and transcription factors (22). Acetylated residues can recruit proteins containing bromodomains. Also, autoacetylation leads to conformational changes of proteins with intrinsic HAT activity (histone

acetyltransferases) as is the case with the transcriptional co-activator CBP/p300. In addition, acetylation can inhibit ubiquitination of the same side-chain, resulting in a prolonged half-life of the protein. An example of this last event is the tumor suppressor protein p53 (23).

1.3.2. Signal processing through preassembled multiprotein complexes

Another way to regulate intracellular communication is by the flow of signals through preassembled multiprotein complexes where successive enzymes of a transduction pathway are clustered in an orderly fashion. The molecular glue is a scaffold protein as described above. One example of this modulation is the clustering of the kinases involved in the MAPK (mitogen-activated protein kinase) pathway by scaffold proteins such as KSR and MP-1, which will be thoroughly discussed bellow. The benefit of this kind of modulation is that it enhances the precision and fidelity of signaling events.

1.3.3. Signal regulation by subcellular localization

Another way of spatially restricting signaling events is by compartmentalizing enzymes in close proximity to their substrates. In this manner, many kinase- and phosphatase- binding proteins are recruited to sites where they can receive activating signals and are near their substrates (16).

One family of anchoring proteins are AKAPs (A-kinase anchoring proteins). AKAPs organize protein kinase A (PKA) holoenzyme, guanine nucleotide exchange factors (Epac) and phosphodiesterases (PDE) into cAMP-inducible complexes. There are about 20 AKAP genes and about 75 alternately spliced transcripts that are targeted to different organelles within the cell. As a result PKA can anchor to different isoform targets in different localizations and restrict the action of PKA to only a few of its substrates.

1.3.4. Temporal control of signal transduction

A different way to modulate cellular events is to induce changes in either the composition or the amount of enzyme complexes over time. This usually involves synchronized phosphorylation events, ubiquitin-mediated degradation, and translocation of signaling components. A good example is the activation mechanism of NF-kB (nuclear factor kB), which involves the phosphorylation and ubiquitination of several components (24).

2. Tyrosine kinases

2.1. Introduction

Protein tyrosine kinases (PTKs) catalyze tyrosine residue phosphorylation, by transferring the g-phosphoryl group of adenosine triphosphate (ATP) to the hydroxyl

group in the substrate. Phosphotyrosine (pTyr or pY) modifications can modulate the enzymatic activity of target proteins and can also disrupt or stabilize protein-protein interactions. Many tyrosine kinases have the potential to cause cancer and are considered oncogenes (25). There are approximately 100 PTKs encoded in the human genome, from which about 40 are nonreceptor tyrosine kinases (NRTKs) and 60 are receptor tyrosine kinases (RTKs).

2.2. Structure of protein tyrosine kinases

Receptor tyrosine kinases are composed of a ligand binding extracellular domain, a transmembrane helix domain and an intracellular portion with tyrosine kinase activity **(Figure 3)** (15,26).

Non-receptor tyrosine kinases are mostly localized in the cytoplasm although some are anchored to the cell membrane through modifications such as myristoylation or palmitoylation. NRTKs possess a tyrosine kinase domain and can contain one or more different recruitment or regulatory domains that mediate protein-protein, protein-lipid, and protein-DNA interactions, such as SH2 domains, SH3 domains, or other subfamily-specific domains. Some examples are an integrin-binding domain and a focal adhesion-binding domain in focal adhesion kinase (FAK), or a nuclear localization signal, an F actin–binding domain and a DNA-binding domain in Abl kinase. Another common domain is the pleckstrin homology (PH) domain **(Figure 4)** (15).

The structure of the kinase domain is highly conserved among all tyrosine kinases (15). Kinase domains contain an N-terminal lobe involved in ATP binding, a C-terminal

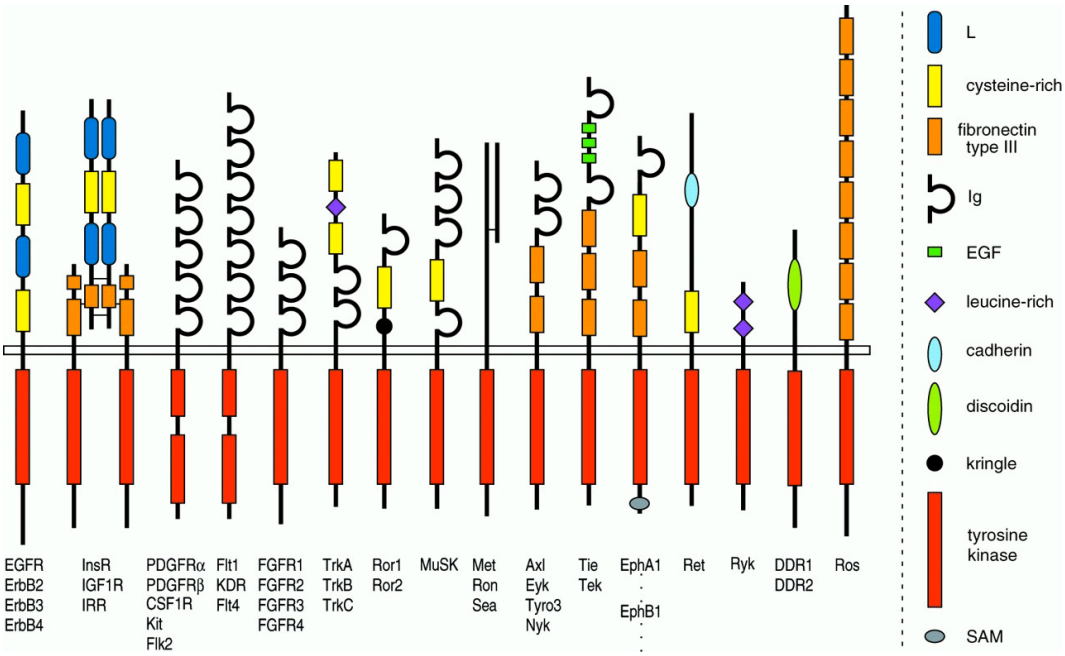

Hubbard SR and Till JH, Annual Review of Biochemistry 2000

Figure 3. Domain organization for a variety of RTKs

The horizontal double line represents the cell membrane. On top of it, the extracellular portion of the receptors is represented, whereas the cytoplasmic portion is on the bottom. The length of the receptor is to approximate scale. The tyrosine kinase symbol (red rectangle) has a break in those receptors that contain a large insert in the tyrosine kinase domain.

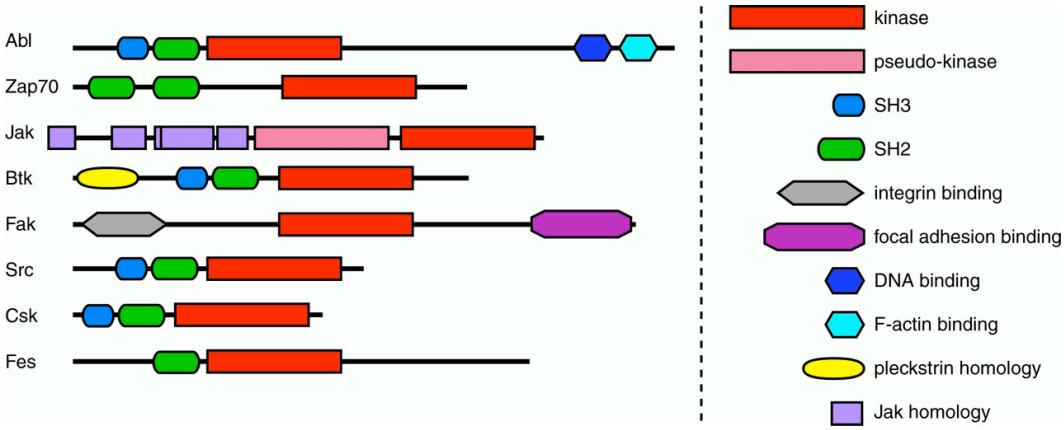

Hubbard SR and Till JH, Annual Review of Biochemistry 2000

Figure 4. Domain organization for a variety of NRTK

The NRTKs are shown from the amino terminus (left) to the carboxy terminus (right).

The length of the NRTKs is to approximate scale.

lobe with catalytic residues and protein substrate recognition elements, and a deep cleft between both lobes where the active site responsible for catalysis is located.

The ATP g-phosphate is oriented outward toward the active site entrance and the adenine is positioned inside a hydrophobic pocket. The ribose interacts with the kinase structure through hydrogen bonds. Mg^{2+} interacts with the two or three of the phosphates of ATP. A catalytic aspartate acts as a base that removes the proton from the hydroxyl group in the substrate tyrosine. There are several other conserved residues involved in substrate positioning and in coordinating the metal ions. Most tyrosine kinases have an activation loop containing at least one regulatory tyrosine. When the tyrosine residue is unphosphorylated, it often interferes with catalysis and autophosphorylation of this tyrosine residue leads to a conformational change in the active site that facilitates activation of the kinase.

2.3. Regulation of protein tyrosine kinases

After decades of research, the developed model of RTK activation is that ligand binding to RTKs stabilizes dimer formation from receptor monomers. This facilitates intermolecular autophosphorylation of the kinases domains in the cytoplasmic region of the RTKs (27,28). Autophosphorylation of up to three tyrosine residues in the activation loop further stimulates the kinase activity (29).

A signal induced from an RTK can be attenuated and terminated through different mechanisms such as inhibitory ligands (30), inactive RTKs with ability to hetero-oligomerize with functional RTKs (31), certain RTK phosphorylation events (32),

receptor-mediated endocytosis (28), ubiquitin-directed proteolysis (33), and protein tyrosine phosphatases (34).

Regulation of NRTKs can be modulated by phosphorylation of tyrosine sites in the activation loop or at other positions. Other forms of regulation are dephosphorylation by tyrosine phosphatases, phosphorylation by serine/threonine kinases, and regulation by protein-protein interactions.

3. Src

3.1. Introduction

Prior to the identification of the *src* gene, a virus called the Rous sarcoma virus (RSV), was discovered by Peyton Rous, and was shown to be the causative agent for the development and transmission of chicken tumors called fibrosarcomas. RSV was later identified as a type of retrovirus and its molecular details were elucidated. Certain tumor-causing retroviruses contain three genes: *gag*, *pol*, and *env*, in addition to a gene called *v-src* that is required for the development of cancer (35). The *v-src* gene was the first oncogene identified. Bishop and Varmus discovered in 1979 that chickens contain a gene that is structurally related to *v-src* and it became known *c-src*, for cellular *src* (36). This discovery led to the groundbreaking realization that a gene that is normally present in the cell could cause cancer and was therefore classified as a proto-oncogene. Erickson, Sefton, and Hunter showed that Src was a protein tyrosine kinase (37).

The gene *v-src* was first sequenced in 1980 (38). v-Src protein is not negatively

regulated as c-Src is, because it lacks a C-terminal inhibitory phosphorylation site (tyrosine 527). This explains why v-Src is constitutively active (oncogene) as opposed to c-Src (proto-oncogene), which is activated specifically in certain cellular stages.

The Src family is composed of eleven tyrosine kinases with a high level of homology: Src, Fyn, Yes, Yrk, Blk, Fgr, Hck, Lck, Lyn, and the Frk subfamily proteins Frk/Rak and Iyk/Bsk. Members of this family are involved in several functions including cellular proliferation, differentiation, survival, adhesion and migration. The functions of Src family kinases are redundant (39). For example, Src, Fyn and Fgr are involved in cellular adhesion through integrins, cadherins, selectins, and focal adhesion kinase (FAK). Src, Yes and Fyn play roles in RTK activation pathways. Fyn, Hck, Fgr, Lck, Lyn, Src, and Yes are involved in cytokine receptor activation.

3.2. Domains of Src

Src is composed of the following domains, from N to C-terminus: SH4, unique domain, SH3, SH2, linker region, catalytic domain (SH1), and C-terminal tail, as shown in **Figure 5**.

The SH2 and SH3 domains cooperate in the auto-inhibition of the kinase domain. C-Src is phosphorylated on an inhibitory tyrosine near the C-terminus of the protein. This produces a binding site for the SH2 domain which, when bound, facilitates binding of the SH3 domain to a low affinity polyproline site within the linker between the SH2 domain and the kinase domain. Binding of the SH3 domain results in misalignment of residues within the kinase domain's active site, inactivating the enzyme. This allows for multiple

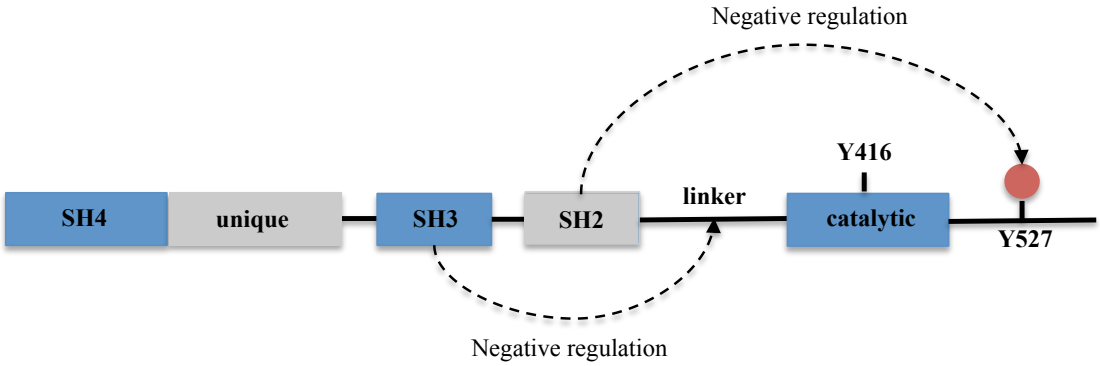

Figure 5. Schematics of c-Src domains

c-Src domain composition: From N to C-terminus: SH4, unique domain, SH3, SH2, linker region, catalytic domain (SH1), and C-terminal tail. C-Src is phosphorylated on Tyr-527, creating a binding site for the SH2 domain. The SH3 domain binds to a low affinity polyproline motif included in the linker between the SH2 domain and the kinase domain, leading to the inactivation of the enzyme. C-Src can be activated by dephosphorylation of Tyr-527, binding of the SH2 domain to a competitive phospho-tyrosine residue, or competitive binding of a polyproline-binding motif to the SH3 domain.

mechanisms for c-Src activation: dephosphorylation of the C-terminal tyrosine by a protein tyrosine phosphatase, binding of the SH2 domain by a competitive phospho-tyrosine residue, as seen in the case of c-Src binding to focal adhesion kinase, or competitive binding of a polyproline binding motif to the SH3 domain, as seen in the case of the HIV NEF protein.

The SH4 domain is essential for Src membrane association, which is key for the biological function of Src, since it allows the flow of signal from the membrane to downstream cytoplasmic substrates. This association occurs mainly through myristoylation (40), the concentration of basic residues in the SH4 domain and palmitoylation (41). This association is also promoted by several signaling pathways (39).The unique domain is the least conserved among the Src family members and its functions remains unclear to date. Ser/Thr kinase Cdc42 is thought to phosphorylate Thr-34, Thr-46, and Ser-72 residues (42,43) in this domain. There may be specific functions associated with each Src family member related to this region.

The β-barrel fold comprised of β-strands in the SH3 domain of Src binds to a left-handed proline type II helix in the linker region of Src (44). The SH3 domain in Src has two functions. It helps maintain Src in its basal state, by maintaining its repressed conformation. It also provides a docking site for substrate binding and cellular localization. As described before, the consensus sequence in the proline rich region that binds to the SH3 domain contains the PXXP pattern (X being any amino acid). Binding between Src's SH3 domain and its peptide ligand has been measured by *in vitro* binding assays: a dissociation constant of 10 μM shows a moderate binding affinity (44), which can be higher with intact proteins due to cellular localization or other long-range proteins

interactions. SH3 domains are also commonly found in dozens of other signaling proteins.

The SH2 domain of Src serves a dual function: it binds phosphorylated Tyr-527 of the Src C-terminal tail to maintain Src in its repressed state. In addition, it serves as a docking site for substrates or adaptors by binding to phosphotyrosine containing proteins, such as focal adhesion kinase (FAK), p130Cas, the p85 subunit of PI3-Kinase, and p68Sam (45). The SH2-phosphotyrosine binding usually occurs through a two-pocket mode. The first pocket of the SH2 domain contains one or more Arg residues and binds the phosphotyrosine residue. The second pocket usually binds to a hydrophobic residue located at position +3 after the phosphotyrosine residue. The binding affinity of the binding between the SH2 domain and the phosphorylated tyrosine is in the range of 1.0 μM. This affinity is strongly reduced (1000-fold or more) when tyrosine is unphosphorylated (46).

The Src catalytic domain contains a small N-terminal lobe, an activation loop (residues 404 to 432), and large C-terminal lobe. The activation loop contains an autophosphorylation site (Tyr-416) that facilitates the activity of Src. When unphosphorylated, this tyrosine probably blocks the substrate binding to the catalytic site. Autophosphorylation relieves the inhibition and allows substrate binding (47). The Src catalytic domain is homologous to hundreds of other human protein kinase domains.

Unlike v-Src, c-Src contains a C-terminal tail (48). This domain contains the key residue, Tyr-527. This residue is phosphorylated by Csk and Chk (49). Subsequently, Src's SH2 domain binds phosphorylated Tyr-527 and locks Src in its inactive

conformation. However, phosphotyrosine-containing proteins may be able to displace the tail to open Src and enhance its activity.

3.3. Crystal structure of Src

c-Src is normally maintained in a repressed conformation by two main interactions (50). The first one is the interaction between the phosphorylated Tyr-527 and the SH2 domain and the second the interaction between the SH3 domain and short polyproline Type II helix in the linker between the SH2 domain and the kinase domain. It is thought that these two interactions might limit autophosphorylation of Tyr-416 in the activation loop. When Tyr-416 is not phosphorylated, it forms hydrophobic interactions with residues in the catalytic cleft, blocking substrate binding (50).

3.4. The Role of Src in the cell: v-Src

The v-Src phenotype on cell biological function has been intensively studied. Infection or transfection of fibroblasts with the v-Src oncogene leads to several morphological changes: the cells that initially formed an ordered monolayer, lose the intercellular, integrin-based cytoskeletal attachments and, as a result they round up, disaggregate, and float in the media. These cells also have increased motility and invasiveness. After several weeks, when cells have lost their density inhibition, v-Src transformation leads to the formation of foci, or overgrown clumps of cells (51) **(Figure 6)**.

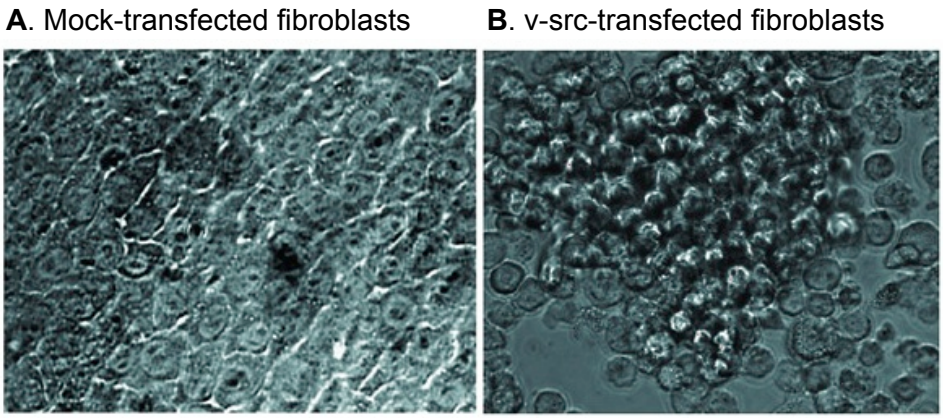

Adapted from Yeatman TJ, Nature 2004.

Figure 6. Photomicrographs showing the v-Src phenotype

Photomicrographs showing the transformed phenotype caused by v-Src transfection. **A.** Normal rat fibroblast culture stably transfected with a control vector. The cells are fusiform and show density inhibition. **B.** Transformed rat fibroblasts stably transfected with v-Src. Cells rounding up and detaching from the substratum eventually form visible foci.

Loss of contact inhibition is a hallmark of a cancer cell. In fact, v-Src transformed cells undergo processes that resemble metastatic cells when they disaggregate from the primary tumor, invade surrounding tissues, and travel to distant organs.

In normal cells, v-Src increases the proliferation rate, reducing doubling times and increasing nutrient requirements *in vitro*. When cells are transfected *in vivo*, they grow faster than normal cells and form tumors a few days after injection. The tumors can metastasize both locally and to distant sites (51).

3.4.1. Induced signaling in v-Src transformed cells

The transformational activity of v-Src is likely to be mediated by certain STAT proteins (Signal Transducers and Activators of Transcription). STAT3 promotes transcription of cell-cycle regulator D-type cyclins, cyclin E, $p21^{WAF1/CIP1}$ and Myc. Myc synthesis is a critical feature in v-Src transformed cells (52). STAT3 activation also stimulates VEGF (Vascular Endothelial Growth Factor) in v-Src transformed cells (53). Another STAT, STAT5, may also contribute and is associated with cell cycle progression, cell survival, and anchorage-independent growth (54).

3.4.2. v-Src and adhesion

3.4.2.1. Stress fiber disorganization

As cells encounter an ECM that induces adhesion, cells form stress fibers, which are complex structures that comprise cytoskeletal structures and other cytoplasmic components. The cytoskeletal structures are formed by actin, which assemble into actin filaments (previously called microfilaments) that generate the actin cytoskeleton. Actin filaments can assemble between two separated and stable adhesions into stress fibers that can generate high traction forces (55). Crosslinking proteins that bind two or more filaments together, and myosin II motors are the cytoplasmic components of stress fibers. The myosin motors move, sliding actin filaments past one another, allowing the fibers to contract.

The fibers must be anchored in order for contraction to generate forces. Stress fibers are linked to the exterior through focal adhesions, which are formed by the assembly of many proteins. The contraction of the fibers against these fixed external substrates allows the traction forces generated by the myosin motors to modulate the mechanical homeostasis of the cell by moving and reshaping it (56). This process responsible for stabilizing the cell structure and transducing mechanical information from the cell exterior that leads to the production of force that promotes changes in cell shape and ECM remodeling (57).

Cofilin is an actin-binding protein that disassembles actin filaments through two different mechanisms: severing filaments (58) and increasing off-rate for actin monomers from the pointed end (59). Cofilin activity is regulated by the RhoA-ROCK-LIM kinase pathway, and the loss of stress fibers is thought to be associated with disruption of this pathway (60). Src also plays a role in cofilin activity by indirectly mediating cofilin

dephosphorylation on Ser-3, which leads to cofilin activation and subsequently actin filament disassembly.

3.4.2.2. Focal adhesion disruption

3.4.2.2.1. v-Src-induced proteolysis of FAK

One of the key features of v-Src transformed cells is the disruption of focal adhesions. This event will be discussed in detail below. As a brief introduction, v-Src mediates phosphorylation of FAK and its proteolysis by the calpain-calpastatin proteolytic system. Calpain promotes FAK proteolysis and thus induces focal adhesion turnover. Calpastatin is calpain endogenous inhibitor. V-Src can both increase the synthesis of calpain 2 and the degradation of calpastatin, therefore promoting the turnover of focal adhesions (61) **(Figure 7)**.

3.4.2.2.2. v-Src effects on integrin function

Integrins are key components on the linkage between the ECM and the cytoskeleton. Tyrosine phosphorylation of integrins can reduce cell adhesion. V-Src can induce tyrosine phosphorylation of certain integrins, such as b1A integrin on sites Tyr -783 and Tyr-795 (62), or b3 integrin on sites Tyr-783 and Tyr-795 (63). Phosphorylation of integrins is normally transient and reversed by phosphatases but in v-Src transformed

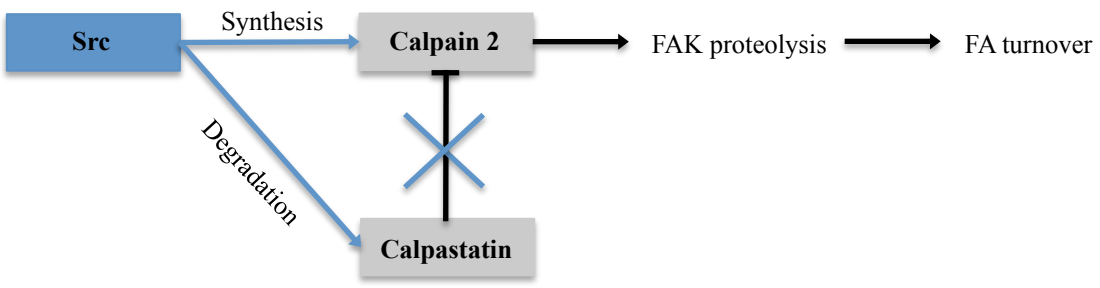

Figure 7. Schematics of the mechanism of v-Src –induced proteolysis of FAK

v-Src-induced proteolysis of FAK by the calpain-calpastatin proteolytic system. Src is thought to promote calpain synthesis as well as calpastatin degradation. Calpastatin is a calpain inhibitor so its degradation enhances the effect of Src on calpain. Calpain promotes FAK proteolysis and the consequent focal adhesion turnover.

cells, constitutively active Src might break this balance and promote focal adhesion disassembly.

Another way of regulating integrin function is by phosphorylation of the small GTPase R-Ras by v-Src (64), suppressing integrin activity and affecting cell-matrix adhesion.

3.4.2.3. Disruption of adherens junctions

Adherens junctions are cell-cell junctions that connect the actin cytoskeleton of two cells through protein complexes that contain, among other proteins, cadherins and catenins. Cadherins are transmembrane proteins that form homodimers in a calcium-dependent manner with other cadherin molecules on adjacent cells.

v-Src can induce cadherin degradation in different ways: hakai is a Src-binding protein which functions as an E3 ligase that ubiquitylates C-cadherin promoting its degradation (65). P120CTN is tyrosine phosphorylated by Src (66) and modulates E-cadherin (epithelial cadherin function), reducing cell-cell adhesion. Loss of E-cadherin complexes at cell-cell adhesions as well as enhancement of integrin-dependent cell-ECM contacts, are related to the induction of epithelial to mesenchymal transition (EMT), which is a key event in metastatic events.

3.4.2.4. Disruption of Gap junctions

Gap junctions are intercellular junctions that connect the cytoplasm of two cells,

allowing the free interchange of molecules and ions between cells (67,68). Gap junctions' channels are composed of two conexons (or hemichannels) which connect across the intercellular space (69). These hemichannels are primarily homo- or hetero-hexamers of conexins proteins. v-Src can phosphorylate connexin 43 on Tyr-247 and Tyr-265 leading to gap junction disruption (70).

3.4.2.5. v-Src and FAK induced expression of MMPs (matrix metalloproteinases)

Matrix metalloproteinases (MMPs) are zinc-dependent endopeptidases that degrade different types of ECM proteins as well as several bioactive molecules. They are known to have several functions including the cleavage of cell surface receptors, release of apoptotic ligands or chemokine/ cytokine activation (71). In addition, MMPs play important roles in cell proliferation, migration, differentiation, apoptosis and angiogenesis.

v-Src induces FAK signaling to JNK (c-Jun N-terminal kinase), promoting the downstream expression of MMP2 and MMP9 (72,73). In addition, v-Src induces phosphorylation and activation of FAK, which recruits DOCK180 (a Crk-binding adaptor) and p130Cas to lamellipodial focal contacts (74). DOCK180 induces Rac activation through Crk/p130Cas complexes. Elevated activities of Rac1 and JNK promote MMP expression, leading to matrix re-modeling and increased invasion (73).

3.5. c-Src

c-Src affects cell proliferation in fibroblasts. This event may be related to the fact that Src-family kinases are thought to play roles in mitosis, specifically in the progression from phase G2 to phase M during cell cycle (75). C-Src transfected cells experience decreased intercellular adhesion and increased invasion and motility, particularly in epithelial cells and in cancer cells in late stages of progression (76).

Among the Src family, c-Src is the member most often associated with cancer. Several cancer types have shown c-Src overexpression or an increase in its activity (77). Some examples are gastrointestinal-tract cancers such as colorectal cancer (78), hepatocellular, pancreatic, gastric and oesophageal (77), breast (79), ovarian (79,80), and lung cancers. C-Src is necessary for cell division in fibroblasts (75) and may also stimulate the proliferation of precancerous cells, playing a role in tumorigenesis (production of new tumors). However, it has also been shown that there is no correlation between Src activity and in vitro colon tumor cell proliferation rates or in vivo tumor growth rates. Instead, when c-Src is overexpressed in human colon cancer cells, it stimulates the assembly of integrin adhesions, which increase the ability of cells to spread on a substrate (81). In the same manner, the cooperation between c-Src and epidermal growth factor receptor (EGFR) is not associated with increased proliferation, but with enhanced invasiveness of cancer cells (82). A suggested explanation for these observations is that c-Src plays a role in cell proliferation during the initial process of tumorigenesis and enhances adhesion and invasiveness during later stages of tumor progression (76). It is important to note that the effects of c-Src are believed to be distinct in epithelial cells vs. fibroblasts.

3.5.1. Localization of c-Src in the cell

The subcellular localization of Src influenced by three regions within the N-terminus of Src. Amino acids 1-14 are responsible for Src myristoylation and attachment to cytoplasmic granules (83). Amino acids 38-111 promote the association to the plasma membrane and perinuclear membrane. Amino acids 204-259 facilitate the association with perinuclear membranes (84). C-Src localizes also at the membrane-cytoskeletal interface in focal adhesions, lamellipodia and filopodia as a result of the regulation mediated, in part, by the small G proteins RhoA, RAC1 and CDC42 (84,85). The recruitment of Src to focal adhesions by FAK will be described in the next section.

3.5.2. Regulation of Src activity in the cell

As described earlier, phosphorylation of Src's C-terminal Tyr-527 leads to its intramolecular interaction with the Src SH2 domain, locking Src's structure into its "inactive" form. Disruption of this intramolecular interaction by either removal of the phosphate group from Tyr-527 or by engagement of the SH2 and/or SH3 domains with other proteins can effect activation of Src.

3.5.2.1. Phosphorylation on C-terminal tyrosine (Tyr-527)

There are two known upstream tyrosine kinases responsible for Src C-tail phosphorylation. Csk (c-Src tyrosine kinase) and its homologue Chk (C-terminal Src

Kinase-homologous Kinase) (49). The reverse process (dephosphorylation) also occurs in the cell and is mediated by protein tyrosine phosphatases that remove the phosphate from Tyr-527, thereby activating Src (51). Several phosphatases have demonstrated to be able to promote this dephosphorylation, such as CD45 (86), PTP (protein tyrosine phosphatases)-a, PTP-g, PTP1B, SHP-1 (SH2-containing phosphatases 1) and SHP-2 (84,87,88).

3.5.2.2. Interaction with binding partners

A number of proteins can bind to Src in the cell. These interactions generally occur through Src's non-catalytic domains, particularly its SH2 and SH3 domains. As described in the previous section, FAK binds Src's SH2 domain and p130Cas binds to Src's SH3 domain (89,90). In this manner, FAK and p130Cas disrupt the inactive conformation and relieve Src autoinhibition. It is important to note that these interactions are also responsible for Src's colocalization with substrate proteins in specific sites of the cell. The local concentration of the substrate proteins is an important determinant of Src substrate specificity.

3.5.2.3. Receptor-mediated activation of Src

When certain receptor tyrosine kinases become activated through phosphorylation on one or more tyrosine residues in their cytoplasmic regions, Src's SH2 domain binds these phosphorylated tyrosines driving Src to its active conformation. Some of these

receptors are Epidermal Growth Factor Receptor (EGFR), Platelet-Derived Growth Factor Receptor (PDGFR), Human Epidermal growth factor Receptor 2 (Her2/Neu or ErbB2), Fibroblast Growth Factor Receptor (FGFR), colony-stimulating factor 1 and Hepatocyte Growth Factor Receptor (HGFR) (45,52,91-94)

3.5.3. c-Src in signaling pathways

3.5.3.1. Src-FAK complex

The relationship between c-Src and FAK deserves special attention. Focal adhesion kinase (FAK) was one of the first discovered Src substrates (95). FAK's association with Src is well studied and considered a key event in Src's role in cell signaling (96). FAK is a non-receptor tyrosine kinase involved in cell-cycle progression (cell proliferation), cell survival, and cell migration, as well as growth-factor- and integrin-mediated cellular motility, adhesion and invasion (72,97). FAK localizes to focal adhesions, which are cytoskeletal structures responsible for cell-extracellular matrix (ECM) connections. In particular, integrins in focal adhesions link the actin cytoskeleton with the ECM **(Figure 8)**.

FAK is phosphorylated after cellular contact with the ECM and can be activated by both growth factors and integrins (98). Integrin clustering, actin polymerization and actomyosin contractility facilitate FAK autophosphorylation and activation (73). FAK associates with integrins through its COOH-terminal domain. FAK recruits Src to focal adhesions through binding of c-Src's SH2 domain to FAK, forming a transient signaling

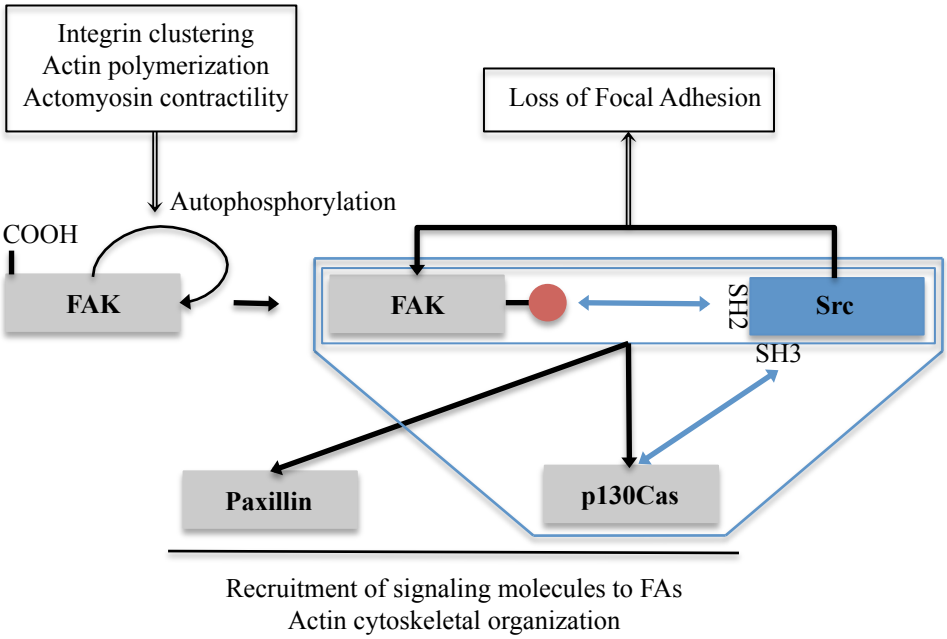

Figure 8. Schematics of the interactions of Src, FAK, p130Cas and paxillin in focal adhesions

Integrin clustering, actin polymerization and actomyosin contractility facilitate FAK autophosphorylation and activation. Phosphorylated FAK binds Src in a transient complex and thus recruits it to focal adhesions. C-Src stimulates tyrosine phosphorylation and activation of FAK. As a result, Src promotes turnover of focal adhesions. Src's SH3 domain binds p130Cas. Src, FAK, and p130Cas form a trimeric complex, where the FAK-Src complex phosphorylates p130Cas and paxillin, creating heavily phosphorylated sites that serve as a recruitment dock for other molecules involved in signaling and actin cytoskeletal organization. FA: Focal adhesion.

complex with c-Src (99,100). This recruitment of Src to FAK promotes turnover of these junctions, contributing to cell motility. C-Src stimulates tyrosine phosphorylation and activation of FAK, which results in the loss of focal adhesions (100,101). Src also binds p130Cas through its SH3 domain. Src, FAK, and p130Cas form a trimeric complex that is stabilized through mutual interactions among the three proteins (99). The FAK-Src complex phosphorylates p130Cas and paxillin, creating heavily phosphorylated sites of recruitment for other molecules and therefore facilitating actin cytoskeletal organization (102).

Quantitative assays to determine levels of kinase and adaptor molecules in focal adhesions have demonstrated that the FAK- c-Src complex, p130Cas, paxillin, extracellular signal-regulated kinase p42 (Erk) and myosin light-chain kinase (MLCK) are crucial for adhesion turnover at the cell front (101). Erk is a target of Src-FAK signaling (96) and it is also the upstream kinase of calpain. Activated calpain can induce proteolysis of FAK and promote the breakdown of focal adhesions (61).

3.5.3.2. Src targets in adhesion, motility and invasion

There are two main cytoskeletal structures that regulate adhesion, motility and invasion: focal adhesions and adherens junctions (51). Src is thought to enhance cellular motility by both disrupting adherens junctions and promoting focal adhesion turnover.

Focal adhesions are the cytoskeletal structures responsible for cell-matrix attachments, and also play an essential role in regulating proliferation and gene transcription (96). As cells move along the extracellular matrix, focal adhesions are

disassembled and Src is believed to play a major role in disruption of focal adhesions and stress fibers (103). The current understanding of this connection is Src induced tyrosine phosphorylation of FAK and the subsequent degradation of FAK by the calpain-calpastatin proteolytic system (61).

In the context of adherens junctions, Src is also thought to play a role in the disruption of adherens junctions. Src's contribution seems to be associated with its ability to phosphorylate E-cadherin, leading to E-cadherin's ubiquitylation and subsequent displacement (65). An additional role of Src in adhesion is its ability to regulate metalloproteinases (MMPs) and tissue inhibitors of matrix metalloproteases (104), thus affecting their role in tissue remodeling.

3.5.3.3. Src and the Ras/ MAPK pathway

In the classical MAPK pathway, RTKs are activated and Shc and SHP-2 recruited and phosphorylated by RTKs. The phosphorylation sites on Shc and/or SHP-2 recruit the complex formed between the adaptor Grb2 and its associated molecule Sos, a guanine exchange factor (GEF) for Ras. The Grb2/Sos complex can also be recruited to the membrane through phosphorylation sites in the C-terminal cytoplasmic region of the RTKs (105). Once Sos has been translocated to the membrane, it induces the GTP/GDP exchange and converts Ras to an active form (106). The GTP bound Ras has an enhanced ability to interact with its effectors, Raf, Ral-GEFs and PI3K (phosphatidylinositol 3-kinase), and activate them for downstream signaling (107). Raf is part of the well-established Raf/MEK/ERK pathway, which is known to be activated by Ras (108).

Activated Raf first leads to the stimulation of the dual-specificity kinases MEK1 and MEK2, also known as MAPKK or MAP2K 1 and 2 (mitogen-activated protein kinase kinases). MEK 1 and 2 phosphorylate the MAPK/Erk (mitogen-activated protein kinase/ extracellular signal-regulated kinases) proteins Erk1 (p44) and Erk2 (p42). This Ser/ Thr protein kinase cascade provides opportunities for feedback regulation and signal amplification.

When Src is activated by RTK, it can phosphorylate FAK and recruit it. Tyr-925 is one of the residues in FAK that becomes phosphorylated upon Src activation and it constitutes a binding site for Grb2 (99). The activated Src/FAK complex stimulates Shc tyrosine phosphorylation (99,109). Another possible role for Src in this pathway is that Src is thought to phosphorylate Raf1 in its N-terminal domain that is responsible for Raf1 autoinhibition, therefore inducing Raf1 activation (110-113). The Ras/Raf/MEK/Erk pathway regulates transcription, metabolism and cytoskeletal reorganization with downstream effects associated with cell growth, anti-apoptosis and cell differentiation (114).

3.5.3.4. Induction of DNA synthesis

Several RTK activating growth factors such as EGF, PDGF, and CSF-1 require Src activity to induce DNA synthesis (115). As an example, PDGF-b mediated induction of myc transcription requires Src activity and can be block by a Src selective inhibitor (116). Several signaling molecules are known to be involved in Src-mediated DNA synthesis, such as Shc (117) or PI3K (118).

3.5.3.5. Degradation of Src

c-Src can be ubiquitylated (74) and Cbk ubiquitin ligase (especially the Cbl-c E3 ligase) appears to be responsible for Src ubiquitylation (119). Activated Src seems to be a better substrate for ubiquitylation than the tail-phosphorylated form. Upon ubiquitylation, Src can be degraded by the proteasome as a mechanism for attenuating Src signaling cascades.

4. Methods for identification of tyrosine kinase substrates

Signaling pathways are extremely complex and dynamic. Signaling pathways are not independent units. Instead they are intricately interwoven. Different kinds of mechanisms alter signal flow, including feedback loops and amplifications mechanisms. An initial way to approach the dissection of such a daunting matrix of potential interactions is to determine the *in vivo* interactions/ substrates of a protein of interest. In the case of protein tyrosine kinases, this is particularly challenging given several reasons, among which are the apparent lack of a constant consensus sequence around the Tyr (as opposed to many Ser/Thr kinases), and the fact that many in vitro techniques are not applicable in vivo. We will next summarize some of the employed techniques that have been used towards the goal of tyrosine kinase substrate identification.

4.1 Classical methods

4.1.1. Genetic methods

One broadly used method to identify substrates of tyrosine kinases is to perform genetic screens followed by subsequent analysis of genetic interactions. One disadvantage of such experiments is that it is difficult to infer any direct biochemical linkage. One example is the epistasis analysis perform in Drosophila melanogaster, where Daughter of Sevenless (Dos) was located downstream of the RTK Sevenless (120).

4.1.2 Biochemical Fractionation

When the phosphorylation site is known and the upstream kinase is searched, it is possible to screen different fractions of the cell lysate using radioactive assays or with antiphosphotyrosine antibody blots in order to determine the upstream kinase. As an example, Src's substrate p130Cas was identified in this manner (121).

4.1.3. In vitro identification of kinase substrate

4.1.3.1. Solid phase phosphorylation screening of phage expression libraries

Phage display is used for high-throughput screening of protein interactions. DNA from a cDNA library encoding the proteins or peptides of interest is ligated to genes that encode a coat protein. As a result, a whole library of protein or peptide sequences can be inserted into surface exposed coat proteins in a bacteriophage.

In the case of a phosphorylation screening, the immobilized bacteriophage can be phosphorylated by g-^{32}P-ATP. The phage particles are screened and those that are efficient substrates can be isolated and enriched to produce more phage (by bacterial infection with helper phage). After infecting suitable bacteria, from which the plasmids can be collected, the DNA can be sequenced and identified. As an example, PI3 Kinase p85 was identified as an EGFR downstream substrate using this approach (122).

4.1.3.2. Oriented peptide library screen of optimal substrate motifs

In peptide library screening, a synthetic peptide library is exposed to a tyrosine kinase and the phosphorylated peptides are selected by affinity chromatography. The selected pool can be sequenced by Edman degradation. From the pool of selected peptides, the sequence surrounding the phosphorylated Tyr can be analyzed and consensus sequences identified (11).

4.1.4. *In vivo* identification of kinase substrates

4.1.4.1. Two- dimensional gels

In this methodology, the kinase of study is either activated (i.e.: by overexpression in the cell, stimulation of upstream receptors) or inactivated (i.e.: by specific kinase inhibitors, injection of antibodies, knockouts, RNA interference). The [g-P^{32}] ATP labeled cell lysate is run in a two-dimensional gel by electrophoresis that

provides resolution based on isoelectric point and protein mass. It is unlikely that two proteins will share these identical properties and as a result, this method allows for favorable separation of proteins in the lysate that can be then identified by in gel-trypsinization and mass spectrometry.

4.1.4.2. Protein chips

This novel technology can be used to screen for potential kinase substrates in a high-throughput fashion. The technology was designed for high-through analysis of protein kinase activity over the kinome (123). As an example, Rim11p was identified as a novel tyrosine kinase that could use poly (Glu, Tyr) as substrate in radioactive assays. In vivo validation of its kinase activity on the substrate, Ime1p, was performed.

4.1.4.3. Kinase-substrate crosslinking

In this approach, an ATP analog, with an UV activable crosslinking group azide in both the purine moiety and g-phosphate is applied *in vivo*. The adenine moiety of ATP usually bounds to the kinase active site during phosphorylation and the g-phosphate is usually close to the substrate protein. When using the described ATP analoge, the UV activatable crosslinking generates a ternary complex that can help the identification of the kinase substrate and can then be cleaved by phosphodiesterase. As an example, this approach has been used with Csk, which can be crosslinked to Src by the described ATP analog (124).

4.1.4.4. ATP analog and mutant kinase pair

This methodology combines a kinase mutant with altered ATP binding proteins with an unnatural ATP analog (125). The use of a radioactive [g-P^{32}] ATP analog allows for direct labeling of substrates in cell extracts, but not in the living cell, since ATP analogs are highly negatively charged and are therefore not cell permeable. However, it has received much interest and identified many kinase-substrate interactions for Src, Cdks, and other kinases.

4.1.4.5. Phospho-motif specific antibodies

Based on the consensus sequences obtained using previously descried methods, novel site-specific phosphorylation site antibodies have been generated. These antibodies have been particularly helpful in validating potential novel substrates for specific kinases (126). Given the fact that consensus sequences seem to be more conserved in Ser/Thr kinases, only Ser/Thr kinases substrates have so far been achieved using this approach.

4.1.4.6. Chemical Rescue

One of the critical steps in kinase substrate identification is the method employed for activation/ inhibition of the kinase. Specific modulation of a kinase *in vivo* is particularly challenging. Many of the commonly used methods to activate kinases or

inhibit enzymes are non-specific (i.e. stimulation of upstream receptors, many kinase inhibitors) or achieve their goal a few hours or even days (i.e. overexpression of the kinase in the cell, injection of antibodies, knockouts, RNA interference). In this context, chemical rescue has been of particular use. In this approach, the activity of an inactive mutant protein can be restored by chemical complementation by a small molecule with similar electronic or steric features than the side chain of the mutated amino acid. The activation of the kinase is therefore highly specific and the activation can be observed within minutes upon chemical rescue, providing a specific, rapid, and reversible method for kinase activation. Combining chemical rescue with other methodologies to identify changes in the phosphorylation pattern in the cell upon chemical complementation of the kinase can in principle provide many novel proteins/ residues being phosphorylated upon kinase activation. Chemical rescue will be thoroughly reviewed in the next section.

5. Chemical Rescue

5.1. Introduction of chemical rescue

In an effort to approach the study of protein structure and function, early efforts were focused on using group modifying agents to modulate the activity of macromolecules, like enzymes or proteins. Site-directed mutagenesis methodology followed (127). Both approaches were later combined in chemical complementation (128).

One of the first applications of chemical complementation was the study of serine proteases, endopeptidases in which serine acts as the nucleophilic amino acid at the active site (129). A common feature of most Ser proteases is a Ser-His-Asp catalytic triad (Asp-102, His-57, Ser-195) (130). As mentioned before, Ser-195 is the nucleophile and His-57 acts like the general base (and later, general acid). Asp-102 has a very low pKa of 2, and it is therefore mostly ionized. In that way, it helps stabilize the protonated imidazole ring of His-57 with its negative charge.

Subtilisin is a non-specific serine endopeptidase initially obtained from Bacillus subtilis, a Gram positive bacterium commonly found in soil. While performing site mutagenesis studies, it was found that the catalytic activity of H64A mutant subtisilin could be restored by a substrate that contains the lost histidine at the P2 position (131) as compared with the substrate that contains alanine at the P2 position (factor of 170). For the rescue, the imidazole ring of the His at P2 can almost superimpose on the catalytic His64 in subtilisin, mimicking the function of the catalytic histidine in the wild-type enzyme. In this manner, the activity of the mutant enzyme was restored.

Several studies followed, which not only optimized chemical rescue of different enzymes, but also revealed functionalities of different residues within the catalytic region of the enzymes allowing physicochemical analysis of the catalytic impact of a specified amino acid residue in the enzyme. As an example, site-directed mutagenesis studies of trypsin (132), revealed the important facilitating function of Asp-102 in the triad of serine protease.

Chemical rescue was further developed through the study of aspartate aminotransferase (AATase). AATase is a pyridoxal phosphate (PLP)-dependent

transaminase enzyme that catalyzes the reversible transfer of an α-amino group, facilitating the interconversion of the dicarboxylic amino and ketoacids. The inactive K258A AATase mutant contained a cavity in the catalytic site where several amines with different pK_a values could fit, replacing the lost residue and partially rescue the activity of the AATase (133).

Chemical rescue has been extended to a number of enzymes to establish structure-activity relationships as well as to identify important catalytic residues. Depending on which amino acid is mutated, different small molecules are used for complementation. For example, amines are commonly used for lysine mutations, guanidines for arginine mutations, azide, formate, or fluoride for Glu or Asp mutations, imidazole for histidine mutations, and indole for enzymes with tryptophan mutations.

5.2. Chemical rescue and signaling

Chemical rescue is one of the most efficient ways of manipulating enzyme activity with the use of small molecules or structurally altered substrates (131-133) that functionally substitute for the missing side chain.

The initial applications of chemical rescue were focused on the analysis of enzyme mechanisms and molecular recognition *in vitro*. However, one of the most advantageous aspects of chemical rescue is the fact that it facilitates the challenging spatio-temporal dissection and analysis of complex cellular pathways in the cell. One of the challenges to an *in vivo* application to chemical rescue is that the small molecules used as rescue agents need to be cell-permeable and non-toxic at the relevant

concentrations (sometimes up to molar quantities might be required). If these challenges are met, *in vivo* chemical rescue represents an enzyme activation methodology that is specific (only activates the mutated enzyme), rapid (activation can be less than a minute depending on the enzyme) and reversible (the enzyme can be deactivated by small molecule removal).

Chemical rescue of an enzyme with an altered substrate has been applied to the study of specific G-proteins in cells. EF-Tu is a GTP regulatory protein. The fact that mutant D138N EF-Tu cannot bind GDP efficiently but instead can bind xanthosine 5'-diphosphate efficiently, reveals that Asp138 probably interacts with C-2 of the purine ring. This approach has been used to study other GTPases involved in nuclear protein import.

5.3. Chemical rescue of Src

Previous work in our laboratory used a chemical rescue strategy to learn more about the role of v-Src in the cell (134). The catalytic Arg-388 in all Src's family members is located two residues upstream as compared with its position in other tyrosine kinases **(Figure 9)**.

Src kinase was subjected to site-directed mutagenesis and rendered catalytically inactive. In particular, a set of Src Arg388 mutant recombinant proteins were generated and their potential for chemical rescue was examined. The maximal turnover rate (k_{cat}) of the mutant R388A Src was 0.5% of the k_{cat} of wild-type Src. The k_{cat} after imidazole

SRC ^{382}YVHRDLRAANILV^{394}

CSK FVHRDLAARNVLV

IRK FVHRDLAARNCMV

Adapted from Qiao Y *et al*., *Science* 2006

Figure 9. Position of the catalytc Arg-388 of Src- family kinases as compared to other tyrosine kinases

Selected sequences within the catalytic domain of selected tyrosine kinases. Numbers above sequences correspond to the equivalent residue position in Src.

treatment increased to 30-50% of the k_{cat} of wild-type Src. In summary, Src's activity could be restored by the addition of the cell permeable small molecule imidazole.The Michaelis-Menten constant (K_m) for imidazole was approximately 2.5 mM, which is far below its toxic level. By specifically jump-starting v-Src kinase activity, the immediate contributions of v-Src to different signaling pathways could be identified.

Encouraged by these positive results, the potential of chemical rescue of Src was assessed in living cells. For this purpose, an additional mutation, Y527F was incorporated in order to prevent down-regulation by Csk phosphorylation. In this manner, SYF MEFs were stably transfected with R388A/Tyr-527→Phe (Y527) Src to generate 8A7F cells. A control cell line was generated by stably transfecting SYF MEFs with Src Asp386→Asn (D386N)/ Y527F (6N7F). This Src mutant is catalytically inactive and insensitive to imidazole. In this thesis, when describing the research conducted on c-Src rescue, we will refer to the mutation R388A as R390A, and the mutation D386N as D388N, just as a result of different nomenclature but the site of mutation is the exact same.

8A7F cells were treated with 5 mM imidazole for 0 to 10 minutes and the changes in overall tyrosine phosphorylation level were analyzed by Western blot using the anti-phosphotyrosine antibody 4G10. Some new bands appear and others intensified at 2.5 minutes and plateau by 10 minutes. However, when the same treatment was applied to 6N7F cells no changes were observed **(Figure 10)**.

Chemical rescue conditions were analyzed in greater detail by observing autophosphorylation on its activation-loop tyrosine, Tyr-416, with a site-specific antibody **(Figure 11).** A marked increase in the phosphorylation level was detected after

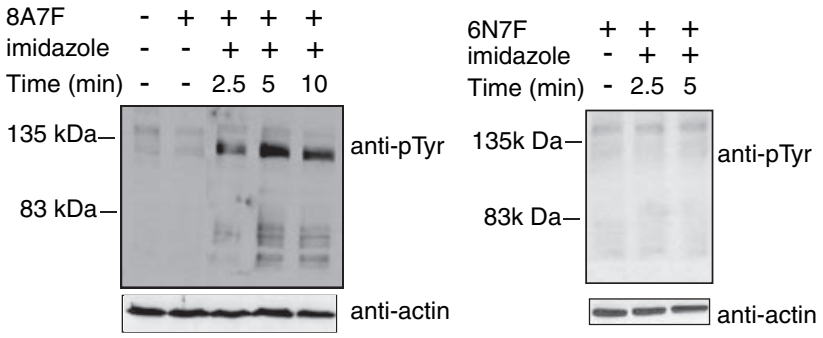

Qiao Y *et al*., *Science* 2006

Figure 10. Time course of tyrosine phosphorylation induced by imidazole treatment of Src R388A/Y527F in SYF cells (8A7F) and Src D386N/Y527F in SYF cells (6N7F cells)

Time course of tyrosine phosphorylation levels induced by 5 mM imidazole treatment of R388A/Y527F in SYF cells (8A7F cells) and D386N/Y527F in in SYF cells (6N7F cells). The lysates were analyzed by Western blot using a 4G10 anti p-tyr antibody and the loading control was performed using an anti-actin antibody.

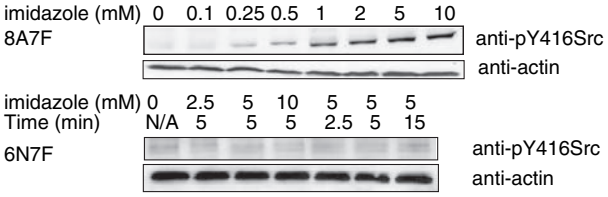

Qiao Y *et al*., *Science* 2006

Figure 11. Src autophosphorylation (Y416) induced by imidazole treatment of Src R388A/Y527F in SYF cells (8A7F) and Src D386N/Y527F in SYF cells (6N7F cells)

Src autophosphorylation (Y416) in R388A/Y527F in SYF cells (8A7F cells) as a function of imidazole concentration after 5 min treatment (top two panels). Src autophosphorylation (Tyr-416) in D386N/Y527F in in SYF cells (6N7F cells) at the indicated concentrations and during the indicated treatment times (top two panels). The lysates were analyzed by Western blot using a phosphospecific antibody against Tyr-416 in Src and the loading control was performed using an anti-actin antibody.

only 5 minutes. As expected from the previous results, control 6N7F were unresponsive to imidazole treatment.

The reversibility of chemical rescue was then analyzed by performing washout experiments that showed that phosphorylation of the activation-loop tyrosine was back to background only 4 minutes after imidazole removal **(Figure 12)**. This result is also an indication of the rapid cellular kinetics of tyrosine phosphatase activity towards Src's tyrosine autophosphorylation site.

The study included functional studies of v-Src's chemical rescue as well as a proteomic study to identify novel v-Src substrates, the relevance of some of which was further explored. This work suggested that this strategy may be applicable to c-Src, the cellular form of c-Src, which is more relevant to human disease, as well to other disease-related enzymes in humans.

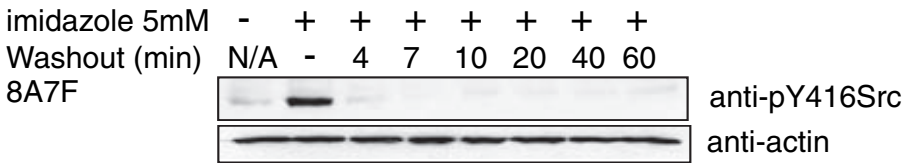

Qiao Y *et al*., *Science* 2006

Figure 12. Reversible Src autophosphorylation (Y416) in R388A/Y527F in SYF cells (8A7F cells) after imidazole washout

Reversible Src autophosphorylation (Y416) in R388A/Y527F in SYF cells (8A7F cells) after treatment with 5 mM imidazole for 5 minutes. Imidazole was removed by replacing the imidazole-containing media for imidazole-free media. Lysates were analyzed 4 to 60 min later using a phosphospecific antibody against Tyr-416 in Src and the loading control was performed using an anti-actin antibody.

CHAPTER 2. IDENTIFICATION AND CHARACTERIZATION OF NOVEL SUBSTRATES OF SRC USING PROTEOMICS

1. Introduction

Proteomics is the large-scale study of proteins, including their structures and functions (135,136). The term "proteomics" was conceived as a blend of "protein" and "genome", to make an analogy with genomics (137). The proteome is the entire set of proteins expressed by a genome, including the modifications made to a particular set of proteins, produced by an organism or system in a given time under defined conditions (138).

Proteomics is more complex than genomics due to the fact that an organism's genome is relatively constant, whereas the proteome is more variable since distinct genes are expressed in particular cell types and specific stages of the cell cycle. In addition, the proteome is larger than the genome, especially in eukaryotes; there are more proteins than genes due to alternative splicing and post-translational modifications (PTMs). Alternative splicing has been estimated to expand the number of distinct mRNA sequences corresponding to the number of open reading frames (ORFs) by approximately three-fold (139). Even though the number of post-translational modifications is unknown, an average redundancy of four- to ten- fold has been estimated by considering combinatorial occupancies. As a result, it is reasonable that greater than one million different protein forms are present in human tissues (140). Moreover, there are at least two more levels of complexity in the proteome, as compared with the genome. The genome is encoded by

the sequence of nucleotides but the diversity of the proteome does not appear to correspond to a code. Moreover, proteins possess complex three-dimensional structures and engage in a plethora of subtle macromolecular interactions relative to the more monotonous conformations of DNA.

In the past, the study of the proteome was primarily grounded in mRNA analysis. However, it has been found that this approach has limitations, since the analyzed specific mRNA level does not correlate tightly with protein abundance (141,142). Modern proteomics assays directly detect the presence and measure the quantity of individual proteins.

In comparison to oligonucleotide and nucleic acid analytes, protein and peptide analytes show a broad array of solubility and chromatographic behavior, in addition to chemical complexity partly resulting from PTMs. Protein-protein interactions represent a key mechanism in signaling, but they are not accessible by conventional expression profiling. As a result, differential profiling experiments require a combination of different strategies for the identification of proteins, the quantification of the relative expression and the assessment of covalent and noncovalent interactions (140).

1.1. Proteomics Methods

An early and still employed method for proteomics analysis involves the separation of proteins by two-dimensional gel electrophoresis (2DE). In the first dimension, the proteins are separated by isoelectric focusing (separation of different molecules by their ionic charge). In the second dimension, proteins are separated by

molecular weight using SDS-PAGE. This methodology reveals levels of protein expression and PTMs using protein staining intensities and electrophoretic mobility.

Mass spectrometry has greatly expanded insights into proteomics. A protein that is cleaved by proteases into short peptides can be identified by matching the observed peptide masses, which can be obtained by peptide mass fingerprinting, against a sequence database. Tandem mass spectrometry provides sequence information from individual peptides by isolating them, colliding them with a non-reactive gas, and labeling the fragment ions produced. One of the most promising proteomics mass spectrometry approaches is multidimensional liquid chromatography coupled with tandem mass spectrometry (MudPIT, multidimensional LC-MS/MS) or 'bottom up' shotgun proteomics **(Figure 13)**. In this strategy, a complex mixture of proteins is subjected to solution proteolysis. The resulting mixture of peptides is separated by multidimensional chromatography and analyzed by LC-MS/MS (143). An alternative methodology to analyze protein mixtures involves first separating the protein by SDS-PAGE followed by in-gel digestion (144). Current mass spectrometric software facilitates peptide sequencing through data dependent acquisition, by which ions are automatically selected and fragmented by MS/MS. As a result thousand of spectra can be collected from a single reversed phase run (145,146).

The coverage of identified proteins by shotgun proteomics as compared to 2DE is much higher. The number of distinct ORFs detected in yeast, bacteria, and mouse by 2DE ranges from 1.5-5.1% of ORFs (147-149), whereas shotgun proteomics has led to the identification of 25% of ORFs from Saccharomyces cerevisiae, 61% of ORFs from

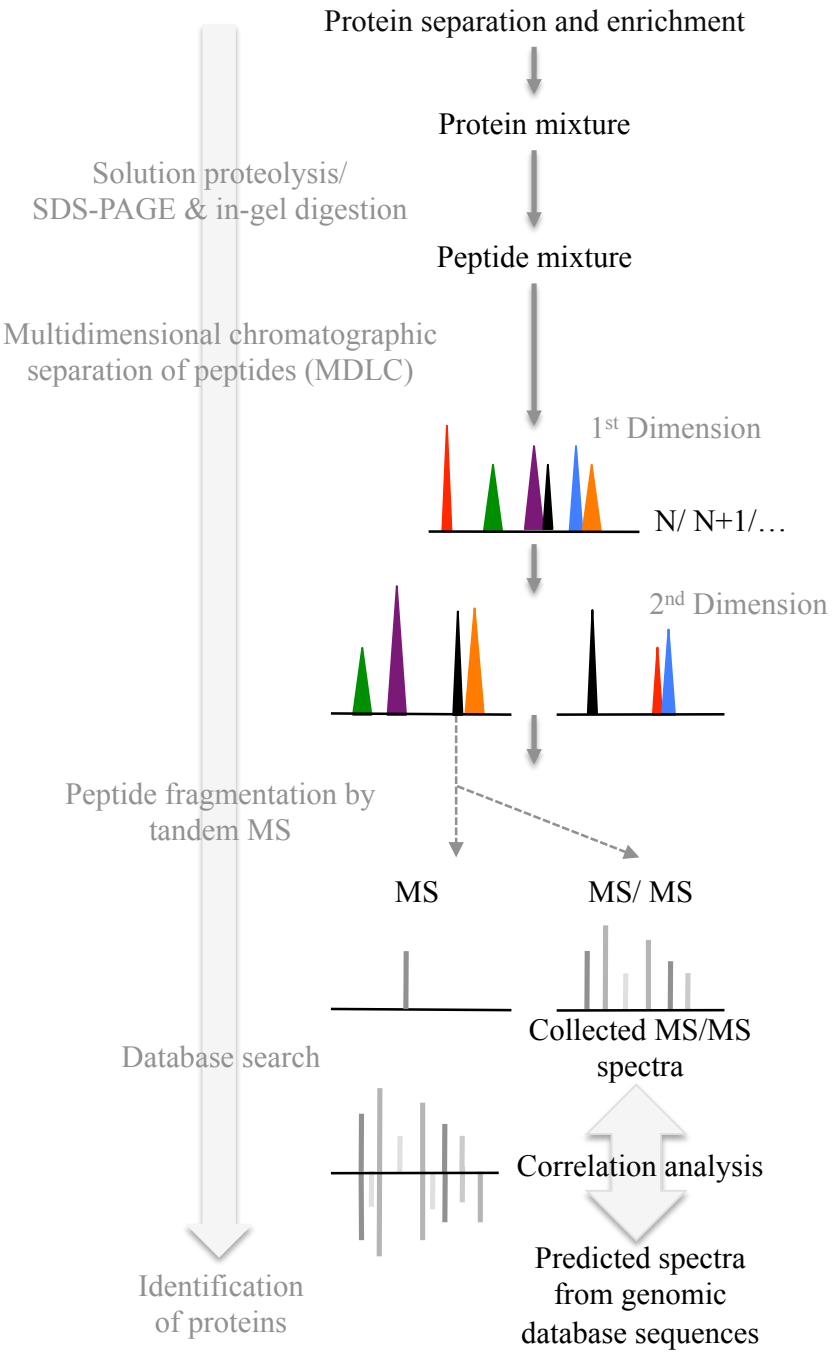

Figure 13. Schematics of MudPIT (multidimensional LC-MS/MS) or 'bottom up' shotgun proteomics

Schematics of the flowtrough of MudPIT, multidimensional LC-MS/MS or 'bottom up' shotgun proteomics. A complex mixture of proteins is subjected to proteolysis and the

resulting mixture of peptides is separated by multidimensional chromatography and analyzed by LC-MS/MS.

Deinococcus radiodurans, 46% of ORFs from Plasmodium falciparum and 15% of ORFs from human erythroleukemia cells (150-153). Moreover, shotgun proteomics detects hydrophobic proteins more efficiently, leading to a more successful detection of proteins from intracellular organelles (154,155).

Quantifying peptide and protein abundances is a critical aspect of shotgun proteomics. A key difficulty is the fact that a peptide that ionizes inefficiently can show unreliable intensity when it coelutes with different peptides within a mixture showing charge competition (ion suppression). Such uneven ionization can be addressed by labeling peptides with differential isotopes or mass tags **(Figure 14)**. After mixing and proteolyzing the lysates from both samples, the relative abundances of distinct peptides can be detected by comparing the intensities of their isotopically separable masses corresponding to the two (or more) different samples (156,157).

Quantitation measured from MS peak intensities based on stable isotopes has been shown to be feasible. Peak intensities of peptide ions show good correlation with relative protein abundance as demonstrated with statistical modeling of peak intensities (158,159). In the ICAT methodology (isotope-coded affinity tag), labeling is performed by covalently coupling the samples (typically through Cys or Lys residues) to isotopically labeled reactants (e.g. ^{12}C vs. ^{13}C). In the SILAC methodology (stable isotope labeling with amino acids in cell culture) lysates are metabolically labeled within normal cell growth in media containing isotopically distinguishable amino acids.

1.2. Applying proteomics to signaling networks: detection of phosphorylation

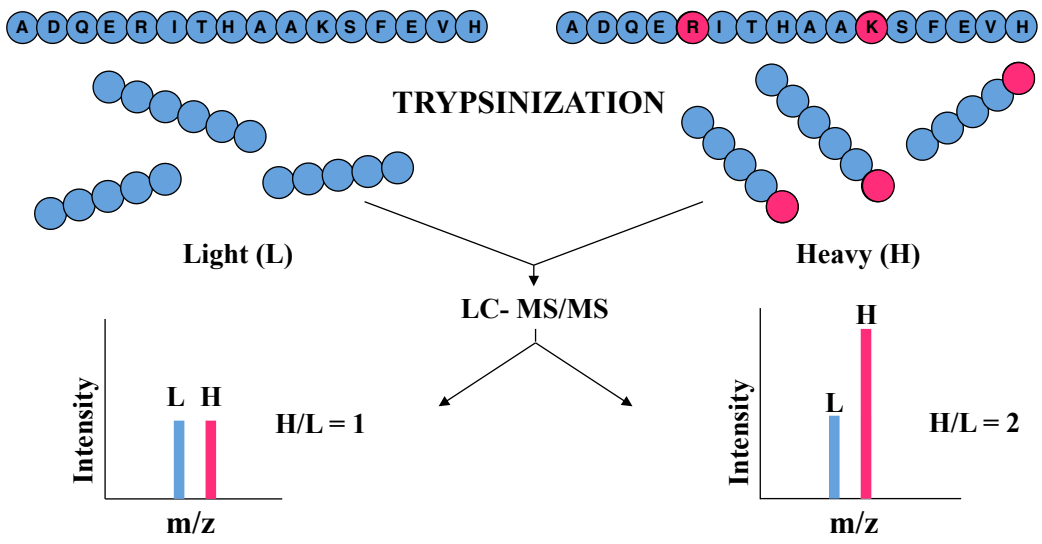

Figure 14. Peptide labeling with isotopically labeled amino acids

Isotopical labeling of amino acids allows distinguishing and comparing the intensities of the isotopically separable masses corresponding to two (or more) different samples.

Shotgun proteomics combined with peptide quantitation by isotope labeling has been very helpful to unveil changes in the proteome as a result of signaling and cell regulation. PTMs are difficult to detect in complex mixtures due in part to the fact that they are only present at low stoichiometry. Therefore, enrichment of modified proteins or peptides through affinity-based purification is an important strategy before LC-MS/MS.

1.2.1. Phosphospecific antibodies

Phosphospecific antibodies produced to detect and enrich tyrosine phosphorylated proteins and peptides have been especially helpful. However, antibodies for phosphorylated serine or threonine have been more difficult to generate, though certain antibodies that are specific for oligopeptides containing pSer/pThr have been successfully applied to immunoaffinity purification (160).

1.2.2. IMAC

IMAC (immobilized metal affinity chromatography) can be used to enrich for phosphopeptides. The mixture of proteins is run through a resin chelated with trivalent metals ions (i.e. Fe (III) or Ga (III)) that will adsorb phosphopeptides and phosphoproteins through ion pair interactions (161) **(Figure 15).**

A limitation of this methodology is that the phosphorylated residues compete with acidic or other metal ligand residues for binding to the resin. This results in low binding

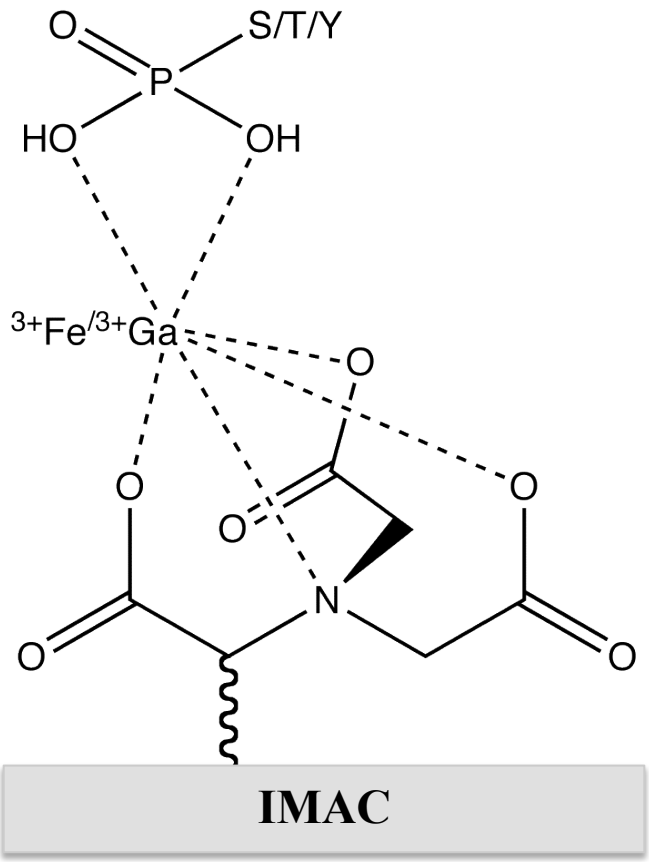

Figure 15. Schematics of IMAC (immobilized metal affinity chromatography)

capacity and high false-positive frequency. Enhanced methods to increase selectivity of phosphopeptide binding are needed.

There are other methods to enrich for phosphopeptides that involve covalent modification (162-164). These strategies usually involve multiple steps of chemical derivatization and purification, which create reproducibility and recovery challenges.

There is not a single method to analyze an entire proteome and its PTMs comprehensively. However, the methodology employed for the enrichment of modified peptides prior to LC-MS/MS analysis is helpful for improving breadth of protein sites identified. Still abundantly expressed proteins are easier to detect than scarce proteins. In fact, a comparison of the number of yeast ORFs that are quantifiable by Western blot analysis (and confirmed by microarray estimates) with the ORFs detected by mass spectrometry indicate that proteins represented in profiling studies are the mostly highly expressed proteins (165).

1.2. Src proteomics

Several biochemical and cellular strategies have been followed to identify direct and indirect tyrosine phosphorylated substrates of Src. Some of them involve immunoprecipitation of significant Src complexes (166), cDNA library screening (167), as well as *in vitro* determination of optimal peptide phosphorylation sequences (168).

1.3.1. v-Src proteomics

Some of the cellular substrate identification studies have used the hyperactive, dysregulated form of Src, v-Src, which lacks normal downregulation by C-terminal phosphorylation on Tyr-527. V-Src's direct substrates and mechanisms of cell transformation are still not fully understood (95). A chemical genetic screen for direct v-Src substrates used a tagging method for specifically radiolabeling the direct cellular substrates of the oncoprotein v-Src (169). This strategy consisted of using a v-Src mutant capable of accepting a non-natural phosphate donor substrate (ATP= N6 (benzyl)ATP) that is weakly used by wild-type kinases *in vivo* (125,170,171). In this way, the direct substrates of v-Src could be detected in cell lysates more cleanly. A global analysis using this technique in combination with 2DE and mass spectrometry led to the identification of 20 proteins that were phosphorylated by the v-Src mutant. After a focused screen with protein preparations enriched for potential direct substrates of v-Src (by isolating v-Src immune complexes), a restricted set of candidate direct v-Src substrates was revealed. Dok-1 was one of the identified proteins and the role of its direct phosphorylation by v-Src was further studied. A disadvantage of this method is that it uses cell lysate as the pool of potential v-Src substrates. The cell lysate may not be representative for the phosphorylation events that occur in the living cell.

A study from the Cole laboratory approached the search of v-Src substrates using the described strategy of chemical rescue that overcomes the limitation of having to use whole cell lysates as a starting material and allowed us to observe the effects of direct v-Src activation in living cells (134). Chemical rescue of v-Src led to the rapid and specific activation of mutated v-Src. Tyrosine phosphorylation in the cell was detected by enriching the combined lysates from the control and treatment cell populations with

antiphosphotyrosine antibody and analyzing them by LC-MS/MS. Quantitation of the global changes in tyrosine phosphorylation upon v-Src activation was performed through two different methodologies. In the first one, immunoprecipitated proteins were separated on an SDS-PAGE gel and detected with silver staining. Bands that showed an apparent enrichment were identified by LC-MS/MS. The second strategy relied on metabolically labeling the control and treatment cell populations with different isotopically labeled amino acids. The combined results led to the identification of 24 proteins, 18 of which were unknown substrates at the time. The results were further validated by immunoprecipitation and Western blot and further studies were performed to explore the relevance of the phosphorylation by v-Src on some of the identified substrates.

1.3.2. Proteomics using constitutively active c-Src mutants

Several studies have used constitutively active Src mutants. In one of the studies, 293T cells were transiently transfected with either an inactive form of c-Src (K298M) as a control or a constitutively active form of Src (Y527F) (172). Cells from both populations were labeled following the described SILAC methodology. Cells transfected with the constitutively active form of c-Src were harvested 12 or 24 hours after transfection. A more significant increase in phosphorylation was detected after 24 hours so this condition was selected. Lysates from the cells transfected with the inactive form of c-Src and the constitutively active form of c-Src were combined, enriched by immunoaffinity purification with an anti-phosphotyrosine antibody and analyzed by LC-MS/MS. The study identified 10 known substrates and interactors of c-Src and Src family

kinases as well as 26 novel substrates. Four of the novel substrates were validated by *in vitro* kinase assays and cotransfection experiments. The study also used a c-Src specific inhibitor to demonstrate that three of the novel substrates contribute to PDGF signaling.

In a different study, p130Cas -/- mouse embryonic fibroblasts (MEFs) were either transformed with oncogenic Src-F529 or transfected with the empty retroviral vector (173). p130Cas expression was reconstituted by a separate retroviral vector. Phosphotyrosine peptides were enriched with an anti-phosphotyrosine antibody and analyzed by LC-MS/MS. A total of 867 peptides (563 distinct pTyr sites on 374 different proteins) were identified from the Src-transformed cells, while 514 peptides (275 pTyr sites on 167 proteins) were identified from nontransformed cells. Quantitation was performed by both spectral counting and SILAC and forty-three pTyr sites corresponding to 32 proteins were considered to be potential novel Src substrates. Interestingly, the proteins exhibiting increased phosphorylation in Src-transformed cells included many metabolic enzymes as well as RNA and protein synthesis processing machinery.

Interestingly, v-Src forms are rarely found in human cells, even in cancer (174). Instead, it would be informative to pursue these studies focusing on the cellular proto-oncogene *c-src*, which unlike the oncogene *v-src*, is regulated by Csk phosphorylation in the cell. This difference in activity regulation may confer different behavior of the kinase in the cell, including distinct substrates.

1.3.3. c-Src proteomics

There has been one previous proteomics study, which actually focused on mammalian c-Src (175). In this study NIH/3T3 fibroblasts were stimulated with PDGF in the presence or absence of the Src-family kinase inhibitor SU6656. A SILAC–based quantitative proteomic approach was combined with enrichment for tyrosine phosphorylated proteins and followed by LC-MS/MS analysis. The study detected changes in tyrosine phosphorylation patterns of 43 potential c-Src kinase substrates in PDGF receptor signaling. From the 23 known c-Src substrates, 7 had never been shown to play roles in PDGF signaling. From the 20 previously unknown substrates, 5 were reported as PDGF receptor signaling intermediates, while 15 have never been reported as players in PDGF receptor signaling. This study was particularly valuable in revealing the role of c-Src as a mediator of the mitogenic response to PDGF in fibroblasts. However, there may be benefits of analyzing cellular protein tyrosine phosphorylation targets of c-Src using a proteomics strategy that can directly and specifically monitor c-Src kinase action rather than an indirect method such as the one performing growth factor stimulation.

One of the goals of this thesis was to achieve specific and rapid activation of c-Src in living cells that will allow identification of substrates temporarily close to c-Src activation. An attractive strategy to pursue these objectives involves chemical rescue of mutant c-Src tyrosine kinase. Previous work in our lab combined chemical rescue of v-Src and proteomics (134). In order to repeat this strategy for the mammalian c-Src, the first step would be to optimize the conditions for c-Src chemical rescue. After this was accomplished in living cells, we decided to combine c-Src chemical rescue with a shotgun proteomic strategy.

By combining the specific and controlled activation of c-Src by chemical rescue with the ability of quantitative SILAC phosphoproteomics to provide the phosphorylation fingerprint of cells in different conditions, we have identified a number of potential novel c-Src targets and discuss the potential ramifications of these phosphorylation events in cell signaling.

2. Methods

2.1. Cell Culture and SILAC

For regular tissue culture, Src-, Yes-, and Fyn- triple knockout mouse embryonic fibroblast cells (hereafter referred to as SYF cells) (ATCC) stably transfected with either R390A c-Src or D388N c-Src constructs as previously described (134) were cultured in Dulbecco's Modified Eagle's Medium (DMEM) (Invitrogen) supplemented with 10% (v/v) qualified fetal bovine serum (FBS) (Invitrogen), 1% (v/v) of penicillin-streptomycin-glutamine (PSG) (Invitrogen) and 300 μg/ml of Hygromycin B (Roche) and incubated at 37ºC in the presence of 5% CO_2. When starved, cells were cultured in the same medium lacking serum. Chemical rescue experiments were performed from cells actively growing and motile at ~75% confluency. Untransfected SYF MEFs cells and wt MEFs were grown as above without hygromycin treatment.

For SILAC experiments, R390A c-Src SYF MEF cells (hereafter referred to as R390A/ SYF MEF cells) were adapted to the SILAC media. A detailed protocol for SILAC media preparation can be obtained from http://www.silac.org. Arginine-, lysine-,

and tyrosine-free DMEM media were bought from Athena Enzyme Systems (SILAC experiment at the protein level) or from Invitrogen (SILAC experiment at the peptide level). R390A/ SYF MEF cells were cultured in Arg-/ Lys-/ Tyr- free DMEM media supplemented with light ($^{12}C_6$ Arg/ $^{12}C_6$ Lys/ $^{12}C_6$ Tyr) amino acids from Sigma or heavy ($^{13}C_6$ Arg/ $^{13}C_6$ Lys) amino acids from Cambridge Isotope Laboratories, Inc. "Light media" was supplemented with $^{12}C_6$ Arg, $^{12}C_6$ Lys, and $^{12}C_6$ Tyr. "Heavy media" was supplemented with $^{13}C_6$ Arg, $^{13}C_6$ Lys, and $^{12}C_6$ Tyr. A table with the used concentrations of stable isotopic amino acids used in SILAC media is included **(Table 1)**. Both media contained 10% qualified FBS (Invitrogen), 1% PSG (Invitrogen) and 300 μg/ml of Hygromycin B (Roche). The cells were adapted to the SILAC medium by growing them in these media for at least 5 replication cycles, as described earlier (176). When starved, cells were cultured in the same medium lacking serum. The p-Tyr proteomes were assessed from cells actively growing and motile at ~75% confluency.

2.2. Cell treatment

For other chemical rescue experiments, including Western blots, immunoprecipitations and Western blots, and coimmunoprecipitations and Western blots, R390A/SYF cells and D388N/SYF cells were serum-starved for 16-20 hours. Cells were either treated with 10 mM imidazole, pH 7.5 for 5 minutes or left untreated (control) also for 5 minutes. Both cells sets were then washed once with ice cold PBS (Invitrogen) and immediately lysed in RIPA buffer (50 mM Tris-HCl pH 8.0, 0.25% Na-deoxycholate, 150 mM NaCl, 1 mM EDTA, 1% NP-40 (Igepal), 1 mM Na_3VO_4, 1 mM NaF, 1 mM

PMSF, Complete protease inhibitor cocktail (Roche)), mixed for 30 minutes at 4°C. The lysate was then cleared by centrifugation at 13,000 x g for 15 minutes and the supernatant collected.

For SILAC experiments, approximately thirty 150-mm diameter plates of R390A/SYF cells (per condition) were serum-starved for 16 hours. Cells grown in $^{13}C_6$ Arg/ $^{13}C_6$ Lys- containing media (heavy media) were treated with 10 mM imidazole, pH 7.5 for 5 minutes, whereas cells grown in $^{12}C_6$ Arg/ $^{12}C_6$ Lys- containing media (light media) were left unstimulated and used as a control. Both cells sets were then washed once with ice cold PBS (Invitrogen) and immediately lysed RIPA buffer (SILAC experiment at the protein level). In the SILAC experiment at the peptide level the lysis was perfomed with Urea lysis buffer (20 mM HEPES, pH 8.0, 9 M urea, 1 mM sodium orthovanadate, 2.5 mM sodium pyrophosphate, 1 mM ß-glycerophosphate) by 3 bursts of ultrasonication (Duty cycle 40%, output control at 4, on Sonifier 250, Branson) at 4 °C. After sonication, the lysate was cleared by centrifugation at 20,000 x g for 15 minutes and the supernatant collected.

2.3. SILAC experiment at the protein level

SYF/MEF cells stably transfected with R390A c-Src were cultured, isotopically labeled and treated as described above. Phosphotyrosine protein profile with and without imidazole treatment was analyzed by immunoaffinity purification of phosphoproteins with 4G10 anti-phosphotyrosine antibody followed by Western blot using 4G10 anti-phosphotyrosine antibody **(Figure 16.A.)**.

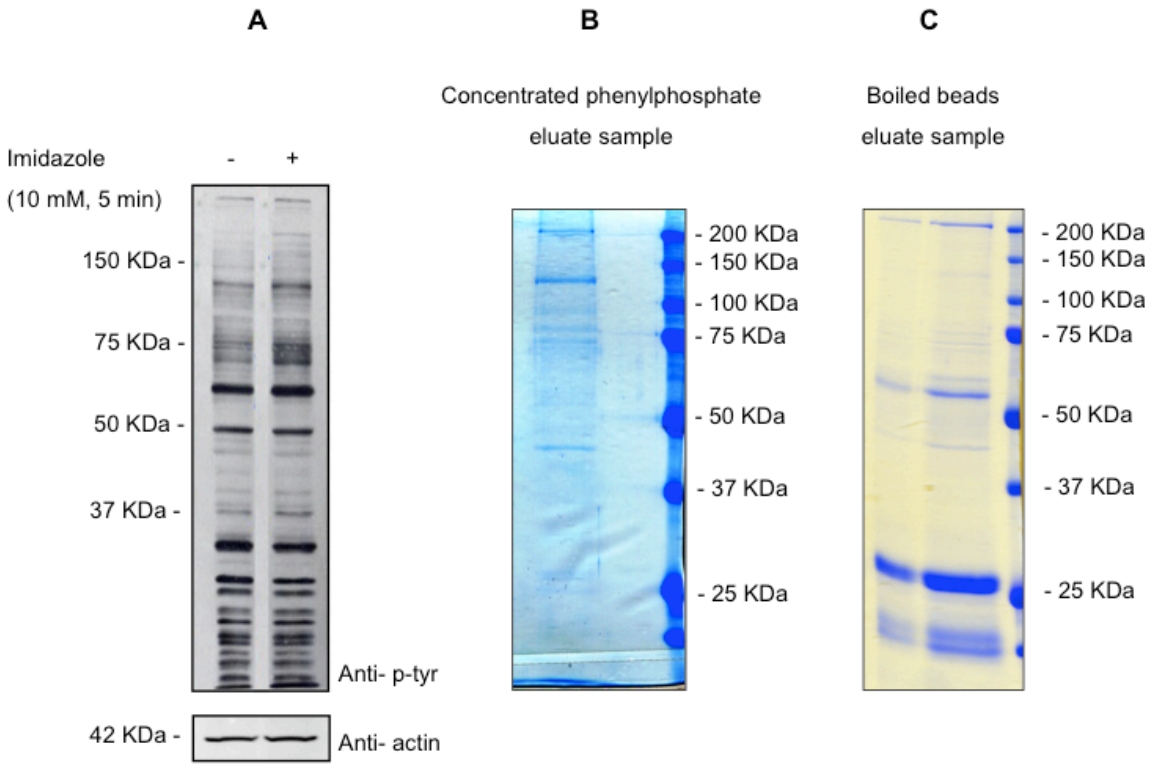

Figure 16. Identification and quantitation of tyrosine phosphorylated proteins by SILAC and LC-MS/MS. Anti-phosphotyrosine immunoblot revealing chemical rescue. SDS-Page and colloidal Coomassie stained gels of immunoprecipitated eluates.

A. Western blot against whole lysate of R390A/ SYF MEF cells using 4G10 anti-phosphotyrosine antibody. Loading control was performed with anti-actin antibody. **B.** Phenylphosphate eluate run in a SDS-Page gel and stained with colloidal Coomassie. **C.** Boiled beads eluate run in a SDS-Page gel and stained with colloidal Coomassie.

2.3.1. Tyrosine phosphoprotein enrichment and quantitative analysis

Immunoaffinity purification of tyrosine-phosphorylated proteins was carried out as described previously (134). The agarose beads were eluted using two different procedures, one after the other. First, the beads were subjected to competitive elution with 100 mM phenyl phosphate. The eluate was concentrated and separated by SDS-Page **(Figure 16.B.)**. Hereafter, the beads were treated with beta-mercaptoethanol and boiled at 95ºC for 5 minutes. This sample was also separated by SDS-Page **(Figure 16.C.)**. Both samples were processed independently from this step. The enriched tyrosine-phosphorylated proteins were subjected to in-gel digestion as described previously (134). The resulting tryptic peptides were analyzed by reversed phase LC-MS/MS using a quadrupole-time-of-flight mass spectrometer (QSTAR Pulsar, MDS Sciex, Concord, Ontario, Canada) coupled to an 1100 series CapLC (Agilent, Santa Clara, CA). The raw data obtained from both analyses was first queried separately and then the raw data obtained from both analyses were combined and queried again. Queries were performed against the RefSeq protein database (v.26, containing 20311 entries) using MASCOT v.2.2.2 (Matrixscience, London, England). Quantitation of obtained SILAC data was conducted using MSQuant v1.4.3a39. Acquired data were queried against the RefSeq mouse protein database using the following search parameters precursor and fragment ions mass tolerance of 1.1 and 0.1 Da, respectively. Carbamidomethylation of cysteines was set as a fixed modification while N-terminal acetylation, deamidation of asparagine and glutamine, oxidation at methionine, phosphorylation at serine, threonine and tyrosine

together with 'heavy' lysine and arginine was allowed as variable modifications. Quantitation was performed using MSQuant as described on http//msquant.sourceforge.net. As described before data from the two elutions were first treated separately and then merged, analyzed and quantitated together.

2.4. SILAC experiment at the peptide level

Three biological replicates were conducted. Protein concentrations were determined by Bradford **(Figure 17.A)**. As a further loading control equal amount of lysates (50 μg) were mixed with SDS loading buffer and boiled at 95ºC for 5 minutes, analyzed by SDS-PAGE and stained with Colloidal Coomasie **(Figure 17.B)**.

Phosphotyrosine protein profile with and without imidazole treatment was analyzed by immunoaffinity purification of phosphoproteins with 4G10 anti-phosphotyrosine antibody followed by Western blot using 4G10 anti-phosphotyrosine antibody **(Figure 18)**.

"Heavy" and "Light" lysates were mixed in protein concentration ratios 1:1. As a result, a total amount of 35 mg (first biological replicate), 50 mg (second biological replicate) and 52 mg (third biological replicate) were generated for phosphotyrosine peptide profiling. Two of the 3 biological replicates had two technical replicates with respect to LC-MS/MS. LC-MS analysis of sample aliquots was performed to observe the equal mixing of heavy and light cell lysate proteins using a Micromass quadrupole time-of-flight mass spectrometer (QTOF) Ultima API (Waters) **(Figure 19)**.

A

Biological replicate

Biological replicate	1		2		3	
	L	H	L	H	L	H
Concentration (µg/ml)	1271	1274	1348	1285	1366	1357

B

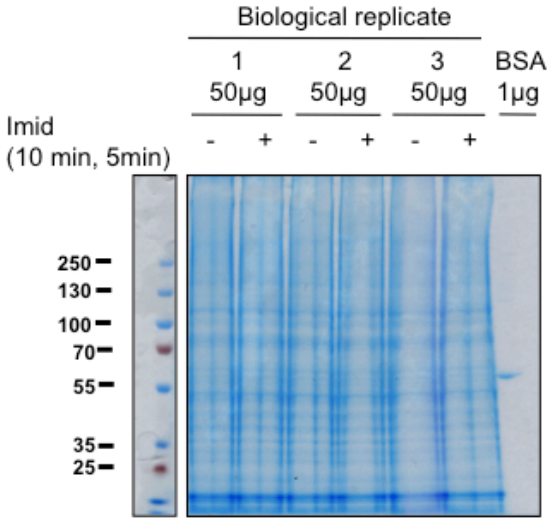

Figure 17. Site-specific mapping and quantification. Control 1

Quality control studies of proteomics samples used for phosphotyrosine-site mapping. **A.** Loading controls: protein concentrations were calculated by Bradford assay. **B.** 50 µg samples from both the heavy and light lysates from each biological replicate were separated and stained with colloidal Coomassie for further validation

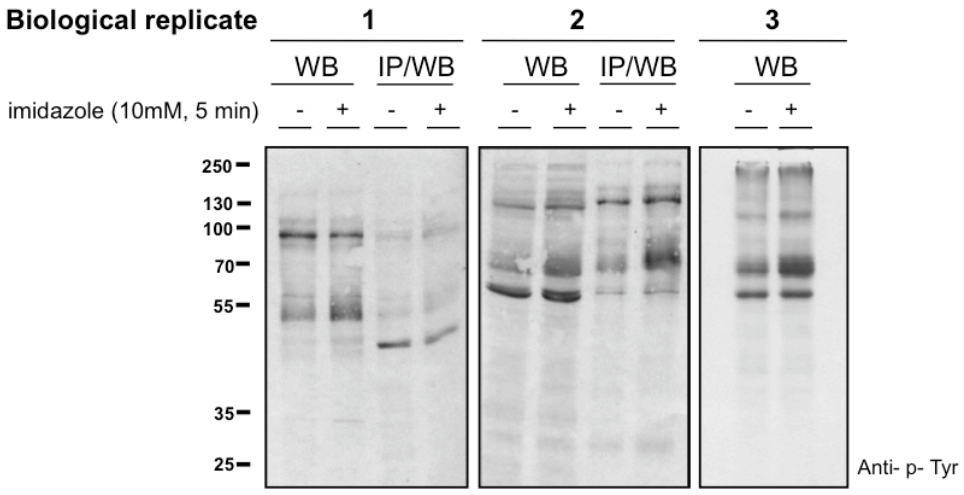

Figure 18. Site-specific mapping and quantification. Control 2

Quality control studies of proteomics samples used for phosphotyrosine-site mapping. Chemical rescue controls: Anti-phosphotyrosine 4G10 Western Blot (WB) and immunprecipitation (IP/WB) of three biological replicates before and after R390A c-Src chemical rescue in R390A/ SYF MEF cells.

	Biological Replicate		
	1	2	3
Normalization Ratio	0.9-1	0.9-1	0.9-1

Figure 19. Site-specific mapping and quantification. Control 3

Quality control studies of proteomics samples used for phosphotyrosine-site mapping. Normalization controls: QTOF analysis of sample aliquots was performed to assure good normalization for each biological replicate.

2.4.1. Peptide preparation

Proteins were reduced with DTT at a final concentration of 4.5 mM and alkylated with 10 mM iodoacetamide. Lysates were diluted to a final concentration of 2 M urea, 20 mM HEPES (pH 8.0). 1/100 vol/vol of 1 mg/ml trypsin- TPCK (Worthington Biochemical Corporation) was added to the diluted protein extracts and digestion was performed overnight at 25 ºC. The lysates were analyzed before and after digestion as a control **(Figure 20)** using SDS-PAGE and colloidal Coomassie staining.

The protein digests were acidified with trifluoroacetic acid (TFA) at a final concentration of 1%. The acidified peptide solutions were centrifuged at 1,800 x g for 5 minutes to remove the precipitate. The clear supernatants were loaded onto Sep-Pak C_{18} cartridges (Waters, cat no: WAT051910) previously wetted with 100% acetonitrile and equilibrated with 0.1% TFA. Acidified peptide samples were passed through cartridge by gravity and the cartridges were then washed with 0.1% TFA. The peptides were eluted by 40% acetonitrile/ 0.1% TFA. The eluted peptide solutions were lyophilized to remove residual TFA completely.

2.4.2. Immunoaffinity purification of tyrosine phosphopeptides

Anti-phospho-tyrosine antibody based immunoaffinity purification (IAP) of phosphopeptides was carried out according to the manufacturer's protocol (177). Lyophilized peptides from each of the fractions (3 biological replicates, 2 technical replicates) were dissolved with 1.4 ml of IAP buffer (50 mM MOPS, pH 7.2, 10 mM

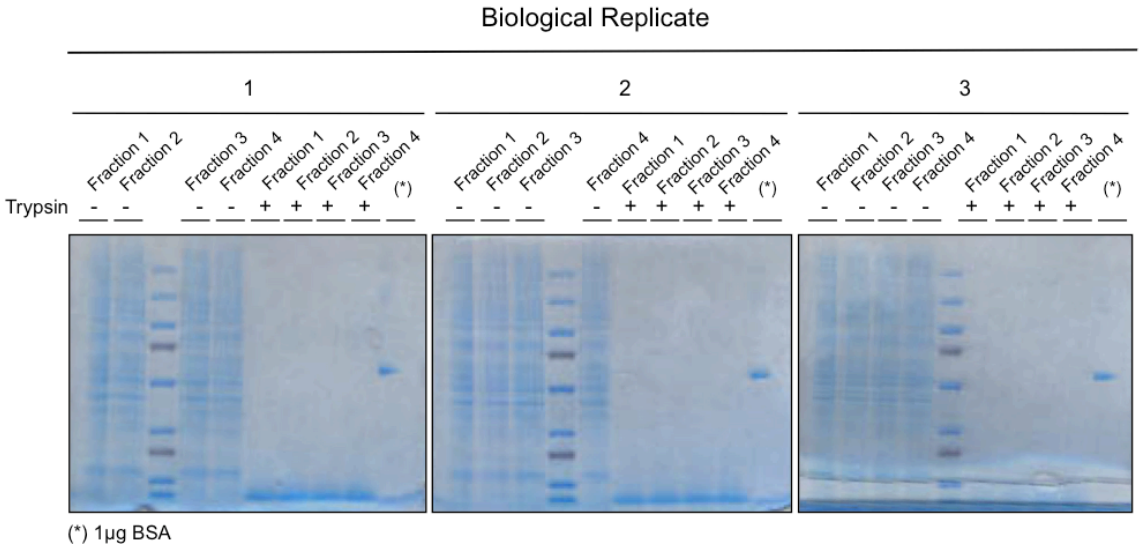

Figure 20. Site-specific mapping and quantification. Control 4

Quality control studies of proteomics samples used for phosphotyrosine-site mapping. Control of trypsinization of proteomic samples used for phosphotyrosine-site mapping. Samples from each biological control before and after trypsinization were separated on a SDS-Page gel and stained with colloidal Coomassie to ensure complete trypsinization.

sodium phosphate, 50 mM NaCl) aided by shaking and brief sonication. Solution was cleared by centrifugation for 5 minutes at 1,800 x g. The phosphotyrosine antibody-linked beads (Cell Signaling Technology) were washed with IAP buffer (1.4 ml IAP buffer, mix by invert 5 times) once and incubated with the cleared peptide solution for 30 minutes at 4ºC with gentle shaking. The phosphopeptide bound antibody beads were washed twice with IAP buffer and twice with water at 4ºC. Phosphopeptides were eluted from the beads by incubation with 55 µl of 0.15% TFA at 20-25ºC for 10 minutes followed by second extraction with 45 µl of 0.15% TFA.

The eluted phosphopeptides were desalted using Stage-Tip protocol described previously (178). The peptide eluate was then dried at 25ºC in Speed-Vac for mass spectrometry analysis.

2.4.3. LC-MS/MS analysis of tyrosine phosphorylated peptides

LC-MS/MS analysis of phosphopeptides enriched by IAP was carried out using a reversed-phase liquid chromatography system interfaced with Fourier transform LTQ-Orbitrap Velos mass spectrometer (FT-MS) on a "high-high" mode (both MS and MS/MS analyses were carried out in FT-MS mode) (Thermo Scientific). The reversed phase setup consisted of a trap column (2 cm × 75 µm, Magic C_{18} AQ material 5µm, 100 Å) and an analytical column (10 cm × 75 µm, Magic C_{18} AQ material 5 µm, 100 Å). After concentration and desalting on the pre-column, peptides were eluted and separated on the analytical column using a gradient increasing from 100% solvent A/ 0% solvent B (Solvent A: 0.1% formic acid, solvent B: 100% acetonitrile, 0.1% formic acid) to 40%

buffer A/60% solvent B in 135 min. Each survey scan involved precursor scan from 350-1600 m/z at 60,000 resolution and data dependent higher energy collision dissociation (HCD) MS/MS scans for the 10 most intense precursor ions at 7,500 resolution. Normalized collision energy was 35% and monoisotopic precursor selection enabled with isolation width of 1.9 m/z.

2.4.4. Data analysis

The acquired mass spectra were processed and searched using MaxQuant (version 1.2) (179), Mascot (180) and Sequest (181) since these algorithms are complementary which can broaden protein and site identification (182). Searches using the latter two were submitted via Proteome Discoverer (version 1.3, Thermo Scientific), which allowed merging search results and quantitating the SILAC pairs. All MS/MS spectra were searched against the RefSeq mouse protein database (v. 40, containing 31,183 entries). For all searches, two missed cleavages were allowed; carbamidomethylation of cysteines were set as a fixed modification. N-terminal acetylation, deamidation of asparagine and glutamine, oxidation at methionine, phosphorylation at serine, threonine and tyrosine together with the 'heavy' lysine and arginine were used as variable modifications.

Monoisotopic peptide tolerance was set to 10 p.p.m. for precursors and 0.05 mDa for MS/MS fragment ions. Peptides fulfilling a FDR of 1% were reported. Peptides with inconsistent ratios or unusual high ratios were manually checked. We established a threshold H/L ratio value of 1.2. Phosphopeptides showing an average (from the three biological replicates) SILAC ratio of 1.2 or above from Proteome Discoverer, MaxQuant,

or both were considered upregulated upon c-Src rescue. Four filtering criteria were used to obtain a high-confidence data set of quantified phosphotyrosine peptides. If manual validation was satisfactory and showed a rounded SILAC ratio of 1.2 or above, the peptides were included on the list. A detailed flow-chart of the process is included in **Figure 21**.

2.5. Network Modeling and Literature Curation

Phosphosite (http://phosphosite.org), Human Protein Research Database (HPRD) (22) (http://hprd.org), and literature curation were used to differentiate previously unidentified and known substrates from the list of proteins showing increased phosphorylation upon c-Src rescue. Phosphosite was used to establish the protein type classification of the detected proteins (Figure 26). The Ingenuity pathway analysis software (Ingenuity ® Systems, www.ingenuity.com) and literature curation were used to investigate previously observed connections between c-Src and the protein of study.

The Ingenuity pathway analysis software was used to perform ontology and canonical pathway enrichment analysis of the proteins associated with the found tyrosine phosphopeptides experiencing an increase in their tyrosine phosphorylation level upon c-Src rescue. The online web tool DAVID Bioinformatics Resources 6.7 (http://david.abcc.ncifcrf.gov) (183) and the Ingenuity pathway analysis software were used to obtain a representation of the role of c-Src on focal adhesion pathways. The list of proteins corresponding to the peptides identified as upregulated upon c-Src rescue

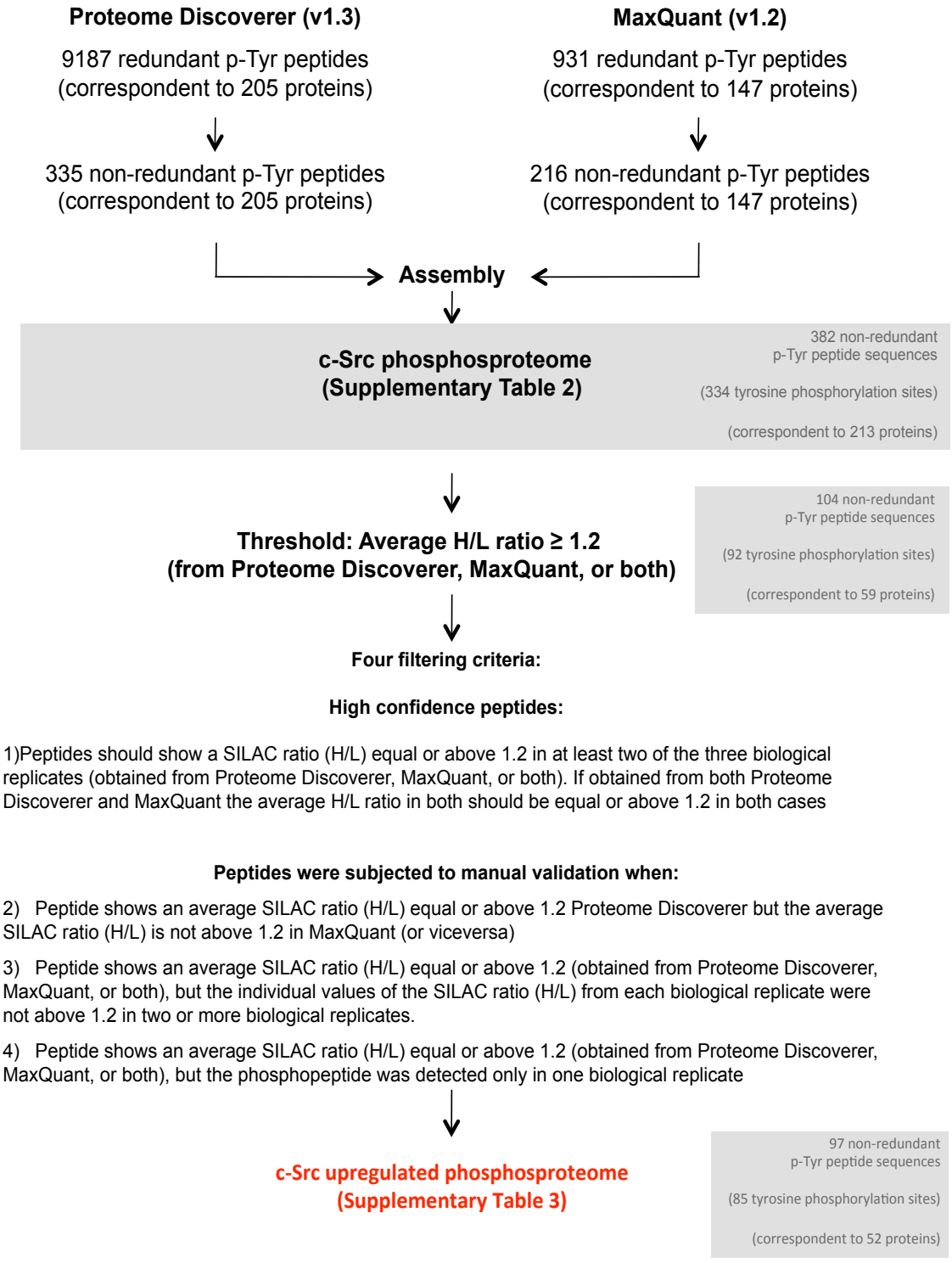

Figure 21. Flow-chart representing the complete data analysis process corresponding to the phosphopeptide enrichment by SILAC and LC-MS/MS

was uploaded in the DAVID tool, which incorporated the newly discovered proteins to the pathway. The pathway was completed using Ingenuity Systems. Both the known and the newly discovered potential c-Src phosphorylation sites were incorporated to the graph manually and validated with Phosphosite and HPRD.

2.6. Immunobloting and Immunoprecipitations

After imidazole treatment cells were washed once with PBS and lysed for 30 min at 4ºC in RIPA buffer (Tris-HCl, 50 mM, pH 7.4, Na-deoxycholate 0.25%, NaCl, 150 mM, EDTA, 1mM, 1% NP-40), Na_3VO_4 1 mM, NaF 1 mM, PMSF 1 mM and protease inhibitor cocktail tablets (Roche), and centrifuged at 16,000 x *g* at 4ºC. The supernatants were collected for immunobloting and immunoprecipitation. For immunobloting the supernatants were mixed with SDS loading buffer and boiled at 95ºC for 5 minutes, analyzed by SDS-PAGE. The proteins were electroblotted onto nitrocellulose or PVDF membrane (Invitrogen). The membrane was blocked with 5% BSA in TBST for 1 hour at 4ºC. The membrane was then probed with appropriate antibody, followed by incubation with the correspondent HRP- conjugated secondary antibody. Antibodies were used at the recommended concentration in the manufacturer's instructions. Bands were visualized using SuperSignal West Pico chemiluminescent substrate (Pierce). For immunoprecipitation, the supernatants were pre-cleared with protein A or G agarose beads and subsequently incubated one hour with the antibody at 4ºC. Antibodies were used at the recommended concentration in the manufacturer's instructions. Mixtures were treated with protein A or G agarose beads and then incubated at 4ºC overnight. The

agarose beads were subsequently washed three times by RIPA buffer, resuspended in SDS loading buffer with β-mercaptoethanol and boiled. The eluates were analyzed by SDS-PAGE and Western blot analysis.

Antibodies were obtained as follows: Phosphotyrosine: (4G10) from Upstate Biotechnology. Both HRP-conjugated and non-HRP-conjugated 4G10 pTyr were used. FAK: 06-543 (FAK IP and WB) from Upstate Biotechnology. Paxillin: 05-417 (Paxillin IP and WB) from Millipore. Vimentin: ab8978 (Vimentin IP), ab58462 (Vimentin WB) from Abcam, Inc. C3G: sc869 (C3G IP and WB) from Santa Cruz Biotechnology. Tensin: sc28542 (Tensin IP and WB) from Santa Cruz Biotechnology. Matrin 3: sc55724 (Matrin IP and WB) from Santa Cruz Biotechnology. Nucleophosmin: ab10530 (Nucleophosmin IP and WB) from Abcam. Gsk3β: CST9315 (Gsk3β IP) from Cell Signaling Technology, sc81462 (Gsk3β WB) from Santa Cruz Biotechnology. C3G: sc-15359 (C3G IP and WB) from Santa Cruz Biotechnology. Western blots of experiments done with the rescuable cell lines (R390A/ SYF) were performed at least twice and results shown are representative except the IP-WB for tensin and matrin 3: tensin IP-WB in R390A/SYF cells have at least one reliable and clear immunoblot and one that is less/ non-reliable (poor quality blot, abundance of non-specific bands that make the interpretation difficult). However, the identification of upregulated tyrosine phosphorylation sites in the phosphopeptide search represents further validation of tensin as a c-Src substrate. In fact, the less/non-reliable anti-phosphotyrosine blot for the tensin IP was performed in the same membrane that another non-reliable duplicate of matrin 3 which we will describe in detail in the Appendix 1 (Appendix 1 Figure 3.A). The IP-WB for matrin 3 was very challenging (specifically the anti-phosphotyrosine Western blot)

and, although attempted 5 times, we only obtained one reliable experimental repeat (**Figure 28**). FAK and paxillin IP-WB were only performed with the rescuable cell lines (R390A/ SYF) and only once (n=1).

Western blots of experiments done with the non-rescuable cell lines (D388N/ SYF) were performed at least twice and results shown are representative, except in the IP-WB for tensin and matrin 3, where we only have one reliable biological replicate.

The validation of matrin 3 through immunoprecipitation and Western blotting deserves further attention since the results obtained in the only valid biological replicate have modest quality, are ambiguous and present several caveats. The Appendix 1 is dedicated fully to the description of the methodology, results and interpretation of the matrin 3's validation experiment and the modest evidence it provided, some of which supported the marginal increase in phosphorylation of matrin 3 upon c-Src rescue. Briefly, the initial experiment **(Appendix 1 Figure 3.A)** was performed following the standard protocol described above. We observed signal in the first attempt but the blot had bands that we suspect correspond to non-specific binding, making the interpretation unreliable, as we will explain in the Appendix 1. The next three repeats/ biological replicates **(Appendix 1 Figure 3.B-D)** were also performed following the standard protocol described above with slight modifications. Matrin 3 phosphorylation was very hard to detect, and the Western blot using phosphotyrosine antibody (4G10) showed no signal in these three experimental repeats. After three attempts when phosphorylation was not detected, we included some additional steps to be able to visualize phosphorylation. After incubation with the mouse HRP-conjugated 4G10 anti-pTyr antibody, we developed the blot and, as before, no phosphorylation was observed **(Appendix 1 Figure**

6). In order to detect matrin 3 phosphorylation, a sandwich reaction had to be performed **(Appendix 1 Figure 7-8)**: we performed an incubation with an HRP-conjugated anti-mouse secondary antibody. The first incubation with the secondary antibody (first sandwich reaction) was performed at 4ºC for approximately one hour. After washing the membrane we developed the membrane using SuperSignal West Femto chemiluminescent substrate (Pierce) diluted 1 to 10 in water **(Appendix 1 Figure 7-8)**. We then washed the membrane again and developed **(Appendix 1 Figure 9)**. The membrane was then washed and incubated again with anti-mouse secondary antibody (second sandwich reaction). This second incubation was performed at 4ºC overnight as indicated in my notebook. After washing the membrane we developed the membrane using SuperSignal West Femto chemiluminescent substrate (Pierce) diluted 1 to 2 in water **(Appendix 1 Figure 10-12)**. The resulting blot was very dark but could be scanned successfully with the help of an external lamp **(Figures 28 and Appendix 1 Figure 11)**. The summarized workflow for the additional steps included to allow visualization of matrin 3 phosphorylation is presented in **Appendix 1 Figure 4**. It should be noted that baseline values between rescuable and non-rescuable cells may not be the same due to subtle alterations in the cell passage number, growth conditions, or Western blot conditions.

3. Results

3. 1. c-Src chemical rescue optimization

The chemical rescue of mutant v-Src provides precise temporal control of its intracellular kinase activity (134) and is a very useful tool to specifically activate v-Src in living cells. In order to test whether we could observe similar results with cellular c-Src and combine this technique with a proteomics approach, we used SYF MEF cells stably transfected with R390A c-Src (R390A/SYF cells). The triple knockout reduces the background from endogenous c-Src, as well as two other members of the Src kinase family, Yes and Fyn (184). We observed that treatment of SYF MEF cells stably transfected with R390A c-Src using a range of 2.5-5 minutes and 2-10 mM imidazole induced a time- and dose-dependent increase in range and intensity of tyrosine-phosphorylated protein bands as visualized by Western blot analysis of whole cell lysate with 4G10 anti-phosphotyrosine antibody **(Figure 22 and 23)**. After a series of optimization experiments, we selected 10 mM imidazole and 5 minutes exposure as favorable conditions for c-Src rescue in R390A/SYF cells. The imidazole-insensitive inactive c-Src mutant D388N/SYF cells were used as a negative control since they express an inactive Src kinase at similar levels (134) and should be most similar to the untreated R390A/SYF cells. In prior studies (134), it was shown that D388N/SYF cells are unresponsive to imidazole. We confirmed here that D388N/SYF cells showed no such change in protein tyrosine phosphorylation with 10 mM imidazole and 5 minute treatment, compared with the imidazole-sensitive R390A/SYF c-Src mutant **(Figure 23)**, suggesting that the imidazole effect was specific. The baseline Western blot differences (minus imidazole) between D388N/SYF and R390A/SYF cells likely represent subtle differences in passage numbers and clonal populations.

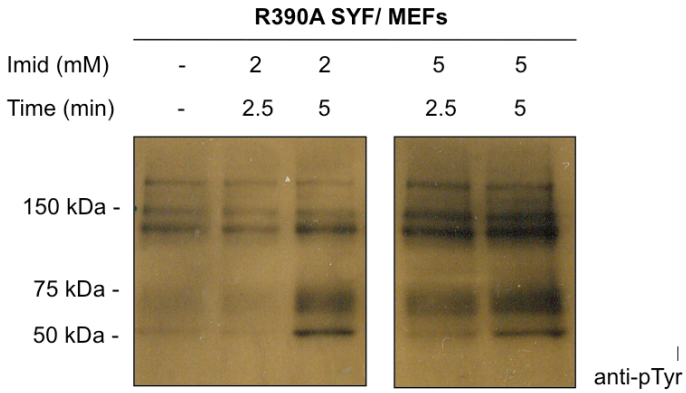

Figure 22. Western blot experiment to optimize c-Src rescue conditions

Optimization of c-Src rescue conditions. Time course imidazole treatment (2 mM and 5 mM) of c-Src R390A SYF cells. Overall tyrosine phosphorylation level was performed by subjecting the lysates to Western blot analysiswith a 4G10 anti- phosphotyrosine antibody.

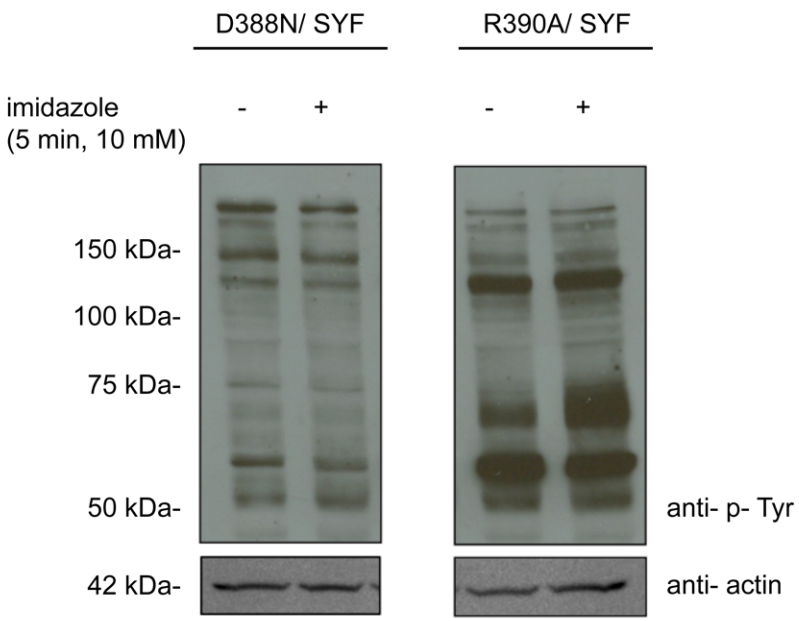

Figure 23. Western blot experiment showing c-Src chemical rescue in R390A/ SYF cells but not in D388N/ SYF cells

c-Src chemical rescue by imidazole. Comparison of the phosphotyrosine profile of imidazole-treated cells compared to that of untreated cells. Tyrosine phosphorylation induced by imidazole treatment (10 mM, 5 minutes) of SYF cells stably transfected with c-Src R390A and D388N SYF (negative control). Cells were subjected to lysis and whole lysates were subjected to Western blotting with 4G10 anti- phosphotyrosine antibody.

To further ensure that imidazole had no major effects on cellular tyrosine phosphorylation outside of chemical rescue under these conditions, we investigated its effect on SYF MEF and WT MEF cells. As shown in **(Figure 24)**, there were no appreciable changes in anti-pTyr Western blots of cell lysates treated with or without imidazole.

3.2. Phosphoprotein identification and quantitation

Since our goal was to identify the c-Src-induced phosphoproteome, we combined c-Src chemical rescue with mass spectrometry and stable isotope labeling with amino acids in cell culture (SILAC) (185). R390A c-Src-expressing SYF cells were labeled with either $^{13}C_6$-Arg/ $^{13}C_6$-Lys (heavy) or $^{12}C_6$-Arg/ $^{12}C_6$-Lys (light). "Heavy" cells were treated with 10 mM imidazole for 5 minutes and "light" cells were left untreated (control) to distinguish the c-Src induced tyrosine phosphorylation events from the background of steady-state tyrosine phosphorylated proteins in the cell. As an initial approach to test the combined advantages of chemical rescue and a proteomics analysis, protein enrichment was performed by immunoprecipitation with anti-phosphotyrosine antibody **(Figure 25).**

The phosphotyrosine proteins were analyzed by tandem mass spectrometry. As described in the method section, two lists were generated after analyzing the two different elution samples (phenyl phosphate elution and boiled-beads elution) coming from the beads used in the phosphotyrosine protein enrichment. Both tables **(Tables 2 and 3)** are included as well as the table generated after analyzing the raw data from both samples.

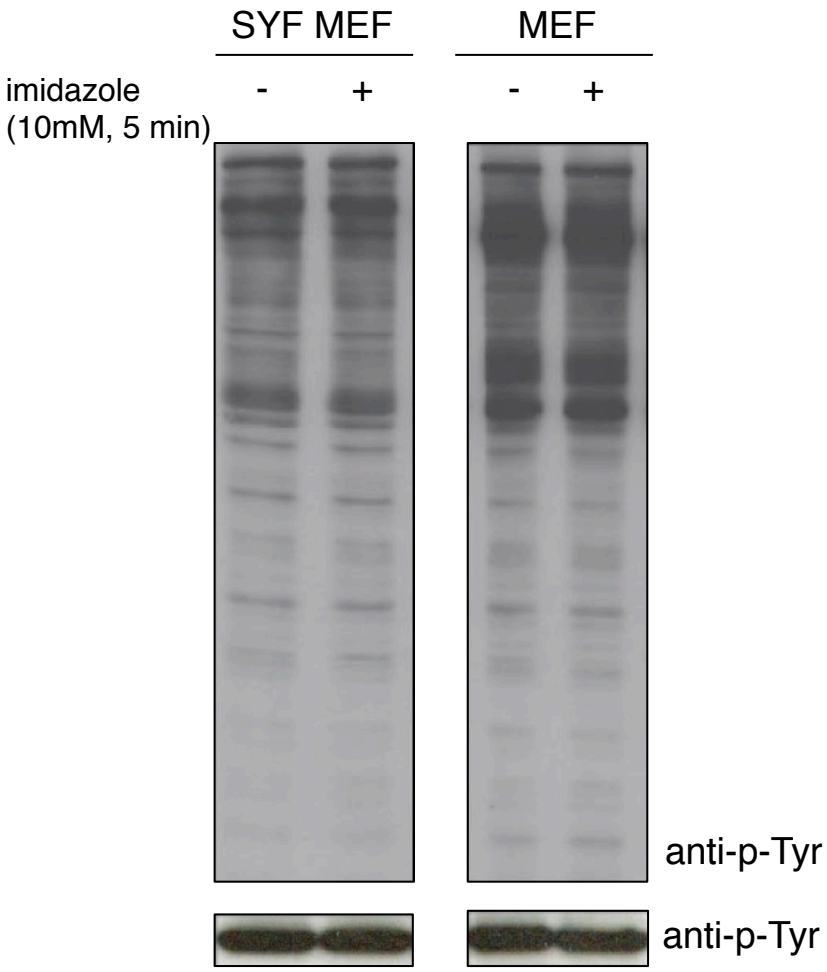

Figure 24. Control Western blot experiment showing no effects of c-Src chemical rescue in SYF MEF and MEF cells

c-Src chemical rescue by imidazole. Comparison of the phosphotyrosine profile of imidazole-treated cells compared to that of untreated cells. Tyrosine phosphorylation induced by imidazole treatment (10 mM, 5 minutes) of SYF MEF cells and MEF cells

(negative controls). Cells were subjected to lysis and whole lysates were subjected to Western blotting with 4G10 anti- phosphotyrosine antibody.

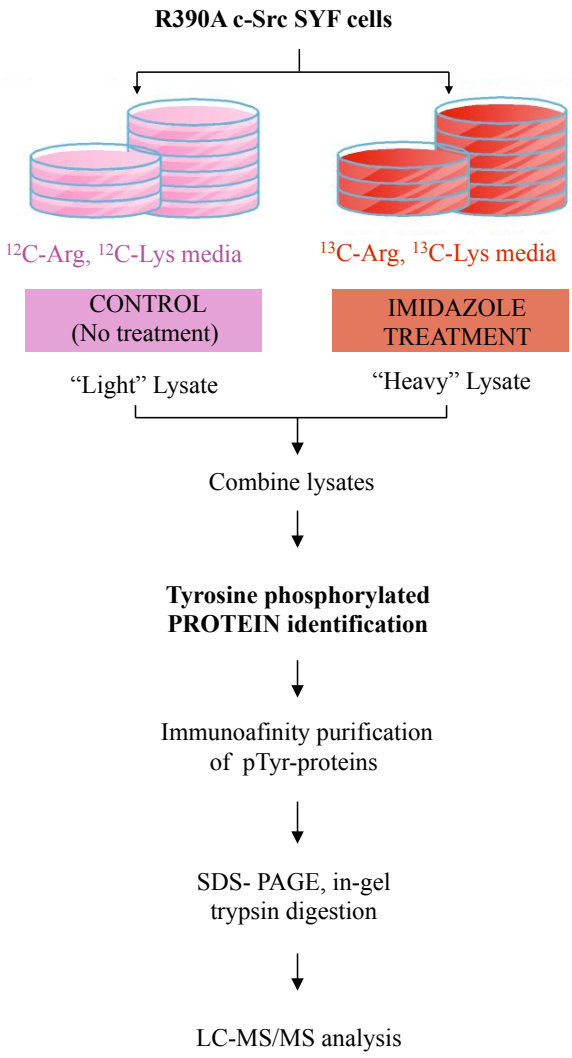

Figure 25. Scheme of the experimental design of SILAC-based quantitative phosphoproteomic approach. Protein level

R390A/SYF MEF cells were divided into two populations that were grown in 'light' or 'heavy' medium. Heavy cells were treated with 10 mM imidazole for 5 minutes and 'light' cells were untreated. Cell lysates were combined in equal proportions. The protein mixture was incubated with anti-phosphotyrosine antibodies for enrichment of tyrosine-phosphorylated proteins. The enriched fraction was subjected to in-gel trypsinization. The enriched sample was analyzed by LC- MS/MS.

The list of identified proteins resulting from analyzing the combined raw data is shown in **Table 4** and **Table 5** (simplified). A summary of fold change in phosphorylation upon c-Src chemical rescue for all proteins included in Table 4 is included in **Figure 26**.

We propose that many of the 35 proteins showing SILAC ratios equal to or above 1.2 are potential targets of c-Src-mediated tyrosine phosphorylation. The cutoff of 1.2 was based on the standard deviation of the SILAC ratios as well as prior experience with this technique. In fact, at least six of these 35 proteins are previously documented c-Src substrates. It could be assumed that larger SILAC ratios suggest greater confidence in undergoing c-Src-mediated phosphorylation. However, this is not necessarily the case. For example, the well-established c-Src substrate focal adhesion kinase (FAK) showed a modest ratio of 1.2. The group of proteins that shows an increase in their phosphorylation level upon c-Src chemical rescue were sub-classified into five categories **(Figure 26.B.)** according to the Phosphosite bioinformatics resource (www.phosphosite.org) (186). The most highly represented cellular functions were signaling pathways (37%) – with proteins such as nucleophosmin, G3BP-2, Map kinase, C3G, and cullin 5 – and adhesion and cytoskeleton (26%) – vimentin, tensin 1, matrin 3, plectin 1, fibronectin 1, and myosin X. A subset of the 29 potentially novel c-Src targets have been functionally linked to c-Src signaling pathways. They have never been identified as c-Src substrates, although the experiments here show unique evidence that they are closely temporally linked to c-Src kinase action. Two examples are vimentin (187) and nucleophosmin (188).

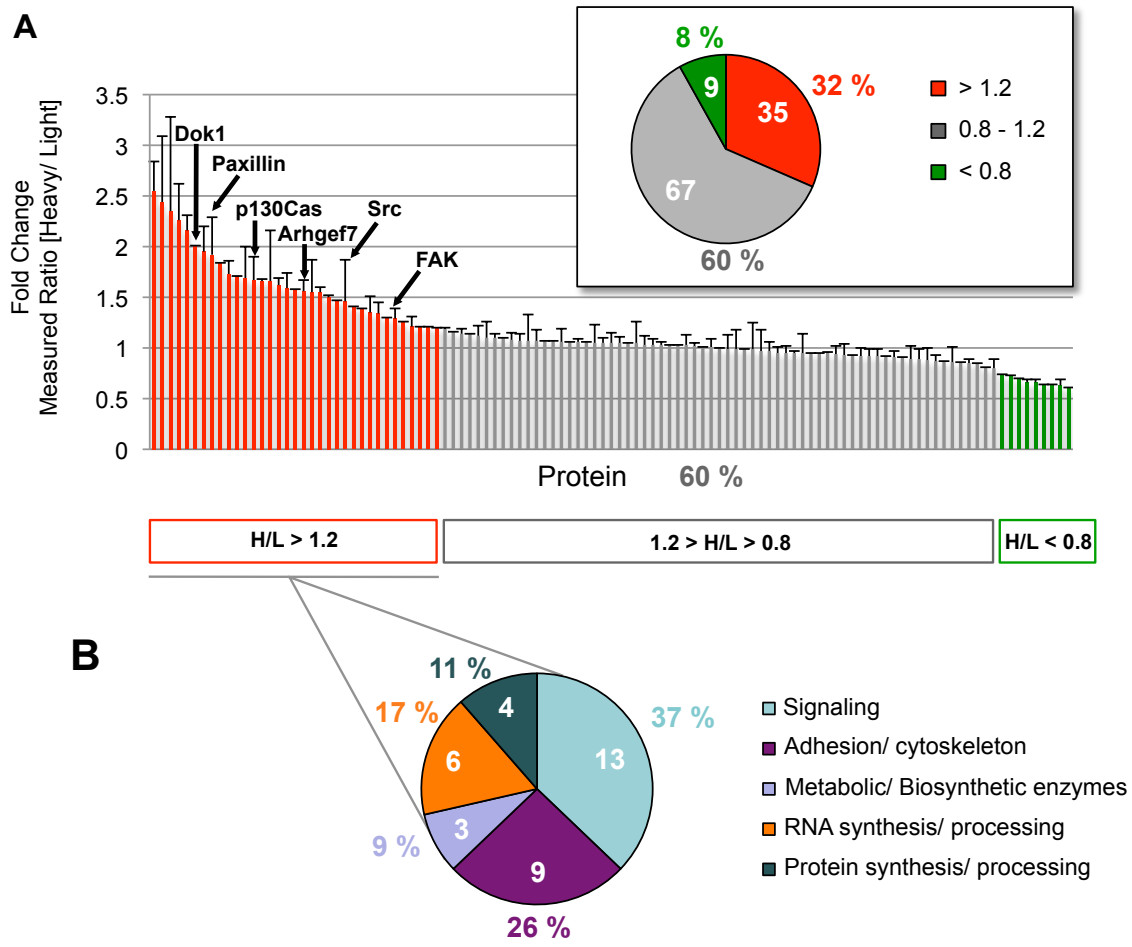

Figure 26. Graph showing the distribution of identified and quantified phosphoproteins

A. Summary of fold change in phosphorylation upon c-Src chemical rescue for all proteins in R390A/ SYF MEF cells. Known Src protein substrates within the group with increased phosphorylation level (H/L > 1.2) are indicated. Proteins with a heavy to light (H/L) ratio > 1.2 (red) increased their tyrosine phosphorylation level, and those with H/L ratio < 0.8 (green) decreased their tyrosine phosphorylation level. Proteins that showed no significant change in their tyrosine phosphorylation level (0.8 < H/L ratio < 1.2) are indicated in gray. The pie chart indicates the distribution of proteins with either up

regulated (H/L >1.2), constant (0.8 < H/L < 1.2) or down-regulated (H/L <0.8) tyrosine phosphorylation levels. **B.** Functional distribution of identified proteins with increased tyrosine phosphorylation level upon c-Src rescue.

3.3. Validation of potential c-Src targets by immunoprecipitation-Western blot analysis

We selected a set of identified proteins to confirm chemical rescue-induced tyrosine phosphorylation using an immunoprecipitation-Western blot approach in c-Src R390A/SYF cells. The D388N/SYF cells serve as negative controls. As a positive control, we first selected two well-established c-Src's susbtrates: paxillin and Fak showed imidazole-enhanced signal intensity when blotting with 4G10 anti-phosphotyrosine antibody after immunoprecipitation from R390A/SYF cells's lysates **(Figure 27).**

We then chose a set of representative potential new c-Src substrates from the different functional classes represented in our screening. We showed that C3G, vimentin, tensin 1, matrin 3 (n=1), nucleophosmin, and Gsk-3ß could be efficiently immunoprecipitated from SYF cells **(Figure 28)**. The loading controls were performed by immunoprecipitation with a specific protein antibody followed by blotting with an antibody against the same protein. Analysis of these immunoprecipitated proteins with anti-phosphotyrosine antibody showed an increase in the phosphorylation of each of these proteins from R390A/SYF but not D388N/SYF cells when treated with 10 mM imidazole for 5 minutes. These data suggest that tyrosine phosphorylation of each of these proteins depends on c-Src kinase activity, with a close temporal connection to c-Src rescue. The evidence obtained in the case of matrin 3 was not as strong as the one for other proteins. The quality of the blot was low given the extra steps we had to include to detect phosphorylation. Some of the evidence obtained supports matrin 3's increased phosphorylation upon c-Src but we say they with reservations and recommend further

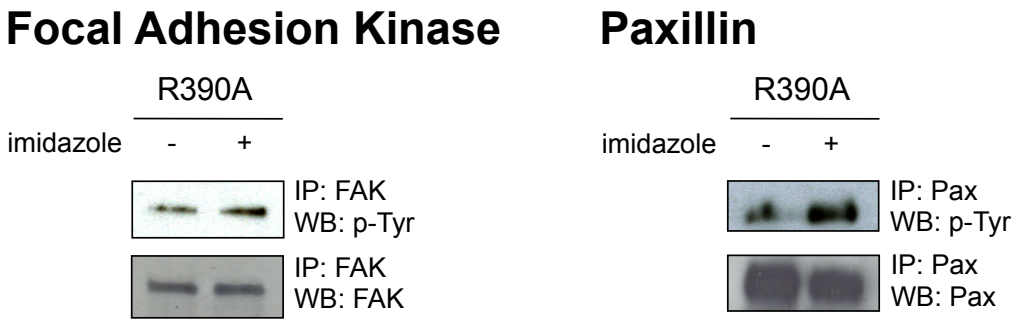

Figure 27. Validation of protein phosphorylation of known Src substrates Fak and paxillin upon c-Src rescue

Validation of protein phosphorylation of known Src substrates Fak and paxillin by immunoprecipitation- immunoblot analysis of R390A/ SYF cells after treatment with 10 mM imidazole for 5 minutes. Immunoprecipitation was carried out with commercially available antibodies corresponding to the protein of interest and immunoblotting was carried out with the 4G10 pTyr-antibody as well as protein specific antibodies (n=1). Focal adhesion kinase and paxillin are two well-known studied c-Src substrates that were also found in ourexperiment. Validation of these two proteins was done once and was used as a control. Note that these results confirm Y Qiao et al. Science (2006).

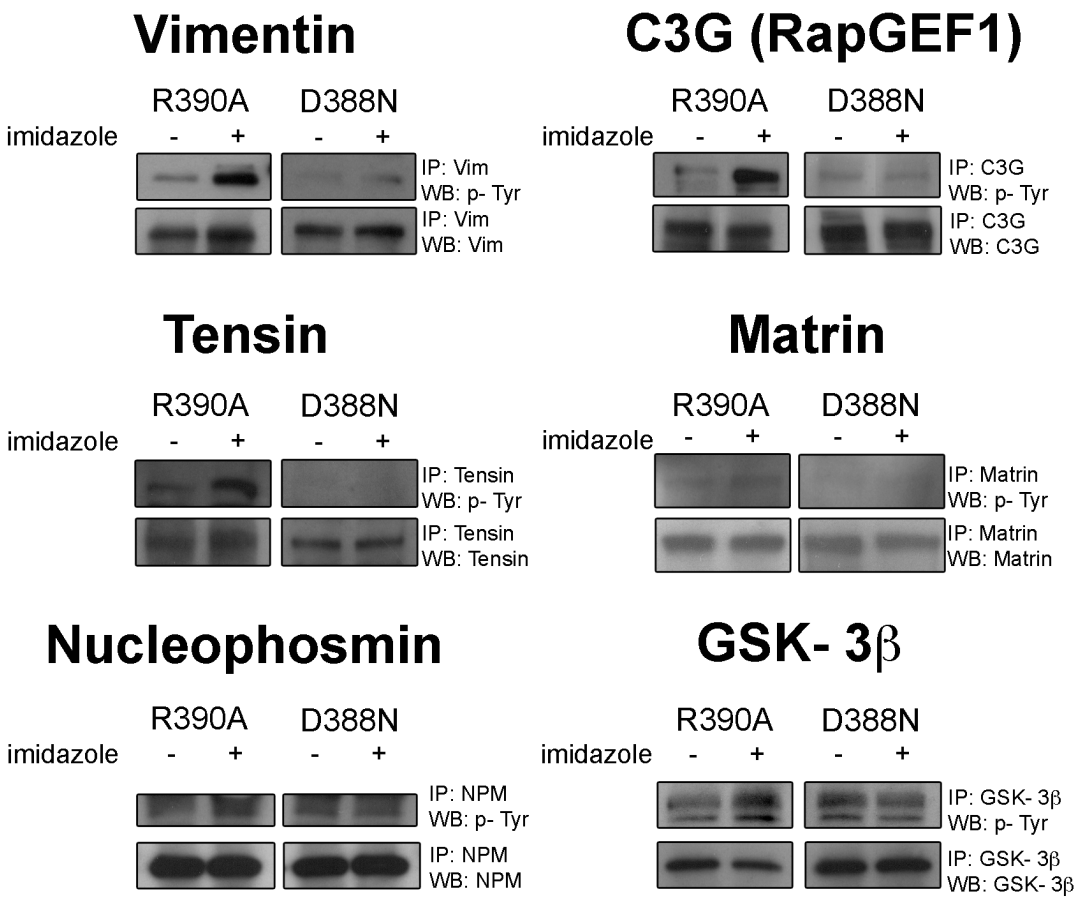

Figure 28. Validation of six identified potential novel c-Src substrates

Validation of protein phosphorylation by immunoprecipitation- immunoblot analysis of R390A and D388N c-Src SYF cells after treatment with 10 mM for 5 min. Immunoprecipitation was carried out with commercially available antibodies corresponding to the protein of interest and immunoblotting was carried out with the 4G10 pTyr- antibody as well as protein-specific antibodies. The blots were performed at least twice for R390A/ SYF MEF cells, except for matrin 3 and tensin where n=1. The blots were performed at least twice for D388N/ SYF MEF cells, except for matrin 3 and tensin where n=1.

validation with alternative methodologies to confirm the possibility that matrin 3 is a potential downstream target of c-Src.

In fact, I would like to pay special attention to matrin 3. Matrin 3 was identified as one of the proteins that experienced an increase in its tyrosine phosphorylation level upon c-Src chemical rescue. The mass spectrometry data evidencing the identification and quantification of this protein is shown in **Appendix 1 Figure 1** (MS/MS) and **Appendix 1 Figure 2** (MS). Since matrin 3's validation was particularly challenging, the procedure, results and interpretation have been thoroughly developed in the Appendix 1, created exclusively with the purpose of presenting the data obtained in an extensive and clear manner. See Appendix 1 for further details.

3.4. Phosphosite mapping by chemical rescue of mutant c-Src

Given the positive outcome of our preliminary attempt to combine c-Src chemical rescue and phosphoproteomics, we decided to perform an extensive phosphopeptide mapping

and quantitation of phosphorylation changes in the cell upon c-Src rescue. The protocol described above for quantitative analysis of protein tyrosine phosphorylation was modified such that trypsin proteolysis of extracted proteins was performed prior to affinity based enrichment with anti-phosphotyrosine antibody **(Figure 29)**.

As described above, three biological replicates and two technical replicates were

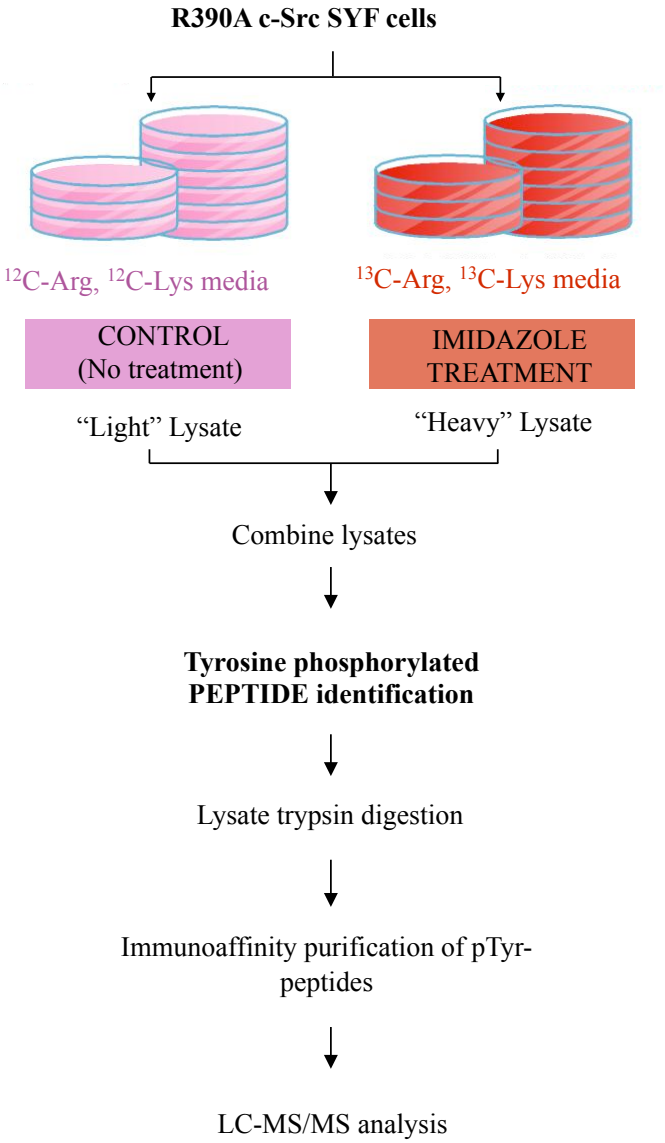

Figure 29. Scheme of the experimental design of SILAC-based quantitative phosphoproteomic approach. Peptide level

SYF MEF cells stably transfected with R390A c-Src were divided into two populations that were grown in 'light' or 'heavy' medium. The population of cells cultured in 'heavy' medium was treated with 10 mM imidazole for 5 minutes and the one cultured in 'light' media was left untreated. Cell lysates were combined in equal proportions. The protein

mixture was first digested with trypsin and then incubated with anti-phosphotyrosine antibodies for enrichment of tyrosine- phosphorylated peptides. The enriched sample was analyzed by LC- MS/MS.

performed and analyzed using high resolution, high accuracy mass spectrometry (189). Mascot and Sequest led to the identification of an initial list of 9,187 tyrosine phosphopeptides spectrum matches (corresponding to 205 proteins). These translated into a list of 335 non-redundant peptide sequences (corresponding to 205 proteins). In parallel, the quantitative proteomics software MaxQuant led to the identification of an initial list of 931 tyrosine phosphopeptide spectrum matches (corresponding to 147 proteins). The tables containing all this information and raw data associated with the phosphopetide screening were uploaded to ProteomeCommons.org Tranche where they can be downloaded from, http://proteomecommons.org/tranche/, using the following hash code:04W8a1fu+GSc7GMzdx0PJMaHuN+TEK8OpXcdzz07rrnT9h7USvqudUouF1vSinkQgXwrp+SA6WuF5IBCwMuF4oCtFDgAAAAAAAAJSg==.

Combining the two sets of data, we assembled a proteome comprising 382 non-redundant peptide sequences, corresponding to 334 tyrosine phosphorylation sites on 213 proteins **(Table 6)**.

We again set a threshold value of 1.2-fold for SILAC ratio (heavy vs. light ≥ 1.2) to filter for tyrosine-containing peptides with increased phosphorylation level upon c-Src rescue. A high-confidence data set of quantified phosphotyrosine peptides was obtained through a four filtering criteria described in the Methods section. After manual validation we obtained a list of 97 non-redundant peptide sequences, revealing 85 tyrosine phosphorylation sites (corresponding to 52 proteins), as upregulated in response to chemical rescue of c-Src, suggesting that they may be downstream c-Src targets. A

complete list of the mapped proteins with sites showing an increased phosphorylation level upon c-Src chemical rescue is provided in **(Table 8)**.

Several of these sites were identified in proteins that also showed an increased phosphorylation level at the protein level (such as C3G, tensin 1, Pard3 and Lpp), adding further confidence to their significance. The proteins containing the tyrosine residues which showed an increased phosphorylation level upon c-Src rescue can be classified into several categories **(Figure 30)** including actin modeling, adaptor/scaffold, adhesion, guanine exchange factors/GTPase-activating proteins, non-receptor protein kinases, phosphatases, cell polarity, receptor tyrosine kinases, and a group of proteins with diverse functionalities.

We analyzed the c-Src upregulated phosphoproteome with the Ingenuity Pathways Knowledge Software (Ingenuity ® Systems, http://www.ingenuity.com) and looked for enrichment of both canonical pathways **(Figure 31. A)** and ontology **(Figure 31.B)**. Not surprisingly two of the most enriched pathways are the integrin and the focal adhesion signaling pathways. The 'cellular movement' category appears to be the functionality that is especially impacted upon c-Src activation. The combination of integrin-mediated focal adhesion formation and adherens junction formation and focal adhesion disassembly (turnover) mediate cellular motility and are involved in cancer invasiveness and progression (51). A significant proportion of the identified sites are involved in cell adhesion, particularly in focal adhesion regulation, where c-Src plays a key role (190,191). In this context, several phosphosites are found in potential novel c-Src substrates. Also, novel sites in well-established c-Src substrates show an increased tyrosine phosphorylation level **(Figure 32)**.

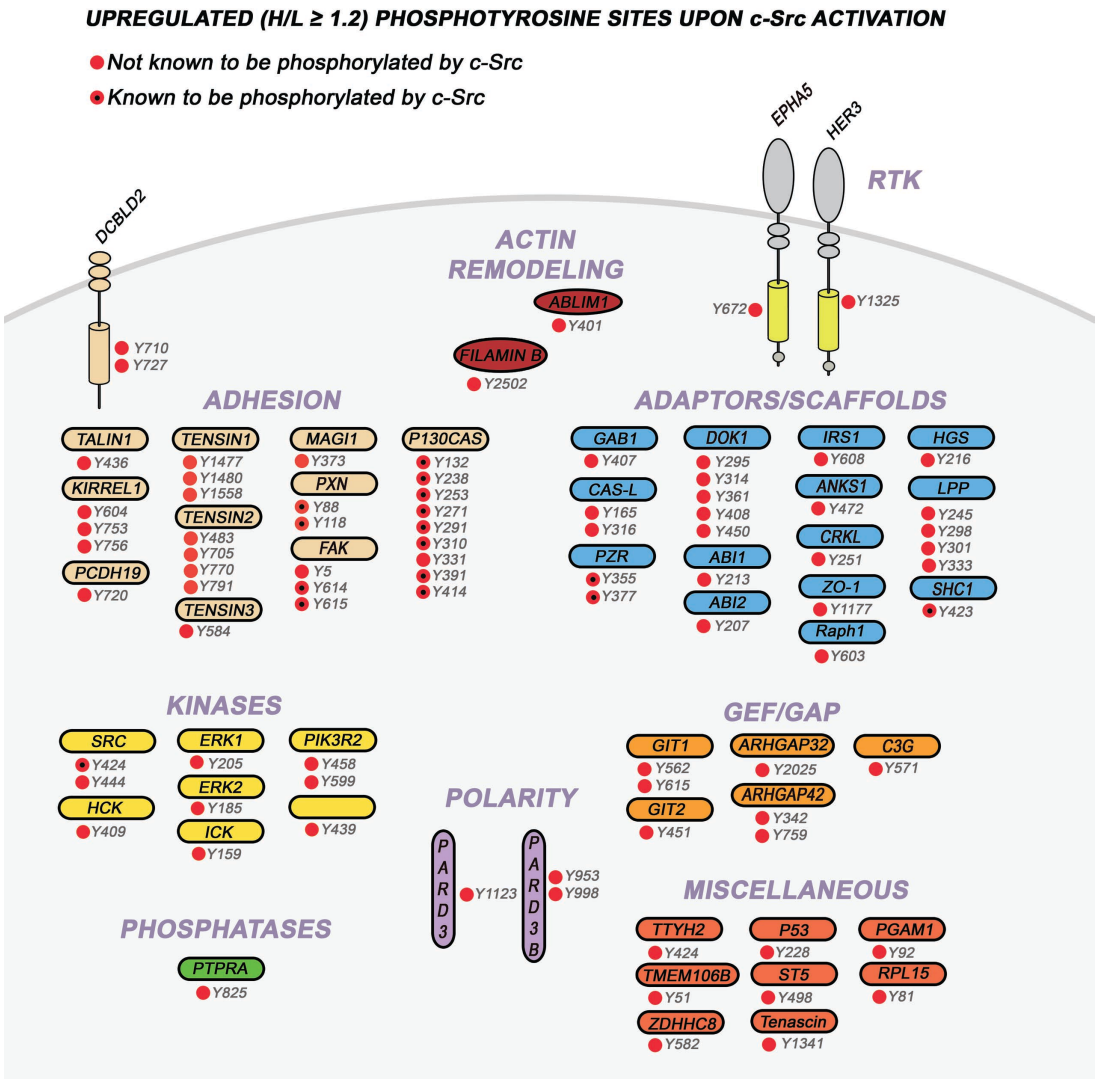

Figure 30. Overview of identified phosphopeptides with upregulated tyrosine phosphorylation upon c-Src rescue in R390A c-Src SYF MEF cells

All the detected upregulated phosphopeptides are shown whether they are novel (red) or known (red and black dot) c-Src substrate sites. As shown, the corresponding proteins span a wide variety of cellular functions, such as polarity, actin remodeling, adaptors, kinases, phosphatases, GEF/GAP proteins.

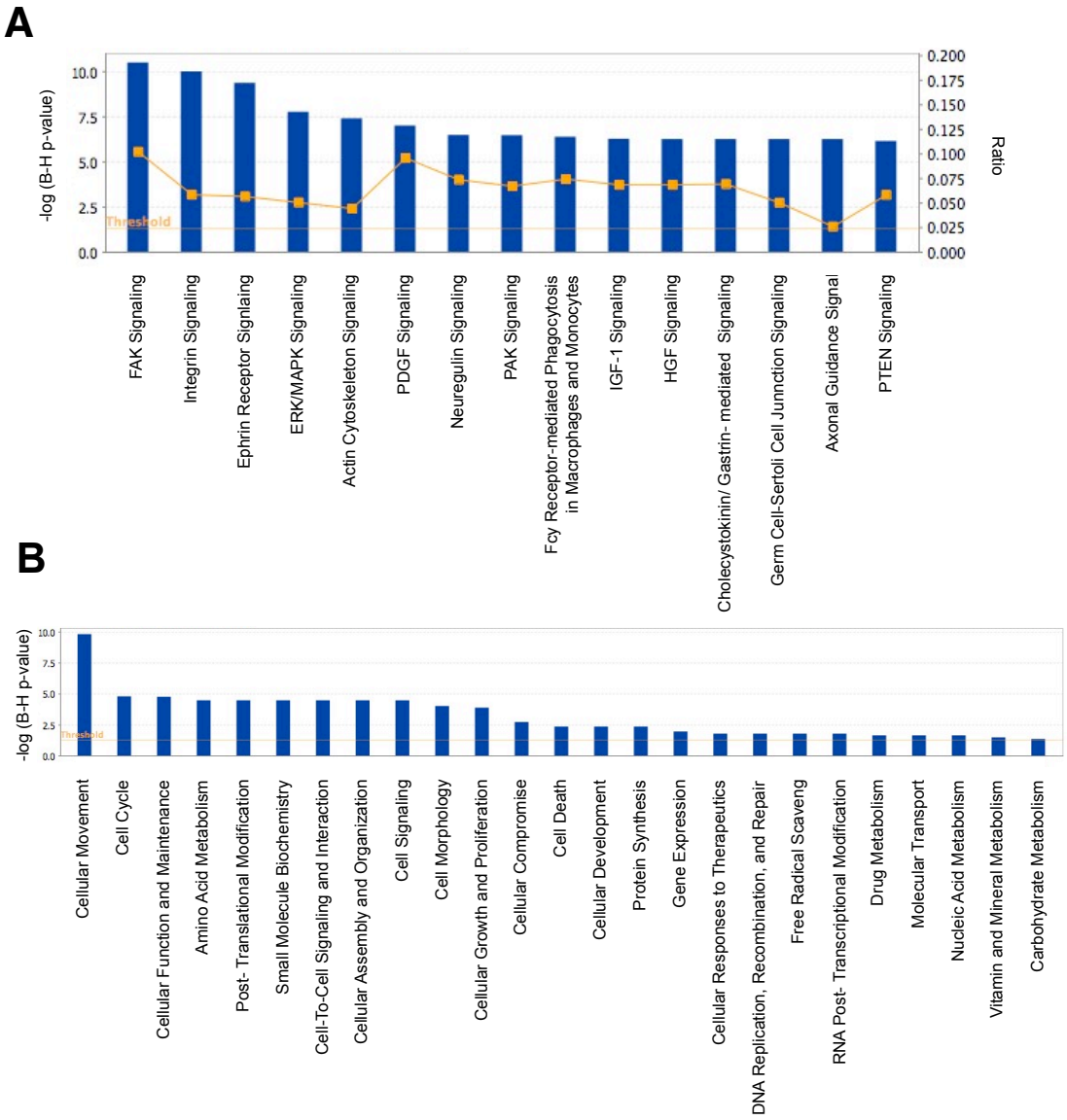

Figure 31. Ingenuity Pathway analysis of the c-Src upregulated phosphoproteome

A. Enrichment plots of canonical pathways (x-axis) built on the list of 52 c-Src upregulated phosphoproteins. The right y-axis (line) represents the percentage enrichment (ratio between the number of c-Src upregulated proteins and the total number of proteins included in the pathway). The left y-axis (bars) represents the significance of the enrichment, which was calculated using the Benjiamini-Hochberg multiple testing correction, as $-\log_{10}$ of *P*-values. From the complete list of pathways obtained from the list of the c-Src upregulated phosphoproteins by Ingenuity Systems, the ones with a value of –log (BH-*P*) ≥ 6 are represented. **B.** Enrichment plots of ontology (x-axis) built on the list of 52 c-Src upregulated

phosphoproteins. The y-axis represents the significance of the enrichment, which was calculated using the Benjiamini-Hochberg multiple testing correction, as $-\log_{10}$ of *P*-values.

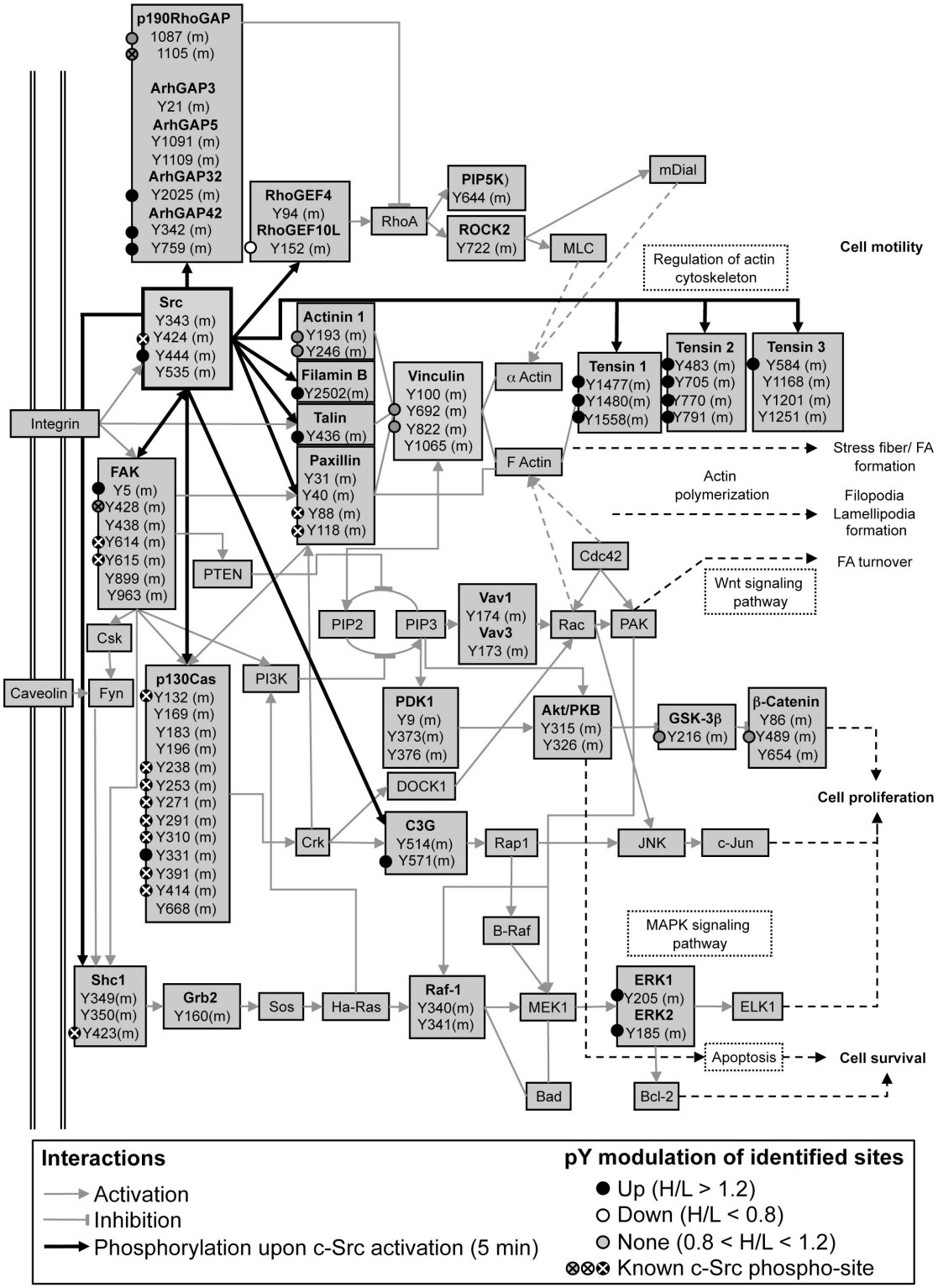

Figure 32. Role of c-Src in focal adhesion signaling

The signaling pathways involved in focal adhesion activation by integrins and the resulting downstream signaling events are represented. The biological functions resulting from focal adhesions are also summarized. For each of the proteins involved the sites that are known substrates of c-Src are indicated. The modulation of phosphotyrosine sites that were identified in our experiment is indicated as significantly increased (black), not modulated (gray), or decreased (white). Among the identified sites some are known c-Src substrates (marked with an "X").

Although the tyrosine phosphoproteome provided here is not likely to include the entire c-Src phosphoproteome, it is the first snapshot of the tyrosine phosphorylation events that take place immediately (5 minutes) after c-Src specific activation and the first one that has been obtained through high-resolution, high accuracy mass spectrometry.

Discussion

As described above, previous studies have focused on the proteomic analysis of oncogenic v-Src and other dysregulated Src mutants (134,172,173), which may respond very differently to wild type c-Src in a cellular context. Moreover, some of these studies have examined tyrosine phosphorylation patterns several hours or even days after Src is expressed, allowing chronic changes in phosphoproteins to be determined. Such analyses are well-suited to identification of possible biomarkers in v-Src expressing tumors, which appear to be very rare, but likely reflect many secondary changes in cellular protein levels relating to Src's well established effects on growth and gene expression.

The most recent study on Src proteomics did focus on cellular c-Src's kinase action in response to treatment with SU6656 inhibitor and posterior stimulation with platelet-derived growth factor (PDGF) (175). Proteomic analysis after acute activation of tyrosine kinases by ligands such as growth factor have been particularly informative because they have revealed how a cascade of signaling is initiated in a temporal fashion. They also have provided information on how the kinase of study is involved in the

signaling pathways that are usually activated by such growth factors. However, this methodology is unlikely to reflect the effects of exclusively activating a single kinase.

In order to identify direct or temporally connected substrates of the proto-oncogene c-Src, it would be ideal to use a method to rapidly and specifically switch on c-Src activity in the cell. In contrast to receptor tyrosine kinases, most non-receptor tyrosine kinases cannot be readily controlled in this fashion. However, the chemical rescue of the R390A c-Src mutant provides a strategy that nicely fits this purpose since it provides a rapid, specific and reversible mechanism of c-Src activation, permitting the detection of the immediate effects of the restored c-Src activity in live cells (134).

Combining the power of chemical rescue with a proteomics approach that incorporates tyrosine-phosphorylated protein enrichment led to the identification of 28 potential novel c-Src protein substrates. When the enrichment was done at the peptide level, we were able to identify 85 potential novel tyrosine phosphorylation sites (corresponding to 52 proteins), which showed an increased phosphorylation level upon c-Src rescue. It is reassuring that several of the putative protein substrates of c-Src that we have uncovered in this work have been linked to Src in prior studies. However, only 16 of the proteins found here using c-Src rescue were found among the 140 putative Src kinase targets identified in a combined list **(Table 8)** of the four prior mass spec phosphoproteomics studies (134,172,173,175) reported previously. The lack of greater overlap is likely due in part to the divergent experimental approaches.

It should be noted that even chemical rescue cannot unequivocally assign a protein as a direct kinase substrate of c-Src since the changes in phosphorylation we see can result from secondary effects, which can happen within the time frame used in our

observations (5 minutes). Indeed, the class of proteins that show a decrease in tyrosine phosphorylation likely reflects examples of a secondary phenomenon where a protein tyrosine phosphatase is activated by phosphorylation. For example, protein tyrosine phosphatases SHP1 and SHP2 are known to be activated by tyrosine phosphorylation and such a mechanism could contribute to specific dephosphorylation events (192,193). Nevertheless, in order to define the characteristics of signaling networks, it is helpful to elucidate the temporal connections among phosphoprotein changes, even if the protein interactions are indirect.

Activation of c-Src by growth factors or activating mutations leads to increased cellular proliferation, invasion and motility and decreased cell-cell (adherens junctions) and cell-matrix adhesion (focal adhesions) (51). As revealed by the Ingenuity analysis **(Figure 31)**, a significant number of the phosphopeptides detected in our chemical rescue analysis are involved in cell adhesion and, in particular, in focal adhesion pathways **(Figure 32)**. C-Src is known to play a role in the regulation and disassembly of focal adhesions, which link the extracellular matrix to the actin cytoskeleton (194) and are also involved in signaling pathways that regulate proliferation and gene transcription (195). Our work here provides a number of possible novel connections between c-Src and focal adhesion pathways. A network map that includes the role of c-Src in focal adhesions and highlights the novel proteins and phosphopeptides identified in our study is shown in **Figure 32**.

Focal adhesions form when integrin connects the ECM to a complex of proteins that act as a link between integrins and the actin cytoskeleton. These supramolecular complexes include structural cytoskeletal proteins like talin, vinculin and alpha-actinin,

as well as signaling molecules, including c-Src, FAK, p130Cas and paxillin (196). In fact, focal adhesions serve at least two significant cellular functions: transmitting force at adhesion sites in order to maintain strong attachments to the underlying ECM and acting as signaling centers from which several intracellular pathways originate and are involved in cell growth, survival and gene expression (197,198). Several tyrosine sites from cytoskeletal proteins that are part of this supramolecular structure and have not previously been described as c-Src substrates experienced an increase in their phosphorylation level include talin (Tyr-436), filamin B (Tyr-2502), tensin 1 (Tyr-1477, Tyr-1480, Tyr-1558), and tensin2 (Tyr-483, Tyr-705, Tyr-770, Tyr-791). Tensin 3 is a recently discovered c-Src target (199) but the site found in this study, Tyr-584, has never been shown to be phosphorylated by c-Src.

Regarding the effects of c-Src on the signaling molecules mentioned above, our study led also to interesting findings about potential novel c-Src tyrosine phosphorylation sites. C-Src is known to autophosphorylate on site Tyr-424 leading to an increase in its activation. We were able to detect this site, which indeed showed an increase in phosphorylation. However, we also identified a second phosphorylation site within the catalytic domain, Tyr-444 that was also detected in a previous study (173) and has no known role in Src activity or binding with other partners. It is established that c-Src phosphorylates and activates FAK at sites Tyr-614 and Tyr-615 promoting maximal FAK catalytic activity (200). Interestingly we detected a new FAK phosphorylation site, Tyr-5, which underwent a c-Src mediated increase in phosphorylation and has never been identified as a c-Src substrate. Similarly, p130Cas is a well-known substrate of active FAK-Src. Several known sites and a new phosphorylation site, Tyr-331, showed an

increased phosphorylation level upon c-Src rescue.

The activation of the small GTP binding protein RhoA is one of the key events of focal-adhesion assembly (201). C-Src blocks downstream signalling by RhoA through activation of p190-RhoGAP, leading to focal-adhesion disruption and increased motility. In this manner, c-Src regulates EGF-dependent actin cytoskeleton reorganization through phoshorylation of p190-RhoGAP (202). Two other RhoGAPs are known to be phosphorylated by c-Src: RhoGAP3 (Tyr-21 (203)), and RhoGAP5 (204) (Tyr-1091, 1109). Interestingly, we detected two other RhoGAPs that have never been described as c-Src substrates: RhoGAP42 (Tyr-342-unknown; Tyr-759-unknown) and RhoGAP32 (Tyr-2025-unknown).

Among other new sites identified, one is particularly worth mentioning since we will focus on its connection with c-Src through the next chapter. Previous studies have shown a correlation between C3G phosphorylation and different potential tyrosine kinases, including Src family kinases (205-207). However, we believe it is the first time that such a temporarily connected correlation has been established between c-Src and C3G in living cells. This connection was established through the above proteomic approach and revealed an increase in phosphorylation of the C3G protein, as well as a new site (Tyr-571), that has a remarkably high SILAC ratio upon c-Src chemical rescue. In addition, the work described in the next chapter has further explored the connection between c-Src-mediated C3G's phosphorylation, its activation and the consequent ramifications in c-Src-Crk-C3G-Rap1 signaling.

CHAPTER 3: THE ROLE OF C-SRC IN THE PHOSPHORYLATION AND ACTIVATION OF C3G

1. Introduction

1.1. C3G

C3G (for Crk SH3 domain-binding guanine nucleotide-releasing factor) or Rap1 guanine exchage factor (Rap1GEF) is a guanine nucleotide exchange factor for the small G-proteins Rap1, Rap2, and R-Ras (208, 209). C3G was first identified as one of two major proteins that bind the SH3 domain of the adaptor Crk (210, 211). A 4.1-kb C3G cDNA containing a 3.2-kb open reading frame encodes a 121-kDa protein that has three major types of domains **(Figure 33)**. The C-terminal domain catalyzes the guanine-nucleotide exchange reaction for Rap1, a Ras family protein (208). Mutational analysis of C3G revealed that a 50-amino acid central region containing a proline-rich sequence is responsible for binding to Crk's SH3 domain (211). The function of the amino-terminal region of C3G remains incompletely understood but p130Cas, a major Crk SH2-binding protein, binds this region *in vitro* (212).

C3G, among other guanine exchange factors, is responsible for stimulating the dissociation of bound GDP and binding of GTP to Rap1 (208) and Rap2 (213).

1.2. p130cas

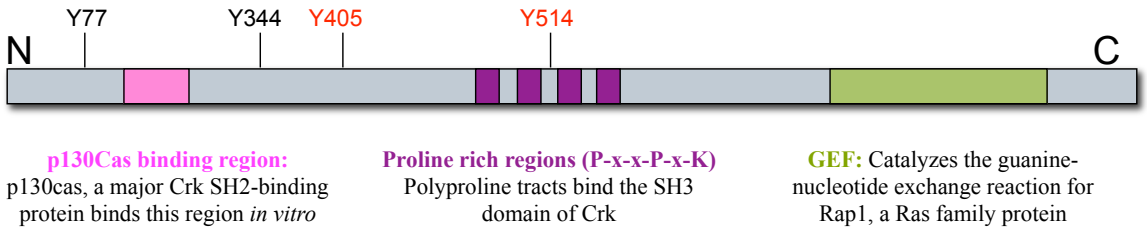

Figure 33. C3G domain structure

The amino-terminal is known to bind p130Cas. The central region contains a proline-rich sequence that binds the SH3 domain of Crk. The carboxyl-terminal domain catalyzes the guanine-nucleotide exchange reaction for Rap1.

p130Cas (Cas; crk-associated substrate) was identified as a highly phosphorylated protein of 130 kDa in v-Src and v-Crk transformed rat 3Y1 fibroblasts (214). p130Cas is a docking molecule that contains one NH_2-terminal SH3 domain followed by a stretch of proline-rich sequences, a central substrate domain composed of a cluster of potential SH2-binding sites, and a COOH-terminal domain which contains consensus binding sites for the SH3 and SH2 domains of c-Src (215). The SH3 domain is known to bind focal adhesion kinase (FAK) (216) among other molecules, but C3G was also identified as a direct interactor both *in vitro* and *in vivo*. Analysis of several mutants revealed a proline-rich Cas-binding site located NH_2-terminal of C3G. The site is defined by the consensus sequence XXPXKPX, which is recognized by the p130Cas SH3 domain. As a docking molecule, p130Cas may serve to bring C3G to specific compartments within the cell (212).

1.3. Crk

v-crk was identified first as an oncogene of CT10 avian sarcoma virus (10). Crk belongs to a group of adaptor-type SH2-containing molecules, together with GRB2/ASH and Nck proteins. The human *crk* gene is translated into two products by alternative mRNA splicing, CrkI and CrkII (217). v-Crk, its cellular homologs Crk II, Crk I, and the paralog CrkL, constitute a class of regulatory proteins that function as adaptors. These adaptors contain SH2 and SH3 domains that participate in the assembly of multiprotein complexes and act as convergence points in tyrosine kinase signaling (218). **Figure 34** shows the structure of the Crk family of proteins. The domains are boxed: SH2; SH3;

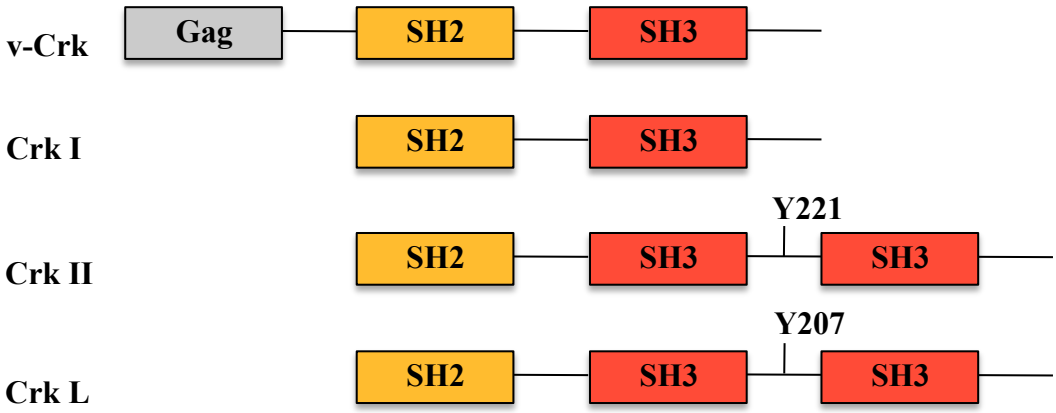

Adapted from Birge RB *et al*. Cell Commun Signal, 2009

Figure 34. Crk domain structure

v-Crk is a viral protein containing a Gag, SH2 and SH3 domains. There are two splice forms of huan Crk, CrkI (containing one SH2 domain and one SH3 domain) and CrkII (containing one SH2 domain and two SH3 domains). The paralog CrkL shares CrkII's domain structure.

Gag, viral group specific antigen.

The SH2 domain of Crk binds to phosphotyrosine-containing proteins such as paxillin and p130Cas (214,218). Two major proteins bound to the amino-terminal SH3 Domain, SH3(N), have been identified as C3G and DOCK180. Apart from these major binding proteins, Abl family tyrosine kinases and Sos, a guanine nucleotide exchange protein for Ras, are also known to bind to SH3 (N) (219-223).

A peculiar feature of Crk (CrkII) is that unlike other adaptor proteins such as Grb2 and Nck, CrkII itself is phosphorylated on tyrosine. Tyr-221 (Crk) or Tyr-207 (CrkL) are negative regulatory phosphorylation sites. Crk is negatively regulated by tyrosine phosphorylation on Tyr-221, which occurs as a result of various types of stimulation. C-Abl kinase binds to the first Crk SH3 domain and is proposed to phosphorylated Crk on Tyr-221 (**Figure 35**). The phosphorylation of c-Crk Tyr-221 creates a binding site for the Crk SH2 domain. c-Crk lacking phosphorylation on Tyr-221 can bind specifically to several proteins. It is likely that protein-binding activity of Crk is regulated by a mechanism similar to that of the Src family kinases. The intramolecular binding of phosphorylated Tyr-221 to the SH2 domain blocks SH3 (1)- dependent protein binding. The activation of Crk may be linked to the action of a cellular phosphatase. Once the first SH3 domain is unmasked, Crk forms a complex with specific proteins. It is currently unknown if the Crk SH2 domain has more than a negative regulatory function *in vivo* and what the function of the second SH3 domain is (224).

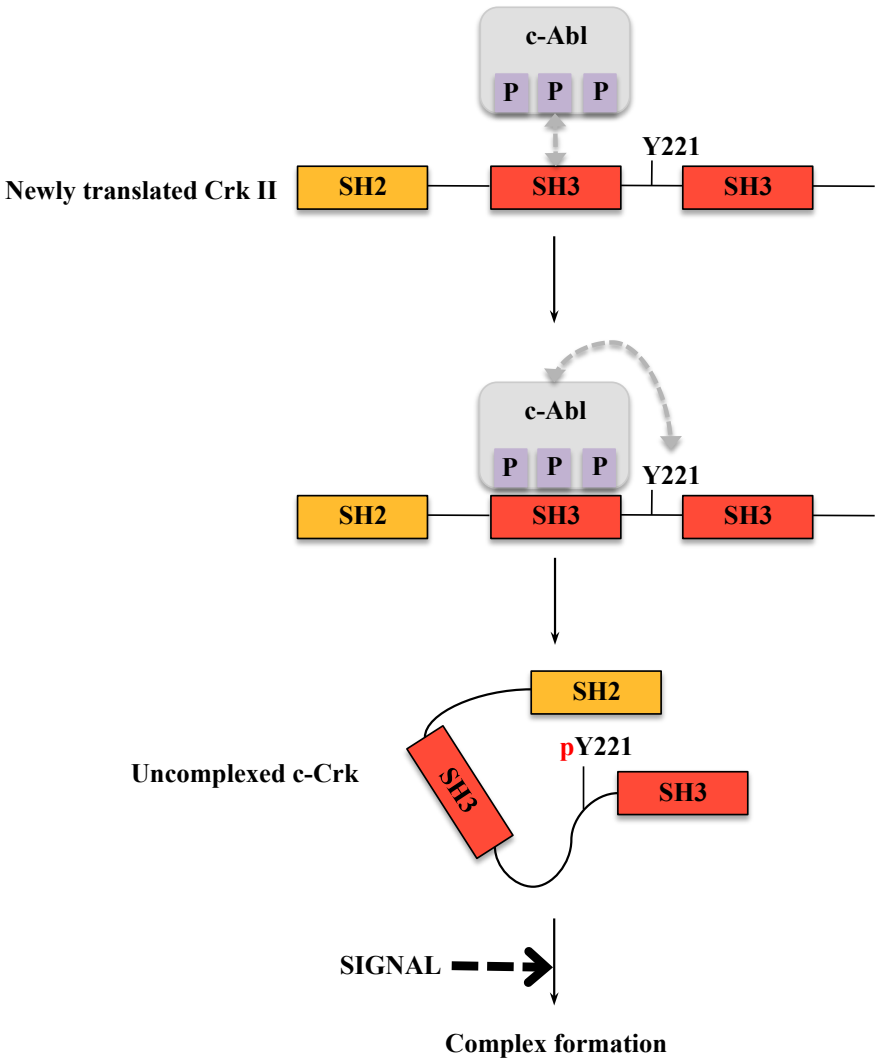

Adapted from Feller SM *et a*l. EMBO J, 1994

Figure 35. Crk negative regulation by phosphorylation on Tyr-221 by c-Abl

c-Abl binds to Crk's SH3 domain, facilitating phosphorylation of Crk on Tyr-221. Phosphorylated Tyr-221 binds intramolecularly to Crk's SH2 domain, regulating the ability of Crk to bind other proteins.

1.4. Rap1

Rap 1 is a small G-protein of the Ras family that antagonizes Ras activity by sequestering Raf-1, a common target, in the inactive form (224) and therefore competitively suppresses Ras-dependent transformation and ERK/ MAP kinase activation (225,226). Rap is implicated in a variety of biological processes that affect the cytoskeleton, adhesion molecules and/or intracellular trafficking. These functions of Rap include the regulation of integrin-mediated cell adhesion, cell–cell junction formation, establishment of cell polarity, exocytosis and cell proliferation (227).

Rap proteins have been shown to localize to multiple membrane compartments including the plasma membrane (PM), the perinuclear Golgi apparatus and endoplasmic reticulum, endocytic vesicles, secretory vesicles, and the nuclear envelope. Lipid modifications within the C-terminal tail are responsible for anchoring of Rap to the membrane (228). Rap is likely to be further compartmentalized at the membrane into distinct molecular complexes (229). The dynamic localization of Rap is partly controlled by post-translational modifications (228).

1.5. THE SRC-CRK-C3G-RAP1 PATHWAY

The members of the Crk family are not just conduits for intracellular signal transduction: they can also regulate the amplitude of signaling (230): Crk-mediated transformation leads to an increase in p130Cas-associated activity of Src family kinases

(SFK) (231), phosphorylation of FAK by SFKs, and the recruitment of PI3K to FAK (232,233). It has been shown that Crk overexpression in tumor cells induces an increase in the tyrosine phosphorylation of p130Cas and the activation of an intracellular feedback loop that further increases Crk activity with the consequent increase in motility of cancer cells signaling (230) **(Figure 36).**

1.6. C3G activation

1.6.1. C3G- Crk binding and membrane recruitment

C3G activation occurs mainly through membrane recruitment (205, 234). Binding to the Crk/ CrkL SH2 domains to newly generated target sites on activated receptors and their substrate proteins leads to a redistribution of C3G within the cell, presumably to sites where Rap 1 is located. In fact, the adaptor protein Crk has been identified to mediate Src-dependent Rap1 activation (235). Expression of Crk in COS cells leads to C3G activation concomitant with its translocation to the cell membrane.
Besides the relocation of this complex, some studies suggest Crk-C3G association itself may be regulated, thereby affecting downstream signaling (236). As described above, the binding sites of C3G for Crk and CrkL have been mapped as several P-x-x-P-x-K motifs in the center of the protein (237,238). CrkII is more abundant than CrkI in normal cells and is therefore the major adaptor for C3G (217). It was reported in a previous study that CrkII is constitutively associated with C3G (239). However, even though Crk and CrkL exist in constitutive complexes with C3G in many cell types, regulation of these

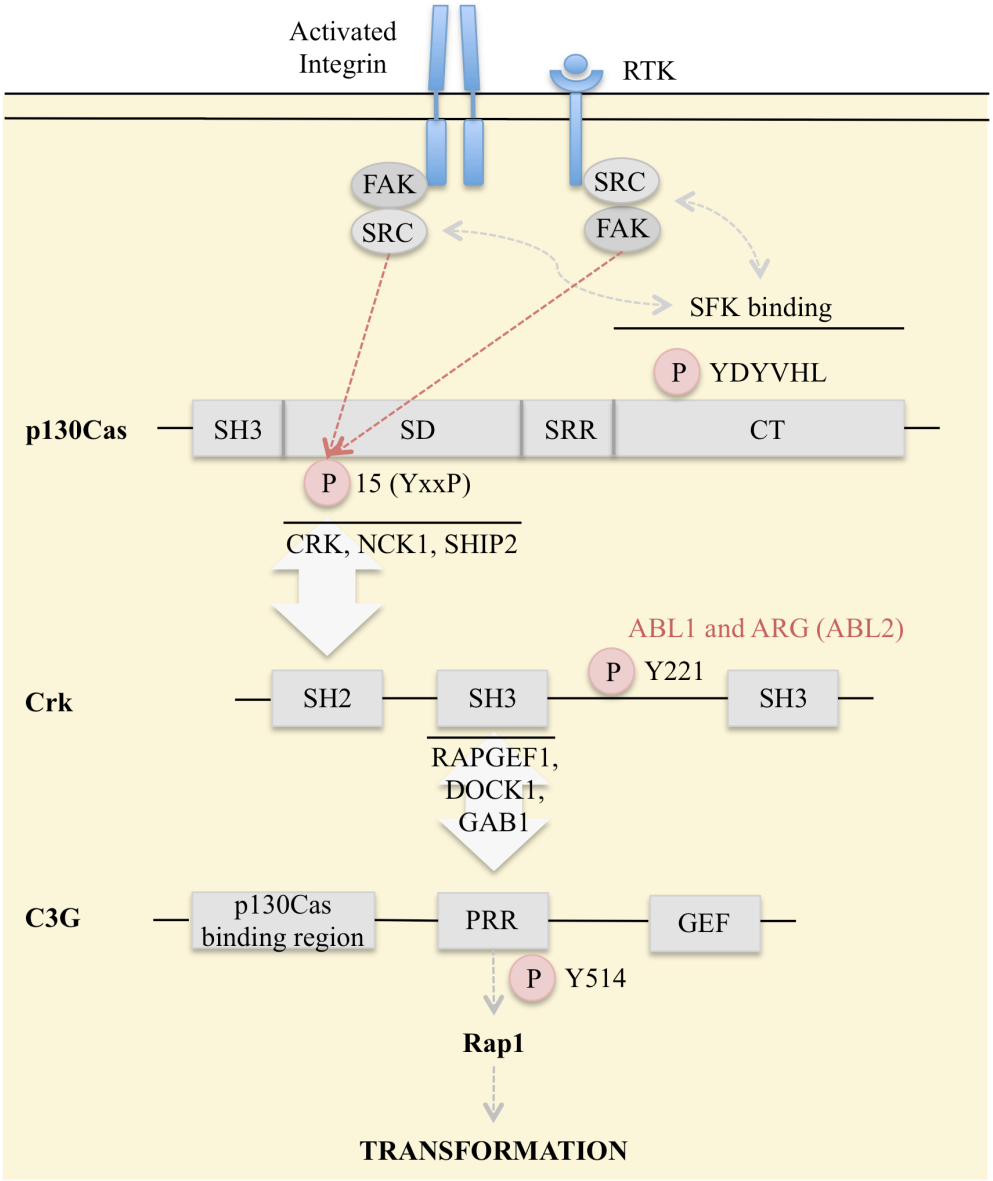

Adapted from Cabodu S, *et al*. Nature Reviews Cancer, 2010

Figure 36. The Src-Crk-C3G-Rap1 pathway

Growth factors activate RTKs. Crk's SH2 domain binds to activated receptors or newly tyrosine phosphorylated proteins, such as p130Cas. The SH3 domain of Crk binds proline-rich-effector molecules such as C3G, which is redistributed to sites where its effector, Rap1, is located. C3G is tyrosine-

phosphorylated on Tyr-514 and this phosphorylation is thought to regulate its activity. This event may occur when C3G is close to the membrane and in the vicinity of activated tyrosine kinases. Activated Rap1 recruits B-Raf, stimulating a signaling cascade. SFK: Src family kinases; SD: substrate domain; SRR: serine-rich region; CT: carboxy-terminal; PR: proline rich region; GEF: guanine exchange factor

complexes has also been reported in response to a variety of stimuli such as insulin receptor activation and integrin stimulation (236,240,241).

The requirement of the SH2 domain of Crk for the enhancement of guanine nucleotide exchange activity for Rap1 could be replaced by the addition of a farnesylation signal to Crk (234). These results suggest that Crk may be able to enhance the guanine nucleotide exchange activity of C3G by recruitment of C3G to the membrane.

1.6.2. C3G phosphorylation

Membrane recruitment may not be the sole mechanism of C3G activation by Crk. While a previous study showed that Crk did not stimulate the guanine nucleotide exchange activity of C3G for Rap1 *in vitro* (234), an indirect tyrosine phosphorylation mechanism has been proposed. It has been shown that an increase in the catalytic activity of C3G correlated with its tyrosine phosphorylation (206). In fact, C3G is the first example of a guanine nucleotide exchange factor for Ras family proteins that can be activated by tyrosine phosphorylation.

It has been observed that activation of C3G by CrkI expression is accompanied by C3G tyrosine phosphorylation, playing a significant role in the activation of C3G (242). Several growth factors and cytokines stimulate the recruitment of the Crk-C3G complex to the membrane where tyrosine kinases are located, such that a C3G tyrosine residue may phosphorylated with a resultant increase in its GEF activity (205,206).

A previous study constructed a series of C3G deletion mutants in order to understand the mechanism by which C3G is phosphorylated and activated by Crk (**Figure 37**) (206). This 1999 study described a negative regulatory region within C3G. Deletion of the amino-terminal third had been shown to activate C3G to the level of C3G co-expressed with Crk, strongly suggesting the presence of a cis-acting negative regulatory function in the noncatalytic domain of C3G (206). When C3G was truncated to amino acid 390 (C3G-delta390), C3G showed the same level of activity as wild-type C3G before and after Crk coexpression. Deletion of the amino terminus of C3G to amino acid 579 (C3G-d579) increased GTP-bound Rap1 to the level of wild-type C3G in the presence of Crk, irrespective of the presence of Crk. As a result, Ichiba *et al*. concluded that C3G-delta579 is a catalytically active form and the negative regulatory region is located between residues 391 and 579.

The Ichiba *et al*. study then defined the location of Crk-induced tyrosine phosphorylation. C3G-delta390 was still phosphorylated on tyrosine. C3G-d579 exhibited significant reduction in the Crk-dependent tyrosine phosphorylation. As a result, Ichiba et al. deduced that the tyrosine phosphorylation sites on C3G are located between residues 391 and 579. Integrin stimulation-dependent tyrosine phosphorylation of C3G had been reported (237) but the exact site had not been mapped. In order to do so, Ichiba et al. substituted all seven tyrosine residues in this region for phenylalanine. The C3G-Y504F mutant was remarkably less activated and phosphorylated than the wild type. All the other substitution mutants were activated and tyrosyl-phosphorylated after the expression of Crk. The authors conclude that CrkI activates C3G by the phosphorylation of tyrosine 504, which represses the cis-acting negative regulatory

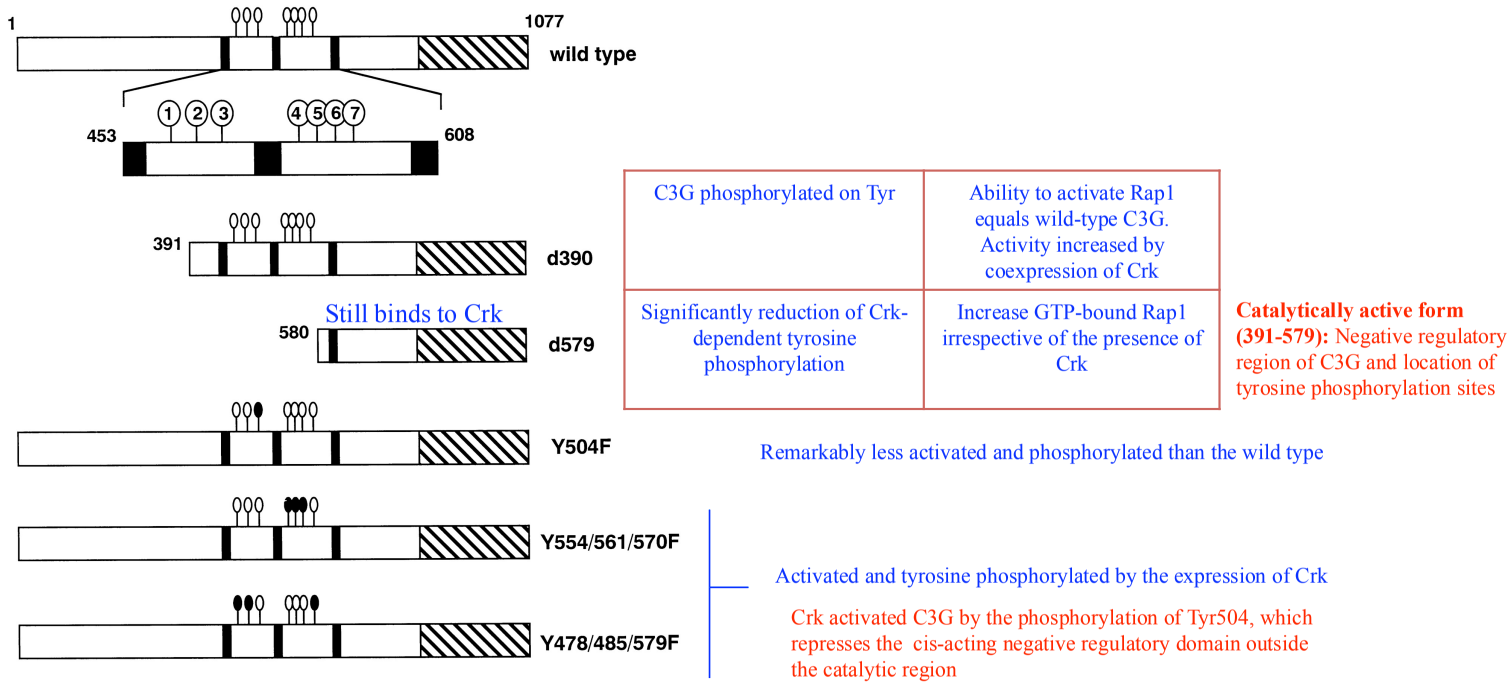

Adapted from Ichiba T, *et al.* J. Biol. Chem, 1999.

Figure 37. Mechanism of Crk-induced phosphorylation and activation of C3G

A series of C3G deletion mutants were created to investigate the mechanism by which C3G is phosphorylated and activated by Crk. The amino-terminal noncatalytic third was deleted (C3G-delta 390) and shown to activate C3G to the level of wild-type C3G before and after co-expressed with Crk. This suggests the presence of a cis-acting

C3G-delta 579 exhibited significant reduction in the Crk-dependent tyrosine phosphorylation, leading to the conclusion that the tyrosine phosphorylation sites are located between residues 391 and 579. All seven tyrosine residues in this region were substituted for phenylalanine. The C3G-Y504F mutant was substantially less activated and phosphorylated than the wild type whereas the other substitution mutants were activated and tyrosyl-phosphorylated after the expression of Crk. As a result, it was concluded that CrkI activates C3G by the phosphorylation of tyrosine 504 (tyrosine 514 in mice).

domain outside the catalytic region. When the amino-terminal region, including Y504 is deleted, the catalytic activity is intact. In wild type C3G, phosphorylation may be required for the suppression of cis-acting negative regulation. Previous studies have shown a correlation between C3G phosphorylation and activation of different potential tyrosine kinases: Activation of Src family kinase Hck increased C3G phosphorylation on Y504 (205). When NIH-3T3 cells were treated with growth hormone both JAK2 and c-Src were activated (239). Tyrosine phosphorylation of C3G occurs in cells transformed by v-Crk or v-Src. When C3G comes into the vicinity of activated tyrosine kinases, phosphorylation of the regulatory tyrosine residue (Y504) could occur, although prior to this thesis research, C3G-Y504 phosphorylation had so far only been observed in certain oncogene-transformed cells with hyperactive tyrosine kinases (206). Src-dependent Rap1 activation is indispensable for integrin-mediated cell adhesion and formation of focal adhesion structures (243).

Growth hormone treatment stimulates tyrosine phosphorylation of C3G, and the increased phosphorylation level of C3G observed in these conditions required the combined activities of both JAK2 and c-Src (244). However, a systematic analysis of kinases that may have contributed to this phosphorylation has not been completed.

In addition, a study showed that transfection of Src family kinases or pervanadate treatment of cells, which may mimic stimulation by growth factors, has also induced tyrosine phosphorylation of C3G at Y504 (207). Upon expression of Src family kinases or pervanadate treatment of cells, C3G phosphorylated on Y504 was predominantly located at the Golgi complex and the subcortical actin cytoskeleton unlike non-phosphorylated C3G, which was largely cytosolic (207).

1.6.3. C3G binding to p130Cas

p130Cas has been shown to bind directly to C3G (212). Pro-267 and Pro-270 of C3G are essential for the binding of the SH3 domain of p130Cas. When the prolines responsible for binding to the SH3 domain of p130Cas were deleted in the C3G-delta390 mutant described above, C3G could not be activated effectively by the expression of Crk, even though C3G-delta390 is tyrosyl-phosphorylated to a similar extent as the wild-type C3G. Therefore, binding of p130Cas may be required for optimal activation of C3G after the phosphorylation of Tyr 504 (206).

Therefore, there are three events that are hypothesized to occur in the process of C3G activation: C3G binding to Crk and consequent membrane recruitment, C3G phosphorylation, and C3G binding to p130Cas. All three events seem to contribute to C3G activation. However, the order or the possible connections between these events remains largely unknown.

2. Methods

2.1. Cell treatment and lysate preparation

R390A/SYF cells and D388N/SYF cells were serum-starved for 16 hours. Different dishes from each cell line were either treated with 10 mM imidazole, pH 7.5 for 5 minutes or left unstimulated and used as a control. Cells sets were then washed once

with ice cold PBS (Invitrogen) and immediately lysed in RIPA buffer (Tris-HCl 50 mM, pH 7.4, Na-deoxycholate 0.25%, NaCl 150 mM, EDTA 1mM, 1% NP-40, Na_3VO_4 1 mM, NaF 1 mM, PMSF 1 mM). The lysate was collected and transfer to pre-chilled micro centrifuge tubes. The tubes were placed in a rotor at 4ºC during 30 minutes. The lysate was cleared by centrifugation at 13,000 rpm for 15 min at 4ºC and the supernatant collected. Protein concentrations were calculated by the Bradford method.

2.2. Immunobloting and Immunoprecipitations

For immunobloting a volume of the lysate corresponding to 10-30 μg was mixed with SDS loading buffer with β-mercaptoethanol, boiled at 95ºC for 5 minutes, and analyzed by SDS-PAGE. The proteins were electroblotted into PVDFs membrane (Invitrogen) using the iBlot system (program 3/ 5.5 minutes). The membrane was blocked with 5% BSA in 1X TBST for one hour at room temperature. After a quick rinse in 1X TBST, the membrane was probed with appropriate primary antibody, followed by incubation with the correspondent HRP-conjugated secondary antibody. Antibodies were used at the recommended concentration in the manufacturer's instructions. Bands were visualized using SuperSignal West Pico chemiluminescent substrate (Pierce) and ECL film (GE Healthcare Amersham).

For immunoprecipitation, a volume corresponding to approximately 1 mg of lysate was cleared by incubating it with 40 μl of 50/50 protein A or G agarose magnetic bead slurry (Invitrogen) rotating for one hour at 4ºC. Using a magnet, the beads were separated from the supernatant. Beads were discarded and the supernatant was kept on

ice. 40 µl of 50/50 protein A or G agarose magnetic bead slurry were mixed with the volume of antibody corresponding to 10 µg 200 µl of RIPA modified buffer was added to facilitate mixing. Samples were incubated for one hour rotating at 4°C. Using a magnet, the bead-antibody complex was separated from the supernatant, which was discarded. The cleared lysate was added to the antibody-bead complex. Incubation was performed overnight rotating at 4ºC. Antibodies were used at the recommended concentration in the manufacturer's instructions. The beads were subsequently washed six times with RIPA buffer, resuspended in SDS loading buffer with beta-mercaptoethanol and heated at 95-100°C for 5 minutes. The eluates were analyzed by SDS-PAGE, electroblotted into PVDF membrane and subjected to Western blot analysis as described above.

Antibody against C3G (C3G WB), sc-15359 from Santa Cruz Biotechnology; antibody against Tyr(P)-514 of C3G isoforms (Tyr(P)-514-C3G WB), sc32621 from Santa Cruz Biotechnology; C3G IP/ Crk WB: sc-15359 (C3G IP and WB) from Santa Cruz Biotechnology and 610035BD (Crk WB) from BD Transduction Laboratories; Crk (pTyr-221) WB, ab76227 from Abcam. Antibody against tubulin (tubulin WB), ab44928 from Abcam. The results shown are representative of the tendency observed in different experimental repeats. It should be noted that the timing at which increases where detected was not always the exact same but it was similar, and the tendency of the signal intensity of the bands of interest was similar throughout the biological replicates obtained. It should also be noted that baseline values between rescuable and non-rescuable cells may not be the same due to subtle alterations in the cell passage number, growth conditions, or Western blot conditions (such as exposure time).

2.3. Immunofluorescence and Confocal Microscopy

Cells were seeded and grown in 8-well glass microscopy slides (Lab-Tek). Cells were processed for immunofluorescence staining in the following way: after imidazole treatment (10 mM, for 0, 1, 2.5, 5 and 10 minutes), cells were washed once with ice cold PBS. Cells were fixed with 4% formaldehyde (Tousimis Reserch Corporation) for 1 hour at 4°C followed by washing with 10 mM glycine in PBS. Permeabilization was performed with 0.1-0.2% (v/v) of Triton X 100 (or NP-40) in PBS for 5 minutes at room temperature. After washing with PBS, cells were incubated in blocking solution (10-20 mg/ml BSA in PBS) for 1 hour. The primary antibodies used were rabbit polyclonal antibody against C3G (sc-15359 from Santa Cruz Biotechnology) and rabbit polyclonal antibody against pTyr514-C3G (sc-32621 from Santa Cruz Biotechnology). The secondary antibodies used were Alexa-Fluor 555 goat anti-rabbit (A-21430 from Invitrogen) and Alexa-Fluor 488 chicken anti-rabbit (A-21441 from Invitrogen), respectively. The slides were mounted with ProLong® Gold Antifade Reagent (With DAPI) from Invitrogen. Samples were acquired with the Zeiss Meta Confocal Laser Scanning Microscope System, utilizing AIM software version 4.0. An argon laser excited at 488 nm and a red HeNe at 561 nm wavelengths was used to obtain optical sections. Narrow band emission filters (nm) were utilized to eliminate channel crosstalk and a 1.0 μm confocal aperture was used to obtain z-plane sections. Slides were imaged with a 40x and 100x oil immersion Plan Apochromat objective lens (N.A. 1.4) through a Zeiss Axiovert inverted microscope. For quantification, at least 40 cells were counted for each condition and scored according to whether or not they had peripheral staining

(Figure 38). Percent of cells with a peripheral staining was calculated for each 40x window. Averages and standard errors are shown and statistical analysis was done using the Student's t test.

2.4. FRET Microscopy

R390A and D388N c-Src SYF MEF cells were plated to glass bottom dishes (MatTech Corp.) and transiently transfected with 2 μg Raichu-Rap1 (**Figure 39**) (245) reporter using lipofectamine (Invitrogen). The cells were starved for 16 hours. After 15 hours cells were washed once and media was replaced with Hanks Balanced Salt Solution (HBSS). The dish was loaded onto the stage of an inverted Zeiss Axiovert 200M microscope controlled by METAFLUOR software (Universal Imaging, Downingtown, PA). Dual emission ratio imaging was performed using a 420DF20 excitation filter and a 450DRLP dichroic mirror and appropriate emission filters, 475DF40 for CFP and 535DF25 for YFP. Images were captured with a MicroMAX BFT512 CCD camera (Roper Scientific, Trenton, NJ). Baseline values were captured every 30 seconds for 2 minutes. Cells were treated with 10 mM imidazole at time zero and imaged for an additional 15-20 minutes. Images were quantified using the Metafluor software. Regions of interest were selected and average intensities of the pixels in each region for each channel were quantified. FRET ratios were calculated by dividing the yellow emission over the cyan emission at each time point.

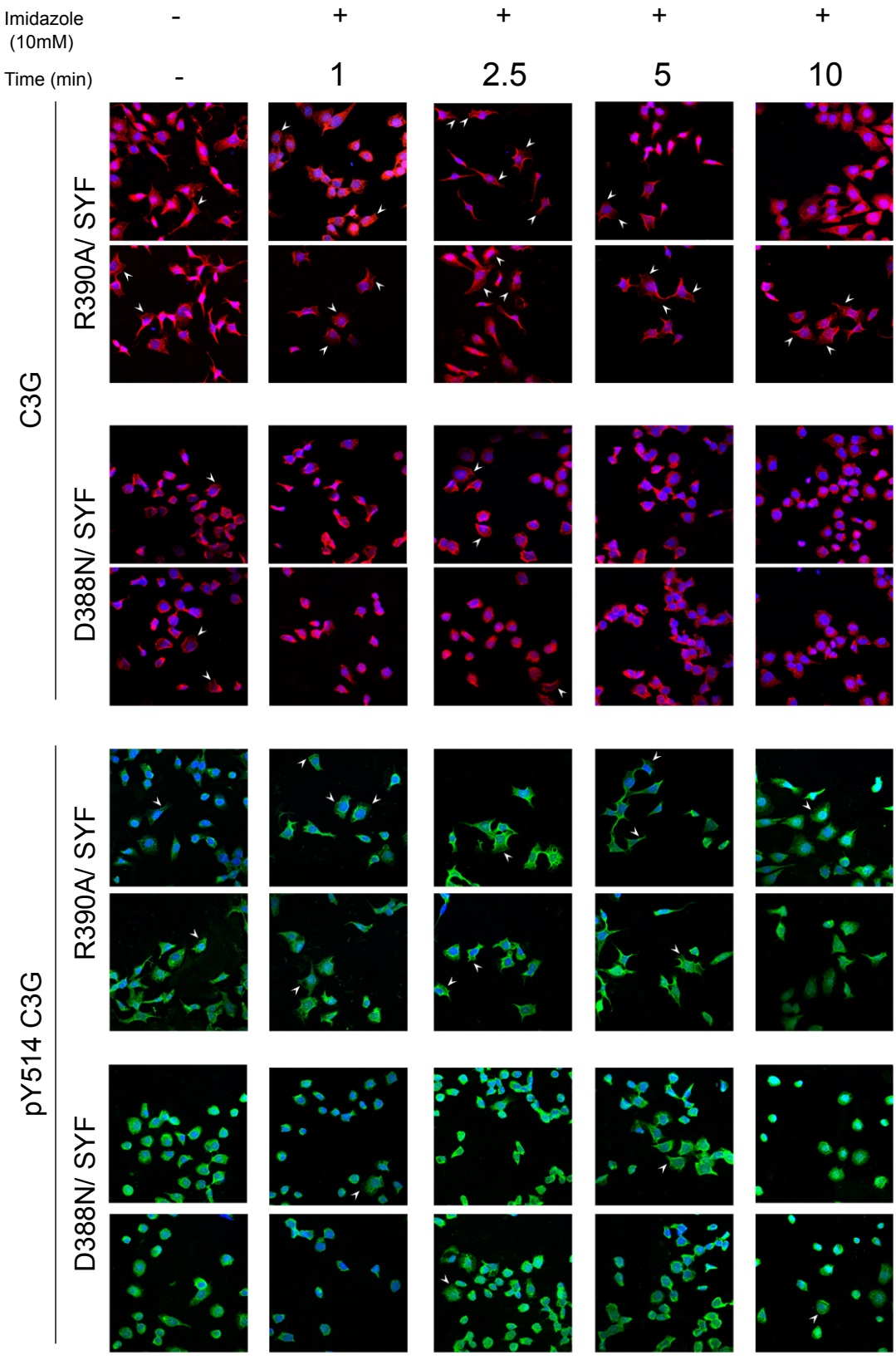

Figure 38. C3G and pTyr-514-C3G increased localization at the cell periphery after c-Src rescue

R390A/SYF and D388N/SYF cells were treated with 10 mM imidazole for 0,1,2.5,5, and 10 minutes and immunostained against C3G or pTyr-514-C3G. Two representative confocal microscopy images at 40X magnification are shown for each condition.

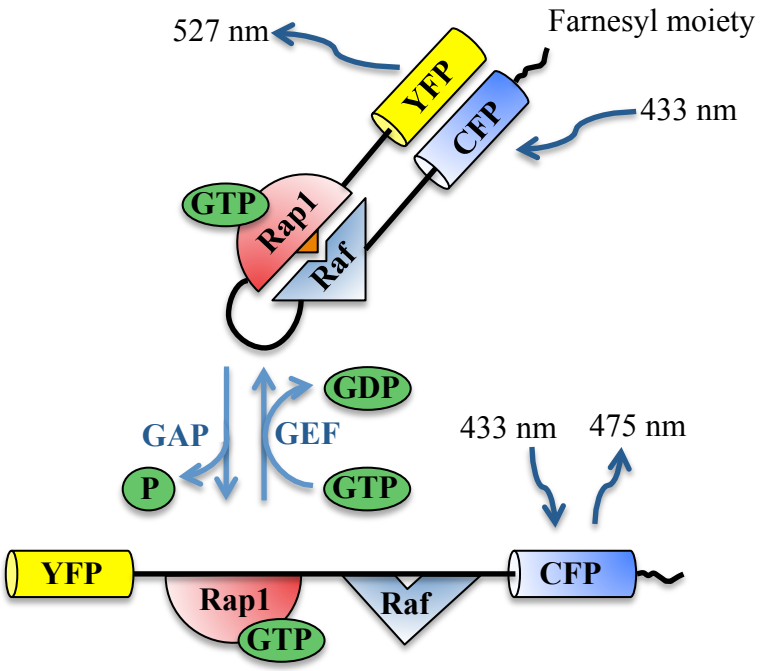

Adapted from Mochizuki N, *et al*. Nature, 2001

Figure 39. Schematic representation of the Raichu-Rap1 reporter bound to GDP or GTP

The difference in the FRET response allows evaluating the difference in the ability of C3G to activate Rap1.

3. Results

3.1. c-Src chemical rescue leads to Rap-1 activation

We had observed in our proteomics study that C3G level of phosphorylation increases upon c-Src rescue. As described above, it is known that phosphorylation of C3G leads to an increase in its guanine exchange factor activity. In order to functionally evaluate the potential effects of c-Src mediated phosphorylation of C3G on Rap1 in our system, we employed the cell-based reporter Raichu-Rap1 (245), which is designed to undergo a FRET change upon Rap1 activation.

As shown in **Figure 40**, imidazole treatment of R388A Src/SYF cells revealed that chemical rescue of c-Src rapidly stimulates Rap1, manifested as an increase of 10-11% FRET ratio. As a control, imidazole treatment of D386N Src/SYF cells did not show a significant increase.

Rap1 is known to localize to the Golgi, lysosomal vesicles and cortical actin cytoskeleton (246). Consistent with expectation, the apparent c-Src-induced activation of Rap1 was mostly observed at the cell periphery where filopodia were formed. Rap1 showed an increase in its activation level immediately after c-Src rescue, and reached the maximum level of activity 5 minutes after treatment.

Once we tested the effects of Src activation on Rap1 activity, we were interested in analyzing possible intermediate steps in a spatio-temporal manner that may contribute to C3G activation.

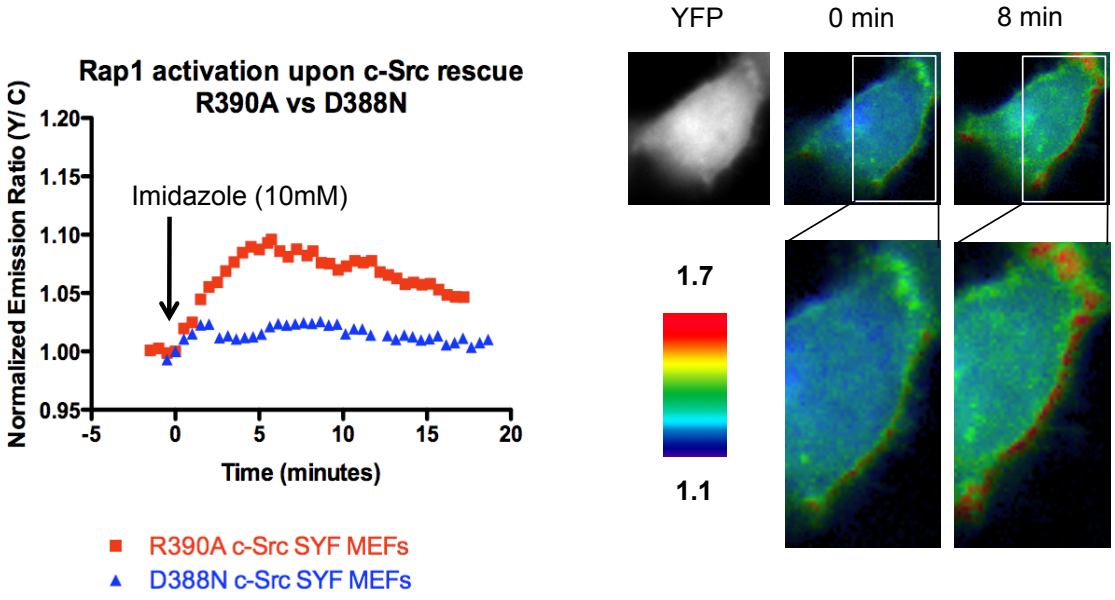

Figure 40. Detection of the effect of c-Src activation on C3G's ability to activate Rap1

Rap1 activation upon c-Src rescue in R390A c-Src SYF cells (red) and D388N c-Src SYF cells (blue). The FRET-based GTPase sensor, Raichu-Rap1 showed a 10% increase in FRET (Rap1activation indicator) along the cell membrane after 8 min of treatment with imidazole to rescue c-Src activity.

3.2. Effects of c-Src activation on C3G phosphorylation

As discussed above, we have previously detected increased phosphorylation levels of C3G in the cell after rescuing catalytically inactive c-Src. Based on previous reports where different members of the Src family of tyrosine kinases have shown an effect on C3G phosphorylation on Tyr-504 (human)/ Tyr-514 (mouse), we wanted to look for site-specific tyrosine phosphorylation with our chemical rescue approach. Using a commercially available anti pTyr514-C3G site-specific antibody, Western blot analysis revealed enhanced C3G modification with imidazole treatment of R388A Src/SYF cells, but not D386N Src/SYF cells (**Figure 41**).

This increase was observed within 1 minute of imidazole exposure, supporting the possibility of direct targeting of C3G by c-Src. It must be noted that we detected an increase in one band that corresponds to a slightly smaller molecular weight than the strong band usually observed when we perform a Western blot against C3G or an immunoprecipitation with C3G antibody followed by Western blot against C3G. However, in previous immunoprecipitation with C3G antibody followed by Western blot against C3G, we have also observed a weaker lower band at around 120 kDa and we suggest that it may corresponds to one of the different known C3G isoforms, which are known to exist as a result of alternative spliced transcript variants. **Figure 42** shows two biological replicates where the same observation was made. The figure includes the complete films obtained from Western blot experiments with the anti pTyr514-C3G site-specific antibody. The blot shows multiple bands suggesting that the antibody specificity may not be very strong. However, C3G has many isoforms and some of these bands

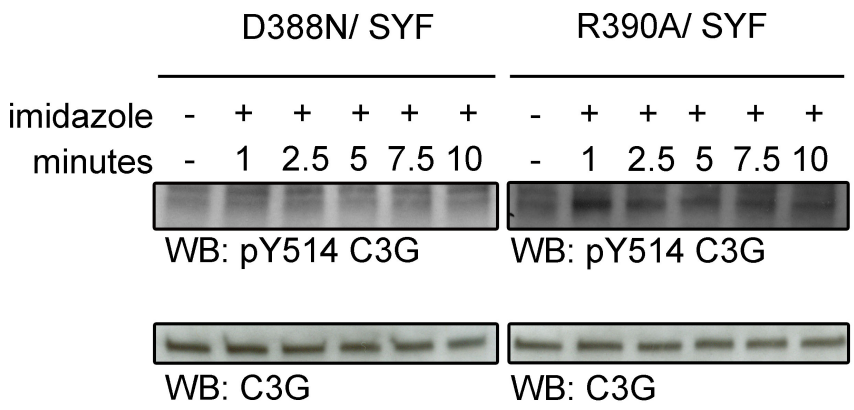

Figure 41. Detection of the effect of c-Src activation on C3G's phosphorylation on Tyr-514

Western blot using anti pTyr514-C3G antibody showed an increase in the phosphorylation level of tyrosine 514 in a C3G isoform after 1 minute upon c-Src rescue in R390A c-Src SYF cells but not in D388N c-Src SYF cells. From the several bands observed in the blot against pTyr514-C3G, we detected an increase in one band that corresponds to a slightly smaller molecular weight than the strongest band usually observed when we perform a Western blot against C3G or an immunoprecipitation with C3G antibody followed by Western blot against C3G. However, we have also observed a weaker band just bellow the strongest band in C3G immunoprecipitation and western blot that we understand corresponds to one of the different C3G isoforms. The molecular weights are indicated in the blot to illustrate this point. Western blot using an antibody against C3G shows equal loading along the different time points in both R390A c-Src SYF and D388N c-Src SYF cells.

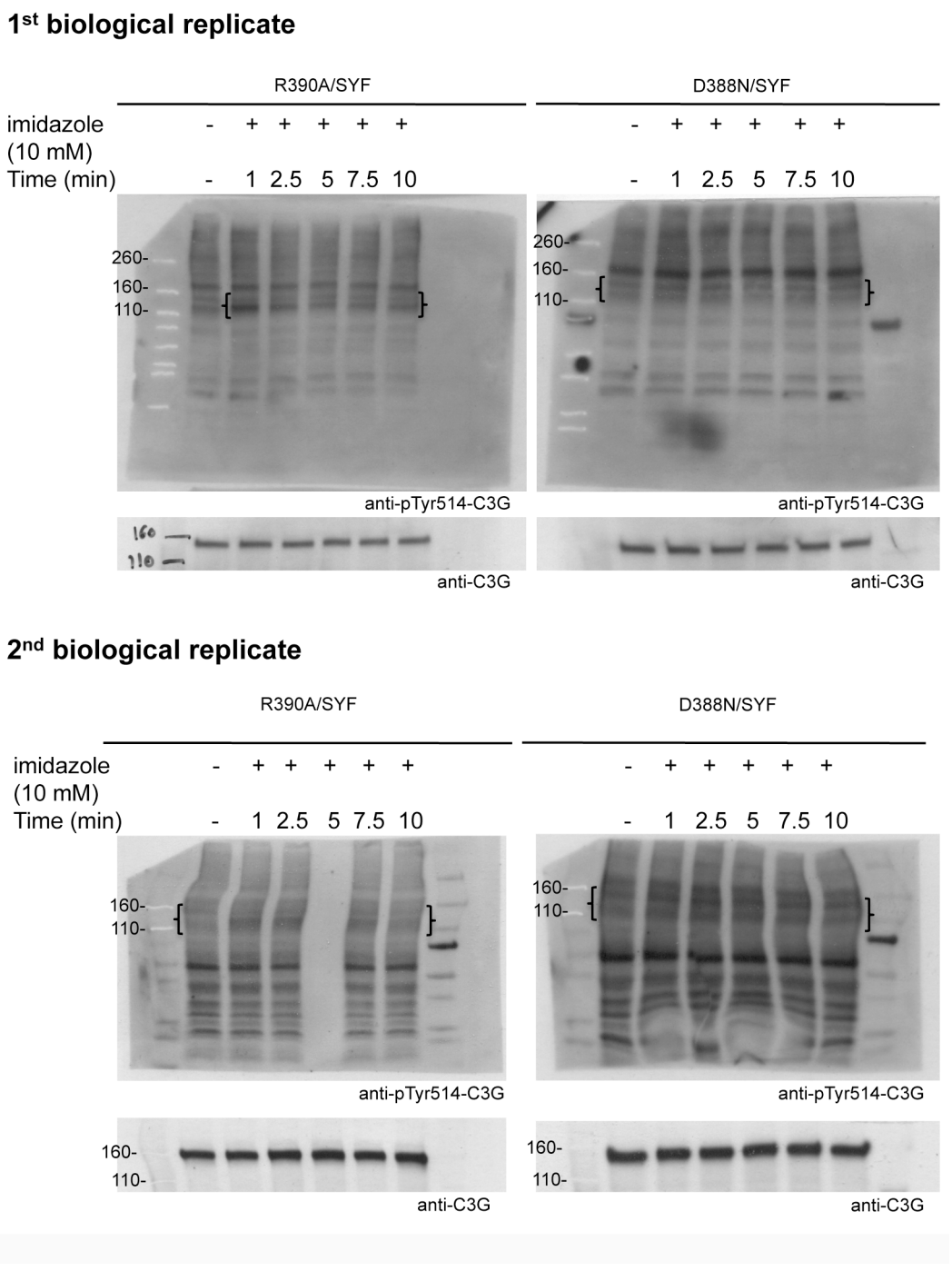

Figure 42. Biological replicates for the experiment to detect the effect of c-Src activation on C3G's phosphorylation on Tyr-514

The entire anti-pTyr514-C3G immunoblot is shown for both repeats to show the entirety of bands appearing. In the case of the anti-C3G-immunoblot, the band presented was the

major and stronger band of the blot. Western blot using anti pTyr514-C3G antibody showed an increase in the phosphorylation level of tyrosine 514 in a C3G isoform after 1 minute upon c-Src rescue in R390A c-Src SYF cells but not in D388N c-Src SYF cells. From the several bands observed in the blot against pTyr514-C3G, we detected an increase in one band that corresponds to a slightly smaller molecular weight than the strongest band usually observed when we perform a Western blot against C3G or an immunoprecipitation with C3G antibody followed by Western blot against C3G. However, we have also observed a weaker band just bellow the strongest band in some C3G immunoprecipitation and Western blot experiment. We interpret that this lower band corresponds to one of the different C3G isoforms. The molecular weights are indicated in the blot to illustrate this point. Western blot using an antibody against C3G shows equal loading along the different time points in both R390A c-Src SYF and D388N c-Src SYF cells.

could correspond to different C3G isoforms. In the anti pTyr514-C3G immunoblot we indicate two bands. One corresponds to the band at the molecular weight were we usually observe C3G in the C3G immunoblot. The other band is the one that consistently increases in intensity one minute upon c-Src rescue and that we believe corresponds to a C3G isoform. The molecular weights are indicated in the blot to illustrate this point.

3.3. Effects of c-Src activation on C3G-Crk binding

As mentioned above, it has been shown that different stimuli lead to an increase in C3G-Crk binding. In order to further dissect this signaling process and investigate whether c-Src specific activation can result in an increase in binding between C3G and Crk, we explored potential changes in protein-protein interactions between C3G and Crk.

After imidazole treatment of R388A/SYF cells, C3G protein was immunoprecipitated and Crk binding was analyzed by Western blot (**Figure 43**).

It was shown that increased Crk was pulled down by C3G immunoprecipitation after only 1 minute of rescue of R388A/SYF cells, but not in D388N/SYF cells. The peak binding of C3G and Crk was reached at 2.5 minutes and began to decrease by 5 minutes.

It is important to warn that the exact timing at which these observations are made differs slightly from one biological replicate to the other but the pattern of an immediate increase and a consequent decrease is consistent. In the biological replicate shown in **Figure 44**, we performed two different co-immunoprecipitations. In one of them the incubation of the lysate with the antibody and beads occurred overnight and in the other

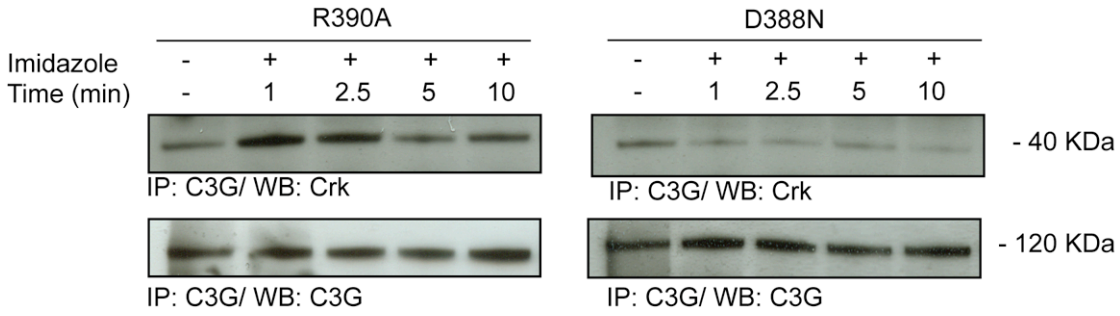

Figure 43. Detection of the effect of c-Src activation on C3G- Crk binding

Co-Immunoprecipitation using C3G immunoprecipitation and Crk blotting showed an increase in C3G-Crk binding after 1 minute upon imidazole treatment which was sustained until 2.5 minutes and decreased at minute 5 in R390A c-Src SYF cells but not in D388N c-Src SYF cells.

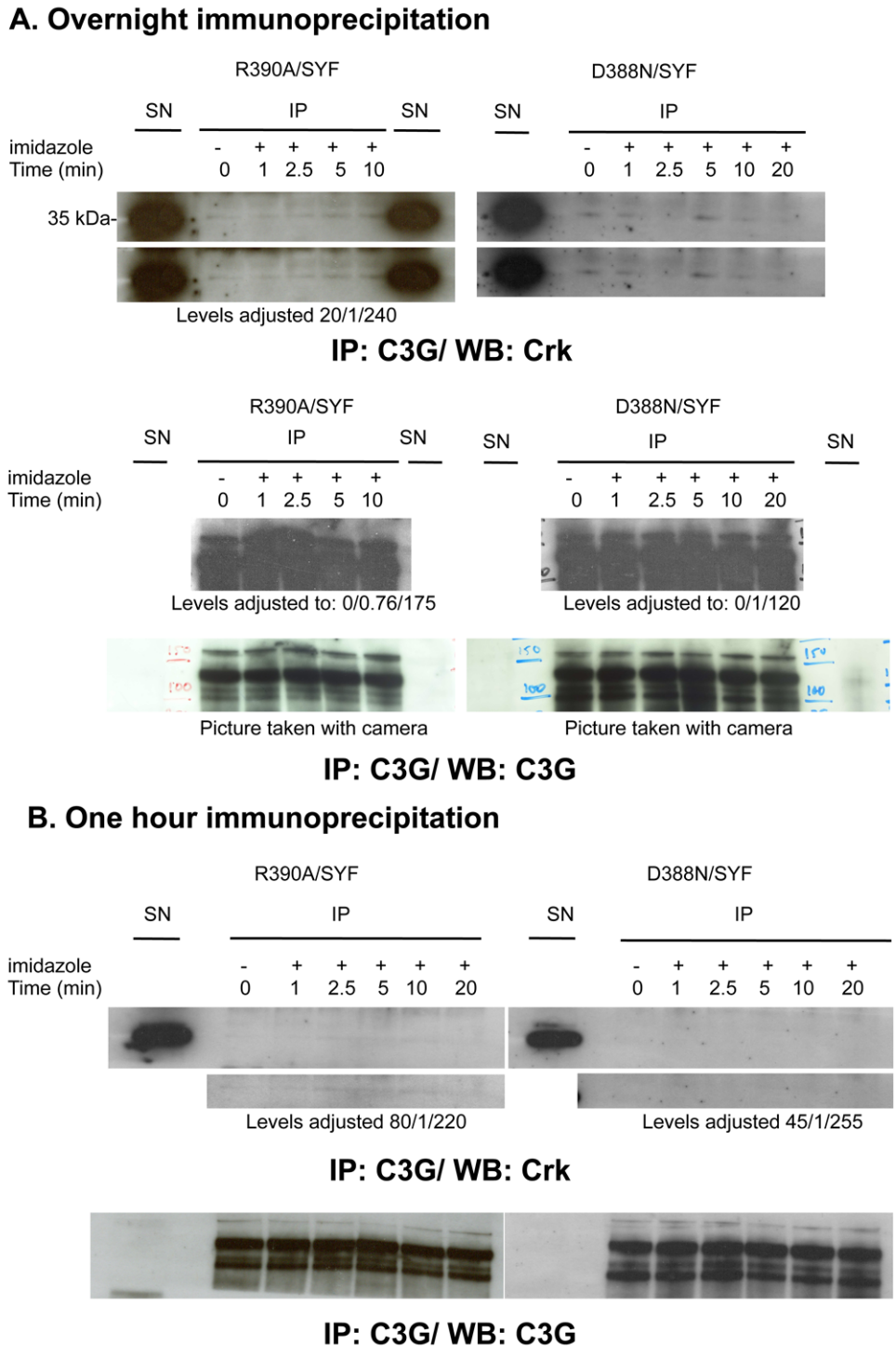

Figure 44. Biological replicates for the experiment to detect the effect of c-Src activation on C3G-Crk binding

A. Co-Immunoprecipitation using C3G immunoprecipitation and Crk blotting showed an increase in C3G-Crk binding after 2.5 minutes upon imidazole treatment in R390A c-Src SYF cells but not in D388N c-Src SYF cells. **B.** Co-Immunoprecipitation using C3G immunoprecipitation and Crk blotting showed an increase in C3G-Crk binding after 2.5 minute supon imidazole treatment which was sustained until 10 minutes and decreased at minute 20 in R390A c-Src SYF cells but not in D388N c-Src SYF cells.

for just one hour. In both of them we observed a mild increase in C3G-Crk binding after 2.5 minutes upon c-Src chemical rescue. This increase was maintained until 10 minutes. The overnight-incubation experiment did not have a lane corresponding to 20-minute treatment due to a mistake, but the experiment where the incubation was performed for one hour showed a decrease in Crk-C3G binding 20 minutes upon c-Src rescue. We could therefore conclude that c-Src activation leads to an immediate increase in binding between C3G and Crk followed by a consequent decrease.

3.4. Tyr-221 Crk phosphorylation and Crk-C3G complex dissociation

It has previously been shown a that phosphorylation of Crk on Tyr-221 (241) is an important event that mediates for Crk-C3G dissociation after insulin-stimulation of Chinese hamster ovary cells. Phosphorylation of Crk on Tyr-221 (241) allows the intramolecular binding of Crk's SH2 domain to Tyr-221 (223, 247).

In order to test if phosphorylation of Crk on Tyr-221 was responsible for the observed decrease in C3G-Crk binding, we measured the phosphorylation level of this particular site with a phosphospecific antibody (**Figure 45**) at the same time points used to observe C3G-Crk binding. We performed both experiments simultaneously from the same cell lysates to reduce experimental variability. Indeed, in Figure 45 phosphorylation of Crk on Tyr-221 increases just after 1 minute and reaches a peak at 5 minutes, which correlated with the time at which binding between C3G and Crk decreases.

The biological replicate shown in **Figure 46** also suggests an increase in Tyr-221

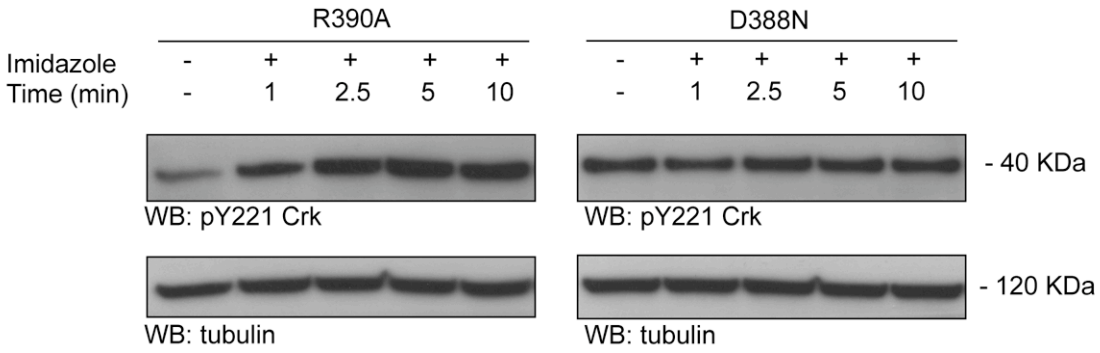

Figure 45. Detection of the effect of c-Src activation on Crk's phosphorylation on Tyr-221

Western blot using anti-pTyr-221in Crk showed a gradual increase in phosphorylation upon c-Src rescue reaching the highest level of phosphorylation at minute 5 in R390A c-Src SYF cells but not in D388N c-Src SYF cells. The maximum level of phosphorylation was reached at the same point at which C3G and Crk showed a decreased binding.

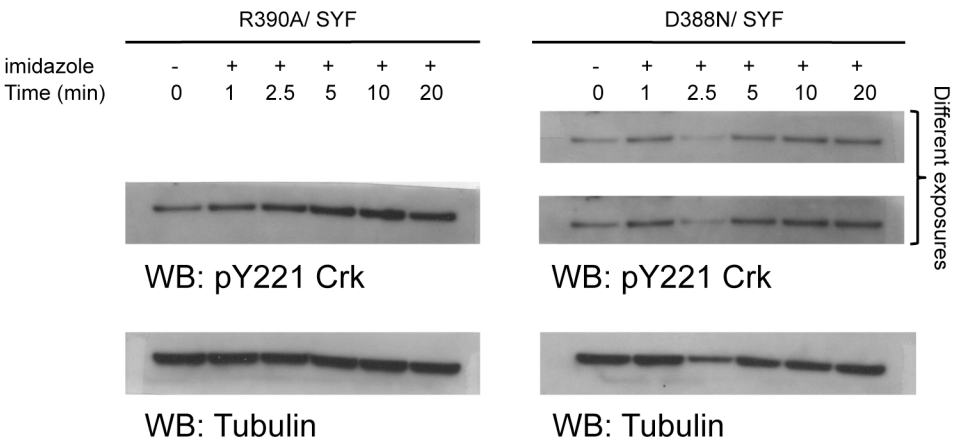

Figure 46. Biological replicates for the experiment to detect the effect of c-Src activation on Crk's phosphorylation on Tyr-221

Western blot using anti-pTyr-221in Crk showed a gradual increase in phosphorylation upon c-Src rescue reaching the highest level of phosphorylation at minute 5-10 in R390A c-Src SYF cells but not in D388N c-Src SYF cells.

phosphorylation of Crk.

3.5. Effects of c-Src activation on C3G subcellular localization

As discussed above, in addition to C3G phosphorylation, C3G activation occurs mainly through membrane recruitment (205,234). To further examine the connections between c-Src and C3G, we explored the subcellular localization of C3G using immunocytochemistry and confocal microscopy after chemical rescue (**Figure 47**).

As shown, upon imidazole treatment of R390A/SYF cells but not D388N/SYF cells, there is an apparent movement of C3G protein to the cell periphery from the cytosol. This movement occurs within 1 minute and persisted for at least 5 minutes and then began showing a decrease about 10 minutes after c-Src rescue.

4. Discussion

The Rap1 guanine exchange factor, C3G, was first detected in our SILAC experiment as a protein with increased phosphorylation upon c-Src rescue. It was further validated by immunoprecipitation and Western blot and showed a clear increase in tyrosine phosphorylation. A phosphopeptide from C3G was subsequently detected in our mass spectrometric phosphopeptide screening, Tyr-571, and showed an apparent 2.5-fold increase in its phosphorylation level that was consistent among the three biological replicates.

Rap1 is a Ras-like small GTPase that is activated by many extracellular stimuli

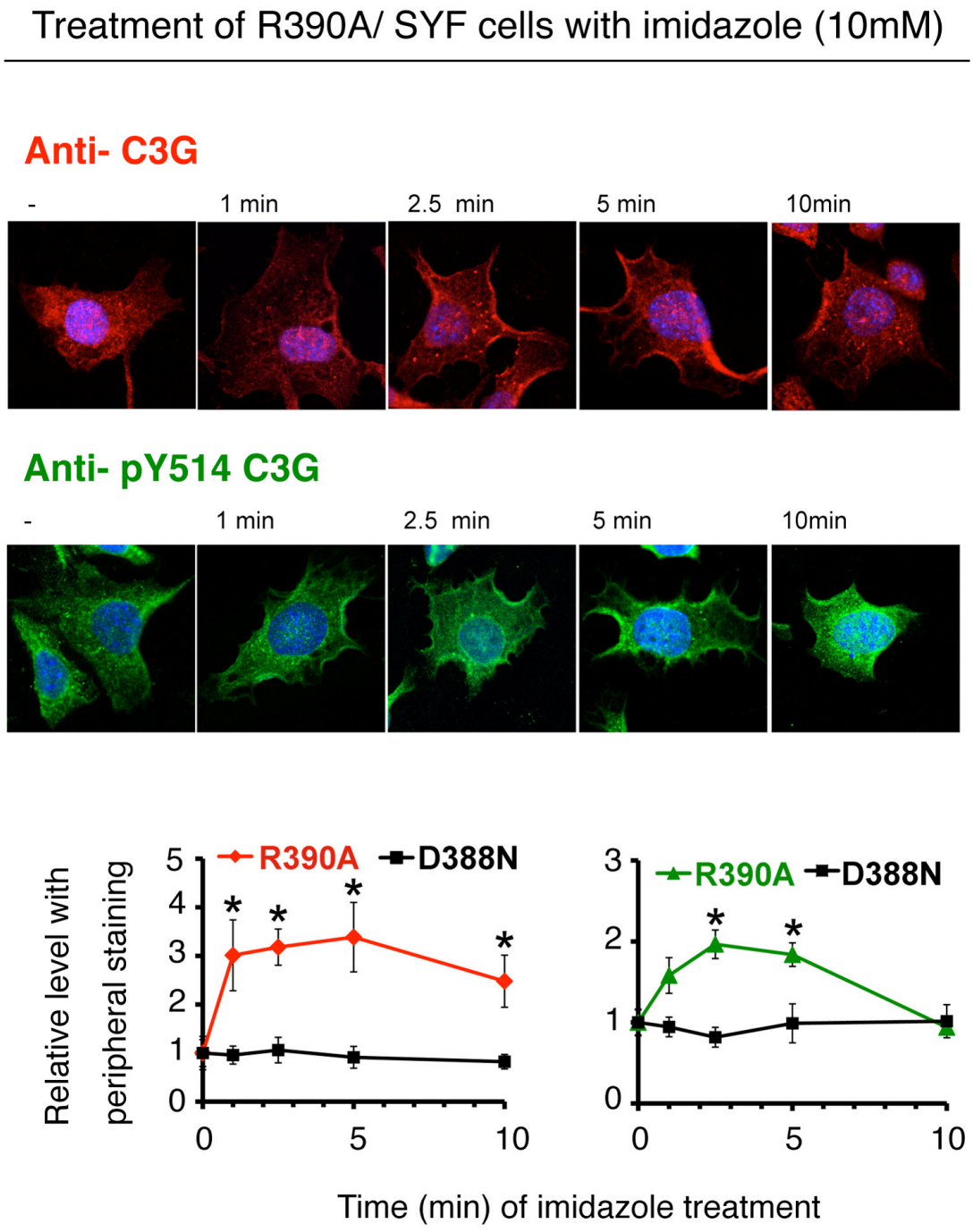

Figure 47. Detection of the effect of c-Src activation on C3G's subcellular localization

R390A c-Src/SYF cells were treated with 10 mM imidazole for various time points before being fixed. Localization of both C3G and pTyr514-C3G was detected by staining with C3G (Rhodamine) and pTyr514-C3G (FITC) and nuclei stained by DAPI. Images were acquired by confocal microscopy. Representative images at 100x magnification are shown. Cells ($n>40$) were categorized according to phenotype (cytosolic vs peripheral) and quantified. Quantitative analysis of C3G and pTyr514-C3G cellular localization was measured as a function of imidazole treatment time. Images were captured by confocal microscopy at 40x magnification. Six representative images (at least 40 cells) were quantified for each condition. Each cell was scored for whether it had peripheral staining. The fraction of cells with peripheral staining was calculated for each image and averages were calculated by combining the six images for each condition. Each time point was normalized to time zero and standard errors are shown. Statistical significance ($p<0.05$) compared with time zero was calculated using a Student's T test and is indicated with an asterisk (*).

and strongly implicated in the control of integrin-mediated cell adhesion. Recent evidence indicates that Rap1 also plays a key role in formation of cadherin-based cell-cell junctions. Rap1 has been reported to play an essential role in the spatial and temporal control of adhesion. It is therefore not surprising that several Rap1 GEFs, such as C3G, have been implicated in the regulation of adhesion complexes (248,249).

Despite the considerable interest in understanding the process of C3G activation, the spatiotemporal regulation of this process has been largely unclear. The ability of c-Src chemical rescue to specifically and rapidly activate c-Src allowed us to gain greater insight into the spatiotemporal process of C3G activation, as well as to propose a molecular mechanistic pathway for Rap1 control. After we found that c-Src activation led to an increase of GTP-bound Rap1 in the cell periphery within 5 minutes, we pursued this molecular mechanism in greater detail.

Although it has been reported that Crk is constitutively associated with C3G (239), it has also been shown that this association can be induced by different stimuli (236,240,241). We show that rapid activation of c-Src enhances interaction between C3G and Crk by 1 minute. Such regulation of this complex may account for reported responses after the stimulation of cells by insulin, integrin engagement, and other natural triggers. Presumably, as the adaptor protein Crk forms a complex with C3G, it recruits C3G to the cell periphery, where we detected C3G rapidly after c-Src rescue. Interestingly, the binding between C3G and Crk began to decrease approximately 5 minutes post stimulation, possibly initiating retrograde signaling in this pathway. In support of this idea, a previous study reported that both insulin and epidermal growth factor (EGF) stimulation of cells resulted in a time-dependent dissociation of the Crk-

C3G complex (240).

Crk is negatively regulated by tyrosine phosphorylation on Tyr-221. The intramolecular binding of phosphorylated Tyr-221 to the SH2 domain blocks SH3 dependent protein binding responsible for the formation of the C3G-Crk complex (223). Pretreatment of the cells with genistein (tyrosine kinase inhibitor), decreased the tyrosine phosphorylation of Crk that correlated inversely with the amount of Crk that was immunoprecipitated with C3G (240). We showed that the level of phosphorylation of Crk on Tyr-221 increases upon c-Src activation. Interestingly the observed decrease in Crk-C3G binding occurs when phosphorylation of Crk on Tyr-221 reaches a maximum level. There thus seems to be an inverse correlation between Crk phosphorylation on Tyr-221 and C3G-Crk binding. Subsequently, Rap1 activation appears to be indirectly modulated downward in a fashion that is also correlated with Crk phosphorylation on residue Tyr-221.

Since Rap1 suppresses Ras signaling by sequestering its common target, Raf1, it is logical that the ability of growth factors to activate the Ras/Raf/MEK/ERK cascade requires a mechanism for the inactivation of Rap1 function. Phosphorylation of Crk on Tyr-221 and the consequent dissociation of the C3G-Crk complex may well contribute to this negative regulation of Rap1 activity. In fact, a similar negative feedback loop involving another aspect of the same pathway has been reported already and a parallel can be made with our pathway of study (**Figure 48**). Sos is a RasGEF that associates with the adaptor Grb2. A kinase downstream of MEK or maybe MEK itself, can phosphorylate Sos on serine/threonine (250,251). As a result, the ability of Sos to activate Ras diminishes and there is attenuation in ERK activation. As represented in **Figure 48**,

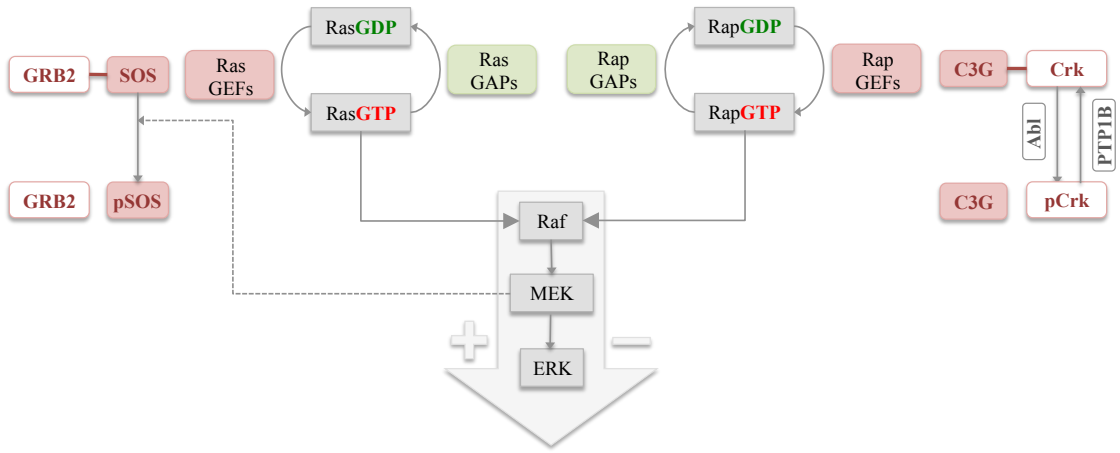

Figure 48. Hypothetical parallelism between the phosphorylation of the RasGEF Sos and the adaptor protein Crk as events for the regulation of the Raf/MEF/ERK cascade

Sos associates with the adaptor Grb2 and activates Ras leading to an activation of the Raf/MEF/ERK cascade. However, when Sos is phosphorylated, its ability to both bind Grb2 and to activate Ras decreases. Crk's phosphorylation on Tyr-221 by Abl seems to decrease its ability to serve as an adaptor of C3G, leading to a downstream inactivation of Rap1 and a activation of the Raf/MEF/ERK cascade.

phosphorylation of Crk may be the key event of a similar feedback mechanism.

Abl kinase has been identified as a Crk upstream kinase that can phosphorylate Tyr-221 (252). In this regard, our phosphopeptide mapping revealed that site Tyr-439/393 of Arg (Abl2)/Abl, which has additive effects on Abl activation (253) and has not been described previously as a c-Src substrate, experienced a significant increase in its phosphorylation level 5 minutes after c-Src chemical rescue. In this way, tyrosine phosphorylation on Tyr-221 of Crk, may regulate MAPK activity through Crk-C3G formation. In support of this idea, oncogenic Bcr-Abl may lead to constitutive phosphorylation of Crk, dissociation of the Crk-C3G complex and reversal of the suppressive effects of RAP on ERK activity. This would contribute to the oncogenic effects of Bcr-Abl. It is worth mentioning one more study that supports this idea of a feedback mechanism mediated by phosphorylation of Tyr-221 on Crk in a different context: Tyr-221 was reported to also be phosphorylated by other tyrosine kinases, such as epidermal growth factor (EGF) receptor upon EGF stimulation. This phenomenon was also detected in a c-Abl-deficient cell line. Tyrosine-phosphorylated Crk was detected at the periphery of the cells, where ruffling is prominent, suggesting that signaling to Crk may be involved in EGF-dependent cytoskeletal reorganization. Moreover, recombinant Crk protein was phosphorylated *in vitro* by EGF receptor. These results suggested that EGF receptor may directly phosphorylate Crk. Mutational analysis revealed that the Crk's SH2 domain was essential for the phosphorylation of Crk by EGF receptor but not by c-Abl, arguing that these kinases phosphorylate Crk by different phosphorylation mechanisms. This may be due to the fact that the SH2 is required for recruiting Crk to the proximity of EGFR, but not for cytosolic Abl. It was also found that Crk initiated

dissociation from EGF receptor within 3 minutes even with sustained tyrosine phosphorylation of EGF receptor. This led to the conclusion that the phosphorylation of Tyr-221 of Crk correlated with its dissociation from the EGF receptor, implicating the phosphorylation of Tyr-221 in the negative feedback of the SH2-mediated binding of Crk to EGF receptor (252). Previous studies have provided some evidence that PTP1B may be able to dephosphorylate Crk (236,241) and have a role in the regulation of the Crk-C3G complex formation. In addition, PTP1B has been shown to bind to p130Cas, allowing it to locate near potential substrates, such as Crk (254). In fact, phosphorylation of p130Cas may also be important, as this is required to create an SH2-docking site for Crk as well as c-Src and other kinases that may be involve in the phosphorylation of C3G and other components of the signaling complex.

It was known previously that C3G is phosphorylated on tyrosine 514 and this PTM has been suggested to influence its ability to activate Rap1. We observed an increase in Tyr-514 phosphorylation level within 1 minute after activation of c-Src. Indeed, increased phosphorylation of C3G on Tyr-514 facilitate C3G's activity to catalyze GTP exchange on Rap1 in our system, as revealed in our live cell reporter assay, which also showed a maximum level of activity at 5 min.

Interestingly, a previous study revealed that even the C3G-Y504F mutant was also activated slightly by Crk expression (206). Because the C3G-Y504F mutant was still phosphorylated weakly on tyrosine, it is possible that phosphorylation of other tyrosine residue(s) may replace the function of Y504F phosphorylation. In this regard, it is also noteworthy that rescue induced an ~3-fold increase in phosphorylation of a new site, Tyr-571 (**Figure 49**), on C3G that may also modulate C3G's ability to activate Rap1. This

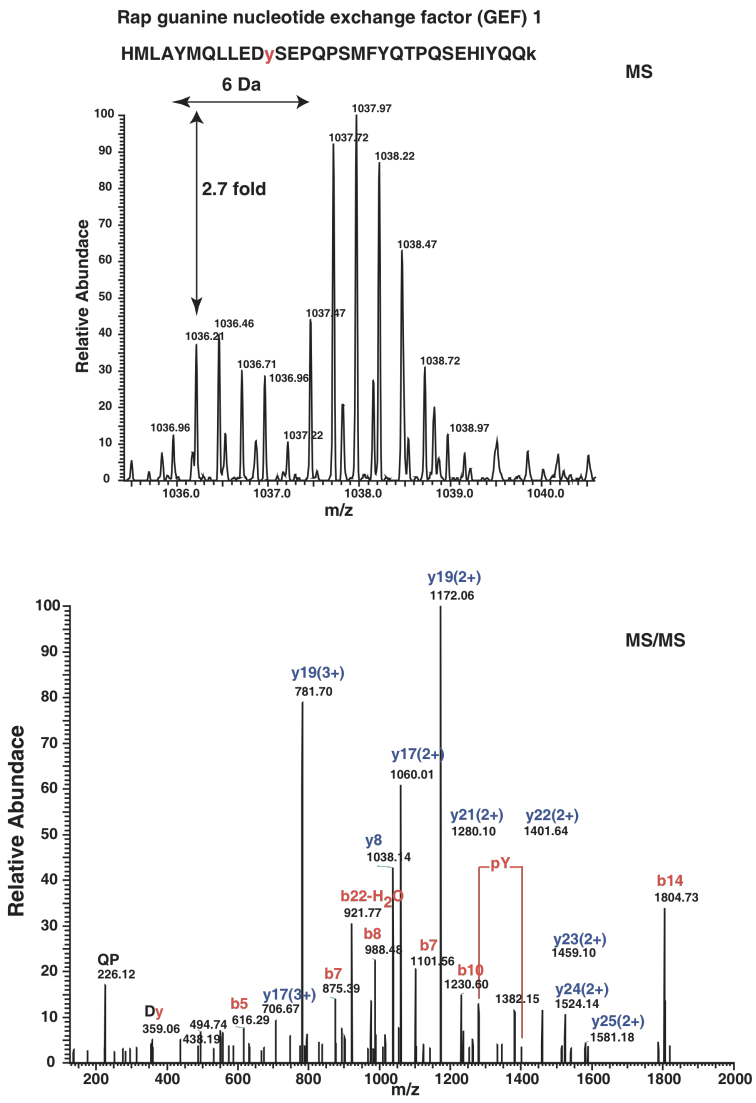

Figure 49. Novel tyrosine phosphorylation site in C3G (Tyr-571) as evidenced by MS/MS

Tyr-571 showed upregulated phosphorylation level upon c-Src's activation as evidenced by mass spectra showing the increase in the relative abundance of phosphopeptides.

site, similar to Tyr-514, is located between two proline rich regions in C3G that bind the SH3 domain of Crk.

The preferred binding motif for the Crk SH2 domain is pY-x-x-P. This preference was initially identified by an in vitro approach (255) and subsequently confirmed by mutational analyses of several Crk SH2 domain-binding partners. Multiple pY-x-x-P motifs are present in prominent Crk SH2 domain binding partners like paxillin (256,257) or p130Cas (214,258). Interestingly, the newly discovered phosphorylation site in C3G fits the sequence of this preferred binding motif (**Figure 50**).

It would be informative to reveal whether or not C3G phosphorylation and Crk-C3G complex formation are interdependent. Growth factor stimulation leads to the formation of a large multiprotein signaling and Crk plays a major role in recruiting some of these proteins. An increase in the association between FAK, c-Src and JAK2 has been reported (239). Crk may facilitate the formation of this triple kinase complex together with C3G. As a result, it could be the case that increased Crk binding to C3G, and the consequent C3G translocation to the membrane, facilitated phosphorylation of C3G by Src due to the local proximity. However, it is also possible that phosphorylation of C3G leads to an increase in binding with Crk.

Both phosphorylation of C3G on Tyr-514 and C3G-Crk binding showed an increase after only 1 minute upon c-Src rescue in our system, showing that both phenomena are temporarily related. However, it is not clear whether the occurrence of one phenomenon depends on the other or both phenomena are independent. In fact, while both C3G phosphorylation and C3G-Crk binding experience a significant increase within 1 minute after c-Src rescue, phosphorylation of C3G on Tyr-514 did not seem to

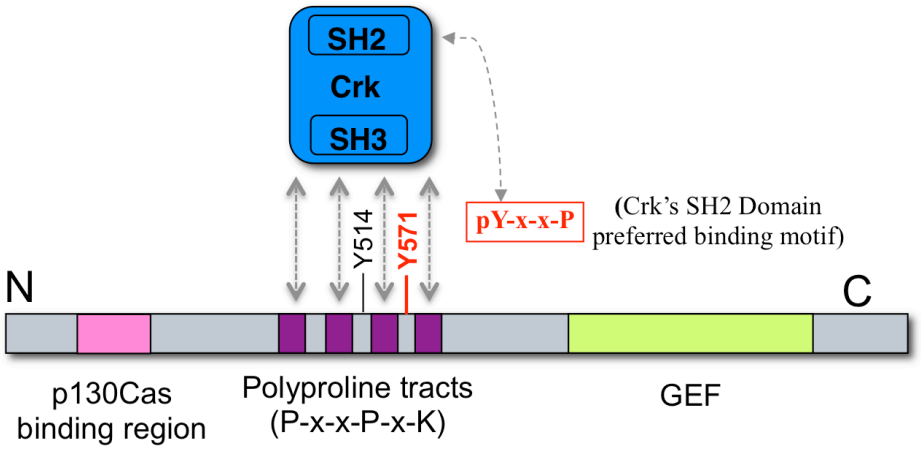

Figure 50. Schematics of a hypothetical C3G-Crk interaction based on Tyr-571 phosphorylation

pY-x-x-P is the preferred binding motif for the Crk SH2 domain and is included in many Crk SH2 binding partners. The newly discovered and upregulated phosphorylation site in C3G (Tyr-571) fits the described sequence.

follow the trend of C3G-Crk binding. C3G-Crk association decreases after 2.5 minutes (although this phenomenon can be detected later since there is some experimental variability) and reaches a minimum at 5 minutes, when Crk's phosphorylation on Tyr-221 reaches a maximum level. It is worth emphasizing that the timing is variable but experiments shown in Figue 43 and Figure 45 were performed from the same sample coming from the same experimental repeat so the timing between these two events can be compared in a more convincing way, since we are avoiding experimental variability.

If both phenomena were interdependent, further research would hopefully allow dissecting which of the two events occurs first and facilitates the second.

This leaves us with two possible mechanisms of C3G activation and consequent Rap activation, as represented below (**Figure 51**). Both phosphorylation of C3G on Tyr-514 and recruitment to the membrane by Crk are needed but we cannot conclude from our data if one of these events is required or facilitates the occurrence of the other. The figure also summarizes all the observations made in this study and suggests a mechanism of Crk-C3G dissociation caused by Crk's phosphorylation on Tyr-221 (likely by c-Abl) as a hypothetical retrograde signaling in this pathway.

Additional phosphorylation of C3G may play a role in its activation. We have identified a novel site that shows a significant increase in phosphorylation at the time GTP-bound Rap1 signal reaches its highest level. Either this or other unknown tyrosine or serine/ threonine phosphorylations might affect C3G's ability to interact with Crk.

The chemical rescue approach has allowed a temporal description of such

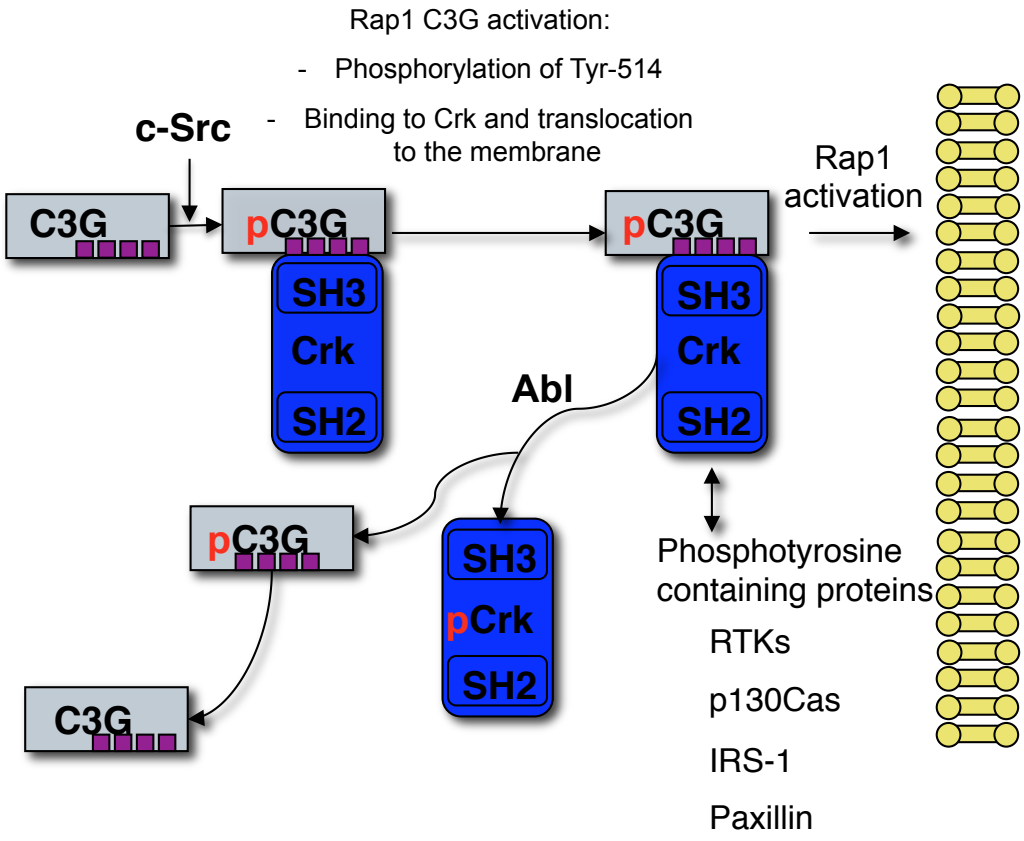

Figure 51. Schematics of the observations made on the Crk-C3G-Rap1 pathway

C3G is activated by both phosphorylation on Tyr-514 and by binding to Crk, which then recruits C3G to the membrane. There is an increased localization of C3G in the peripheral region and an increased in Rap1 activity which is known to be mediated by C3G. The figure also represents the hypothetical retrograde signaling that takes place when Crk becomes phosphorylated on Tyr-221 by Abl leading to a disruption of C3G-Crk binding and a consequent observed decrease in C3G phosphorylation.

signaling events that would otherwise have been difficult to obtain. In principle, this technique can be applied to other non-receptor PTKs to provide a more complete portrait of tyrosine phosphorylation networks in cell signaling.

Tables

Table 1. Stable isotopic amino acids used in SILAC media

Stable isotopic amino acids (Molecular Weight)	Concentration in DMEM	Mass difference	Cambridge Isotope laboratories (Catalog No.)	Sigma-Aldrich (Catalog No.)
L-Lysine·H_2O (164.20)	131.0 mg/l (0.798 mM)	0 Da	-	62855
L-Lysine·$2H_2O$ ($^{13}C_6$) (164.20)	179.6 mg/l (0.798 mM)	6 Da	CLM-2247	-
L-Arginine (174.20)	69.3 mg/l (0.398 mM)	0 Da	-	A8094
L-Lysine·$2H_2O$ ($^{13}C_6$) (164.20)	86.2 mg/l (0.398 mM)	6 Da	CLM-2265	-
L- Tyrosine disodium salt (225.15)	89.6 mg/l (0.398 mM)	0 Da	-	T1145

Table 2. List of identified proteins from the SILAC experiment at the protein level. Phenylphosphate elution.

No.	GI	MW	NAME [Mus Musculus]	Heavy/ Light	Std. Dev
1	gi|9506909	239143	Myosin X	2.6	0.34
2	gi|94365254	144931	PREDICTED: similar to tensin	2.3	0.4
3	gi|27370424	108910	Hypothetical protein LOC244895	2.1	0.25
4	gi|21281693	62198	Paxillin isoform alpha	2.0	0.31
5	gi|6754632	41648	Mitogen activated protein kinase 1	2.0	0.18
6	gi|31981796	52789	Docking protein 1	2.0	0
7	gi|31982290	67339	LIM domain containing preferred translocation partner in lipoma	1.9	0.13
8	gi|27476057	84520	Discoidin, CUB and LCCL domain containing 2	1.8	0.14
9	gi|31560712	51254	c-src tyrosine kinase	1.7	0.04
10	gi|40254593	94455	Breast cancer anti-estrogen resistance 1	1.7	0.25
11	gi|31980859	73497	Rho guanine nucleotide exchange factor (GEF7)	1.6	0.15
12	gi|21489933	43381	mitogen activated protein kinase 3	1.6	0
13	gi|51921285	86046	G protein-coupled receptor kinase-interactor 1	1.6	0.17
14	gi|70794809	60366	Rous sarcoma oncogene isoform 2	1.5	0.39
15	gi|31982755	53712	Vimentin	1.5	0.17
16	gi|84875504	136510	Rap guanine nucleotide exchange factor (GEF) 1 isoform 2	1.5	0.06
17	gi|6679741	119939	PTK2 protein tyrosine kinase 2	1.3	0.13
18	gi|10092590	41489	Mitogen activated protein kinase 14	1.3	0.19
19	gi|9790077	47194	Glycogen synthase kinase 3 beta	1.3	0
20	gi|46849812	276017	Fibronectin 1	1.3	0
21	gi|51766344	32925	PREDICTED: similar to 40S ribosomal protein SA (p40) (34/67 kDa laminin receptor)	1.1	0.08
22	gi|6679321	81601	Phosphatidylinositol 3-kinase, regulatory subunit, polypeptide 2 (p85)	1.1	0
23	gi|70608146	87806	X kin of IRRE like 1	1.1	0.03

24	gi|32484983	110265	Eph receptor A2	1.1	0.23
25	gi|68299809	53708	phosphatidylinositol 3-kinase, regulatory subunit, polypeptide 1 isoform 1	1.1	0.14
26	gi|6681273	50764	Eukaryotic translation elongation factor 1 alpha 2	1.0	0.15
27	gi|94387987	74363	PREDICTED: similar to heat shock protein 8	1.0	0.1
28	gi|7106439	50095	tubulin, beta 5	1.0	0.07
29	gi|9845265	15004	Ubiquitin A-52 residue ribosomal proteína fusion product 1	1.0	0.17
30	gi|31981722	72492	Heat shock 70 kD protein 5 (glucose-regulated protein)	1.0	0.04
31	gi|9507003	57723	Polypyrimidine tract binding protein 2	1.0	0
32	gi|82993679	70418	PREDICTED: similar to Heat shock 70 kDa protein 1B (HSP70.1) isoform 5	1.0	0
33	gi|6671509	42052	Actin, beta, cytoplasmic	1.0	0.05
34	gi|6678469	50562	tubulin, alpha 6	1.0	0.02
35	gi|94392981	198322	PREDICTED: pleckstrin homology domain containing, family H (with MyTH4 domain) member 1 isoform 1	1.0	0
36	gi|66841385	431301	cardiomyopathy associated 3	1.0	0
37	gi|94363502	43081	PREDICTED: similar to non-catalytic region of tyrosine kinase adaptor protein 2 isoform 2	0.9	0.04
38	gi|7948995	117788	Tyrosine kinase, non-receptor, 2	0.9	0.05
39	gi|34328187	43092	non-catalytic region of tyrosine kinase adaptor protein 1	0.9	0.07
40	gi|82887378	50313	PREDICTED: molybdenum cofactor synthesis 3	0.9	0
41	gi|94377125	293560	PREDICTED: similar to Filamin-C (Gamma-filamin) (Filamin-2) (Protein FLNc) (Actin-binding-like prot	0.9	0
42	gi|39841025	82811	FCH and double SH3 domains 2	0.9	0.07
43	gi|6753620	73455	DEAD/H (Asp-Glu-Ala-Asp/His) box polypeptide 3, X-linked	0.9	0
44	gi|46560563	189575	SH3 domain protein 1B	0.9	0.04

45	gi|68989251	60110	tweety 2	0.9	0
46	gi|49258190	79207	NCK interacting protein with SH3 domain	0.8	0
47	gi|40556608	83571	Heat shock protein 1, beta	0.8	0
48	gi|47059093	110370	Eph receptor B4	0.8	0.09
49	gi|7305295	223983	Myosin, heavy polypeptide 11, smooth muscle	0.8	0.05
50	gi|33598964	229824	Myosin heavy chain 10, non-muscle	0.7	0.04
51	gi|66955868	18368	hypothetical protein LOC67288	0.7	0
52	gi|86262157	56249	hypothetical protein LOC239796	0.7	0.03
53	gi|91598596	68147	Sorting nexin associated golgi protein 1	0.6	0.02
54	gi|23956222	47783	ARP3 actin-related protein 3 homolog	0.6	0
55	gi|6680920	15556	Centromere autoantigen A	0.5	0
56	gi|13386452	13986	Histone 3, H2ba	0.4	0
57	gi|70778882	71740	Chaperone, ABC1 activity of bc1 complex like	0.2	0.06
58	gi|94369415	46522	PREDICTED: similar to arylacetamide deacetylase	0.1	0

Table 3. List of identified proteins from the SILAC experiment at the protein level. Boiled beads elution.

No.	GI	MW	NAME [Mus Musculus]	Heavy / Light	Std. Dev
1	gi|70794809	59853	Rous sarcoma oncogene isoform 2	3.32	0
2	gi|31982755	53655	Vimentin	2.63	0.51
3	gi|24429590	149489	DEAH (Asp-Glu-Ala-His) box polypeptide 9	2.39	0.69
4	gi|6754632	41249	Mitogen activated protein kinase 1	1.83	0.22
5	gi|25141233	94572	Matrin 3	1.79	0
6	gi|21313308	77597	Heterogeneous nuclear ribonucleoprotein M	1.75	0.07
7	gi|51921285	85247	G protein-coupled receptor kinase-interactor 1	1.64	0.12
8	gi|7949051	87837	Heterogeneous nuclear ribonucleoprotein U	1.58	0.28
9	gi|40254593	94227	Breast cancer anti-estrogen resistance 1	1.55	0.19
10	gi|31980859	72984	Rho guanine nucleotide exchange factor (GEF7)	1.53	0.09
11	gi|6679108	32540	Nucleophosmin 1	1.53	0.31
12	gi|46849812	272368	Fibronectin 1	1.5	0.02
13	gi|21281693	60772	Paxillin isoform alpha	1.49	0.18
14	gi|41322927	506145	Plectin 1 isoform 4	1.47	0.3
15	gi|28316750	14228	Histone 1, H2ba	1.47	0.75
16	gi|21450625	46125	Eukaryotic translation initiation factor 4A1	1.47	0
17	gi|31980648	56265	ATP synthase, H+ transporting mitochondrial F1 complex, beta subunit	1.43	0
18	gi|6671509	41710	Actin, beta, cytoplasmic	1.41	0.15
19	gi|7305237	71375	LIM domains containing 1	1.35	0.08
20	gi|94370505	14540	PREDICTED: similar to heterogeneous nuclear ribonucleoprotein H2	1.29	0.04
21	gi|7305075	51797	Ras-GTPase-activating protein SH3-domain binding protein	1.27	0
22	gi|6679741	119141	PTK2 protein tyrosine kinase 2	1.26	0.09

23	gi|23956078	71736	ATP-binding cassette, sub-family F (GCN20), member 2	1.26	0
24	gi|10946928	49168	Heterogeneous nuclear ribonucleoprotein H1	1.23	0.06
25	gi|31982757	54055	Ras-GTPase-activating protein (GAP120) SH3-domain binding protein 2 isoform a	1.21	0
26	gi|15809050	148969	Partitioning-defective protein 3 homolog isoform 3	1.21	0
27	gi|13195690	17939	Ribosomal protein S27a	1.2	0.03
28	gi|6754524	36475	Lactate dehydrogenase 1, A chain	1.17	0.31
29	gi|10092590	41261	Mitogen activated protein kinase 14	1.16	0.12
30	gi|86990450	128483	Myosin IB	1.15	0.51
31	gi|8394460	39478	Tropomodulin 3	1.14	0
32	gi|47271404	111785	Rho/rac guanine nucleotide exchange factor (GEF) 2	1.14	0
33	gi|33598964	228855	Myosin heavy chain 10, non-muscle	1.11	0.54
34	gi|31542366	34085	Cell division cycle 2 homolog A	1.11	0.08
35	gi|6677805	29579	Ribosomal protein S4, X-linked	1.11	0.24
36	gi|7242171	28766	Proliferating cell nuclear antigen	1.11	0.12
37	gi|31981690	70827	Heat shock protein 8	1.09	0.31
38	gi|6679937	35787	Glyceraldehyde-3-phosphate dehydrogenase	1.09	0.02
39	gi|31560030	32689	Tropomyosin 1, alpha	1.08	0.19
40	gi|6680748	59716	ATP synthase, H+ transporting, mitochondrial F1 complex, alpha subunit, isoform 1	1.08	0
41	gi|31980798	70256	Nuclear RNA export factor 1	1.07	0
42	gi|82993679	70133	PREDICTED: similar to Heat shock 70 kDa protein 1B (HSP70.1) isoform 5	1.06	0.11
43	gi|83816893	69223	DEAD (Asp-Glu-Ala-Asp) box polypeptide 5	1.06	0.07
44	gi|6678097	42571	Serine (or cysteine) proteinase inhibitor, clade B, member 6a	1.06	0.48
45	gi|9506843	52620	Lamin A isoform C2	1.06	0.03
46	gi|12963531	54564	Non-POU-domain-containing, octamer	1.05	0

			binding protein		
47	gi|6997239	36861	Poly(rC) binding protein 2	1.05	0
48	gi|6755002	95950	Programmed cell death 6 interacting protein	1.05	0
49	gi|6679321	81201	Phosphatidylinositol 3-kinase, regulatory subunit, polypeptide 2 (p85)	1.05	0
50	gi|68533246	108114	Thyroid hormone receptor associated protein 3	1.05	0.07
51	gi|6753620	73056	DEAD/H (Asp-Glu-Ala-Asp/His) box polypeptide 3, X-linked	1.04	0.17
52	gi|6755372	26657	Ribosomal protein S3	1.03	0.09
53	gi|86262142	69406	RNA binding motif protein 14	1.03	0.12
54	gi|6680047	35055	Guanine nucleotide binding protein (G protein), beta polypeptide 2 like 1	1.03	0.06
55	gi|23956214	75394	Splicing factor proline/ glutamine rich (polypyrimidine tract binding protein associated)	1.02	0.07
56	gi|6678986	118082	Myosin IC isoform b	1.02	0
57	gi|31560686	69599	Heat shock protein 2	1.01	0
58	gi|6681273	50422	Eukaryotic translation elongation factor 1 alpha 2	1	0.14
59	gi|6754256	73483	Heat shock protein 9A	0.99	0.2
60	gi|40556608	83229	Heat shock protein 1, beta	0.99	0.4
61	gi|34328251	72372	Drebrin 1	0.99	0.22
62	gi|31560560	32893	Laminin receptor 1	0.96	0.03
63	gi|31981562	57808	Pyruvate kinase 3	0.95	0.11
64	gi|61743961	603866	AHNAK nucleoprotein isoform 1	0.95	0
65	gi|19526792	40957	CD34 antigen	0.94	0
66	gi|33859482	95253	Eukaryotic translation elongation factor 2	0.93	0.2
67	gi|7305295	223128	Myosin, heavy polypeptide 11, smooth muscle	0.92	0.08
68	gi|31981722	72378	Heat shock 70 kD protein 5 (glucose-regulated protein)	0.91	0.09
69	gi|6671672	32947	Capping protein (actin filament) muscle Z-line, alpha 2	0.91	0.08

70	gi|23956398	40730	Protein-L-isoaspartate (D-aspartate) O-methyltransferase domain containing 2	0.91	0.08
71	gi|76677817	60183	Fuse-binding protein-interacting repressor isoform a	0.91	0.11
72	gi|6678465	49928	Tubulin, alpha 1 a	0.87	0.12
73	gi|6754994	37474	Poly(rC) binding protein 1	0.86	0
74	gi|7948995	116761	Tyrosine kinase, non-receptor, 2	0.84	0.06
75	gi|6753262	30609	Capping protein (actin filament) muscle Z-line, beta	0.81	0.29
76	gi|49258190	78523	NCK interacting protein with SH3 domain	0.79	0
77	gi|21536246	69733	DEAD (Asp-Glu-Ala-Asp) box polypeptide 41	0.68	0.04
78	gi|91598596	67748	Sorting nexin associated golgi protein 1	0.63	0.02
79	gi|23956222	47327	ARP3 actin-related protein 3 homolog	0.61	0
80	gi|6753226	192750	Complement component 4 (within H-2S)	0.39	0
81	gi|19111160	36193	prostasin	0.3	0.1
82	gi|28395018	81749	Junction plakoglobin	0.29	0.1
83	gi|10946866	78269	Solute carrier organic anion transporter family, member 1c1	0.27	0.1
84	gi|31982171	165193	Murinoglobulin 1	0.25	0.21
85	gi|6678083	45825	Serine (or cysteine) proteinase inhibitor, clade A, member 1c	0.21	0.13
86	gi|94419105	105453	PREDICTED: similar to Development and differentiation-enhancing factor 2 (Pyk2 C-terminus associate)	0.15	0.08
87	gi|50363232	207000	Nestin	0.13	0.14
88	gi|94390864	93809	PREDICTED: similar to Y39A1A.9 isoform 1	0.13	0.09
89	gi|6753220	26701	Complement component 1, q subcomponent, B chain	0.12	0.19
90	gi|6671684	85416	Catenin (cadherin associated protein), beta 1, 88 kDa	0.12	0
91	gi|83008262	13646	PREDICTED: similar to Ig heavy chain V region 108A precursor	0.11	0.13
92	gi|94377464	12891	PREDICTED: similar to Ig kappa chain	0.11	0.08

			V-VI region NQ2-17.4.1		
93	gi|27370470	85462	Phosphatidylinositol-3-phosphatase associated protein	0.09	0.02
94	gi|94385430	21645	PREDICTED: similar to Myosin light polypeptide 6 (Myosin light chain alkali 3) (Myosin light chain	0.06	0.14

Table 4. List of identified proteins from the SILAC experiment at the protein level. Phenylphosphate and Boiled beads elutions combined.

Protein No.	Peptide No.	Heavy/Light ratio	St. Dev	GI	Mass [Da]	Description	Peptide Sequence	m/z	Charge	Score
1	1	2.55	0.29	gi|9506909	237319	myosin X	YSGMLETVR	531.2703	2	23
1	2						VEGQEFIVR	541.7942	2	60
1	3						TSFLEGTLR	515.2854	2	42
1	4						TIVADVLAK	468.2754	2	21
1	5						TFTPYER	460.238	2	34
1	6						QLLAEKR	435.2859	2	35
1	7						LLNEATR	411.7417	2	38
1	8						IVDYLLEK	499.7991	2	35
1	9						EIEDLQR	454.7456	2	37
2	1	2.44	0.65	gi|31982755	53655	vimentin	VEVERDNLAEDIMR	572.9616	3	36
2	2						VEVERDNLAEDIMR	572.9659	3	22
2	3						TYSLGSALRPSTSR	499.2764	3	42
2	4						TYSLGSALRPSTSR	503.3027	3	20
2	5						SYVTTSTR	460.7439	2	38
2	6						SYVTTSTR	460.7411	2	41
2	7						SYVTTSTR	460.7541	2	35
2	8						SSVPGVR	351.1989	2	52
2	9						SSVPGVR	354.2128	2	45
2	10						SSVPGVR	354.2181	2	37
2	11						SLYSSSPGGAYVTR	725.8761	2	55
2	12						QVDQLTNDKAR	433.9129	3	24
2	13						QVDQLTNDKAR	429.9083	3	42
2	14						QQYESVAAK	512.2586	2	25
2	15						QQYESVAAK	515.2666	2	62
2	16						QQYESVAAK	515.2819	2	56
2	17						QQYESVAAK	515.2888	2	35
2	18						QQYESVAAK	515.2856	2	30
2	19						QDVDNASLAR	547.7911	2	84
2	20						NLQEAEEWYK	658.3205	2	45
2	21						NLQEAEEWYK	658.3316	2	39
2	22						MFGGSGTSSRPSSNR	519.2566	3	36
2	23						MFGGSGTSSRPSSNR	515.2534	3	32
2	24						LQDEIQNMKEEMAR	593.6254	3	29
2	25						LQDEIQNMKEEMAR	593.6412	3	32
2	26						LLEGEESR	466.7409	2	58
2	27						LLEGEESR	469.7498	2	66
2	28						LLEGEESR	469.7574	2	33
2	29						KVESLQEEIAFLK	515.9863	3	45
2	30						KLLEGEESR	358.2197	3	30
2	31						ISLPLPTFSSLNLR	782.4772	2	38
2	32						ILLAELEQLKGQGK	517.9962	3	38
2	33						ILLAELEQLKGQGK	518.0084	3	47
2	34						FADLSEAANRNNDALR	596.9824	3	33
2	35						FADLSEAANR	550.2779	2	63

2	36						FADLSEAANR	550.2895	2	59
2	37						EYQDLLNVK	564.3161	2	37
3	1	2.35	0.93	gi|24429590	149489	DEAH (Asp-Glu-Ala-His) box polypeptide 9	YTQVGPDHNR	398.2154	3	20
3	2						LPIEPR	365.7411	2	27
3	3						LGGIGQFLAK	505.3134	2	29
3	4						ILTTEGR	398.2441	2	27
3	5						DFVNYLVR	516.2927	2	22
4	1	2.26	0.36	gi|94365254	144475	PREDICTED: similar to tensin	SYVESVAR	458.7536	2	30
4	2						SYVESVAR	458.7574	2	33
4	3						LLSGFGVDR	485.3182	2	22
4	4						LFGFVAR	408.257	2	30
4	5						LFGFVAR	408.2612	2	24
4	6						HFLIETGPR	538.3086	2	27
4	7						GAYGLAMK	416.7264	2	24
4	8						GAYGLAMK	416.728	2	23
5	1	2.16	0.15	gi|27370424	107827	hypothetical protein LOC244895	VQEFNNCLNR	650.3205	2	56
5	2						STSSPYHASNLLQR	522.9381	3	31
5	3						SSVKVPETHK	375.2175	3	25
5	4						SPNLSEIK	447.2591	2	24
5	5						SPNLSEIK	447.2527	2	47
5	6						SAPTSPTATNISSK	684.3675	2	55
5	7						LVTSAQSEPPPPFPPPR	608.3553	3	31
5	8						IQRPTQEPAGK	412.919	3	32
5	9						IQRPTQEPAGK	412.9093	3	36
5	10						IQKDPSTKPVTSPPSK	428.2498	4	26
5	11						IAVHTEKPESK	417.5839	3	26
5	12						EIAGLEATPPVR	629.8547	2	69
5	13						ANTLSPVR	472.2493	2	36
6	1	2.01	0	gi|31981796	52390	docking protein 1	VGQAQDILR	503.288	2	64
6	2						TWAVLYPASPHGVAR	544.2989	3	40
7	1	1.95	0.25	gi|6754632	41249	mitogen activated protein kinase 1	VADPDHDHTGFLTEYVATR	743.9977	3	51
7	2						NYLLSLPHK	364.2256	3	29
7	3						LKELIFEETAR	454.2658	3	52
7	4						LFPNADSK	449.2416	2	33
7	5						ISPFEHQTYCQR	524.5866	3	32
7	6						ICDFGLAR	476.2466	2	40
7	7						GQVFDVGPR	490.7686	2	48
7	8						GQVFDVGPR	490.7845	2	31
7	9						ELIFEETAR	557.292	2	27
7	10						DLKPSNLLLNTTCDLK	619.6872	3	50
7	11						APEIMLNSK	512.786	2	31
7	12						APEIMLNSK	509.7607	2	40
7	13						APEIMLNSK	512.7877	2	56
7	14						ALDLLDK	397.2494	2	48
7	15						ALDLLDK	394.2411	2	33
8	1	1.92	0.37	gi|21281693	60772	paxillin isoform alpha	YAHQQPPSPLPVYSSSAK	655.0199	3	50
8	2						VVTALDR	387.2331	2	37

8	3						VVTALDR	390.248	2	26
8	4						VVTALDR	387.2401	2	55
8	5						VVTALDR	387.2314	2	29
8	6						VVTALDR	390.2406	2	48
8	7						VVTALDR	390.232	2	20
8	8						VVTALDR	390.2472	2	36
8	9						VVTALDR	387.2248	2	23
8	10						RGSLCSGCQKPITGR	419.985	4	45
8	11						NFFER	356.6888	2	24
8	12						NFFER	359.6998	2	21
8	13						NFFER	356.6857	2	24
8	14						NFFER	359.6857	2	23
8	15						LGVATVAK	379.7341	2	31
8	16						LGVATVAK	382.7609	2	48
8	17						LGVATVAK	382.7617	2	55
8	18						LGVATVAK	382.7657	2	36
8	19						LGVATVAK	379.7287	2	38
8	20						LGVATVAK	379.7227	2	39
8	21						LGVATVAK	379.712	2	25
8	22						LGVATVAK	382.7594	2	35
8	23						LGVATVAK	379.7498	2	34
8	24						LGVATVAK	379.7517	2	42
8	25						KPIAGQVVTAMGK	439.2709	3	57
8	26						KPIAGQVVTAMGK	443.2617	3	30
8	27						KPIAGQVVTAMGK	439.2684	3	60
8	28						KPIAGQVVTAMGK	443.2543	3	26
8	29						KFHPEHFVCAFCLK	458.7491	4	37
8	30						KDYFDMFAPK	430.5607	3	57
8	31						KDYFDMFAPK	425.2324	3	50
8	32						ISASSATR	399.7402	2	24
8	33						GSLCSGCQKPITGR	511.598	3	41
8	34						GSLCSGCQKPITGR	511.6095	3	57
8	35						ELDELMASLSDFKFMAQGK	735.3865	3	25
8	36						ELDELMASLSDFK	757.3842	2	58
8	37						DYHSLFSPR	376.5365	3	24
8	38						DYFDMFAPK	578.2772	2	27
8	39						DYFDMFAPK	567.2712	2	31
8	40						DGQPYCEKDYHSLFSPR	525.5088	4	30
8	41						AGEEEHVYSFPNK	504.921	3	43
9	1	1.84	0	gi|31982290	65800	LIM domain containing preferred translocation partner in lipoma	YAPVVAPKPK	361.2409	3	32
9	2						STGEPLGHVPAR	409.5754	3	33
10	1	1.73	0.13	gi|21313308	77597	heterogeneous nuclear ribonucleoprotein M	MGPAIER	398.2191	2	55
10	2						MGPAIER	395.205	2	30
10	3						MGLVMDR	430.2266	2	33
11	1	1.71	0	gi|25141233	94572	matrin 3	LAEPYGK	392.2341	2	35
12	1	1.69	0.31	gi|27476057	83721	discoidin, CUB and LCCL domain containing 2	YSTSEVSHLSAR	448.254	3	26
12	2						FTQVLQPR	497.799	2	38
13	1	1.67	0.23	gi|40254593	94227	breast cancer	VLPPEVADGSVVD	852.1058	3	35

						anti-estrogen resistance 1	DGVYAVPPPAER			
13	2						VLGQLAAA	371.7258	2	37
13	3						TQQGLYQAPGPNPQFQSPPAK	754.0436	3	69
13	4						TKAPGPGPEGSSSLHPNPTDK	522.2858	4	29
13	5						TKAPGPGPEGSSSLHPNPTDK	519.2798	4	50
13	6						TGGLGPSDR	433.2392	2	49
13	7						RVLGQLAAA	452.7907	2	31
13	8						RPGPGTLYDVPR	447.2675	3	37
13	9						RPGPGTLYDVPR	443.2494	3	44
13	10						QGKGQLELQQLK	461.2806	3	40
13	11						QGIVPGNR	420.7412	2	22
13	12						QGIVPGNR	423.7416	2	38
13	13						LVFIGDTLSR	563.8469	2	58
13	14						LVFIGDTLSR	563.8301	2	57
13	15						LVFIGDTLSR	563.8427	2	29
13	16						HLLAPGPQDIYDVPPVR	631.686	3	56
13	17						GWEGTKPPAK	357.529	3	24
13	18						GSPGFTPEDLDRLVACSR	663.6592	3	40
13	19						GSPGFTPEDLDR	648.821	2	55
13	20						GQLELQQLK	531.8093	2	33
13	21						GAVSNATHTSDR	407.8735	3	45
13	22						GAVSNATHTSDR	407.8778	3	31
13	23						ASSIQSRPLPSPPK	492.9652	3	33
13	24						ASSIQSRPLPSPPK	492.961	3	42
13	25						ALYDNVAESPDELSFR	609.3046	3	67
13	26						ALYDNVAESPDELSFR	916.4366	2	52
13	27						AAALQYPSPSAAQDMVDR	638.311	3	77
14	1	1.66	0.02	gi|21489933	43039	mitogen activated protein kinase 3	NYLQSLPSK	528.3014	2	45
14	2						ALDLLDR	408.2391	2	46
14	3						ALDLLDR	411.2538	2	41
15	1	1.66	0.5	gi|82887378	49344	PREDICTED: molybdenum cofactor synthesis 3	VPPPPLAPR	475.3003	2	53
15	2						VPPPPLAPR	475.3145	2	26
15	3						VPPPPLAPR	475.3088	2	25
16	1	1.62	0.07	gi|31560712	50684	c-src tyrosine kinase	SVLGGDCLLK	534.2907	2	28
16	2						NVLVSEDNVAK	597.3231	2	48
17	1	1.59	0.15	gi|51921285	85247	G protein-coupled receptor kinase-interactor 1	YQMLAFVHK	386.8891	3	26
17	2						VNSSLSDELRR	425.901	3	42
17	3						TPIDYAR	421.2411	2	37
17	4						TPIDYAR	418.232	2	33
17	5						TGNLETCLR	535.2849	2	57
17	6						SLSSPTDNLELSAR	745.4058	2	66
17	7						SLSSPTDNLELSAR	748.4102	2	60
17	8						SAVPFLPVNPEYSATR	877.489	2	30

17	9						SAVPFLPVNPEYSATR	877.48	2	31
17	10						RPALEPVR	469.2943	2	40
17	11						QLVTITTR	460.7959	2	36
17	12						QLHSSVR	408.2427	2	40
17	13						QAGHHELAER	379.5361	3	34
17	14						NIQELLR	446.285	2	29
17	15						NIQELLR	446.287	2	36
17	16						NIQELLR	446.2642	2	33
17	17						LVECQYELTDR	716.3648	2	45
17	18						LQALSNR	404.2555	2	39
17	19						LQALSNR	404.2518	2	43
17	20						LQAENLQLR	542.8238	2	56
17	21						LQAENLQLR	545.8197	2	41
17	22						LPCRDDDGVTAK	453.5799	3	20
17	23						LLSLGAQANFFHPEK	559.9899	3	36
17	24						LLSLGAQANFFHPEK	559.9986	3	22
17	25						LLNASAYR	457.2814	2	40
17	26						LLNASAYR	457.2737	2	49
17	27						LLNASAYR	457.2621	2	21
17	28						LAFYLCGR	503.2966	2	22
17	29						LAFYLCGR	500.2734	2	40
17	30						LAFYLCGR	503.2868	2	24
17	31						KLQALSNR	471.3139	2	45
17	32						GVLVCDECCSVHR	532.9268	3	44
17	33						GTTPLHVAAK	497.7983	2	45
17	34						AEHTLMGPGGSTHR	368.9472	4	42
18	1	1.58	0	gi|28076981	90916	cullin 5	LVHAER	365.7453	2	27
19	1	1.56	0.11	gi|31980859	72984	Rho guanine nucleotide exchange factor (GEF7)	VIEAYCTSAK	574.2993	2	51
19	2						VGGCFLSLMPQMR	767.3954	2	27
19	3						TGWFPSNYVR	616.8285	2	52
19	4						STAALEEDAQILK	697.9097	2	68
19	5						SPPKGFDTTAINK	459.2687	3	41
19	6						SNGQTVIEEK	553.2873	2	81
19	7						SLVDTVYALKDEVQELR	664.0517	3	58
19	8						SLEEEQRAR	377.2228	3	25
19	9						NLSAQCQEVR	605.8151	2	52
19	10						NAFEISGSMIER	685.3394	2	56
19	11						NAFEISGSMIER	688.3584	2	24
19	12						NAFEISGSMIER	680.359	2	47
19	13						MSGFIYQGK	566.7582	2	44
19	14						MSGFIYQGK	566.7609	2	36
19	15						LPTTGMTITK	542.8077	2	64
19	16						LPTTGMTITK	542.8257	2	35
19	17						LPTTGMTITK	542.824	2	32
19	18						LPTTGMTITK	542.8106	2	48
19	19						LPTTGMTITK	534.8231	2	49
19	20						LDKYPTLLK	368.2464	3	38
19	21						LDKYPTLLK	368.2398	3	28
19	22						LDKYPTLLK	368.2329	3	40
19	23						KPSDEEFAVRK	441.9297	3	36
19	24						KPSDEEFAVR	397.2208	3	41
19	25						IIVEETK	419.2689	2	33
19	26						GFDTTAINK	486.7646	2	40

19	27						GFDTTAINK	483.7627	2	39
19	28						GDVIHVTR	448.7604	2	66
19	29						GASSPGILVLTTGLSKPFMR	683.4067	3	49
19	30						ESAPQVLLPEEEKIIVEETK	765.0932	3	22
19	31						ELELQILTEPIR	730.437	2	55
19	32						EIKPSEKPVSPK	452.9625	3	38
19	33						EIKPSEKPVSPK	446.9509	3	25
20	1	1.55	0.05	gi|16905083	121847	Rap guanine nucleotide exchange factor (GEF) 1 isoform 3	VAVVAPMSR	476.274	2	28
20	2						VAVVAPMSR	476.2654	2	32
20	3						RQSAPSPTR	506.7647	2	29
20	4						RQSAPSPTR	506.7586	2	38
20	5						RQSAPSPTR	506.7602	2	32
20	6						RQSAPSPTR	506.7627	2	43
20	7						RQSAPSPTR	506.7599	2	34
20	8						RQSAPSPTR	506.7662	2	34
21	1	1.55	0.32	gi|6679108	32540	nucleophosmin 1	VTLATLK	373.2528	2	23
21	2						GPSSVEDIKAK	377.5513	3	31
21	3						GPSSVEDIK	469.2599	2	49
22	1	1.5	0.02	gi|46849812	272368	fibronectin 1	LTAGLTR	369.2423	2	26
22	2						LGVRPSQGGEAPR	445.9319	3	35
22	3						LGVRPSQGGEAPR	445.9337	3	26
22	4						APITGYIIR	505.3098	2	33
23	1	1.47	0	gi|21450625	46125	eukaryotic translation initiation factor 4A1	VLITTDLLAR	560.8733	2	37
24	1	1.46	0.41	gi|70794809	59853	Rous sarcoma oncogene isoform 2	VADFGLAR	427.7443	2	63
24	2						LTTVCPTSKPQTQGLAK	614.6861	3	53
24	3						LLLNAENPR	523.3054	2	43
24	4						LIEDNEYTAR	615.3117	2	71
24	5						KLDSGGFYITSR	452.5897	3	30
24	6						GPSAAFVPPAAEPK	669.8598	2	47
24	7						EVLDQVER	497.2609	2	23
24	8						EVLDQVER	494.2589	2	60
24	9						EVLDQVER	497.2573	2	25
24	10						EVLDQVER	497.287	2	41
24	11						DAWEIPR	446.7387	2	26
25	1	1.41	0	gi|7949051	87837	heterogenous nuclear ribonucleoprotein U	NGQDLGVAFK	527.7952	2	69
25	2						NGQDLGVAFK	528.2864	2	40
25	3						LNTLLQR	432.2828	2	60
25	4						FIEIAAR	410.2494	2	35
26	1	1.39	0	gi|31980648	56265	ATP synthase, H+ transporting mitochondrial F1 complex, beta subunit	ILQDYK	393.2238	2	23
26	2						IGLFGGAGVGK	491.2992	2	33
27	1	1.35	0.16	gi|41322927	506145	plectin 1 isoform 4	VPLDVAYAR	505.2954	2	28
27	2						VPGAQDGVR	449.7492	2	32

27	3						VLADPSDDTK	533.7846	2	23
27	4						QLAEGTAQQR	551.2933	2	32
27	5						LTVDEAVR	454.7751	2	46
27	6						LSVAAQEAAR	511.2928	2	58
27	7						LRAETEQGEQQR	486.27	3	33
27	8						LQAEEVAQQK	575.323	2	30
27	9						LLEAAAQSSK	512.2999	2	39
27	10						LLAEENQR	489.7771	2	27
27	11						LKAEVTEAAR	363.216	3	38
27	12						LAAISEATR	469.2878	2	47
27	13						EVAEADSVR	488.2538	2	42
27	14						ATVSAPFGK	442.2648	2	46
27	15						AGVVGPELHEK	381.2187	3	21
28	1	1.34	0.11	gi|7305237	71375	LIM domains containing 1	SYLSVSAPLSSTAGK	737.4149	2	68
28	2						GAGNNPEFEETRR	492.9147	3	25
28	3						DSGLGYEASGR	556.2725	2	55
28	4						DSGLGYEASGR	559.2823	2	46
29	1	1.29	0.1	gi|6679741	119141	PTK2 protein tyrosine kinase 2	YMEDSTYYK	608.2519	2	41
29	2						YMEDSTYYK	608.2626	2	45
29	3						VYENVTGLVK	564.318	2	29
29	4						VKHVACYGFR	416.8988	3	47
29	5						TLLATVDETIPALPASTHR	669.3861	3	50
29	6						TLLATVDETIPALPASTHR	669.3689	3	50
29	7						THLGTGMER	501.2454	2	32
29	8						SYWEMR	439.2053	2	25
29	9						SNYEVLEK	491.2509	2	47
29	10						SNYEVLEK	491.2644	2	35
29	11						SNDKVYENVTGLVK	522.6277	3	67
29	12						SNDKVYENVTGLVK	526.6223	3	79
29	13						SNDKVYENVTGLVK	522.9644	3	41
29	14						SLLDSVK	381.235	2	22
29	15						SLLDSVK	384.2428	2	25
29	16						SLLDSVK	381.2245	2	40
29	17						SLLDSVK	384.2417	2	28
29	18						SFLQVR	375.2272	2	22
29	19						SFLQVR	375.2353	2	39
29	20						SFLQVR	378.2399	2	39
29	21						SFLQVR	378.2307	2	37
29	22						SFLQVR	375.2254	2	35
29	23						SEEVHWLHVDMGVSSVR	498.0016	4	52
29	24						SDYMQEIADQVDQEIALK	704.665	3	68
29	25						QQQEMEEDQRWLEKEER	577.5194	4	26
29	26						QQQEMEEDQRWLEKEER	764.001	3	50
29	27						QQQEMEEDQRWLEKEER	764.693	3	38
29	28						QMLTAAHALAVDAK	487.9323	3	47
29	29						QMLTAAHALAVDAK	487.9519	3	38
29	30						QMLTAAHALAVDAK	482.6054	3	47

29	31	QMLTAAHALAVDAK	722.9066	2	81
29	32	QMLTAAHALAVDAK	722.8778	2	101
29	33	QMLTAAHALAVDAK	714.8811	2	82
29	34	QFANLNREESILK	778.9328	2	47
29	35	QFANLNR	434.7376	2	31
29	36	QFANLNR	431.7459	2	25
29	37	NVLVSSNDCVK	620.8313	2	68
29	38	NVLVSSNDCVK	617.8247	2	54
29	39	NVLVSSNDCVK	617.8077	2	48
29	40	NNDVIGR	394.2032	2	45
29	41	NNDVIGR	397.2296	2	44
29	42	NLLDVIDQAR	581.8312	2	53
29	43	NLLDVIDQAR	578.8368	2	56
29	44	NLLDVIDQAR	578.8269	2	63
29	45	NLLDVIDQAR	578.8079	2	53
29	46	NLLDVIDQAR	578.8351	2	57
29	47	MLGQTRPH	478.2532	2	52
29	48	LVNGATQSFIIRPQK	558.3307	3	46
29	49	LVNGATQSFIIRPQK	558.3252	3	49
29	50	LVNGATQSFIIRPQK	558.3038	3	33
29	51	LVNGATQSFIIRPQK	558.0133	3	35
29	52	LQPQEISPPPTANLDR	592.6669	3	26
29	53	LQPQEISPPPTANLDR	594.6568	3	61
29	54	LQPQEISPPPTANLDR	594.6668	3	73
29	55	LPMPPNCPPTLYSLMTK	664.6544	3	44
29	56	LLNSDLGELISK	651.3829	2	78
29	57	LLNSDLGELISK	651.368	2	84
29	58	LLNSDLGELISK	654.368	2	66
29	59	LLNSDLGELISK	651.3825	2	65
29	60	LKMLGQTRPH	403.579	3	31
29	61	LKMLGQTRPH	403.5744	3	35
29	62	LIQQTFR	456.2809	2	58
29	63	LIQQTFR	453.2551	2	49
29	64	LIQQTFR	453.7579	2	35
29	65	LIQQTFR	453.3102	2	47
29	66	LGDFGLSR	432.7419	2	63
29	67	LGDFGLSR	432.7485	2	52
29	68	LGDFGLSR	432.7402	2	51
29	69	LGDFGLSR	432.7271	2	57
29	70	LGDFGLSR	435.75	2	35
29	71	LGDFGLSR	435.7479	2	32
29	72	LGDFGLSR	435.7474	2	32
29	73	LGDFGLSR	432.7485	2	59
29	74	LGCLEIRR	508.7903	2	46
29	75	LGCLEIR	430.7483	2	49
29	76	LGCLEIR	433.7438	2	55
29	77	LGCLEIR	402.2566	2	23
29	78	LAQQYVMTSLQQEYKK	662.7009	3	35
29	79	LAQQYVMTSLQQEYKK	662.6783	3	45
29	80	LAQQYVMTSLQQEYKK	657.3598	3	44
29	81	KSNYEVLEKDVGLKR	445.2536	4	38

29	82	KSNYEVLEK	370.5394	3	32
29	83	KSNYEVLEK	370.5458	3	21
29	84	KQMLTAAHALAVDAK	532.6475	3	46
29	85	KGMLQLK	409.2516	2	47
29	86	IQPAPPEEYVPMVK	540.6401	3	21
29	87	IQPAPPEEYVPMVK	540.6217	3	37
29	88	IQPAPPEEYVPMVK	538.632	3	29
29	89	IQPAPPEEYVPMVK	535.2964	3	53
29	90	HVACYGFR	508.248	2	42
29	91	GMLQLK	356.2077	2	24
29	92	GMGQVLPPHLMEER	544.6077	3	27
29	93	GMGQVLPPHLMEER	544.6231	3	20
29	94	FLQEALTMR	565.8173	2	44
29	95	FLQEALTMR	565.8158	2	51
29	96	FLQEALTMR	562.7865	2	48
29	97	FLQEALTMR	565.8122	2	34
29	98	FLQEALTMR	554.7934	2	55
29	99	FLKPDVRLSR	437.573	3	21
29	100	FLKPDVR	437.7733	2	40
29	101	FLKPDVR	443.7825	2	49
29	102	FFEILSPVYR	635.8618	2	44
29	103	FFEILSPVYR	635.8451	2	45
29	104	FFEILSPVYR	635.859	2	36
29	105	FDKECFK	493.2589	2	20
29	106	FDKECFK	493.2356	2	20
29	107	EVGLALR	382.2463	2	36
29	108	EVGLALR	379.2449	2	24
29	109	EVGLALR	379.2347	2	42
29	110	EVGLALR	379.2416	2	50
29	111	EVGLALR	379.2311	2	41
29	112	EVGLALR	382.2387	2	34
29	113	EVGLALR	379.2272	2	37
29	114	EVGLALR	382.231	2	32
29	115	EVGLALR	379.2429	2	50
29	116	ERIELGR	442.7718	2	27
29	117	EKYELAHPPEEWKYELR	555.0383	4	50
29	118	EKFLQEALTMR	465.2693	3	23
29	119	EKFLQEALTMR	465.2597	3	32
29	120	EIEMAQK	427.7414	2	32
29	121	EESILK	359.7129	2	23
29	122	DYEIQR	415.2274	2	26

29	123						DYEIQR	415.2064	2	29
29	124						DYEIQR	412.2118	2	28
29	125						CWAYDPSR	530.7433	2	40
29	126						AVIEMSSK	435.7382	2	36
29	127						AQLSTILEEEKVQQEER	681.3852	3	72
29	128						AQLSTILEEEKVQQEER	681.3603	3	77
29	129						AQLSTILEEEKVQQEER	677.3695	3	57
29	130						ALPSIPK	366.2539	2	40
29	131						ALPSIPK	366.243	2	31
29	132						ALPSIPK	366.2549	2	26
30	1	1.26	0	gi|31982757	54055	Ras-GTPase-activating protein (GAP120) SH3-domain binding protein 2 isoform a	VDAKPEVQSQPPR	488.2873	3	30
31	1	1.21	0.1	gi|10092590	41261	mitogen activated protein kinase 14	TLFPGTDHIDQLK	497.6111	3	46
31	2						TIWEVPER	518.28	2	27
31	3						TIWEVPER	518.2925	2	24
31	4						NYIQSLAQMPK	657.8442	2	55
31	5						NYIQSLAQMPK	657.8666	2	42
31	6						MLVLDSDKR	368.881	3	22
31	7						LVGTPGAELLKK	409.2551	3	36
31	8						LVGTPGAELLKK	409.2693	3	22
31	9						LVGTPGAELLK	549.3185	2	32
31	10						LVGTPGAELLK	552.3599	2	23
31	11						ILDFGLAR	455.783	2	36
31	12						ILDFGLAR	455.7818	2	35
31	13						DLLIDEWK	519.283	2	28
31	14						DLLIDEWK	519.2944	2	30
32	1	1.21	0	gi|23956078	71736	ATP-binding cassette, sub-family F (GCN20), member 2	MMASGLTER	514.2493	2	41
33	1	1.21	0	gi|61888842	66568	partitioning-defective protein 3 homolog isoform 2	TLGLLVK	372.2589	2	21
33	2						LNIQLK	364.7349	2	25
33	3						INDGDLR	401.7284	2	33
34	1	1.2	0	gi|94370505	14540	PREDICTED: similar to heterogeneous nuclear ribonucleoprotein H2	YVEVFK	392.7164	2	22
34	2						YVEVFK	392.7282	2	23
34	3						YIEIFK	406.7357	2	23
34	4						HTGPNSPDTANDGFVR	564.2916	3	54

35	1	1.19	0.01	gi|10946928	49168	heterogeneous nuclear ribonucleoprotein H1	VHIEIGPDGR	366.8919	3	29
35	2						IQNGAQGIR	481.795	2	32
35	3						FIYTR	350.1983	2	22
36	1	1.16	0	gi|7305075	51797	ras-GTPase-activating protein SH3-domain binding protein	EAGEPGDVEPR	581.2846	2	39
37	1	1.14	0.05	gi|31542366	34085	cell division cycle 2 homolog A	SPEVLLGSAR	514.8035	2	59
37	2						NLDENGLDLLSK	668.874	2	90
37	3						LADFGLAR	434.7629	2	37
37	4						IGEGTYGVVYK	633.308	2	54
37	5						EISLLK	351.7317	2	32
37	6						AFGIPIR	387.2455	2	37
38	1	1.14	0	gi|8394460	39478	tropomodulin 3	LVEVNLNNIK	581.3741	2	50
38	2						LLSYLEK	433.2575	2	22
38	3						LLSYLEK	433.2693	2	30
39	1	1.12	0.1	gi|32484983	108782	Eph receptor A2	YSEPPHALTR	392.8831	3	25
39	2						VVQMSNEDIKR	445.5759	3	31
39	3						VIGAGEFGEVYK	637.8506	2	69
39	4						TLADFDPR	470.7593	2	58
39	5						TASVSINQTEPPKVR	546.9796	3	41
39	6						SEQLKPLK	477.8206	2	31
39	7						NILVNSNLVCK	640.3728	2	63
39	8						NILVNSNLVCK	637.3386	2	46
39	9						NGVSGLVTSR	498.2881	2	64
39	10						MVGPLTR	395.2299	2	27
39	11						LPSTSGSEGVPFR	667.3509	2	67
39	12						LNVEER	380.2139	2	40
39	13						LNVEER	380.2088	2	34
39	14						LEGVVSK	369.234	2	23
39	15						IFIELK	381.7519	2	24
39	16						IFIELK	381.7482	2	35
39	17						IAYSLLGLK	489.3087	2	61
39	18						GELGWLTHPYGK	455.2599	3	40
39	19						FTTEIHPSCVAR	475.2596	3	28
39	20						FADIVSILDK	563.8411	2	66
39	21						EVVLLDFAAMK	626.3525	2	52
39	22						EKDGEFSVLQLVGMLR	617.0149	3	23
39	23						EIPVAIK	388.2584	2	36
39	24						AINDGFR	396.7117	2	35
39	25						ACSPGFFK	460.2363	2	45
40	1	1.1	0.16	gi|31560030	32689	tropomyosin 1, alpha	SLEAQAEK	441.2482	2	47
40	2						SIDDLEEK	474.7457	2	43
40	3						QLEDELVSLQK	654.3726	2	61
40	4						LATALQK	375.7515	2	26
40	5						LATALQK	375.7502	2	30
40	6						HIAEDADR	466.7405	2	23
41	1	1.1	0.04	gi|6679937	35787	glyceraldehyde-3-phosphate dehydrogenase	VVDLMAYMASKE	697.8499	2	47

41	2						VGVNGFGR	403.719	2	20
41	3						LTGMAFR	406.2206	2	31
41	4						GAAQNIIPASTGAAK	685.3845	2	36
42	1	1.1	0	gi|6680748	59716	ATP synthase, H+ transporting, mitochondrial F1 complex, alpha subunit, isoform 1	LTELLK	358.7469	2	22
42	2						AVDSLVPIGR	513.7972	2	23
42	3						AVDSLVPIGR	513.8113	2	22
42	4						APGIIPR	362.2389	2	28
43	1	1.08	0.07	gi|94407081	64081	PREDICTED: similar to DEAD (Asp-Glu-Ala-Asp) box polypeptide 3, Y-linked	VGSTSENITQK	582.3038	2	67
43	2						VGSTSENITQK	585.3131	2	28
43	3						VGSTSENITQK	585.323	2	84
43	4						VGSTSENITQK	585.3143	2	87
43	5						SSFFGDR	408.2038	2	38
43	6						SPILVATAVAAR	587.8849	2	50
43	7						QSSGASSSSFSSSR	681.3143	2	76
43	8						IVEQDTMPPKGVR	495.9441	3	32
43	9						HAIPIIK	399.2762	2	44
43	10						HAIPIIK	396.2625	2	21
43	11						GLDISNVK	423.2533	2	28
43	12						FSGGFGAR	402.7222	2	26
44	1	1.07	0	gi|12963491	47095	enolase 1, alpha non-neuron	YNQILR	406.7444	2	20
44	2						YNQILR	406.7519	2	21
44	3						TIAPALVSK	450.2858	2	24
44	4						IGAEVYHNLK	383.8834	3	23
44	5						IGAEVYHNLK	381.8761	3	25
44	6						IEEELGSK	455.7547	2	41
45	1	1.07	0	gi|31980798	70256	nuclear RNA export factor 1	NASPEEIQR	522.2729	2	32
46	1	1.07	0.26	gi|49258190	78523	NCK interacting protein with SH3 domain	LSDLQATLR	508.8013	2	44
46	2						ALYAFR	370.7254	2	21
46	3						AIEAVHNTAMR	410.2281	3	22
46	4						AAAETVVPR	457.2728	2	65
46	5						AAAETVVPR	457.2672	2	71
47	1	1.07	0.11	gi|7106439	49639	tubulin, beta 5	YLTVAAVFR	523.313	2	41
47	2						TAVCDIPPR	514.7689	2	67
47	3						LAVNMVPFPR	580.3126	2	57
47	4						LAVNMVPFPR	580.3341	2	33
48	1	1.07	0.07	gi|83816893	69223	DEAD (Asp-Glu-Ala-Asp) box polypeptide 5	TIVFVETK	471.8016	2	42
48	2						TIVFVETK	468.7826	2	41
48	3						TGTAYTFFTPNNIK	790.9148	2	31
48	4						TAQEVDTYRR	413.5605	3	26
48	5						TAQEVDTYRR	413.5576	3	23
48	6						QVSDLISVLR	568.3588	2	39

48	7						LMEEIMSEKENK	504.918	3	25
48	8						LMEEIMSEKENK	504.9179	3	24
48	9						LLQLVEDRGSGR	452.2819	3	23
48	10						LLQLVEDR	496.3127	2	62
48	11						LLQLVEDR	493.2965	2	60
48	12						APILIATDVASR	613.8734	2	62
48	13						APILIATDVASR	613.8695	2	51
49	1	1.06	0	gi|47271396	-1	GNAS complex locus isoform a	LLLLGAGESGK	529.3407	2	71
50	1	1.06	0	gi|6680047	35055	guanine nucleotide binding protein (G protein), beta polypeptide 2 like 1	VWQVTIGTR	533.3165	2	43
50	2						LWDLTTGTTTR	635.859	2	63
51	1	1.06	0.13	gi|82993679	70133	PREDICTED: similar to Heat shock 70 kDa protein 1B (HSP70.1) isoform 5	YKAEDEVQR	379.8723	3	23
51	2						VQVNYKGESR	397.9071	3	31
51	3						VQVNYK	375.7211	2	28
51	4						SAVEDEGLK	474.257	2	46
51	5						NALESYAFNMK	652.3189	2	31
51	6						LSKEEIER	502.2883	2	29
51	7						DNNLLGR	401.2392	2	27
51	8						DAGVIAGLNVLR	599.3729	2	45
51	9						DAGVIAGLNVLR	599.3623	2	46
51	10						ATAGDTHLGGEDF DNR	561.2862	3	39
52	1	1.06	0.03	gi|9506843	52620	lamin A isoform C2	LSPSPTSQR	489.7752	2	36
52	2						LSPSPTSQR	489.7767	2	49
52	3						LSPSPTSQR	486.7678	2	48
53	1	1.05	0	gi|12963531	54564	non-POU-domain-containing, octamer binding protein	MGQMAMGGAMGI NNR	534.9006	3	58
53	2						ALIEMEK	428.2463	2	24
53	3						AFNLEK	361.2105	2	25
54	1	1.05	0.1	gi|51766344	32640	PREDICTED: similar to 40S ribosomal protein SA (p40) (34/67 kDa laminin receptor)	LLVVTDPR	456.785	2	30
54	2						LLVVTDPR	456.7848	2	46
54	3						FAAATGATPIAGR	605.3592	2	57
54	4						FAAATGATPIAGR	605.3329	2	67
54	5						FAAATGATPIAGR	602.3388	2	49
55	1	1.05	0.18	gi|6671509	41710	actin, beta, cytoplasmic	VAPEEHPVLLTEAP LNPK	652.0387	3	38
55	2						VAPEEHPVLLTEAP LNPK	652.02	3	23
55	3						VAPEEHPVLLTEAP LNPK	654.0398	3	46
55	4						SYELPDGQVITIGNE R	597.65	3	33

55	5						SYELPDGQVITIGNER	898.9823	2	57
55	6						RGILTLK	400.7818	2	27
55	7						QEYDESGPSIVHR	508.2675	3	69
55	8						MQKEITALAPSTMK	527.616	3	38
55	9						LDLAGRDLTDYLMK	547.3163	3	20
55	10						IKIIAPPERK	388.9293	3	34
55	11						IKIIAPPER	350.244	3	33
55	12						IKIIAPPER	518.8471	2	27
55	13						IIAPPERK	462.2967	2	31
55	14						IIAPPERK	462.2843	2	25
55	15						IIAPPER	401.2602	2	38
55	16						IIAPPER	401.2442	2	25
55	17						IIAPPER	401.2438	2	39
55	18						IIAPPER	398.2346	2	20
55	19						IIAPPER	398.2513	2	50
55	20						HQGVMVGMGQK	396.5437	3	41
55	21						GYSFTTTAER	566.7815	2	46
55	22						GYSFTTTAER	566.7631	2	41
55	23						GYSFTTTAER	569.7852	2	22
55	24						GYSFTTTAER	566.7782	2	54
55	25						EITALAPSTMK	589.3176	2	36
55	26						EITALAPSTMK	589.303	2	38
55	27						EITALAPSTMK	589.3063	2	34
55	28						EITALAPSTMK	592.3389	2	32
55	29						EITALAPSTMK	581.3286	2	50
55	30						EITALAPSTMK	581.3058	2	48
55	31						DSYVGDEAQSKR	452.2229	3	55
55	32						DSYVGDEAQSKR	452.2328	3	44
55	33						DSYVGDEAQSK	599.7844	2	65
55	34						DSYVGDEAQSK	602.7911	2	56
55	35						DLYANTVLSGGTTMYPGIADR	746.3755	3	46
55	36						DLTDYLMK	510.7622	2	30
55	37						DLTDYLMK	507.7349	2	23
55	38						DLTDYLMK	510.7722	2	27
55	39						DLTDYLMK	499.7562	2	39
55	40						CDVDIRK	453.2381	2	31
55	41						AVFPSIVGRPR	404.26	3	21
55	42						AVFPSIVGRPR	400.2615	3	33
55	43						AVFPSIVGRPR	400.2671	3	28
55	44						AVFPSIVGRPR	404.2584	3	23
55	45						AVFPSIVGRPR	400.2543	3	27
55	46						AVFPSIVGRPR	400.2607	3	23
55	47						AGFAGDDAPR	488.7405	2	72
55	48						AGFAGDDAPR	491.7354	2	54
55	49						AGFAGDDAPR	488.7237	2	44
55	50						AGFAGDDAPR	491.7491	2	47
55	51						AGFAGDDAPR	488.7461	2	47
56	1	1.05	0.21	gi|6754524	36475	lactate dehydrogenase 1, A chain	VTLTPEEEAR	572.8052	2	57
56	2						LVIITAGAR	460.3051	2	41
57	1	1.05	0.05	gi|6755372	26657	ribosomal protein S3	TQNVLGEK	447.7643	2	34
57	2						TEIIILATR	518.3447	2	47
57	3						QGVLGIK	357.741	2	43
57	4						LLGGLAVR	402.7864	2	31
57	5						GGKPEPPAMPQPVPTA	795.4161	2	27

57	6						FIMESGAK	449.7381	2	34
57	7						ELAEDGYSGVEVR	715.3662	2	93
57	8						AELNEFLTR	549.81	2	56
58	1	1.05	0.06	gi|86262142	69406	RNA binding motif protein 14	INVELSTK	455.2817	2	52
58	2						AQPSVSLGAPYR	626.3545	2	62
58	3						AQPSVSLGAAYR	613.3488	2	34
59	1	1.03	0.09	gi|31981690	70827	heat shock protein 8	VQVEYKGETK	394.2254	3	31
59	2						VQVEYKGETK	394.2253	3	22
59	3						VQVEYKGETK	394.2285	3	33
59	4						VQVEYKGETK	394.227	3	20
59	5						VQVEYK	383.2176	2	23
59	6						VEIIANDQGNR	614.8315	2	56
59	7						VEIIANDQGNR	617.8396	2	57
59	8						VEIIANDQGNR	614.8253	2	40
59	9						VCNPIITK	475.7948	2	27
59	10						VCNPIITK	475.7927	2	30
59	11						TVTNAVVTVPAYF NDSQR	663.3573	3	37
59	12						TTPSYVAFTDTER	744.3718	2	68
59	13						TTPSYVAFTDTER	744.383	2	67
59	14						STAGDTHLGGEDFD NR	566.6011	3	65
59	15						SQIHDIVLVGGSTR	496.6311	3	38
59	16						SFYPEEVSSMVLTK	544.943	3	41
59	17						SFYPEEVSSMVLTK	816.9095	2	36
59	18						RNTTIPTK	471.8095	2	31
59	19						QATKDAGTIAGLN VLR	543.3184	3	20
59	20						NTTIPTK	390.7358	2	31
59	21						NTTIPTK	387.7278	2	42
59	22						NTTIPTK	390.7409	2	22
59	23						NSLESYAFNMK	660.3191	2	54
59	24						NSLESYAFNMK	652.3191	2	71
59	25						NQVAMNPTNTVFD AKR	607.9936	3	83
59	26						NQVAMNPTNTVFD AK	833.4086	2	51
59	27						MVQEAEKYK	381.208	3	21
59	28						MKEIAEAYLGK	427.5876	3	55
59	29						MKEIAEAYLGK	418.2365	3	58
59	30						LSKEDIER	495.2707	2	52
59	31						LSKEDIER	495.2768	2	56
59	32						LLQDFFNGKELNK	522.959	3	34
59	33						LLQDFFNGK	544.3138	2	47
59	34						LDKSQIHDIVLVGG STR	617.3713	3	44
59	35						ITITNDKGR	509.2966	2	66
59	36						ITITNDK	405.7428	2	23
59	37						IINEPTAAAIAYGLD KK	596.6945	3	67
59	38						IINEPTAAAIAYGLD KK	596.6845	3	62
59	39						IINEPTAAAIAYGLD K	555.9947	3	74
59	40						GTLDPVEK	429.752	2	24
59	41						GTLDPVEK	432.7507	2	42
59	42						FELTGIPPAPR	599.342	2	41
59	43						FEELNADLFR	630.3428	2	75
59	44						EIAEAYLGK	497.2781	2	49

59	45						DAGTIAGLNVLR	600.3571	2	64
59	46						DAGTIAGLNVLR	603.3608	2	39
59	47						DAGTIAGLNVLR	600.346	2	62
59	48						ARFEELNADLFR	494.2704	3	68
60	1	1.03	0.1	gi|34328251	72372	drebrin 1	MAPTPIPTR	500.2608	2	34
60	2						LSNGLAR	368.7387	2	34
61	1	1.03	0	gi|6678986	118082	myosin IC isoform b	LGTEEISPR	501.286	2	63
62	1	1.03	0.03	gi|6679321	81201	phosphatidylinositol 3-kinase, regulatory subunit, polypeptide 2 (p85 beta)	ILLNSER	425.7624	2	33
62	2						DGTFLIR	411.2411	2	35
62	3						APGPGPPSAAR	492.2877	2	48
63	1	1.03	0.06	gi|6754256	73483	heat shock protein 9A	VQQTVQDLFGR	645.8472	2	67
63	2						VLENAEGAR	479.7657	2	60
63	3						VLENAEGAR	479.7595	2	55
63	4						TTPSVVAFTADGER	728.8831	2	68
63	5						RYDDPEVQKDTK	374.2107	4	27
63	6						RYDDPEVQKDTK	504.6137	3	27
63	7						QAVTNPNNTFYATKR	579.6545	3	26
63	8						QAASSLQQASLK	619.3526	2	79
63	9						QAASSLQQASLK	619.3498	2	51
63	10						ETGVDLTKDNMALQR	569.6374	3	32
63	11						ETGVDLTKDNMALQR	569.6408	3	36
63	12						ETGVDLTK	431.7466	2	30
63	13						DAGQISGLNVLR	621.8638	2	70
63	14						DAGQISGLNVLR	624.8701	2	40
63	15						ASNGDAWVEAHGK	450.2343	3	33
63	16						AQFEGIVTDLIKR	497.2994	3	52
64	1	1.03	0	gi|7242171	28766	proliferating cell nuclear antigen	YLNFFTK	469.7731	2	43
64	2						MPSGEFAR	455.7145	2	43
65	1	1.02	0.03	gi|23956214	75394	splicing factor proline/glutamine rich (polypyrimidine tract binding protein associated)	YGEPGEVFINK	626.8255	2	39
65	2						LAQKNPMYQK	412.9043	3	22
65	3						FGQGGAGPVGGQGPR	671.3613	2	48
65	4						FATHAAALSVR	381.8959	3	35
65	5						AVVIVDDRGR	367.2188	3	22
65	6						AVVIVDDR	443.7702	2	41
65	7						AELDDTPMR	535.2614	2	28
66	1	1.01	0	gi|29336026	227620	myosin, heavy chain 14	LKQLKR	393.2847	2	26
67	1	1.01	0.08	gi|6677805	29579	ribosomal protein S4, X-linked	YALTGDEVK	501.2826	2	37
67	2						TIRYPDPLIK	405.9167	3	24
67	3						LTIAEER	419.2457	2	49
67	4						LSNIFVIGK	495.8141	2	31

67	5						LSNIFVIGK	495.8065	2	54
67	6						LIYDTK	376.7213	2	33
67	7						IGVITNR	389.7529	2	41
67	8						DANGNSFATR	527.2525	2	66
68	1	1	0	gi|31560686	69599	heat shock protein 2	GTLEPVEK	439.7622	2	27
69	1	0.99	0	gi|30039680	56665	ROD1 regulator of differentiation 1 isoform 2	VTNLLMLK	474.281	2	46
69	2						NSSTSAGVYANGN DNKK	870.3868	2	22
70	1	0.99	0.14	gi|33859482	95253	eukaryotic translation elongation factor 2	VNFTVDQIR	549.3087	2	58
70	2						VFSGVVSTGLK	550.3269	2	69
70	3						GGGQIIPTAR	488.3006	2	21
70	4						GEGQLSAAER	512.2792	2	58
70	5						FSVSPVVR	445.7717	2	34
71	1	0.99	0.26	gi|40556608	83229	heat shock protein 1, beta	FYEAFSK	449.2491	2	27
71	2						ALLFIPR	418.2828	2	32
71	3						ALLFIPR	418.2843	2	23
71	4						ADLINNLGTIAK	624.8822	2	36
72	1	0.99	0.19	gi|68299809	53366	phosphatidylinositol 3-kinase, regulatory subunit, polypeptide 1 isoform 1	TAIEAFNETIK	618.8433	2	68
72	2						ISEIIDSR	466.7634	2	61
72	3						DGTFLVR	404.229	2	29
73	1	0.97	0.09	gi|31981562	57808	pyruvate kinase 3	VNLAMDVGK	484.7779	2	46
73	2						GDLGIEIPAEK	571.3262	2	34
74	1	0.97	0.21	gi|94377125	290937	PREDICTED: similar to Filamin-C (Gamma-filamin) (Filamin-2) (Protein FLNc) (Actin-binding-like prot	LVSIDSK	384.2351	2	28
74	2						IQQNTFTR	504.2669	2	47
75	1	0.95	0.19	gi|13195690	17939	ribosomal protein S27a	TLSDYNIQK	541.2917	2	35
75	2						TLSDYNIQK	541.2766	2	53
75	3						TLSDYNIQK	541.28	2	37
75	4						TLSDYNIQK	541.287	2	35
75	5						TLSDYNIQK	544.2968	2	21
75	6						TLSDYNIQK	544.3009	2	39
75	7						MQIFVK	391.2389	2	31
75	8						MQIFVK	391.2248	2	40
75	9						MQIFVK	391.2197	2	30
76	1	0.95	0.01	gi|13384620	50944	heterogeneous nuclear ribonucleoprotein K	ILLQSK	351.2382	2	27
76	2						DLAGSIIGK	440.2657	2	24
76	3						DLAGSIIGK	437.271	2	26
77	1	0.95	0.02	gi|6678469	49877	tubulin, alpha	LSVDYGKK	455.2587	2	40

						6				
77	2						DVNAAIATIK	511.3023	2	48
77	3						DVNAAIATIK	508.2953	2	31
77	4						DVNAAIATIK	508.2955	2	37
77	5						DVNAAIATIK	508.3018	2	42
78	1	0.95	0.07	gi|6681273	50422	eukaryotic translation elongation factor 1 alpha 2	TIEKFEK	447.7486	2	41
78	2						TIEKFEK	447.7502	2	40
78	3						TIEKFEK	447.7604	2	37
78	4						QTVAVGVIK	457.7913	2	55
78	5						QLIVGVNK	438.791	2	28
78	6						LPLQDVYK	488.2808	2	47
78	7						LPLQDVYK	488.2891	2	44
78	8						LPLQDVYK	488.2881	2	62
78	9						IGGIGTVPVGR	513.3025	2	65
78	10						IGGIGTVPVGR	516.3175	2	77
78	11						IGGIGTVPVGR	513.3235	2	67
78	12						IGGIGTVPVGR	516.327	2	68
78	13						IGGIGTVPVGR	513.3197	2	35
78	14						IGGIGTVPVGR	516.3341	2	23
79	1	0.95	0	gi|66841385	427993	cardiomyopathy associated 3	QDNDLRK	444.73	2	38
80	1	0.95	0.06	gi|94363502	42853	PREDICTED: similar to non-catalytic region of tyrosine kinase adaptor protein 2 isoform 2	VQLVDSVYCIGQR	768.8876	2	66
80	2						TGYVPSNYVER	642.8039	2	57
80	3						NLKDTLGLGK	353.5428	3	36
80	4						LWLLDDSK	495.2716	2	43
80	5						KAPIFTSEHGEK	448.5749	3	45
80	6						IYDLNIPAFVK	646.8628	2	45
80	7						HQAECALNER	409.858	3	41
80	8						GVEGDFLIR	503.2789	2	54
80	9						GQVGLVPK	402.252	2	36
80	10						FAYVAEREDELSLVK	590.3101	3	43
80	11						FAYVAER	428.2284	2	20
80	12						EWYYGNVTR	597.2802	2	28
80	13						DTLGLGK	355.2128	2	20
80	14						DSESSPSDFSVSLK	745.848	2	76
80	15						APIFTSEHGEK	407.8797	3	38
81	1	0.95	0	gi|94392981	196041	PREDICTED: pleckstrin homology domain containing, family H (with MyTH4 domain) member 1 isoform 1	TLQSHLQK	480.8007	2	39
81	2						SPSDVIR	390.2322	2	26
82	1	0.94	0.08	gi|34328187	42863	non-catalytic region of tyrosine kinase adaptor	TGFVPSNYVER	634.8114	2	38

						protein 1				
82	2						FAGNPWYYGK	601.7896	2	50
83	1	0.93	0.11	gi|6753262	30609	capping protein (actin filament) muscle Z-line, beta isoform b	SVQTFADK	451.2484	2	36
83	2						STLNEIYFGK	589.324	2	78
83	3						LVEDMENKIR	421.5656	3	23
84	1	0.93	0	gi|94379397	103514	PREDICTED: similar to NACHT, leucine rich repeat and PYD containing 4A	VKTLISK	400.7743	2	28
85	1	0.92	0	gi|19526792	40957	CD34 antigen	SWSPTGER	460.243	2	41
86	1	0.92	0.07	gi|31981722	72378	heat shock 70kD protein 5 (glucose-regulated protein)	VYEGERPLTK	397.9032	3	25
86	2						SQIFSTASDNQPTVTIK	612.9986	3	28
86	3						QATKDAGTIAGLNVMR	554.6504	3	28
86	4						NTVVPTK	379.7303	2	28
86	5						NQLTSNPENTVFDAKR	611.9937	3	50
86	6						NGRVEIIANDQGNR	519.6215	3	34
86	7						MKETAEAYLGK	423.5796	3	21
86	8						LYGSGGPPPTGEEDTSEKDEL	726.68	3	28
86	9						LTPEEIER	493.772	2	44
86	10						LTPEEIER	493.7709	2	53
86	11						ITPSYVAFTPEGER	783.9114	2	43
86	12						ITITNDQNR	537.7893	2	65
86	13						IQQLVK	364.7468	2	20
86	14						IQQLVK	364.749	2	24
86	15						ELEEIVQPIISK	699.4099	2	41
86	16						EFFNGKEPSR	404.2243	3	32
86	17						DAGTIAGLNVMR	620.3358	2	40
86	18						DAGTIAGLNVMR	620.3283	2	49
87	1	0.92	0.07	gi|6671672	32947	capping protein (actin filament) muscle Z-line, alpha 2	TSVETALR	441.7675	2	53
87	2						LLLNNDNLLR	599.3524	2	68
88	1	0.92	0.08	gi|7305295	223128	myosin, heavy polypeptide 11, smooth muscle	RQQQLTAMK	373.8745	3	36
88	2						QQQLTAMK	485.2673	2	46
88	3						QQQLTAMK	477.28	2	44
88	4						QLLQANPILEAFGNAK	578.3381	3	49
88	5						QLLQANPILEAFGNAK	855.4749	2	46
88	6						QLLQANPILEAFGNAK	863.9884	2	41
88	7						QKLNVSTK	499.7529	2	24
88	8						QKLNVSTK	499.7549	2	22
88	9						NTDQASMPDNTAA	538.9279	3	36

							QK			
88	10						NTDQASMPDNTAAQK	804.3607	2	47
88	11						LEVNMQALK	531.2921	2	23
88	12						ERNTDQASMPDNTAAQK	635.6515	3	25
88	13						EQADFAIEALAK	653.3592	2	58
88	14						EQADFAIEALAK	653.3587	2	70
88	15						ATDKSFVEK	512.7883	2	37
88	16						AQTKEQADFAIEALAK	578.6559	3	59
89	1	0.91	0.06	gi|7948995	116761	tyrosine kinase, non-receptor, 2	VEQLFGLGLRPR	462.285	3	30
89	2						VEQLFGLGLRPR	462.2864	3	32
89	3						TVSVAVK	355.2343	2	35
89	4						TVSVAVK	352.2273	2	31
89	5						TVSVAVK	352.2253	2	33
89	6						TVSVAVK	355.2377	2	36
89	7						TLCVGPFPR	523.7915	2	30
89	8						TLCVGPFPR	526.7951	2	27
89	9						TLCVGPFPR	523.7769	2	31
89	10						NLLLATR	403.7726	2	35
89	11						NLLLATR	403.7772	2	45
89	12						NLLLATR	403.7632	2	37
89	13						NLLLATR	403.7727	2	34
89	14						LYGVVLTLPMK	625.3834	2	50
89	15						LRDDLNITR	372.5543	3	35
89	16						LGDGSFGVVR	506.7896	2	100
89	17						LGDGSFGVVR	503.7812	2	88
89	18						LGDGSFGVVR	503.7711	2	20
89	19						LGDGSFGVVR	506.7847	2	58
89	20						DFLLEAQPTDMR	729.3608	2	28
89	21						ANFSTNNSNPGARPPSLR	633.9971	3	61
89	22						AGPCILPIVR	551.3339	2	45
89	23						AGPCILPIVR	548.3347	2	31
89	24						AGPCILPIVR	551.3438	2	53
90	1	0.91	0	gi|7949150	32243	syndecan binding protein	SLMDHTIPEV	579.2948	2	29
90	2						ITMTIR	375.7246	2	26
91	1	0.89	0.1	gi|23956398	40730	protein-L-isoaspartate (D-aspartate) O-methyltransferase domain containing 2	TDLVEQAFR	542.8052	2	46
91	2						LVQLPPPAVR	545.3489	2	46
91	3						LPLPDPLK	446.7926	2	32
91	4						EAQYIR	393.2187	2	35
92	1	0.89	0.13	gi|33598964	228855	myosin heavy chain 10, non-muscle	YLFVDR	406.7248	2	22
92	2						VVSSVLQFGNISFKK	555.6835	3	29
92	3						VLQQVK	360.7486	2	21
92	4						VLAYDKLEK	364.2382	3	25
92	5						VLAYDKLEK	364.2231	3	24
92	6						VKPLLQVTR	355.9259	3	56

92	7						VIQYLAHVASSHK	365.4758	4	24
92	8						VIQYLAHVASSHK	363.9677	4	23
92	9						VIQYLAHVASSHK	486.9536	3	40
92	10						VDYKADEWLMK	475.9286	3	37
92	11						TVGQLYKESLTK	456.2724	3	35
92	12						TVGQLYK	407.7509	2	22
92	13						QLEEAEEEATR	652.822	2	62
92	14						QKLQLEK	441.2888	2	22
92	15						QKLQLEK	443.7241	2	29
92	16						QIVSNLEK	465.7792	2	52
92	17						QGFPNR	362.7061	2	24
92	18						QGFPNR	362.7099	2	27
92	19						QGFPNR	362.6962	2	26
92	20						NTNPNFVR	484.2774	2	35
92	21						NTNPNFVR	484.2582	2	37
92	22						NTNPNFVR	484.2726	2	41
92	23						NTNPNFVR	481.2566	2	28
92	24						NTNPNFVR	484.2693	2	35
92	25						NTNPNFVR	481.2602	2	30
92	26						LVWIPSER	500.294	2	29
92	27						LQELEGAVK	496.803	2	55
92	28						LMATLR	355.7296	2	22
92	29						LMATLR	355.7297	2	25
92	30						LDPHLVLDQLR	440.2723	3	37
92	31						LDPHLVLDQLR	442.283	3	33
92	32						KFDQLLAEEK	407.5716	3	54
92	33						KFDQLLAEEK	411.5875	3	46
92	34						KEEELQGALAR	415.2276	3	27
92	35						IVFQEFR	469.7748	2	42
92	36						IVFQEFR	469.7689	2	46
92	37						IVFQEFR	469.7682	2	30
92	38						GGPISFSSSR	497.7659	2	41
92	39						FDQLLAEEK	549.8076	2	53
92	40						FDQLLAEEK	549.8133	2	47
92	41						EQEVAELK	473.2856	2	65
92	42						EQADFAVEALAK	646.3439	2	59
92	43						ELDDATEANEGLSR	763.366	2	67
92	44						ATISALEAK	452.2696	2	45
92	45						ATISALEAK	455.2806	2	60
92	46						ASRDEIFAQSK	417.8981	3	31
92	47						AMVNKDDIQK	393.215	3	36
92	48						AMVNKDDIQK	393.2136	3	25
92	49						ALELDPNLYR	602.3375	2	41
92	50						AGVLAHLEEERDLK	395.7314	4	26
92	51						AGVLAHLEEER	410.5658	3	36
92	52						AGVLAHLEEER	410.5699	3	46
92	53						AGKLDPHLVLDQLR	525.6611	3	37
92	54						ADFCIIHYAGK	432.2336	3	22
92	55						ADFCIIHYAGK	432.2298	3	20
93	1	0.88	0.12	gi|76677817	60183	fuse-binding protein-interacting repressor isoform a	YAMEQSIK	496.2565	2	40
93	2						QAFAPFGPIK	541.3192	2	43
94	1	0.87	0.06	gi|39841025	82355	FCH and double SH3 domains 2	VGQVGYVPEK	538.3059	2	47

94	2						SSQFFPR	434.7373	2	32
94	3						NFISEPAR	467.2594	2	43
94	4						LSLFQSR	428.7669	2	33
94	5						LASQYLK	411.7495	2	25
94	6						INICENYK	527.2686	2	43
95	1	0.87	0	gi|54607098	72539	succinate dehydrogenase Fp subunit	TEDGKIYQR	370.5381	3	22
95	2						AFGGQSLK	407.2423	2	28
96	1	0.86	0.15	gi|6678097	42571	serine (or cysteine) proteinase inhibitor, clade B, member 6a	TGTQYLLR	476.2467	2	26
96	2						TGTQYLLR	476.286	2	47
96	3						QHINTWVAK	368.2255	3	24
96	4						QGLFLSK	388.2346	2	29
96	5						MTYIGEIFTK	612.829	2	47
96	6						LGMTDAFGGR	520.7599	2	47
96	7						ILGEDSSK	427.7395	2	48
97	1	0.86	0	gi|6754994	37474	poly(rC) binding protein 1	QGANINEIR	507.7834	2	79
98	1	0.85	0.04	gi|46560563	188662	SH3 domain protein 1B	TLQDTLNPK	515.2957	2	42
98	2						TGIFPSNYVRPK	460.2796	3	32
98	3						QLLNER	386.7312	2	25
98	4						QLLNER	386.7335	2	26
98	5						LQDVQIR	436.2649	2	20
98	6						LQDVQIR	439.2721	2	27
98	7						LLGPSSER	432.7581	2	36
98	8						LIYLVPEK	487.818	2	43
98	9						ITRYPLLIR	382.2509	3	38
98	10						ALYPFEAR	483.762	2	40
99	1	0.85	0	gi|68989251	58969	tweety 2	LSEIIAAR	436.7845	2	47
100	1	0.81	0	gi|6680942	84674	conserved helix-loop-helix ubiquitous kinase	NTLISASQQLK	603.3207	2	28
101	1	0.8	0.09	gi|47059093	108831	Eph receptor B4	VDTVAAEHLTR	404.5648	3	37
101	2						TGWVPR	358.2139	2	44
101	3						SSPCTTPPSAPR	629.3171	2	46
101	4						ILASVQHMK	521.7994	2	52
101	5						FPQVVSALDK	552.309	2	54
101	6						DLVEPWVAIR	599.3489	2	44
102	1	0.74	0	gi|22122825	44732	actin-related protein 2	ILLTEPPMNPTK	685.3574	2	35
103	1	0.73	0	gi|6756039	27761	tyrosine 3-monooxygenase/tryptophan 5-monooxygenase activation protein, theta polypeptide	VISSIEQK	452.2675	2	34
104	1	0.7	0	gi|6996913	38652	annexin A2	LMVALAK	384.2522	2	28
105	1	0.66	0.03	gi|21536246	69733	DEAD (Asp-Glu-Ala-Asp) box	QTLLFSATMPK	626.8536	2	34

						polypeptide 41				
105	2						GITYDDPIK	511.2823	2	26
105	3						ALMSVKEMAK	380.5422	3	24
						hypothetical protein				
106	1	0.66	0.03	gi|86262157	55621	LOC239796	TAIEHVK	399.232	2	36
106	2						SDPAEHLR	462.7326	2	41
106	3						KLQQLVTENPGK	452.2701	3	42
106	4						AISPYHLR	478.7738	2	37
107	1	0.64	0	gi|31980969	86382	SEC23B	YINTEHGGSQAR	446.8966	3	27
						hypothetical protein				
108	1	0.64	0	gi|66955868	18140	LOC67288	LQALQEKR	493.7989	2	52
						sorting nexin associated				
109	1	0.63	0.06	gi|91598596	67748	golgi protein 1	VGQSFR	350.2074	2	33
109	2						SYISYK	383.7145	2	37
109	3						SYISYK	380.7053	2	26
109	4						SGGEAFVLGEASGFVK	777.9042	2	62
109	5						SENPGEISLR	551.2916	2	60
109	6						SDLSLGSR	417.7287	2	55
109	7						SDLSLGSR	417.7137	2	36
109	8						SDLSLGSR	420.7434	2	42
109	9						LVPTHTQVPVHR	463.9467	3	70
109	10						LAEKFPVISVPHLPEK	454.7905	4	36
109	11						GVSAPPAHQASGAK	428.5754	3	38
109	12						GVSAPPAHQASGAK	426.5717	3	34
109	13						GVSAPPAHQASGAK	428.58	3	49
109	14						GLFPASYVQVIR	678.4085	2	58
109	15						FSTFVK	364.715	2	33
109	16						FSTFVK	364.7142	2	27
109	17						FEEDFISKR	390.8731	3	42
109	18						FEEDFISK	507.7547	2	42
109	19						APEPGPPADGGPGAPAR	505.2667	3	77
109	20						APEPGPPADGGPGAPAR	507.2765	3	43
109	21						APEPGPPADGGPGAPAR	757.384	2	72
109	22						ALYDFK	378.7112	2	32
						ARP3 actin-related protein				
110	1	0.61	0	gi|23956222	47327	3 homolog	LSEELSGGR	474.246	2	48
110	2						LSEELSGGR	474.2648	2	33
110	3						HNPVFGVMS	502.2539	2	36
						murinoglobulin				
111	1	0.33	0	gi|31982171	165193	1	YGAVTFSR	450.7459	2	42
111	2						SSGSLFNNAMK	586.2876	2	39
111	3						ITNKLIFLK	363.9241	3	37
111	4						FSTSQSLPASQTR	705.3749	2	57
111	5						FQVENSNR	497.2462	2	20
112	1	0.11	0.11	gi|50363232	207000	nestin	TLLEAENSR	517.2705	2	29
112	2						TLLEAENSR	517.2693	2	28
112	3						TLLEAENSR	517.2814	2	27
112	4						TLLEAENSR	517.2715	2	32
112	5						TLLEAENSR	517.2751	2	28
112	6						TLLEAENSR	517.2807	2	48
112	7						TLLEAENSR	517.2747	2	33

112	8	TLLEAENSR	517.2831	2	35
112	9	TLLEAENSR	517.2761	2	33
112	10	TLLEAENSR	517.2691	2	33
112	11	TLLEAENSR	517.2578	2	36
112	12	TLLEAENSR	517.2612	2	32
112	13	TLLEAENSR	517.2638	2	35
112	14	TLLEAENSR	517.2736	2	37
112	15	TLLEAENSR	517.2657	2	33
112	16	TLLEAENSR	517.2691	2	31
112	17	TLLEAENSR	517.2726	2	43
112	18	TLLEAENSR	517.2692	2	35
112	19	TLLEAENSR	517.278	2	36
112	20	TLLEAENSR	517.2709	2	33
112	21	TLLEAENSR	517.2854	2	36
112	22	TLLEAENSR	517.2827	2	34
112	23	TLLEAENSR	517.2784	2	26
112	24	TLLEAENSR	517.2814	2	31
112	25	TLLEAENSR	517.2778	2	28
112	26	TLLEAENSR	517.2731	2	46
112	27	TLLEAENSR	517.277	2	34
112	28	TLLEAENSR	517.2737	2	35
112	29	TLLEAENSR	517.2769	2	31
112	30	TLLEAENSR	517.2724	2	28
112	31	TLLEAENSR	517.2812	2	35
112	32	TLLEAENSR	517.283	2	48
112	33	TLLEAENSR	517.2776	2	22
112	34	TLLEAENSR	517.2713	2	23
112	35	TLLEAENSR	517.2826	2	25
112	36	ENVQSPR	416.2069	2	32

Table 5. Simplified list of identified proteins from the SILAC experiment at the protein level. Phenylphosphate and Boiled beads elutions combined.

Proteins with fold change in phosphorylation level ≥ 1.2				
gi code	**Gene symbol**	**Protein**	**H/ L Ratio**	**St Dv**
gi|9506909	Myo10	myosin X	2.55	0.29
gi|31982755	Vim	vimentin	2.44	0.65
gi|24429590	Dhx9	DEAH (Asp-Glu-Ala-His) box polypeptide 9	2.35	0.93
gi|94365254	Tns1	PREDICTED: similar to tensin	2.26	0.36
gi|27370424	C230081A	hypothetical protein LOC244895	2.16	0.15
gi|31981796	Dok1 **(*)**	docking protein 1	2.01	N/A
gi|6754632	Mapk1	mitogen activated protein kinase 1	1.95	0.25
gi|21281693	Pxn **(*)**	paxillin isoform alpha	1.92	0.37
gi|31982290	Lpp	LIM domain containing preferred translocation partner in lipoma	1.84	N/A
gi|21313308	Hnrnpm	heterogeneous nuclear ribonucleoprotein M	1.73	0.13
gi|25141233	Matr3	matrin 3	1.71	N/A
gi|27476057	Dcbld2	discoidin, CUB and LCCL domain containing 2	1.69	0.31
gi|40254593	Bcar1 **(*)**	breast cancer anti-estrogen resistance 1	1.67	0.23
gi|21489933	Mapk3	mitogen activated protein kinase 3	1.66	0.02
gi|82887378	Mocs3	PREDICTED: molybdenum cofactor synthesis 3	1.66	0.5
gi|31560712	Csk	c-src tyrosine kinase	1.62	0.07
gi|51921285	Git1	G protein-coupled receptor kinase-interactor 1	1.59	0.15
gi|28076981	Cul5	cullin 5	1.58	N/A
gi|31980859	Arhgef7 **(*)**	Rho guanine nucleotide exchange factor (GEF7)	1.56	0.11
gi|6679108	Npm1	nucleophosmin 1	1.55	0.32
gi|16905083	Rapgef1	Rap guanine nucleotide exchange factor (GEF) 1 isoform 3	1.55	0.05
gi|46849812	Fn1	fibronectin 1	1.5	0.02
gi|21450625	Eif4a1	eukaryotic translation initiation factor 4^{a}1	1.47	N/A

gi|70794809	Src **(*)**	Rous sarcoma oncogene isoform 2	1.46	0.41
gi|7949051	Hnrnpu	heterogenous nuclear ribonucleoprotein U	1.41	N/A
gi|31980648	Atp5b	ATP synthase, H+ transporting mitochondrial F1 complex, beta subunit	1.39	N/A
gi|41322927	Plec1	plectin 1 isoform 4	1.35	0.16
gi|7305237	Limd1	LIM domains containing 1	1.34	0.11
gi|9790077	Gsk3b	Glycogen synthase kinase 3 beta	1.3	N/A
gi|6679741	Ptk2 **(*)**	PTK2 protein tyrosine kinase 2	1.29	0.1
gi|31982757	G3bp2	Ras-GTPase-activating protein (GAP120) SH3-domain binding protein 2 isoform a	1.26	N/A
gi|10092590	Mapk14	mitogen activated protein kinase 14	1.21	0.1
gi|23956078	Abcf2	ATP-binding cassette, sub-family F (GCN20), member 2	1.21	N/A
gi|61888842	Pard3	partitioning-defective protein 3 homolog isoform 2	1.21	N/A
gi|94370505	LOC545497	PREDICTED: similar to heterogeneous nuclear ribonucleoprotein H2	1.2	N/A

(*) Prior evidence of direct c-Src phosphorylation

Proteins with fold change in phosphorylation level < 1.2				
gi|10946928	Hnrnph1	heterogeneous nuclear ribonucleoprotein H1	1.19	0.01
gi|7305075	G3bp1	ras-GTPase-activating protein SH3-domain binding protein	1.16	N/A
gi|31542366	Cdk1	cell division cycle 2 homolog A	1.14	0.05
gi|8394460	Tmod3	tropomodulin 3	1.14	N/A
gi|32484983	Epha2	Eph receptor A2	1.12	0.1
gi|31560030	Tpm1	tropomyosin 1, alpha	1.1	0.16
gi|6679937	Gapdh	glyceraldehyde-3-phosphate dehydrogenase	1.1	0.04
gi|6680748	Atp5a1	ATP synthase, H+ transporting, mitochondrial F1 complex, alpha subunit, isoform 1	1.1	N/A
gi|94407081	Ddx3x	PREDICTED: similar to DEAD (Asp-Glu-Ala-Asp) box polypeptide 3, Y-linked	1.08	0.07
gi|83816893	Ddx5	DEAD (Asp-Glu-Ala-Asp) box polypeptide 5	1.07	0.07
gi|49258190	Nckipsd	NCK interacting protein with SH3 domain	1.07	0.26
gi|7106439	Tubb5	tubulin, beta 5	1.07	0.11
gi|31980798	Nxf1	nuclear RNA export factor 1	1.07	N/A

gi|12963491	Eno1	enolase 1, alpha non-neuron	1.07	N/A
gi|82993679	Hspa1b	PREDICTED: similar to Heat shock 70 kDa protein 1B (HSP70.1) isoform 5	1.06	0.13
gi|47271396	Gnas	GNAS complex locus isoform a	1.06	N/A
gi|9506843	Lmna	lamin A isoform C2	1.06	0.03
gi|6680047	Gnb2l1	guanine nucleotide binding protein (G protein), beta polypeptide 2 like 1	1.06	N/A
gi|6671509	Actb	actin, beta, cytoplasmic	1.05	0.18
gi|6755372	Rps3	ribosomal protein S3	1.05	0.05
gi|51766344	LOC432548	PREDICTED: similar to 40S ribosomal protein SA (p40) (34/67 kDa laminin receptor)	1.05	0.1
gi|86262142	Rbm14	RNA binding motif protein 14	1.05	0.06
gi|12963531	Nono	non-POU-domain-containing, octamer binding protein	1.05	N/A
gi|6754524	Ldha	lactate dehydrogenase 1, A chain	1.05	0.21
gi|31981690	Hspa8	heat shock protein 8	1.03	0.09
gi|6754256	Hspa9	heat shock protein 9[a]	1.03	0.06
gi|6679321	Pik3r2	phosphatidylinositol 3-kinase, regulatory subunit, polypeptide 2 (p85 beta)	1.03	0.03
gi|6678986	Myo1c	myosin IC isoform b	1.03	N/A
gi|7242171	Pcna	proliferating cell nuclear antigen	1.03	N/A
gi|34328251	Dbn1	drebrin 1	1.03	0.1
gi|23956214	Sfpq	splicing factor proline/glutamine rich (polypyrimidine tract binding protein associated) [Mus muscu	1.02	0.03
gi|29336026	Myh14	myosin, heavy chain 14	1.01	N/A
gi|6677805	Rps4x	ribosomal protein S4, X-linked	1.01	0.08
gi|31560686	Hspa2	heat shock protein 2	1	N/A
gi|33859482	Eef2	eukaryotic translation elongation factor 2	0.99	0.14
gi|68299809	Pik3r1	phosphatidylinositol 3-kinase, regulatory subunit, polypeptide 1 isoform 1	0.99	0.19
gi|30039680	Rod1	ROD1 regulator of differentiation 1 isoform 2	0.99	N/A
gi|40556608	Hsp90ab1	heat shock protein 1, beta	0.99	0.26
gi|94377125	Flnc	PREDICTED: similar to Filamin-C (Gamma-filamin) (Filamin-2) (Protein FLNc) (Actin-binding-like prot	0.97	0.21
gi|31981562	Pkm2	pyruvate kinase 3	0.97	0.09
gi|94363502	Nck2	PREDICTED: similar to non-catalytic region of tyrosine kinase adaptor protein 2 isoform 2 [Mus musc	0.95	0.06

gi|6681273	Eef1a2	eukaryotic translation elongation factor 1 alpha 2	0.95	0.07
gi|6678469	Tuba1c	tubulin, alpha 6	0.95	0.02
gi|13195690	Rps27a	ribosomal protein S27a	0.95	0.19
gi|94392981	Plekhh1	PREDICTED: pleckstrin homology domain containing, family H (with MyTH4 domain) member 1 isoform 1 [	0.95	N/A
gi|66841385	Xirp2	cardiomyopathy associated 3	0.95	N/A
gi|13384620	Hnrnpk	heterogeneous nuclear ribonucleoprotein K	0.95	0.01
gi|34328187	Nck1	non-catalytic region of tyrosine kinase adaptor protein 1	0.94	0.08
gi|6753262	Capzb	capping protein (actin filament) muscle Z-line, beta isoform b	0.93	0.11
gi|94379397	Nalp4d	PREDICTED: similar to NACHT, leucine rich repeat and PYD containing 4[a]	0.93	N/A
gi|7305295	Myh11	myosin, heavy polypeptide 11, smooth muscle	0.92	0.08
gi|31981722	Hspa5	heat shock 70kD protein 5 (glucose-regulated protein)	0.92	0.07
gi|6671672	Capza2	capping protein (actin filament) muscle Z-line, alpha 2	0.92	0.07
gi|19526792	Cd34	CD34 antigen	0.92	N/A
gi|7948995	Tnk2	tyrosine kinase, non-receptor, 2	0.91	0.06
gi|7949150	Sdcbp	syndecan binding protein	0.91	N/A
gi|33598964	Myh10	myosin heavy chain 10, non-muscle	0.89	0.13
gi|23956398	Pcmtd2	protein-L-isoaspartate (D-aspartate) O-methyltransferase domain containing 2	0.89	0.1
gi|76677817	Puf60	fuse-binding protein-interacting repressor isoform a	0.88	0.12
gi|39841025	Fchsd2	FCH and double SH3 domains 2	0.87	0.06
gi|54607098	Sdha	succinate dehydrogenase Fp subunit	0.87	N/A
gi|6678097	Serpinb6a	serine (or cysteine) proteinase inhibitor, clade B, member 6[a]	0.86	0.15
gi|6754994	Pcbp1	poly(rC) binding protein 1	0.86	N/A
gi|46560563	Itsn2	SH3 domain protein 1B	0.85	0.04
gi|68989251	Ttyh2	tweety 2	0.85	N/A
gi|6680942	Chuk	conserved helix-loop-helix ubiquitous kinase	0.81	N/A
gi|47059093	Ephb4	Eph receptor B4	0.8	0.09
gi|22122825	Actr2	actin-related protein 2	0.74	N/A
gi|6756039	Ywhaq	tyrosine 3-monooxygenase/tryptophan 5-monooxygenase activation protein, theta polypeptide	0.73	N/A
gi|6996913	Anxa2	annexin A2	0.7	N/A
gi|21536246	Ddx41	DEAD (Asp-Glu-Ala-Asp) box polypeptide 41	0.66	0.03

gi|86262157	1600021P15Rik	hypothetical protein LOC239796	0.66	0.03
gi|66955868	Srek1ip1	hypothetical protein LOC67288	0.64	N/A
gi|31980969	Sec23b	SEC23B	0.64	N/A
gi|91598596	Snx18	sorting nexin associated golgi protein 1	0.63	0.06
gi|23956222	Actr3	ARP3 actin-related protein 3 homolog	0.61	N/A

Table 6. Complete set of tyrosine phosphorylated peptides quantitated by SILAC at the peptide level.

The proteome is comprised of 382 non-redundant peptide sequences, corresponding to 334 tyrosine phosphorylation sites on 213 proteins

Gene	Protein	Site	Peptide	MaxQuant					Proteome Discoverer				
				1	2	3	Av	St Dv	1	2	3	Av	St Dv
Abi1	Abi1 (abl interactor 1 isoform 5)	213	TLEPVKPPTVPNDyMTSPAR						1.605	1.42	1.419	1.481	0.107
Abi2	Abi2 (abl interactor 2)	207	TLEPVRPPVVPNDyVPSPTR						1.557	1.6	1.621	1.593	0.033
Abl2	Arg (Abelson tyrosine-protein kinase 2)	439	LMTGDTyTAHAGAK	4.95	5.006	6.044	5.333	0.616		5.51		5.51	N/A
Ablim1	abLIM1 (actin-binding LIM protein 1 isoform 1)	401	TSSESIySRPGSSIPGSPGHTIYAK							1.46		1.46	N/A
Acad11	ACAD11 (acyl-CoA dehydrogenase family member 11)	323	LAGISQGVyR							0.99		0.99	N/A
Actb	Actb (Actin, cytoplasmic 1)	198	GySFTTTAER		0.864	0.877	0.871	0.009			0.894	0.894	N/A
Actg1	Actin, cytoplasmic 2	53	DSyVGDEAQSK	1.014	0.951		0.983	0.044					
Actn1	Alpha-actinin-1	193	HRPELIDyGK						1.029	1.07		1.0495	0.029
		246	AIMTYVSSFyHAFSGAQK	0.751	1.079		0.916	0.232					
Adam9	ADAM9 (A disintegrin and metalloproteinase domain 9)	841	ISSQGNLIPARPAPAPPLySSLT								0.909	0.909	N/A
Afap1l2	Afap1l2 (actin filament-associated protein 1-like 2 isoform 3)	68	IESPEGYyEEAEPFDR						0.558	0.85	0.669	0.692	0.147
		413	VAQQPLSLVGCDVLPDPSPDHLySFR						1.158		0.991	1.074	0.118
Agfg1	AGFG1 (arf-GAP domain and FG repeats-containing protein 1)	327	AGLQTADKyAALANLDNIFSAGQGGDQGSGFGTTGK						0.941			0.941	N/A
Anks1	ANKS1 (Ankyrin repeat and SAM domain containing 1)	472	IQSSAPQEEEEHPyELLLTAETK		4.24		4.24	N/A		6.81		6.81	N/A
Anxa1	Annexin A1	21	FLENQEQEyVQAVK	0.895	1.071	1.279	1.082	0.192	0.813	1.14	1.014	0.989	0.165
Anxa2	Annexin A2	199	ELyDAGVK			0.688	0.688	N/A					
		238	SYSPyDMLESIKK	0.747	1.094	0.746	0.862	0.201		1.06	0.826	0.943	0.165
		275	LyDSMK		1.299	1.119	1.209	0.127					
		316	SLyYYIQQDTK		0.992		0.992	N/A					

		317	**SLYyYIQQDTK**		0.868		0.868	N/A	0.586	1.28		0.933	0.491
Anxa5	annexin A5	92	**LYDAyELKHALK**	1.017	1.037		1.027	0.014					
Arhgap32	RICS (RhoGAP involved in the beta-catenin-N-cadherin and NMDA receptor 203hosphata)	2025	**QSSMTVVSQyDNLEDYHSLPQHQR**							1.21		1.21	N/A
Arhgap42	Arhgap42	342	**EPIyTLPAIISK**							1.45	1.166	1.308	0.201
		342	**LWLEAMDGKEPIyTLPAIISK**						1.27		1.349	1.309	0.056
		759	**LDTASSNGyQrPGSVVAAK**						1.25	1.27	1.355	1.292	0.056
		759	**LRLDTASSNGyQRPGSVVAAK**							1.17		1.17	N/A
Arhgef10l	rho guanine nucleotide exchange factor 10-like protein isoform b	152	**GLVyEDVHR**						0.645	0.85	0.756	0.75	0.103
Arhgef40	SOLO (protein SOLO isoform 2; rho guanine nucleotide exchange factor 40 isoform 2)	242	**SPGDGHNAPAEGPEGEyVELLEVTLPVR**							1.17		1.17	N/A
		1014	**AAPSHCSLTPCGEDyEEEGLELAPETDGRPPR**							0.87		0.87	N/A
Atp1a1	sodium/ potassium-transporting ATPase subunit alpha-1 precursor	260	**GIVVyTGDR**							0.87		0.87	N/A
Axl	Tyrosine-protein kinase receptor UFO isoform 1 precursor	697	**KIYNGDYyR**								0.855	0.855	N/A
		696	**KIYNGDyYR**						0.75	0.86	0.813	0.808	0.055
		696	**IYNGDyYR**						0.734	0.8	0.792	0.775	0.036
Bag3	BAG3 (BAG family molecular chaperone regulator 3)	253	**THYPAQQGEYQPQQPVyHK**		0.828		0.828	N/A		0.92		0.92	N/A
Baiap2l1	IRTKS (Insulin receptor tyrosine kinase substrate)	274	**MIGKDyDTLSK**						0.603	0.64	0.619	0.621	0.019
Bcar1	p130Cas (breast cancer anti-estrogen resistance protein 1)	132	**TQQGLyQAPGPNPQFQSPPAK**		2.66		2.66	N/A		3		3	N/A
		238	**VGQGYVYEAAQTEQDEyDTPR**						1.748	1.69	1.542	1.66	0.106
		253	**HLLAPGPQDIyDVPPVR**		2.218	1.611	1.915	0.429	2.822	2.7	2.221	2.581	0.318
		271	**GLLPNQYGQEVyDTPPMAVK**	1.841	2.081	2.01	1.977	0.123	2.101	2.17	2.391	2.221	0.151
		291	**GPNGRDPLLDVyDVPPSVEK**						6.293	3.65	3.071	4.338	1.718
		310	**GLLSSSHHSVyDVPPSVSK**						9.496	2.61	2.111	4.739	4.127
		331	**EETyDVPPAFAK**	1.791			1.791	N/A					
		391	**RPGPGTLyDVPR**							3.12	2.597	2.858	0.37
		414	**VLPPEVADGSVVDDGVyAVPPPAER**							1.59		1.59	N/A
Btc	probetacellulin precursor	99	**GyFGAR**			0.754	0.754	N/A					
Calm1	Calmodulin	100	**VFDKDGNGyISAAELR**						0.985	0.99	1.064	1.013	0.044

Carkd	Carkd (Carbohydrate kinase domain-containing protein precursor)	81	**IGIVGGCQEyTGAPYFAGISALK**		1.043	1.027	1.035	0.011		1	1.065	1.033	0.046
Cars	cysteinyl-tRNA synthetase, cytoplasmic	143	**VTWYCCGPTVyDASHMGHAR**						0.731			0.731	N/A
Caskin2	Caskin-2	253	**NTyNQTALDIVNQFTTSQASR**						1.154	1.08	1.148	1.127	0.041
Cav-1	Caveolin-1	14	**YVDSEGHLyTVPIR**						1.05	0.98	1.027	1.019	0.036
Cbl	CBL (E3 ubiquitin-protein ligase C)	672	**IKPSSSANAIySLAARPLPMPK**							0.94		0.94	N/A
Cdc2	Cdk1 (Cell division control protein 2 homolog, Cyclin-dependent kinase 1)	15	**IEKIGEGtyGVVYK**						0.664	1.25	0.936	0.95	0.293
		15	**IEKIGEGTyGVVYK**						1.051	1	0.992	1.014	0.032
		15	**IGEGtyGVVYK**	0.913	1.055	0.969	0.979	0.071					
		15	**IGEGTyGVVYKGR**						0.995	1.01	1.026	1.01	0.016
		15	**IGEGTYGVVyKGR**						1.001	1.03		1.016	0.021
Cdc42ep1	Cdc42ep1 (cdc42 effector protein 1)	349	**HyTEMDAR**		0.851		0.851	N/A					
Cdk2	Cdk2 (Cell division protein kinase 2 isoform 1)	15	**VEKIGEGtyGVVYK**	0.949	1.055	0.958	0.987	0.058	0.778	1.16	1.012	0.983	0.193
		15	**VEKIGEGTyGVVYK**						1.021	1.04	1.022	1.028	0.011
		19	**IGEGTYGVVyKAK**						1.012	1.06	1.035	1.036	0.024
Cdk5	Cdk5 (Cell division protein kinase 5)	15	**IGEGTyGTVFK**	0.979	1.068	1.005	1.017	0.046	1.089	1.04	1.025	1.051	0.033
Cdk16	Cdk16 (Cell division protein kinase 16)	176	**LGEGTyATVYK**						0.996	0.98		0.988	0.011
Cdk17	Cell division protein kinase 17	203	**LGEGTyATVYK**	1.122	1.055	1.064	1.08	0.036					
Cdk18	cell division protein kinase 18	132	**LGEGTyATVFK**						1.137	0.97		1.053	0.118
Cdkl5	Cdkl5 (cyclin-dependent kinase-like 5)	171	**NLSEGNNANYTEyVATR**						0.949	0.98	0.986	0.972	0.02
Cdv3	Cdv3 (Carnitine deficiency-associated protein 3)	213	**KTPQGPPElySDTQFPSLQSTAK**	0.7	1.093	1.093	0.962	0.227	0.59	1.04	1.025	0.885	0.256
Clf1	Cofulin-1	117	**MIyASSK**		0.89		0.89	N/A					
		140	**HELQANCyEEVKDR**						0.899	0.9	0.893	0.897	0.004
Cltc	Clathrin, heavy chain 1	644	**ALEHFTDLyDIKR**	0.825			0.825	N/A					
Cobll1	COBLL1 (cordon-bleu protein-like 1 isoform 1)	570	**STEGQGPyHPVVGHIGNEDR**							0.99		0.99	N/A
Crkl	Crkl (crk-like protein)	132	**TLyDFPGNDAEDLPFK**		1.07	0.97	1.02	0.071			1.123	1.123	N/A
		251	**RVPCAyDK**						2.914	2.69		2.802	0.158
Ctnnb1	CTNNB1 (Catenin beta-1)	489	**LHyGLPVVVK**		1.033		1.033	N/A		1.14		1.14	N/A
Ctnnd1	CTNND1 (catenin delta-1)	904	**SLDNNySTLNER**						0.807	0.9	0.817	0.841	0.051
Cttn	src substrate cortactin	334	**MDKNASTFEEVVQVPSAyQK**		0.877		0.877	N/A			0.84	0.84	N/A
Dcbld2	DCBLD2 (discoidin, CUB	710	**TAGTQPHALVGTyNTLLSR**						2.332	1.61		1.971	0.511

	and LCCL domain-containing protein 2 precursor)	727	**TDSCSSGQAQyDTPK**	1.887	1.754		1.82	0.094		1.52		1.52	N/A
Ddr2	discoidin domain-containing receptor 2	481	**IFPLRPDyQEPSR**	0.659			0.659	N/A	0.856			0.856	N/A
Ddx3x	DDX3X (ATP-dependent RNA helicase DDX3X)	104	**GRGDyDGIGGR**						0.984	1.02		1.002	0.025
Ddx5	DDX5 (ATP-dependent RNA helicase DDX5)	202	**STCIyGGAPK**		1.094	0.958	1.026	0.096					
Dlg3	Dlg3 (discs large homolog 3)	705	**RDNEVDGQDyHFVVSR**						1.128	1.07	1.108	1.102	0.029
Dok1	DOK1 (docking protein 1)	295	**TVPPPVPQDPLGSPPALyAEPLDSLR**							2.83		2.83	N/A
		314	**IPPGPSQDSVySDPLGSTPAGAGEGVHSK**		2.062		2.062	N/A		1.83	3.135	2.483	0.923
		361	**LTDSKEDPIyDEPEGLAPAPPR**						2.148	2.14	1.874	2.054	0.156
		408	**LKEEGYELPYNPATDDyAVPPPR**						2.887	1.51	1.565	1.987	0.78
		450	**GFSSDTALySQVQK**	1.904	1.437		1.67	0.33	1.775	1.74		1.758	0.025
Drp2	DRP2 (dystrophin-related protein 2)	706	**SKQyFSK**							0.79		0.79	N/A
Dyrk1a	DYRK1A (Dual specificity tyrosine-phosphorylation-regulated kinase 1A)	145	**KVYNDGYDDDNyDYIVK**						0.934	0.99	1.123	1.016	0.097
		145	**VYNDGYDDDNyDYIVK**	1.118	1.11	1.24	1.156	0.073	1.161	1.17		1.166	0.006
		321	**IYQyIQSR**						1.043	1.03	1.036	1.036	0.007
Dyrk3	DYRK3 (dual specificity tyrosine-phosphorylation-regulated kinase 3)	368	**LYTyIQSR**							1.18		1.18	N/A
Dyrk4	DYRK3 (dual specificity tyrosine-phosphorylation-regulated kinase 4)	379	**VYTyIQSR**						1.039	1.06	1.003	1.034	0.029
Eef1a1	Eef1a1 (Elongation factor 1-alpha 1)	29	**STTTGHLIyK**	1.01	1.013	1.021	1.015	0.006	0.934	0.93	0.943	0.936	0.007
		141	**EHALLAyTLGVK**	0.919	0.943	0.879	0.914	0.032	0.942	0.96	0.912	0.938	0.024
Efnb1	Efnb1 (ephrin-B1 precursor)	316	**TTENNYCPHyEK**		0.642		0.642	N/A					
Efnb2	Efnb2	307	**TADSVFCPHyEK**	0.737	0.799	0.816	0.784	0.042	0.7	0.78	0.78	0.753	0.046
		319	**VSGDYGHPVyIVQEMPPQSPANIYYKV**							0.91		0.91	N/A
Egfr	epidermal growth factor receptor isoform 1	1110	**RPAGSVQNPVyHNQPLHPAPGR**						0.709	0.94		0.825	0.163
Eif4a1	Eif4a1 (Eukaryotic initiation factor 4A-I isoform a)	50	**GIYAyGFEKPSAIQQR**							0.96	1.04	1	0.057

Eif4h	Eif4h (eukaryotic translation initiation factor 4H)	12	**AySSFGGGR**						0.614	0.92	0.791	0.775	0.154
Eno1	ENO1 (Enolase 1)	44	**AAVPSGASTGIyEALELR**		0.933		0.933	N/A					
Epha2	EPHA2 (Ephrin type-A receptor 2 precursor)	588	**SEQLKPLKTyVDPHTYEDPNQAVLK**						0.964			0.964	N/A
		595	**TYVDPHTyEDPNQAVLK**						0.823	0.82		0.822	0.002
		588, 595	**TyVDPHTyEDPNQAVLK**	0.870	0.884	0.924	0.893	0.028		0.88		0.88	N/A
		773	**VLEDDPEATyTTSGGK**	0.891	1.015	0.957	0.954	0.062	0.847	0.97	0.91	0.909	0.062
		773	**VLEDDPEATyTTSGGKIPIR**							0.96	0.941	0.951	0.013
Epha5	EphA5 (ephrin type-A receptor 5)	672	**VLEDDPEAAyTTR**							2.03	1.556	1.793	0.335
Epb4.1l2	EPB4.1L2 (band 4.1-like protein 2)	606	**VDGDNIyVR**						0.704	0.69	0.685	0.693	0.01
Ephb3	EPHB3 (Ephrin type-B receptor 3 precursor)	595	**LQQyIAPGMK**		1.094	1.097	1.096	0.002		1.13	1.086	1.108	0.031
		787	**FLEDDPSDPTyTSSLGGK**	0.664	0.798	0.887	0.783	0.112	0.554	0.89	1.02	0.821	0.24
Ephb4	EPHB4 (Ephrin type-B receptor 4 isoform a)	574	**EVEySDKHGQYLIGHGTK**						0.748		0.925	0.837	0.125
		581	**HGQyLIGHGTK**	0.525	1.003	1.185	0.904	0.341		0.92		0.92	N/A
		574, 581	**EVEySDKHGQyLIGHGTK**	0.933	1.024	0.965	0.974	0.046	0.95	0.85	1.061	0.954	0.106
		614	**EIDVSyVK**	1.143	0.99	1.089	1.074	0.078					
		774	**FLEENSSDPTyTSSLGGK**	0.623	0.76	0.737	0.707	0.073	0.643	0.76	0.705	0.703	0.059
		774	**FLEENSSDPTyTSSLGGKIPIR**						0.624			0.624	N/A
Erbb2ip	Erbin (protein LAP2 isoform 2)	1097	**RTEGDyLSYR**						0.783	0.81	0.788	0.794	0.014
		1097	**TEGDyLSYR**	0.942			0.942	N/A	0.811	0.85	0.806	0.822	0.024
Erbb3	HER3 (receptor tyrosine-protein kinase erbB-3 precursor)	1325	**SLEATDSAFDNPDyWHSR**						1.144	1.3		1.222	0.11
Esyt1	Extended synaptotagmin-1	809	**KGTKPPSPyATITVGETSHK**	1.393	0.966		1.18	0.302	1.068			1.068	N/A
F2r	PAR1 (proteinase-activated receptor 1 precursor)	425	**MDTCSSHLNNSIyKK**							1.08	0.973	1.027	0.076
F11r	Junctional adhesion molecule A precursor	281	**VIySQPSTR**	1.06		1.1	1.08	0.028	0.813	1.13		0.972	0.224
Fert2	FER (proto-oncogene tyrosine-protein kinase Fer isoform a)	402	**VQENDGKEPPPVVNyEEDAR**						0.703	0.73	0.789	0.741	0.044
		715	**QEDGGVySSSGLK**		1.014		1.014	N/A		0.93		0.93	N/A
Fgfr1	FGFR1 (growth factor receptor 1 isoform 2)	653	**DIHHIDyYKK**	0.904	1.082	1.308	1.098	0.202	0.897	1.01	1.067	0.991	0.087
		653	**DIHHIDyYK**							1.05		1.05	N/A
Fhl2	FHL2 (Four and a half LIM domains protein 2)	158	**QyALQCVQCK**	0.964	1.135	0.872	0.99	0.133					
		158	**ENQNFCVPCYEKQyALQCVQCK**						0.91	1.11		1.01	0.141
Flnb	FLNB (Filamin-B)	250	**SSTETCySAIPK**							1.2		1.2	N/A

		2											
Flnc	FLNC (Filamin-C)	2666	**GASySSIPK**		0.936		0.936	N/A					
		2684	**TPCEEVyVK**		1.021		1.021	N/A					
Frs2	FRS2 (Fibroblast growth factor receptor substrate 2)	306	**LVyENINGLSIPSASGVR**							0.94		0.94	N/A
		349	**RPALLNyENLPSLPPVWEAR**							0.78	0.63	0.705	0.106
		392	**TPSLNGYHNNLDPMHNyVNTENVTVPASAHK**	0.663	0.663		0.663	0		0.67		0.67	N/A
G6pdx	G6PD (glucose-6-phosphate 1-dehydrogenase X)	401	**VQPNEAVyTK**						0.985			0.985	N/A
Gab1	Gab1 (GRB2-associated binding protein 1)	259	**LTSVSGESSLyNLPR**						0.939	1.09	1.056	1.028	0.079
		407	**DASSQDCyDIPR**	1.276	1.482	1.154	1.304	0.166	1.283	1.24	1.1	1.208	0.096
Gab2	GAB2 (GRB2-associated-binding protein 2 isoform 2)	263	**HNTEFKDSTyDLPR**							0.84	0.864	0.852	0.017
		321	**ELGDLLVDNMDVPTTPLSAyQIPR**							0.7		0.7	N/A
Git1	GIT1 (ARF GTPase-activating protein GIT1)	562	**LQPFHSTELEDDAIySVHVPAGLYR**						1.608	1.89		1.749	0.199
		615	**HGSGADSDyENTQSGDPLLGLEGKR**						2.173	2.06		2.117	0.08
		615	**HGsGADSDyENTQSGDPLLGLEGK**		2.044		2.044	N/A		2.2		2.2	N/A
Git2	GIT2 (ARF GTPase-activating protein GIT2)	451	**QNSTPESDyDNTACDPEPDDTGSTRK**							2.06		2.06	N/A
Gna11	Gna11 (Guanine nucleotide-binding protein subunit alpha-11)	103	**ILYKyEQNK**	1.008	1.06		1.034	0.037					
Grlf1	GRF-1 (Glucocorticoid receptor DNA-binding factor 1), p190RhoGAP	1087	**KSMSSSPWMPQDGFDPSDyAEPMDAVVKPR**						1.226		0.914	1.07	0.221
		1087	**SMSSSPWMPQDGFDPSDyAEPMDAVVKPR**							0.94		0.94	N/A
		1105	**NEEENIySVPHDSTQGK**	1.064	1.091	1.099	1.085	0.018	0.997	0.991	1.07	1.019	0.044
Gsk3b	Glycogen synthase kinase-3 beta	216	**GEPNVSyICSR**						0.976	0.81	0.939	0.908	0.087
		216	**GEPNVsyICSR**		0.94		0.94	N/A					
H2-D1	HLAC (H-2 class I histocompatibility antigen, L-D alpha chain precursor)	342	**GGDyALAPGSQSSEMSLR**							1.18		1.18	N/A
Hck	Hck (Tyrosine-protein kinase HCK)	409	**IIEDNEyTAR**		1.712		1.712	N/A					
Hgs	Hgs (Hepatocyte growth factor-regulated tyrosine kinase substrate isoform 2)	132	**VVQDTyQIMK**	1.132	1.032		1.082	0.071					
		216	**VCEPCyEQLNK**	1.109	0.996	1.139	1.081	0.075	1.505	1.01	1.357	1.291	0.254
Hipk2	homeodomain-interacting protein kinase 2	352	**AVCSTyLQSR**	1.22			1.22	N/A	0.994	1.03	1.08	1.035	0.043

Hist1h2bc	H2B1C (histone H2B type 1-C/E/G)	43	**KESYSVYVyK**	0.606	1.183	1.132	0.974	0.319	1.356	1.11	0.875	1.114	0.241
Ick	ICK (serine/threonine-protein kinase ICK)	159	**SRPPYTDyVSTR**							1.27		1.27	N/A
		159	**SRPPYtDyVSTR**							0.95		0.95	N/A
Ifitm3	IFITM3 (interferon induced transmembrane protein 3)	20	**MNHTSQAFITAASGGQPPNyER**						0.711	0.83	0.951	0.831	0.12
		27	**IKEEyEVAEMGAPHGSASVR**						0.73	0.92	1.007	0.886	0.142
Inppl1	SHIP-2 (SH2 domain-containing inositol-5'-phosphatase 2)	887	**ERLyEWISIDKDDTGAK**		0.851		0.851	N/A					
		987	**NSFNNPAyYVLEGVPHQLLPLEPPSLAR**						0.91	1.06	1.002	0.991	0.076
		1136	**TLSEVDyAPGPGR**							0.94		0.94	N/A
Igf1r	IGF1R (Insulin-like growth factor 1 receptor)	1163	**DIyETDYYR**								1.001	1.001	N/A
		1163	**DIyETDYYRK**							0.79		0.79	N/A
		1167	**DIYETDyYRK**						0.838		0.932	0.885	0.066
		1167	**DIYETDyYR**							0.81		0.81	N/A
		1168	**DIYETDYyR**							0.83		0.83	N/A
Irs1	IRS1 (insulin receptor substrate 1)	608	**GGHHRPDTSNLHTDDGyMPMSPGVAPVPSNR**							1.28		1.28	N/A
Irs2	IRS2 (Insulin receptor substrate 2)	649	**SSSSNLGADDGyMPMTPGAALR**						1.107	1.22	1.011	1.113	0.105
		671	**SDDyMPMSPTSVSAPK**	0.876	0.976	1.021	0.96	0.074	0.881	1.03	0.92	0.944	0.077
		814	**SYKAPCSCSGDNDQyVLMSSPVGR**						0.881	1.03	0.92	0.944	0.077
Itgb1	ITGB1 (integrin beta-1 precursor)	783	**WDTGENPIyK**		0.863		0.863	N/A					
Itsn1	ITSN1 (intersectin-1 isoform 2)	1115	**QIGWFPANyVK**		0.834		0.834	N/A		0.97		0.97	N/A
Itsn2	ITSN2 (intersectin-2)	922	**GEPEALyAAVTK**	0.835	0.889	0.913	0.879	0.04	0.736	0.9	0.957	0.864	0.115
Jak2	JAK2 (tyrosine-protein kinase JAK2)	570	**REVGDyGQLHK**						1.012	0.95		0.981	0.044
		570	**EVGDyGQLHKTEVLLK**	0.992	1.028	1.128	1.049	0.07		1.03	1.216	1.123	0.132
		570	**EVGDyGQLHK**						0.931	0.9	1.068	0.966	0.089
Kirrel1	KIRREL 1 (Kin of IRRE-like protein 1 precursor)	604	**AIySSFKDDVDLK**		1.575		1.575	N/A		1.48		1.48	N/A
		637	**EEYEMKDPTNGyYNVR**						1.006	0.99	0.963	0.986	0.022
		657	**AVLyADYR**						0.944	0.89		0.917	0.038
		660	**AVLYADyRAPGPTR**							0.93		0.93	N/A
		657, 660	**AVLyADyRAPGPTR**	1.049			1.049	N/A					
		679	**LSHSSGyAQLNTYSR**						0.862			0.862	N/A
		685	**LSHSSGYAQLNTySR**								0.848	0.848	N/A
		753	**TPyEAYDPIGK**	1.597	1.979	2.331	1.969	0.367					

		756	**TPYEAyDPIGK**						1.205	1.38	1.485	1.357	0.141
		762	**TPYEAYDPIGK yATATR**							0.65		0.65	N/A
		777	**FSYTSQHSDyG QR**						1.104	1.03	0.823	0.985	0.146
Laptm 4a	LAPTM4A (Lysosomal-associated transmembrane protein 4A)	305	**IPEKEPPPPyLP A**	0.858	0.902	0.971	0.91	0.057					
		10	**IGyPAPNFK**		0.782		0.782	N/A					
		194	**SKEyFSK**		0.984		0.984	N/A					
Ldlr	LDLR (low-density lipoprotein receptor)	849	**SQDGyTYPSR**						0.951	1.02	0.866	0.946	0.077
Lphn2	latrophilin-2	833	**THSLLyQPQKK**		0.952		0.952	N/A					
Lpp	LPP (lipoma-preferred partner homolog isoform 2)	245	**SAQPSPHYMA GPSSGQIyGPG PR**						4.122	2.49	2.338	2.983	0.989
		298	**YyEPYYAAGPS YGGR**						1.513		1.703	1.608	0.134
		301	**YYEPyYAAGPS YGGR**						1.551	2.14		1.846	0.416
		333	**EAAyAPPASG NQNHPGMYPV SGPK**		2.846	2.378	2.612	0.331					
Lyn	LYN (Tyrosine-protein kinase Lyn)	194	**SLDNGGYyISP R**							1.08		1.08	N/A
Magi1	MAGI1 (membrane-associated guanylate kinase, WW and PDZ domain-containing protein 1 isoform c)	373	**IEDPVyGVYYV DHINRK**							6.9		6.9	N/A
Mapk 1	ERK2 (Extracellular signal-regulated kinase 2)	185	**VADPDHDHTG FLtEyVATR**						3.321	2.83	2.562	2.904	0.385
		185	**VADPDHDHTG FLTEyVATR**						2.636	2.07	1.903	2.203	0.384
Mapk 3	ERK1 (Extracellular signal-regulated kinase 1)	205	**IADPEHDHTGF LTEyVATR**						2.72	2.15	2.06	2.31	0.358
		205	**IADPEHDHTGF LtEyVATR**						2.863	2.71	2.14	2.571	0.381
Mapk 7	ERK5 (mitogen-activated protein kinase 7)	221	**GLCTSPAEHQ YFMTEyVATR**						1	1.17	1.014	1.061	0.094
Mapk 8	JNK1 (mitogen-activated protein kinase 8)	185	**TAGTSFMMTPy VVTR**						0.924	1	0.832	0.918	0.084
Mapk 9	JNK2 (mitogen-activated protein kinase 9 isoform beta)	185	**TATCNFMMTPy VVTR**						0.818	1.02	0.817	0.885	0.117
Mapk 11	P38-beta (mitogen-activated protein kinase 11)	182	**QADEEMTGyV ATR**						1.279	1.03		1.155	0.176
Mapk 12	p38-gamma (mitogen-activated protein kinase 12)	185	**QADSEMTGyV VTR**						0.844	1.19	1.01	1.014	0.173
Mapk 14	p38-alpha (mitogen activated protein kinase 14)	182	**HTDDEMTGyV ATR**						1.111	0.9	1.03	1.014	0.106
Melk	MELK (maternal embryonic leucine zipper kinase)	4	**MKDyDELLK**		1.194		1.194	N/A					
Met	TeM (Tyrosine	100	**SVSPTTEMVSN**						0.426			0.426	N/A

	kinase Met)	1	**ESVDyR**										
		1232	**DMYDKEyYSVHNK**	0.569	0.605	0.602	0.592	0.02		0.49		0.49	N/A
Mllt4	Afadin	1230	**EyFTFPASK**	0.51	0.648	0.598	0.585	0.07	0.523	0.62	0.59	0.578	0.05
Mpzl1	PZR (myelin protein zero-like protein 1 isoform a)	355	**SPPSAGSHQGPVIyAQLDHSGGHHSGK**	1.623	1.596	1.429	1.549	0.105		1.53		1.53	N/A
		377	**SESVVyADIR**		1.856		1.856	N/A					
		377	**INKSESVVyADIR**						1.67		1.67	1.67	0
Myh9	myosin-9 isoform 1	8	**AQQAADKyLYVDKNFINNPLAQADWAAK**		1.092		1.092	N/A					
		149	**CQyLQAEK**		1.227		1.227	N/A		1.03		1.03	N/A
		1407	**VAAyDKLEK**	0.887	1.16	1.136	1.061	0.151					
Myo16	Myo16 (Myosin-XVI)	575	**IsTyMLEK**			0.734	0.734	N/A					
Nckipsd	NckIPSD (NCK-interacting protein with SH3 domain)	161	**QHSLPSSEHLGTDGALyQVPPQPR**	0.952			0.952	N/A	1.093	1.07	0.978	1.047	0.061
		161	**QHsLPSSEHLGTDGALyQVPPQPR**						0.68			0.68	N/A
Nebl/ Lasp1	Nebulette/ LIM and SH3 domain protein 1	24	**VNCLDKyWHK**	0.984	1.113	1.155	1.084	0.089					
Nedd9	Cas-L (Enhancer of filamentation 1 isoform 1)	165	**TGHGYVyEYPSR**	1.82			1.82	N/A	1.546			1.546	N/A
		316	**HQSFSLHHAPSQLGQSGDTQSDAyDVPR**						1.254	1.21	1.213	1.226	0.025
		316	**RHQSFSLHHAPSQLGQSGDTQSDAyDVPR**						1.064	1.19		1.127	0.089
		344	**ANPEERDGVyDVPLHNPADAK**						1.021			1.021	N/A
Nme2	Nucleoside diphosphate kinase B	52	**ASEEHLKQHyIDLK**							0.92		0.92	N/A
		52	**QHyIDLK**		0.98	1.427	1.204	0.316					
Nrp1	Nrp1 (Neuropilin-1)	920	**DKLNPQSNySEA**			1.087	1.087	N/A	0.939	0.93		0.934	0.006
Pabpc2	Pacbpc2 (poly A binding protein, cytoplasmic 2)	364	**IVATKPLyVALAQR**								1.104	1.104	N/A
Pacsin2	protein kinase C and casein kinase substrate in neurons protein 2	364	**QLVEKGPQyGTVEK**		0.637		0.637	N/A		0.58		0.58	N/A
Pard3	PARD3 (partitioning defective 3 homolog isoform 3)	489	**DVTIGGSAPIyVK**		0.923		0.923	N/A		0.95		0.95	N/A
		719	**ISHSLySGIEGLDESPTR**						0.945	0.94	0.846	0.91	0.056
		1076	**ERDyAEIQDFHR**						0.813	0.89	0.781	0.828	0.056
		1123	**EGHLMDTLyAQVK**	1.335	1.183		1.259	0.107	1.425	1.22		1.322	0.145
		1201	**QySSLPR**						0.692	0.77		0.731	0.055
Pard3b	PARD3B (partitioning defective 3 homolog B)	186	**QyASLPR**			1.196	1.196	N/A					
		953	**GLVDYATAVTGPVHDMDDDEMDPNyAR**							1.68		1.68	N/A
		998	**DGRPLSPDHLEGLyAK**							1.47		1.47	N/A
		117	**VPVyQEMGR**	0.841	1.752	0.148	0.914	0.805					

		0											
Pcdh19	PCDH19 (protocadherin-19 isoform b)	720	**IAEySYGHQK**		1.352		1.352	N/A					
Pdgfra	PDGFRA (alpha-type platelet-derived growth factor receptor precursor)	742	**QADTTQyVPMLER**						0.765	1.65	0.853	1.089	0.488
		754	**EVSKySDIQR**						0.88	1.03		0.955	0.106
		762	**SLyDRPASYK**							0.9		0.9	N/A
		768	**SLYDRPASyK**								1.097	1.097	N/A
		762,768	**SLyDRPASyK**						0.806	1.07	1.088	0.988	0.158
		1018	**LSADSGyIIPLPDIDPVPEEEDLGKR**						0.677	1.08		0.879	0.285
Pdha1	PDHA1 (pyruvate dehydrogenase E1 component subunit alpha, somatic form, mitochondrial precursor)	301	**YHGHSMSDPGVSyR**							0.51		0.51	N/A
Pdlim5	PDLIM5 (PDZ and LIM domains protein 5 isoform ENH1)	251	**NTEFyHIPTHSDASK**	0.8	0.853		0.827	0.037					
Pebp1	PEBP1 (phosphatidylethanolamine-binding protein 1)	181	**LyEQLSGK**		0.393		0.393	N/A					
Pfn1	Profilin-1	129	**CyEMASHLR**								0.974	0.974	N/A
Pgk1	PGK1 (Phosphoglycerate kinase 1)	196	**ELNyFAK**	1.089	1.147	1.195	1.144	0.053					
Pgam1	PGAM1 (phosphoglycerate mutase 1)	92	**HyGGLTGLNK**						1.015	0.97	0.955	0.98	0.031
		92	**HyGGLTGLNKAETAAK**						1.479			1.479	N/A
Pik3r1	PIK3R1 (phosphatidylinositol 3-kinase regulatory subunit alpha isoform 1)	467	**ESQGLyVVYNKK**	1.083	1.052	1.095	1.08	0.022					
		508	**YSKEyIEK**		1.289		1.289	N/A					
		580	**DQyLMWLTQK**		1.153		1.153	N/A		1.03		1.03	N/A
Pik3r2	PIK3R2 (phosphatidylinositol 3-kinase regulatory subunit beta)	458	**SREYDQLyEEYTR**						1.254	1.25		1.252	0.003
		458	**EYDQLyEEYTR**						1.08	1.1	1.095	1.092	0.011
		599	**NETEDQySLMEDEDALPHHEER**						1.122	1.16		1.141	0.027
		599	**INEWLGIKNETEDQySLMEDEDALPHHEER**							1.2		1.2	N/A
Pkm2	PKM2 (Pyruvate kinase isozymes M1/M2)	83	**LNFSHGTHEyHAETIK**							0.99		0.99	N/A
		105	**EATESFASDPILyRPVAVALDTK**							1.01		1.01	N/A
Pkp4	PKP4 (Plakophilin-4 isoform 2)	477	**NNYALNTAATyAEPYRPVQYR**							0.79	0.71	0.75	0.057
		481	**NNYALNTAATYAEPyRPVQYR**						0.765			0.765	N/A
		486	**NNYALNTAATYAEPYRPVQyR**							0.73		0.73	N/A
		1137	**SyEDPYCDDRVHFPASTDYSTQYGLK**						0.718		0.747	0.733	0.021
		1166	**STTNyVDFYSTK**	0.866	0.787	0.783	0.812	0.047	0.774	0.79	0.747	0.77	0.022
Plcg1	PLCG1 (1-	783	**NPGFyVEANP**		0.968		0.968	N/A		0.93		0.93	N/A

	phosphatidylinositol-4,5-bisphosphate phosphodiesterase gamma-1)		**MPTFK**										
		977	**ACyRDMSSFPETK**						0.93	1.09	1.1	1.04	0.095
Pld3	PLD3 (phospholipase D3)	7	**LMyQELK**	1.075	0.952		1.014	0.087					
Plec	plectin isoform 12alpha	3253	**AVTGYKDPySGK**		0.994		0.994	N/A					
Prpf4b	Prpf4b (serine/threonine-protein kinase PRP4 homolog)	843	**LCDFGSASHVADNDITPyLVSR**						0.993	1.01	0.96	0.988	0.025
Ptk2	FAK (focal adhesion kinase 1 isoform 1)	5	**AAAyLDPNLNHTPSSSTK**	1.615	1.739	2.189	1.848	0.302					
		428	**THAVSVSEtDDYAEIIDEEDTyTMPSTR**						1.094	0.53	1.247	0.957	0.378
		614	**YMEDSTyYK**						1.426	1.51	1.351	1.429	0.08
		614	**YMEDSTyYKASK**							2.21		2.21	N/A
		615	**YMEDSTYyK**						1.424	1.5	1.416	1.446	0.046
		615	**YMEDSTYyKASK**								2.458	2.458	N/A
		614,615	**YMEDSTyyk**						10.249		9.004	9.627	0.88
		614, 615	**YMEDSTyyKASK**						7.369	10.29	8.316	8.658	1.49
Ptpn11	SHP2 (tyrosine-protein 212hosphatases non-receptor type 11 isoform a)	62	**IQNTGDyYDLYGGEK**	1.018	1.014	0.922	0.985	0.054	0.981	0.99	0.893	0.955	0.054
		546	**GHEyTNIK**						0.913	0.95		0.932	0.026
		546	**KGHEyTNIK**	0.909	0.993	1.101	1.001	0.96					
		584	**VyENVGLMQQQR**						0.895	0.95	1.011	0.952	0.058
Ptpra	PTPRA (receptor-type tyrosine-protein 212hosphatases alpha isoform 1)	825	**VVQEYIDAFSDyANFK**	1.375	1.44	1.383	1.399	0.035	1.339	1.41	1.327	1.359	0.045
Ptprm	PTPRM (receptor-type tyrosine-protein 212hosphatases mu precursor)	929	**NRyGNIIAYDHSR**						1.104			1.104	N/A
Pttg1ip	Pttg1ip (Pituitary tumor-transforming gene 1 protein-interacting protein precusor)	171	**EQNPyEKF**	1.135	0.992	1.126	1.084	0.08					
Ptrf	PTRF (polymerase I and transcript release factor)	310	**KSFTPDHVVyAR**							1.1	1.123	1.112	0.016
Pvrl3	poliovirus receptor-related protein 3 isoform alpha	511	**FERPMDYyEDLK**						0.72	0.83	0.693	0.748	0.073
Pxn	Paxillin	88	**YAHQQPPSPLPVySSSAK**						3.317	3.35	3.139	3.269	0.114
		88	**YAHQQPPsPLPVySSSAK**						4.519	6.15		5.335	1.153
		118	**AGEEEHVySFPNK**						2.586	4.05	2.503	3.046	0.87

		118	**AGEEEHVySFPNKQK**	2.674	2.795	2.639	2.703	0.082	2.747	3.21	2.638	2.865	0.304
Rab1b	Rab1b (ras-related protein Rab-1B)	5	**MNPEyDYLFK**		1.052		1.052	N/A			0.855	0.855	N/A
Rab11a	ras-related protein Rab-11A	8	**GTRDDEyDYLFK**							0.77	0.727	0.749	0.03
Rab2a	Ras-related protein Rab-2A	3	**AyAYLFK**		1.121	0.987	1.054	0.095		1		1	N/A
RapGEF1	C3G (Rap guanine nucleotide exchange factor 1)	571	**HMLAYMQLLEDySEPQPSMFYQTPQSEHIYQQK**	2.942	2.66	2.96	2.854	0.168	3.362		3.046	3.204	0.223
Raph1	Raph1 (Ras association (RalGDS/AF-6) and pleckstrin homology domains 1)	603	**SyTSLMPPLSPQTK**							1.53	1.221	1.375	0.218
Rasa1	Rasa1 (RAS p21 protein activator 1)	451	**ElyNTIR**		1.192		1.192	N/A					
Rbm3	RBM3 (RNA binding motif protein 3)	126	**YDSRPGGYGYGyGR**							0.94		0.94	N/A
		151	**YSGGNYRDNyDN**						0.782	0.76		0.771	0.016
Rin1	ras and Rab interactor 1	35	**EKPSTDPLyDTPDTR**						0.894	1.11	1.098	1.034	0.121
Rplp0	RPLP0 (60S acidic ribosomal protein P0)	24	**IIQLLDDyPK**			1.157	1.157	N/A			1.178	1.178	N/A
Rpl15	60S ribosomal protein L15	59	**QGyVIYR**	1.03	1.045		1.038	0.011		1.05		1.05	N/A
		81	**GATyGKPVHHGVNQLK**		1.302		1.302	N/A					
Rps10	40S ribosomal protein S10	12	**IAIyELLFK**	1.135	0.973	1.096	1.068	0.085	1.12	0.97	1.026	1.039	0.076
Rps27l	Rps27l (40S ribosomal protein S27-like)	31	**LVQSPNSyFMDVK**	0.968	1.037	1.05	1.018	0.044	1.027	1.04	0.98	1.015	0.032
Rpsa	RPSA (40S ribosomal protein SA)	139	**ADHQPLTEASyVNLPTIALCNTDSPLR**						1.043	0.94	0.985	0.99	0.052
Scarf2	Scarf2 (scavenger receptor class F member 2 precursor)	615	**SASSVEGPSGALyAR**						0.737	0.71	0.716	0.721	0.014
Sdc2	syndecan-2 precursor	201	**APTKEFyA**		1.094	1.302	1.198	0.147		0.99	1.147	1.069	0.111
Sdc4	syndecan-4 precursor	197	**KAPTNEFyA**		1.075	1.115	1.095	0.028			1.084	1.084	N/A
Sept2	septin-2 a Nedd 5	17	**QQPTQFINPETPGyVGFANLPNQVHR**							1.09	1.121	1.106	0.022
SgK269	SgK269 (tyrosine-protein kinase SgK269)	632	**NAIKVPIVINPNAyDNLAIYK**						1.139	0.98	1.001	1.04	0.086
		632	**VPIVINPNAyDNLAIYK**	1.032	1.05	1.06	1.047	0.014	1.037	1.15		1.094	0.08
Sh2b3	LNK (Lymphocyte-specific adaptor protein Lnk)	536	**AIDNQyTPLSQLCR**							0.89		0.89	N/A
Sh3d19	SH3D19 (SH3 domain-containing protein 19)	87	**EGLTPySSPQEAGITPVTKPELPK**	0.717	0.978	0.862	0.852	0.131	0.76	0.94	0.859	0.853	0.09

Shb	SHB (SH2 domain-containing adaptor protein B)	113	**LDyCGGGGGGDPGGGQR**						0.961	0.81	0.838	0.87	0.08
		240	**DKVTIADDySDPFDAK**						1.019	1.22	1.026	1.088	0.114
		240	**VTIADDySDPFDAK**	0.995	1.281	1.064	1.113	0.149	1.074	1.11	1.039	1.075	0.036
		268	**AGKGESAGyMEPYEAQR**						0.969	1.06	0.976	1.002	0.051
		268	**GESAGyMEPYEAQR**						1.132	1.11	1.085	1.109	0.024
		330	**LPQDDDRPADEyDQPWEWNR**	0.9			0.9	N/A	1.273	0.85		1.061	0.299
Shc1	SHC1 (SHC-transforming protein 1 isoform a)	423	**ELFDDPSyVNIQNLDK**	1.262	1.431	1.484	1.392	0.116	1.249	1.45	1.396	1.365	0.104
Slc12a4	Slc12a4 (solute carrier family 12 member 4)	17	**RGDyDNLEGLSWVDYGER**							1.1		1.1	N/A
Slc38a2	Slc38a2 (sodium-coupled neutral amino acid transporter 2)	41	**SHyADVDPENQNFLLESNLGKK**	0.867	1.057	1.124	1.016	0.133	0.989	1.02	1.165	1.058	0.094
Son	protein SON truncated isoform	904	**LGQDPyRLGHDPYR**							1.1		1.1	N/A
		916	**LAQDPyRLGHDPYR**						0.989	1.02	1.165	1.058	0.094
Sprr1a	Cornifin-A	137	**APEPCHPVVPEPCPSTVTPSPyQQK**	0.373			0.373	N/A					
Src	proto-oncogene tyrosine-protein kinase Fyn isoform b	424	**LIEDNEyTAR**						1.602	1.79	1.887	1.76	0.145
		444	**WTAPEAALyGR**						1.355	1.35	1.228	1.311	0.072
St5	St5 (Suppression of tumorigenicity 5 protein)	498	**ENPyEDVDLK**	1.208	1.562	1.47	1.413	0.184					
Stat3	STAT3 (signal transducer and activator of transcription 3 isoform 3) iso 2	705	**YCRPESQEHPEADPGSAAPyLK**						0.911	0.95	1.008	0.956	0.049
Stat3	STAT3 (signal transducer and activator of transcription 3 isoform 3) iso 3	705	**YCRPESQEHPEADPGAAPyLK**							0.95	1.012	0.981	0.044
Stat5a	STAT5A (Signal transducer and activator of transcription 5A isoform 1)	694	**AVDGyVKPQIK**	0.556	1.275	1.241	1.024	0.406		1.08		1.08	N/A
Stat5b	STAT5B (Signal transducer and activator of transcription 5B)	699	**AADGyVKPQIK**	0.838	1.196	1.305	1.113	0.244	0.807	1.07	1.069	0.982	0.152
Ston1	Stonin-1	2	**MySTNPGSWVTFDDDPAFQSSQK**		0.748		0.748	N/A		1		1	N/A
Synrg	Synrg (synergin gamma isoform 1)	506	**ASTDKyAVFK**		0.743		0.743	N/A					
Tagln2	TAGLN2 (transgelin-2)	192	**GASQAGMTGyGMPR**								0.851	0.851	N/A
Table of Tenc1	Tensin2	483	**GPLDGSPyAQVQR**						3.123	2.65	2.432	2.735	0.353
		705	**LALPTAALyGLR**	2.548			2.548	N/A	3.538		3.018	3.278	0.368
		770	**VGEEGHEGCS**		2.313		2.313	N/A	2.989	2.74		2.864	0.176

			yAVCSEGR										
		791	YGHSGYPALVTYGyGGAVPSYCPAYGR							2.2		2.2	N/A
Tjp2	ZO2 (Tight junction protein 2)	1095	IEIAQKHPDIyAVPIK		1.121		1.121	N/A		1.18		1.18	N/A
TMEM106B	TMEM106B (transmembrane protein 106B)	51	NGDVSQFPyVEFTGR	1.44			1.44	N/A	1.309	1.45		1.379	0.1
Tnc	Tenascin	1341	LIQtIFTTIGLLyPFPR						>50			>50	N/A
Tnk2	Ack (Activated CDC42 kinase 1 isoform 1)	284	ALPQNDDHyVMQEHR		1.384		1.384	N/A		1.07		1.07	N/A
		533	KPTyDPVSEDPDPLSSDFKR							0.96		0.96	N/A
		874	VSSTHyYLLPERPPYLER							0.92	0.863	0.892	0.04
		874	KVSSTHyYLLPERPPYLER								0.878	0.878	N/A
		875	KVSSTHYyLLPERPPYLER							1.16		1.16	N/A
Tns1	Tensin 1	1477	HAAyGGYSTPEDR						2.133	2.03	2.124	2.096	0.057
		1480	HAAYGGySTPEDR							2.27		2.27	N/A
		1558	AGSLPNyATINGK	2.353	2.295	2.314	2.321	0.03	2.292	2.2	2.204	2.232	0.052
Tns3	Tensin 3	584	KPSAPTPVQAYGQSNySTQTWVR						2.196	1.43		1.813	0.542
Tjp1	ZO-1 (tight junction protein ZO-1 isoform 2)	1061	DLEQPSyRYEVSSYTDQFSR							0.34		0.34	N/A
		1066	YEVSSyTDQFSR							0.34		0.34	N/A
		1145	TRyEQLPR						0.701	0.61	0.579	0.63	0.063
		1164	HEEQPAPAyEVHNR						1.142	1.09		1.116	0.037
		1177	YRPEAQPySSTGPK						2.07	1.73		1.9	0.241
Tln1	talin-1	26	TMQFEPSTMVyDACR							0.95		0.95	N/A
		70	ALDyYMLR							1.01		1.01	N/A
		436	STVLQQQyNR								1.88	1.88	N/A
		436	KSTVLQQQyNR						1.6	1.83		1.715	0.163
Tfrc	TFR (transferrin receptor protein 1)	20	SAFSNLFGGEPLSyTR							0.8		0.8	N/A
Trp53	p53 (cellular tumor antigen p53 isoform a)	228	HSVVVPYEPPEAGSEYTTIHyK						1.317	1.13		1.224	0.132
Ttyh2	TTYH2 (Protein tweety homolog 2)	424	DRDyDDIDDDDPFNPQAR							1.89		1.89	N/A
Tyro3	TYRO3 (Tyrosine-protein kinase receptor TYRO3)	671	KIySGDYYR							1.1		1.1	N/A
Ubash3b	UBASH3B (ubiquitin-associated and SH3 domain-containing protein B)	8	AAREELySK		1.944		1.944	N/A					
Vars	Valyl-tRNA synthetase	468	LHEEGVIyR	0.489			0.489	N/A					
Vcl	vinculin	692	ILLRNPGNQAA						1.194			1.194	N/A

			yEHFETMK										
		822	**SFLDSGyR**						0.953	0.94	0.933	0.942	0.01
Vim	Vimentin	53	**SLySSSPGGAY VTR**						1.007	0.89	0.97	0.956	0.06
		117	**FANyIDKVR**	0.541			0.541	N/A	0.846	0.97	0.882	0.899	0.064
Wasl	N-WASP (Neural Wiskott-Aldrich syndrome protein isoform 1)	253	**VIyDFIEK**	0.691	0.817	0.753	0.754	0.063	0.693	0.77	0.766	0.743	0.044
		253	**ETSKVIyDFIEK**						0.657	0.73	0.672	0.686	0.039
Wee1	Wee1-like protein kinase	19	**VGAAySLR**	1.076			1.076	N/A	0.611	0.92	0.762	0.765	0.154
		170	**AMDDPCSPQP DyPSTPPHK**			0.857	0.857	N/A			0.806	0.806	N/A
Wipf2	WIPF2 (WAS/WASL-interacting protein family member 2)	74	**GSSGGyGPGA AALQPK**	0.711	0.908	0.823	0.814	0.099	0.627	0.84	0.73	0.732	0.106
		255	**TGPSGQSLAP PPPPyRQPPGV PNGPSSPTNES APELPQR**		0.588		0.588	N/A					
ZDHHC8	ZDHHC8 (probable palmitoyltransferase ZDHHC8)	582	**SQTDSLFGDS GVYDTPSSySL QQASVLTEGP R**							2.08		2.08	N/A

Table 7. Set of c-Src- induced tyrosine phosphorylated peptides quantitated by SILAC at the peptide level.

Gene	Protein	Site		MaxQuant		Proteome Discoverer	
				Av	St Dv	Av	St Dv
Abi1	Abi1 (abl interactor 1 isoform 5)	213	TLEPVKPPTVPNDyMTSPAR			1.481	0.107
Abi2	Abi2 (abl interactor 2)	207	TLEPVRPPVVPNDyVPSPTR			1.593	0.033
Abl2	Arg (Abelson tyrosine-protein kinase 2)	439	LMTGDTyTAHAGAK	5.333	0.616	5.51	N/A
Ablim1	abLIM1 (actin-binding LIM protein 1 isoform 1)	401	TSSESIySRPGSSIPGSPGHTIYAK			1.46	N/A
Anks1	ANKS1 (Ankyrin repeat and SAM domain containing 1)	472	IQSSAPQEEEEHPyELLLTAETK	4.24	N/A	6.81	N/A
Arhgap32	RICS (RhoGAP involved in the beta-catenin-N-cadherin and NMDA receptor signaling)	2025	QSSMTVVSQyDNLEDYHSLPQHQR			1.21	N/A
Arhgap42	Arhgap42	342	EPIyTLPAIISK			1.308	0.201
		342	LWLEAMDGKEPIyTLPAIISK			1.309	0.056
		759	LDTASSNGyQrPGSVVAAK			1.292	0.056
Bcar1	p130Cas (breast cancer anti-estrogen resistance protein 1)	132	TQQGLyQAPGPNPQFQSPPAK	2.66	N/A	3	N/A
		238	VGQGYVYEAAQTEQDEyDTPR			1.66	0.106
		253	HLLAPGPQDIyDVPPVR	1.915	0.429	2.581	0.318
		271	GLLPNQYGQEVyDTPPMAVK	1.977	0.123	2.221	0.151
		291	GPNGRDPLLDVyDVPPSVEK			4.338	1.718
		310	GLLSSSHHSVyDVPPSVSK			4.739	4.127
		331	EETyDVPPAFAK	1.791	N/A		
		391	RPGPGTLyDVPR			2.858	0.37
		414	VLPPEVADGSVVDDGVyAVPPPAER			1.59	N/A
Crkl	Crkl (crk-like protein)	251	RVPCAyDK			2.802	0.158
Dcbld2	DCBLD2 (discoidin, CUB and LCCL domain-containing protein 2 precursor)	710	TAGTQPHALVGTyNTLLSR			1.971	0.511
		727	TDSCSSGQAQyDTPK	1.821	0.094	1.52	N/A
Dok1	DOK1 (docking protein 1)	295	TVPPPVPQDPLGSPPALyAEPLDSLR			2.83	N/A
		314	TDSCSSGQAQyDTPK	2.062	N/A	2.483	0.923
		361	LTDSKEDPIyDEPEGLAPAPPR			2.054	0.156
		408	LKEEGYELPYNPATDDyAVPPPR			1.987	0.78
		450	GFSSDTALySQVQK	1.671	0.33	1.758	0.025
Epha5	EphA5 (ephrin type-A receptor 5)	672	VLEDDPEAAyTTR			1.793	0.335
Erbb3	HER3 (receptor tyrosine-protein kinase erbB-3 precursor)	1325	SLEATDSAFDNPDyWHSR			1.222	0.11
Flnb	FLNB (Filamin-B)	2502	SSTETCySAIPK			1.2	N/A
Gab1	Gab1 (GRB2-associated binding protein 1)	407	DASSQDCyDIPR	1.304	0.166	1.208	0.096
Git1	GIT1 (ARF GTPase-activating protein GIT1)	562	LQPFHSTELEDDAIySVHVPAGLYR			1.749	0.199
		615	HGSGADSDyENTQSGDPL			2.117	0.08

			LGLEGKR				
		615	HGsGADSDyENTQSGDPLLGLEGK	2.044	N/A	2.2	N/A
Git2	GIT2 (ARF GTPase-activating protein GIT2)	451	QNSTPESDyDNTACDPEPDDTGSTRK			2.06	N/A
Hck	Hck (Tyrosine-protein kinase HCK)	409	IIEDNEyTAR	1.712	N/A		
Hgs	Hgs (Hepatocyte growth factor-regulated tyrosine kinase substrate isoform 2)	216	VCEPCyEQLNK	1.081	0.075	1.291	0.254
Ick	ICK (serine/threonine-protein kinase ICK)	159	SRPPYTDyVSTR			1.27	N/A
Irs1	IRS1 (insulin receptor substrate 1)	608	GGHHRPDTSNLHTDDGyMPMSPGVAPVPSNR			1.28	N/A
Kirrel 1	KIRREL 1 (Kin of IRRE-like protein 1 precursor)	604	AIySSFKDDVDLK	1.575	N/A	1.48	N/A
		753	TPyEAYDPIGK	1.969	0.367		
		756	TPYEAyDPIGK			1.357	0.141
Lpp	LPP (lipoma-preferred partner homolog isoform 2)	245	SAQPSPHYMAGPSSGQIyGPGPR			2.983	0.989
		298	YyEPYYAAGPSYGGR			1.608	0.134
		301	YYEPyYAAGPSYGGR			1.846	0.416
		333	EAAyAPPASGNQNHPGMYPVSGPK	2.612	0.331		
Magi1	MAGI (membrane associated guanylate kinase, WW abd PDZ domain-containing protein 1 isoform c)	373	IEDPVyGVYYVDHINRK			6.9	N/A
Mapk1	ERK2 (Extracellular signal-regulated kinase 2)	185	VADPDHDHTGFLtEyVATR			2.904	0.385
		185	VADPDHDHTGFLTEyVATR			2.203	0.384
Mapk3	ERK1 (Extracellular signal-regulated kinase 1)	205	IADPEHDHTGFLTEyVATR			2.31	0.358
		205	IADPEHDHTGFLtEyVATR			2.571	0.381
Mpzl1	PZR (myelin protein zero-like protein 1 isoform a)	355	SPPSAGSHQGPVIyAQLDHSGGHHSGK	1.549	0.105	1.53	N/A
		377	SESVVyADIR	1.856	N/A		
		377	INKSESVVyADIR			1.67	0
Nedd9	Cas-L (Enhancer of filamentation 1 isoform 1)	165	TGHGYVyEYPSR	1.82	N/A	1.546	N/A
		316	HQSFSLHHAPSQLGQSGDTQSDAyDVPR			1.226	0.025
Pard3	PARD3 (partitioning defective 3 homolog isoform 3)	1123	EGHLMDTLyAQVK	1.259	0.107	1.322	0.145
Pard3b	PARD3B (partitioning defective 3 homolog B)	953	GLVDYATAVTGPVHDMDDDEMDPNyAR			1.68	N/A
		998	DGRPLSPDHLEGLyAK			1.47	N/A
Pcdh19	PCDH19 (protocadherin-19 isoform b)	720	IAEySYGHQK	1.352	N/A		
Pgam1	PGAM1 (phosphoglycerate mutase 1)	92	HyGGLTGLNKAETAAK			1.479	N/A
Pik3r2	PIK3R2 (phosphatidylinositol 3-kinase regulatory subunit beta)	458	SREYDQLyEEYTR			1.252	0.003
		599	INEWLGIKNETEDQySLMEDEDALPHHEER			1.2	N/A
Ptk2	FAK (focal adhesion kinase 1 isoform 1)	5	AAAyLDPNLNHTPSSSTK	1.848	0.302		
		614	YMEDSTyYK			1.429	0.08
		614	YMEDSTyYKASK			2.21	N/A
		615	YMEDSTYyK			1.446	0.046
		615	YMEDSTYyKASK			2.458	N/A
		614, 615	YMEDSTyyk			9.627	0.88
		614, 615	YMEDSTyyKASK			8.658	1.49
Ptpra	PTPRA (receptor-type tyrosine-protein phosphatase alpha isoform 1)	825	VVQEYIDAFSDyANFK	1.399	0.035	1.359	0.045
Pxn	Paxillin	88	YAHQQPPSPLPVySSSAK			3.269	0.114
		88	YAHQQPPsPLPVySSSAK			5.335	1.153
		118	AGEEEHVySFPNK			3.046	0.87
		118	AGEEEHVySFPNKQK	2.703	0.082	2.865	0.304

RapGEF1	C3G (Rap guanine nucleotide exchange factor 1)	571	**HMLAYMQLLEDySEPQPSMFYQTPQSEHIYQQK**	2.854	0.168	3.204	0.223
Raph1	Raph1 (Ras association (RalGDS/AF-6) and pleckstrin homology domains 1)	603	**SyTSLMPPLSPQTK**			1.375	0.218
Rpl15	60S ribosomal protein L15	81	**GATyGKPVHHGVNQLK**	1.302	N/A		
Shc1	SHC1 (SHC-transforming protein 1 isoform a)	423	**ELFDDPSyVNIQNLDK**	1.392	0.116	1.365	0.104
Src	proto-oncogene tyrosine-protein kinase Fyn isoform b	424	**LIEDNEyTAR**			1.76	0.145
		444	**WTAPEAALyGR**			1.311	0.072
St5	St5 (Suppression of tumorigenicity 5 protein)	498	**ENPyEDVDLK**	1.413	0.184		
Tenc1	Tensin2	483	**GPLDGSPyAQVQR**			2.735	0.353
		705	**LALPTAALyGLR**	2.548	N/A	3.278	0.368
		770	**VGEEGHEGCSyAVCSEGR**	2.313	N/A	2.864	0.176
		791	**YGHSGYPALVTYGyGGAVPSYCPAYGR**			2.2	N/A
Tjp1	ZO-1 (tight junction protein ZO-1 isoform 2)	1177	**YRPEAQPySSTGPK**			1.9	0.241
Tln1	talin-1	436	**STVLQQQyNR**			1.88	N/A
		436	**KSTVLQQQyNR**			1.715	0.163
TMEM106B	TMEM106B (transmembrane protein 106B)	51	**NGDVSQFPyVEFTGR**	1.44	N/A	1.379	0.1
Tnc	Tenascin	1341	**LIQtIFTTIGLLyPFPR**			>50	N/A
Tns1	Tensin 1	1477	**HAAyGGYSTPEDR**			2.096	0.057
		1480	**HAAYGGySTPEDR**			2.27	N/A
		1558	**AGSLPNyATINGK**	2.321	0.03	2.232	0.052
Tns3	Tensin 3	584	**KPSAPTPVQAYGQSNySTQTWVR**			1.813	0.542
Trp53	p53 (cellular tumor antigen p53 isoform a)	228	**HSVVVPYEPPEAGSEYTTIHyK**			1.224	0.132
Ttyh2	TTYH2 (Protein tweety homolog 2)	424	**DRDyDDIDDDDPFNPQAR**			1.89	N/A
ZDHHC8	ZDHHC8 (probable palmitoyltransferase ZDHHC8)	582	**SQTDSLFGDSGVYDTPSSySLQQASVLTEGPR**			2.08	N/A

Table 8. Combined list of Src substrates (140) from prior proteomics studies.

Actin, alpha skeletal muscle (Y93)

Alpha enolase (Y43)

Alpha-1 catenin (Y619)

Anaphase promoting complex subunit 2 (Y825)

ANKS1/Odin (Y471)

Annexin A2 (Y23, 237)

ATP citrate lyase

ATP synthase

A-kinase anchor protein 8

Arsenate resistance protein ARS2

Ataxin 2 related protein

Bcl-2-associated transcription factor 1

Calnexin

Caplain 2

Caponin

Caveolin-1 (Y14)

Cbl (Y672)

Cdc42 GTPase-inhibiting protein

CDV3A/B (Y213)

Chaperonin

Chromosome 20 open reading frame 77

Clathrin heavy chain (Y899)

Cleavage and polyadenylation specific factor 5

Cofilin-1 (Y139)

Cortactin* (Y466)

CrkL **POSITIVE**

Cytidine 5'-triphosphate synthase

Cytoplasmic FMR1 interacting protein 1

Cytosolic phospholipase A2

DOK1** (Y314,361,408) **POSITIVE**

DNA damage-binding protein 1 (Y718)

Double-stranded RNA-binding protein Staufen homolog (Y404)

eEF1A1/2 (Y29,141)

eEF2

Elongation complex protein 3 (Y329)

Ephrin receptor A2

Ephrin receptor B1

Ephrin receptor B3

Ephrin receptor B4

Eps15

Eukaryotic translation initiation factor 3, subunit 4

Eukaryotic translation initiation factor 3, subunit 6-interacting protein (Y72)

Eukaryotic translation initiation factor 3, subunit 8

Ewing sarcoma breakpoint region 1

Ezrin

FAK* (Y576,577) **POSITIVE**

Fibronectin **POSITIVE**

FUSE binding protein*

FUSE binding protein 2

FUS interacting protein (serine/arginine-rich) 1

FUS/TLS oncogene

Fyn

Fyn binding protein

GAPDH (Y315)

GTP-binding protein Ran/TC4

GEF eIF-2B

GIT1 (Y554) **POSITIVE**

G6PDH X (Y400)

GMP synthetase

Histone H4 (Y51)

HNRP A3

HNRP AB

HNRP A2/B1

HNRP D

HNRP D-like

HNRP H1

HNRP K*

Homeobox prox 1

HSP9A

HSP90beta (Y483)

HSP1alpha

HSP1beta

KH-type splicing regulatory protein

Intersectin-2 (Y921)

Isoleucine-tRNA synthetase

Lamin A/C*

Lipoma preferred partner, LPP (Y245, 301,302) **POSITIVE**

Map kinase Erk2 **POSITIVE**

Moesin

Myosin heavy chain IX

NCK1 (Y105)

NEFA-interacting nuclear protein

Nice-4

Non-muscle myosin chain 10

OTUd4 (Y458)

p190 RhoGAP (Y943)

p120 catenin (Y96, 228)

p130cas* (Y253, 271, 414) **POSITIVE**

p120(ctn) (Y96)

Paxillin* (Y118) **POSITIVE**

PDGF receptor beta

Phospholipase C, gamma1

PI3K regulatory subunit, p85a** (Y467)

PI3K regulatory subunit, p85b **POSITIVE**

Plectin 1 (Y3250) **POSITIVE**

Polymerase I and transcript release factor (Y310,Y158)

Procollagen, type III, a1

Prolyl endopeptidase (Y71)

Proteasome 26S non-ATPase subunit 2

Proteasome activator subunit 3

Proteasome subunit beta type 5 precursor (Y165)

PSMA2 (Y56,75)

Pyruvate kinase 3

RasGap SH3-domain binding protein* **POSITIVE**

RENT1 (Y930)

RhoGDI

RhoGEF7 **POSITIVE**

Rin1 (Y35)

RNA binding motif protein 4B

RNA binding motif 10

SAK269 (Y632,638)

Septin-2 (Y17)

Seryl-aminoacyl-tRNA synthetase 1

SHC1 (Y423) **POSITIVE**

SHIP2 (Y987)

SHP-2* (Y62)

Similar to Zinc finger CCCH-type domain-containing protein 6

Splicing factor, arginine/serine-rich 3 (Y32)

Splicing factor, arginine/serine-rich 9

Splicing factor 3B subunit 2

Splicing factor proline/glutamine-rich

Src** (Y418,438) **POSITIVE**

Stress-induced phosphoprotein 1

Talin 1 (Y26, 70) **POSITIVE**

Thioredoxin reductase 1, cytoplasmic (Y131)

Threonyl-tRNA synthetase

Thyroid hormone receptor associated protein 3

Tight junction protein ZO-1 (Y1164, 1521)

Trk-fused gene

Tripartite motif protein 28

UAP1 like-1

UBAP2L (Y878)

Unc-84 homolog

U1 snRNP 70 kDa (Y126)

Valosin containing protein

VASP (Y39)

Vimentin (Y52) **POSITIVE**

Vps35

Xanthine dehydrogenase

Zinc finger, CCHC domain containing 8

(Proteins with * , were identified in two prior reports; proteins with ** , were identified in three prior reports; proteins designated as POSITIVE (16) were found in the current study)

APPENDIX 1- VALIDATION OF MATRIN THROUGH IMMUNOPRECIPITATION AND WESTERN BLOT

1. Summary

Matrin 3 was identified in our first SILAC and LC-MS/MS experiment performed to identify and quantify tyrosine-phosphorylated proteins upon c-Src chemical rescue. Matrin 3 was identified among the group of proteins that were eluted after boiling the beads used for enrichment of tyrosine-phosphorylated proteins by immunoprecipitation with antiphosphotyrosine antibody. By mass spectrometry, matrin 3 showed an increase in its tyrosine phosphorylation level upon c-Src chemical rescue with a Heavy/ Light ratio of 1.79 (Std. Dev.: n/a) (Table 3). When the two sets of raw data obtained from both the phenyl-phosphate and boiled beads elutions were combined and searched again, matrin 3 showed a Heavy/ Light ratio of 1.71 (Std. Dev.: n/a) and the score of the matrin 3 peptide was 35. Matrin 3 was identified by the identification of the peptide LAEPYGK. Matrin 3 was detected in MSQuant data analysis software, but not in Scaffold when the same Mascot data file was used as protein-peptide data file. The lists of proteins identified with 95% and 85% confidence by Scaffold are shown in Appendix 1 Tables 1 and 2. Matrin 3 was not found by Scaffold with 50% confidence either but, as described it was detected in MSQuant data analysis softwar and further manual annotation of MS/MS spectra confirmed the sequence. The mass spectrometry data evidencing the identification and quantification of this protein is shown in **Appendix 1 Figure 1** (MS/MS) and

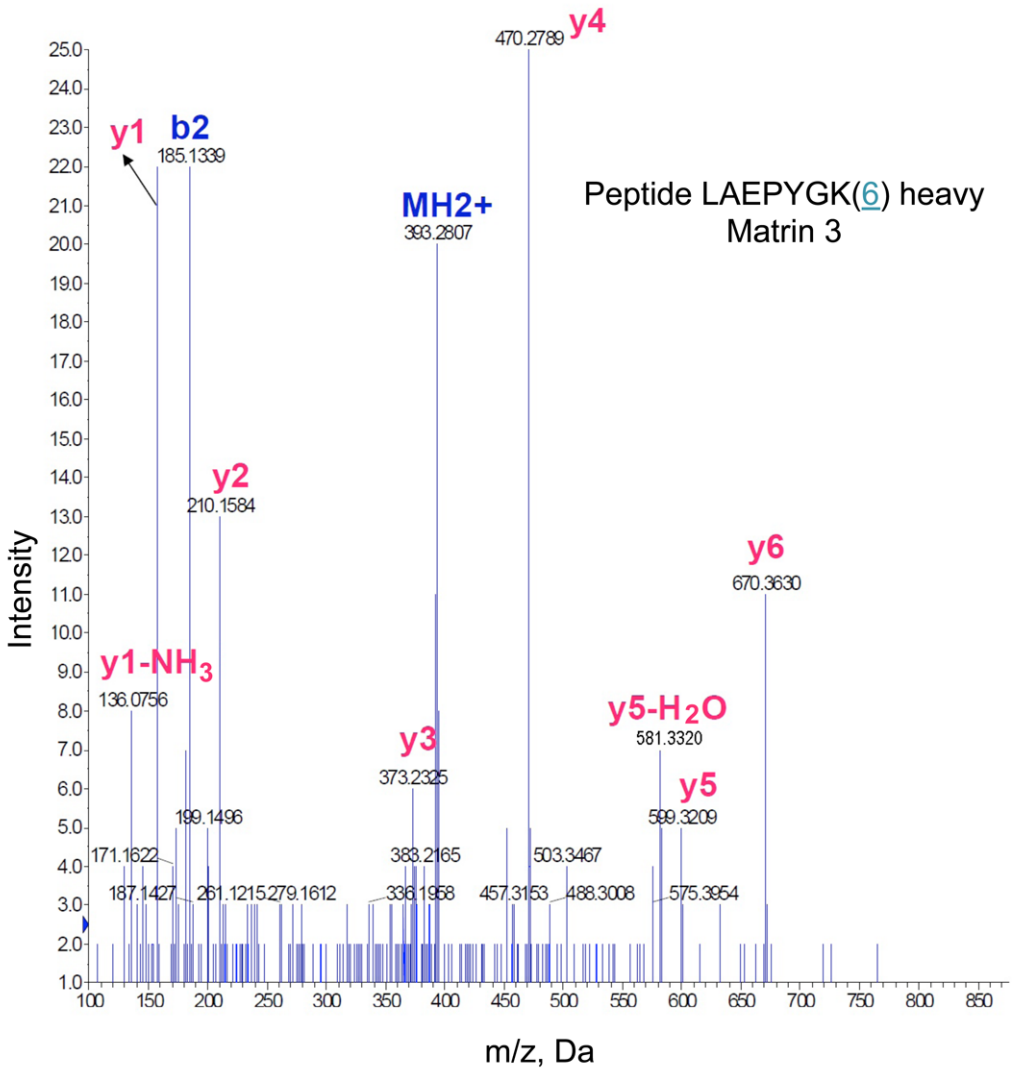

Appendix 1 Figure 1. MS/MS spectrum showing the identified peptide (LAEPYGK) from matrin 3.

Appendix 1 Figure 2 (MS). The experiment detailed in this appendix was performed to validate the results obtained in the SILAC experiment.

Unlike the other proteins selected for validation, it was difficult to detect phosphorylated matrin 3, despite the fact that matrin 3 is tyrosine phosphorylated. Tensin phosphorylation was also hard to detect but increasing the amount of lysate used in the immunoprecipitation was sufficient to overcome the challenge. The methodology that worked for visualization of phosphorylation of C3G, vimentin, GSK-3β, nucleophosmin and, ultimately tensin, did not reveal the expected bands for matrin 3 phosphorylation, and therefore some extra steps were added to the process. We have only one biological replicate of this experiment that showed the appearance of phosphorylated matrin 3, although the experiment was performed 5 times (and an additional attempt to repeat it recently). This led to data of modest quality revealing a borderline result about matrin 3 phosphorylation before and after c-Src chemical rescue, which we explain in detail here, and recommend that it be interpreted with caution. We believe the limitations of the assay for matrin 3 have led to the difficulties that will be next described.

The data obtained about matrin 3 phosphorylation (IP with matrin 3 antibody and Western blot with anti-phosphotyrosine antibody) is complex and ambiguous since multiple blots were obtained from the experiment and they show results by eye that are ambiguous is some cases and inconsistent in one particular blot. All of them have caveats I will thoroughly describe. The different blots obtained through the experimental process used to detect matrin 3 phosphorylation indicate either a borderline increased intensity by eye (and we say this with reservations we thoroughly describe here), a lack of response or even slight decrease in intensity of the bands in one blot (also with reservations we

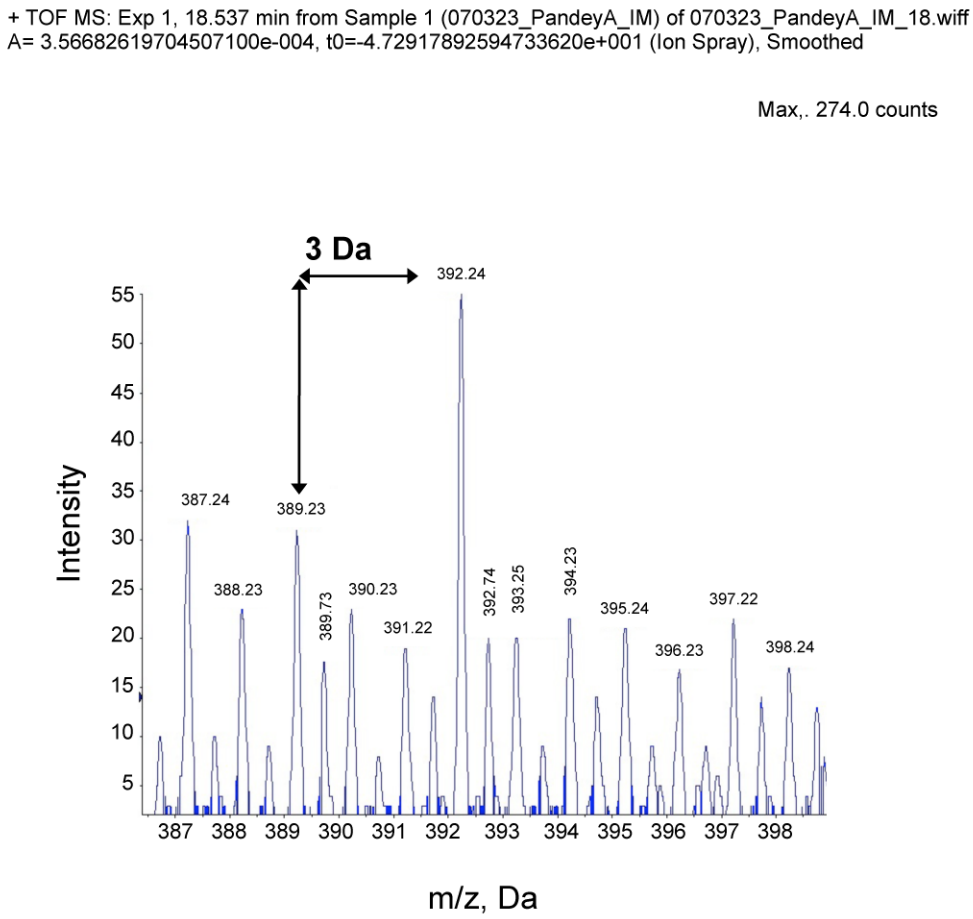

Appendix 1 Figure 2. MS spectrum showing the increase in intensity between the "light" and the "heavy" (isotopically labeled) forms of the peptide (LAEPYGK) from matrin 3.

describe here in detail). We tried employing the Image J methodology to measure the intensity of the bands but the high background and the non-optimal signal-to-noise made this very difficult in some cases and sometimes reflected changes that differ from what one can observe by eye. I believe one of the reasons for this is that the program needs an area of measurement that contains a substantial amount of background to be taken into account for its calculations. The program seems to work optimally when the band is clear and the signal relatively strong and the background is clear and homogeneous. In our case, having to choose such a large area makes it difficult to select areas where there is no heterogeneous background that affects the calculations. In addition, we observe that the methodology used to obtain the images may an effect in the quantitation. We used different methodologies to obtain the images and we believe the best images we obtained resulted from scanning the films. We believe we were successful in obtaining representative quantitation in some cases, even though other caveats were present. Some of the evidence in the experiment supports the mass spectrometry data, but some concerns are present. The few observations that, at least by eye (and not taking into consideration quantitations we believe are not representative of what can be observed by eye), don't show an increase in intensity (and maybe even a decrease), also present caveats. However, we must warn about the limited quality of the evidence due to the fact that this assay was particularly challenging to validate matrin 3 as a potential c-Src target. Some extra steps had to be added to the experimental process for visualization of matrin 3 phosphorylation and they led to some concerns and limitations. I believe the possible increase in phosphorylation of matrin 3 upon c-Src rescue is borderline and data is not

completely unequivocal/ convincing. Therefore, further validation through alternative methodologies is recommended.

2. Methods

The general methods were described in Chapter 2 but additional details are provided here.

After imidazole treatment (10 mM, 5 minutes), cells were washed once with PBS and lysed for 30 min at 4ºC in RIPA buffer (Tris-HCl 50 mM, pH 7.4, Na-deoxycholate 0.25%, NaCl 150 mM, EDTA 1mM, NP-40 1%, Na_3VO_4 1 mM, NaF 1 mM, PMSF 1 mM), and centrifuged at 13,000 x g at 4ºC for 15 minutes. The supernatants were collected for immunoprecipitation.

The supernatants were pre-cleared with protein G agarose. The precleared lysates were mixed with the antibody and incubated for 1 hour at 4ºC. Protein G agarose beads were then added to the mixture that was subsequently incubated overnight at 4ºC. Antibodies were used at the recommended concentration provided in the manufacturer's instructions. The protein G agarose beads were subsequently washed three times with RIPA buffer, resuspended in SDS loading buffer with β-mercaptoethanol and boiled for 5 minutes at 95ºC. The eluates were analyzed by SDS-PAGE and Western blotting.

The antibodies used were obtained as follows: Phosphotyrosine: 4G10 (phosphotyrosine WB) from Upstate Biotechnology. In most cases HRP-conjugated anti-phosphotyrosine antibody was used. Other times (i.e. D388N/ SYF cells) we used non-HRP-conjugated anti-phosphotyrosine antibody. Matrin 3: sc55724 (Matrin IP and WB)

from Santa Cruz Biotechnology. Western blots of experiments done with the rescuable cell lines were attempted 5 times (plus a recent attempt with non satisfactory loading control and poor visualization of matrin 3 phosphorylation), but we only obtained one experimental repeat where we believe we detected phosphorylated matrin 3 (**Figure 28**). The initial experiment **(Appendix 1 Figure 3.A)** was performed following the standard protocol described in Chapter 2. We observed signal in the first attempt but the blot presented bands that we suspect correspond to non-specific binding **(Appendix 1 Figure 3.A)**, making the interpretation unreliable, as we will explain in the result section. The next three repeats/ biological replicates **(Appendix 1 Figure 3.B-D)** were performed with slight modifications to the protocol, but these Western blots using anti-phosphotyrosine antibody (4G10) showed no signal in these three experimental repeats.

In the fifth matrin 3 immunoblot experiment, we included some additional steps to be able to visualize phosphorylation. After incubation with the mouse HRP-conjugated 4G10 anti-pTyr antibody, we developed the blot and, as before, no phosphorylation was observed **(Appendix 1 Figure 6)**. A sandwich reaction then had to be performed **(Appendix 1 Figure 7-8)**: We did a second incubation with an HRP-conjugated anti-mouse secondary antibody. The first incubation with the secondary antibody (sandwich reaction) was performed at 4ºC for approximately one hour as indicated in my lab notebook. After washing the membrane, we developed the membrane using SuperSignal West Femto chemiluminescent substrate (Pierce) diluted 1 to 10 in water **(Appendix 1 Figure 7-8)**. Even though there is the concern that the process of the sandwich reaction may lead to non-specific binding, it is actually a perfectly acceptable technique to increase the signal in a Western blot. Also, the first sandwich reaction was performed for

a short time (4ºC for one hour as I indicated in my notebook, but the exact period of time was not recorded), and exposed for a very short time (seconds to a few minutes). We used a high concentration of substrate for development of the film (1 to 10 femtomolar ECL), which can make the blots very dirty with high background. This is expected and does not necessarily represent a problem but makes the washing and the visualization very difficult.

We then washed the membrane again and developed it with 1 to 10 femtomolar ECL solution. I have a blot (**Appendix 1 Figure 9)** with a clearer background than those showing in Appendix 1 Figure 7-8 (Even though blots corresponding to Appendix 1 Figure 8 and Appendix 1 Figure 9 may have been inadvertently switched in my lab notebook, the pattern of the background suggests that the order of the two blots is as the presented here).

The membrane was then washed and incubated again with anti-mouse secondary antibody. This second sandwich reaction was performed at 4ºC overnight (as indicated in my notebook although the exact period of time was not recorded). After washing the membrane, we developed the membrane using SuperSignal West Femto chemiluminescent substrate (Pierce) diluted 1 to 2 in water **(Appendix 1 Figure 9)**. A sandwich reaction may lead to reduced specificity and artifacts I am not aware of, but it was the only way I could visualize phosphorylation of matrin 3. The resulting blot was very dark but could be scanned using different methodologies **(Figures 28 and Appendix 1 Figure 10-12)**. After the second sandwich reaction, we also had problems with what we believe is loss of signal (or "clearing") that will be described in the Results section.

It should be noted that baseline values between rescuable and non-rescuable cells may not be the same due to subtle alterations in the cell passage number, growth conditions, and/or immunoblot conditions.

The images were acquired through different methodologies: They were scanned with or without the help of a halogen desk lamp that was carefully placed so that it homogeneously illuminated the blot or region of interest. Some of the films we also scanned through translucent scanning, which provided extra illumination to dark blots.. The blots were also placed on top of a light box and pictures were taken with a low-resolution camera in some cases (to get a whole image of a dark blot) or with a Cyber-shot Sony camera. We also took pictures with an Imager (Gel Logic 100, Imaging system) and a white lamp diffuser on top of a UV lamp (Fotodyn lamp). We used a white light diffuser on top of the UV light to attempt homogenous illumination. Images were acquired using Carestream MI GL100. Different images were obtained for different blots depending on the characteristics of the blots.

Images were quantified using Image J with these settings (Set measurements: Area/ Mean Gray Value/ Integrated density; Set Scale: 600 pixel; background was either not subtracted or subtracted with rolling ball radious of 50 or 100, depending of the image). If the orginal image had color they were converted to gray scale by changing the image to both 8-bit and 32-bit as indicated.

3. Results

3.1. First attempt

The first attempt to validate matrin 3 through immunoprecipitation and immunoblot was initially considered successful even though the anti-phosphotyrosine immunoblot was dark and some unexpected bands appeared that we couldn't initially explain **(Appendix 1 Figure 3.A)**. However, we later realized that it might not be reliable due to the following reasons: I believe these bands correspond to a significant amount of non-specific proteins pulled down in the immunoprecipitation experiment that are being co-purified or retained with matrin 3. I believe the signal from these non-specific proteins in the anti-phosphotyrosine immunoblot is quite prevalent and may overlap/ interfere with any band that might show matrin 3's phosphorylation. This was concluded after we observed some evidence for these non-specific proteins as a strong band at around 60 kDa in the immunoprecipitation lane as well as in the lysate lane (to which no antibody was added). Initially it was thought that this band corresponded to the antibody heavy chain (55 kDa) but obviously that cannot appear in the lysate, making us concerned that that band represented a non-specific protein carried in the immunoprecipitation. The fact that the band appears at the same molecular weight in the immunoprecipitation lane and the lysate lane reaffirm the concern. Also, I can clearly see the two bands corresponding to the heavy chain at molecular weight of 50 kDa in the lanes corresponding to the lysates subjected to immunoprecipitation. Also, the pattern of bands observed in the lysate lane in the anti-phosphotyrosine immunoblot clearly resembles the pattern of bands observed in the lanes corresponding to immunoprecipitation, adding weight to the conclusion that the IP did not effectively remove non-specific proteins. This was the first biological

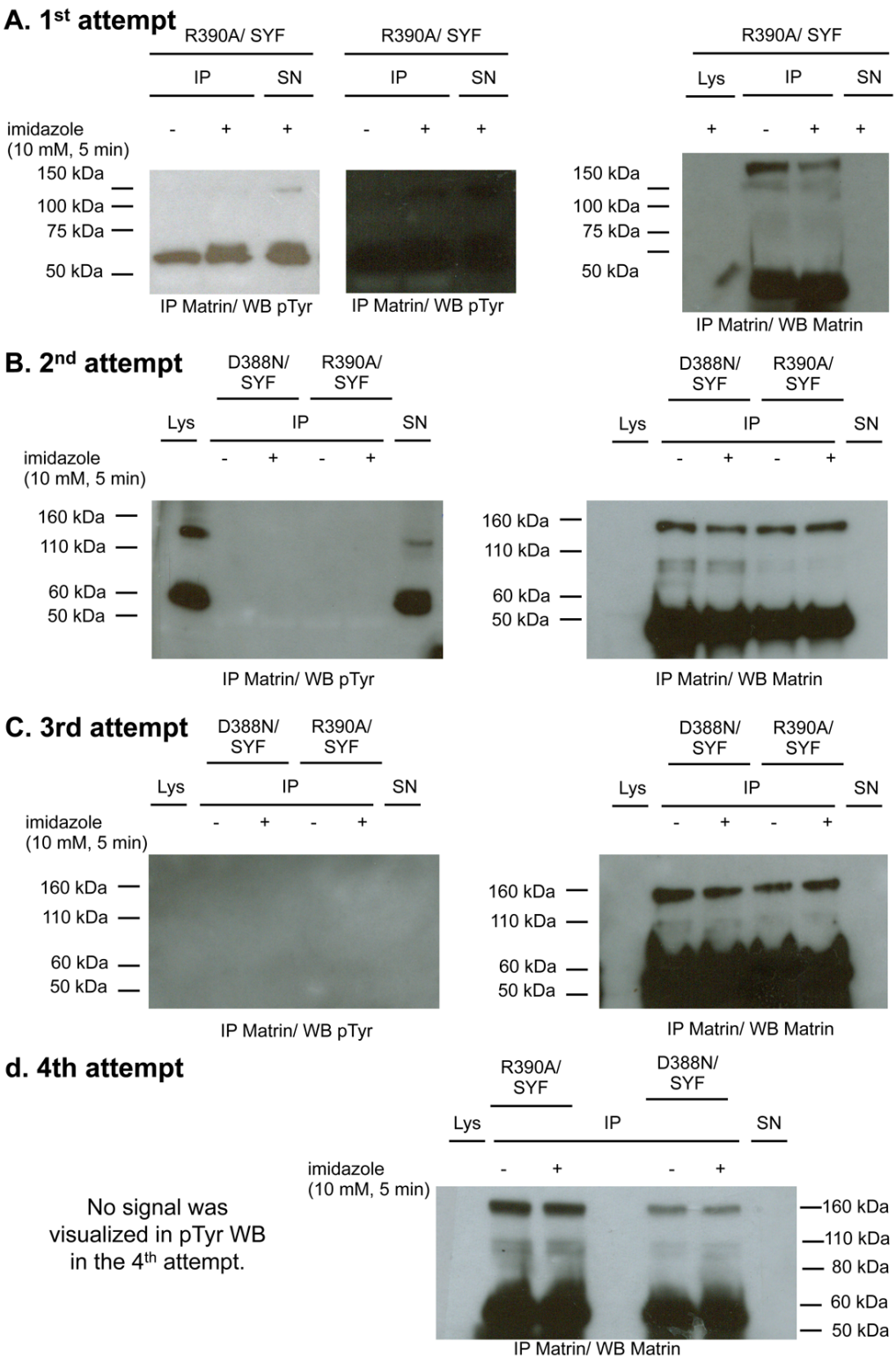
A. 1st attempt
R390A/ SYF
R390A/ SYF
R390A/ SYF
IP
SN
IP
SN
Lys
IP
SN
imidazole
(10 mM, 5 min)
- + + - + +
+ - + +
150 kDa
100 kDa
75 kDa
50 kDa
IP Matrin/ WB pTyr
IP Matrin/ WB pTyr
IP Matrin/ WB Matrin
B. 2nd attempt
D388N/ SYF
R390A/ SYF
Lys
IP
SN
imidazole
(10 mM, 5 min)
- + - +
160 kDa
110 kDa
60 kDa
50 kDa
IP Matrin/ WB pTyr
IP Matrin/ WB Matrin
C. 3rd attempt
D388N/ SYF
R390A/ SYF
Lys
IP
SN
imidazole
(10 mM, 5 min)
- + - +
160 kDa
110 kDa
60 kDa
50 kDa
IP Matrin/ WB pTyr
IP Matrin/ WB Matrin
d. 4th attempt
No signal was visualized in pTyr WB in the 4th attempt.
R390A/ SYF
D388N/ SYF
Lys
IP
SN
imidazole
(10 mM, 5 min)
- + - +
160 kDa
110 kDa
80 kDa
60 kDa
50 kDa
IP Matrin/ WB Matrin

Appendix 1 Figure 3. Repeats of the immunoprecipitation- Western blot experiments to validate the mass spectrometry results that revealed matrin 3 as a potential c-Src substrate.

The control and imidazole treated cells were lysed and immunoprecipitation was performed using matrin 3 antibody. Western blot against matrin 3 was used as a loading control and Western blot against phosphotyrosine was used to detect tyrosine phosphorylation. **A.** Initial attempt where phosphorylation was observed at molecular weights of 60 kDa and 120 kDa, making it difficult to discern whether the top band corresponds to matrin 3 and or a cluster of proteins that was non-specifically bound to matrin 3 and are phosphorylated. **B**, **C**, and **D.** These biological replicates all successfully led to satisfactory loading controls (Matrin 3 western blot) but tyrosine phosphorylation of matrin 3 was not detected.

replicate we performed. In the loading control experiment (immunoprecipitation and Western blot with matrin 3 antibody) we observed two major bands that we believe correspond to matrin 3. One was located at about 150 kDa and the other one at 110-120 kDa. The band that appeared in the phosphotyrosine immunoblot was considered as matrin 3, since it corresponds (has the approximate molecular weight) to the lower band observed in the loading control. However, we then realized that this band in the antiphoshotyrosine Western blot is at the same molecular weight as a strong band in the lane corresponding to the lysate. This was an indication that this band is also very likely a non-specific protein or group of proteins that was pull-down with matrin 3 during the immunoprecipitation the same way we described for the band at 60 kDa. It has actually been observed that these two strong bands usually appear at the approximate molecular weight of 60 kDa and 120 kDa when a whole lysate is blotted using anti-phosphotyrosine antibody (see Figure 23).

In addition to the concern about non-specific binding, our initial experiment may have uneven loading. The amount of increase that can be observed in the band at 120 kDa between the control and treatment immunoprecipitated lysates is very similar to the amount of increase observed in the band at 60 kDa between the control and treatment immunoprecipitated lysates, suggesting that it might not be a real increase but a slight difference in loading. The loading control (immunoprecipitation with matrin 3 antibody and Western blot with matrin 3 antibody) is however satisfactory.

Another concern has to do with the molecular weight of the band initially thought to be matrin 3. The immunoprecipitation effectively retained the matrin 3 protein, as can be observed in the immunoblot against matrin 3 after the immunoprecipitation with

matrin 3 antibody (loading control). As described, in this control blot, matrin 3 can be observed in this blot as a doublet of two strong bands (a stronger upper band and a lower band that is actually a doublet itself). However, in the anti-phosphotyrosine immunoblot, I only can see a band corresponding approximately to the lower molecular weight where the lower doublet was observed. This makes us question even more whether this band is really matrin 3, because one might expect both bands to be detected (band at 120 kDa and doublet at 110 kDa), especially since the top band is the strongest one in the matrin 3 immunoblot.

3.2. Three following unsuccessful attempts

When I tried to reproduce this experiment (3 times) **(Appendix 1 Figure 3.B-D)**, I could always detect matrin 3 in the matrin 3 immunoprecipitation and matrin 3 immunoblot. However, I could not detect phosphorylation in the lanes corresponding to immunoprecipitated lysate in the blot against phosphotyrosine. I had two positive controls in most of the membranes (the lanes corresponding to the lysate and the lanes corresponding to the supernatant after immunoprecipitation) and in one case **(Figure 3.C)** phosphorylation was observed in these lanes, indicating that the antibody and immunoblot protocol were correct. I consider these three repeats as unsuccessful as they do not provide any interpretable results. These three unsuccessful repeats further cause us to question the results of the initial experiment. It is unlikely that I detected phosphorylation in the first attempt but not in the next three attempts when I was optimizing the technique. These three unsuccessful attempts lead us to believe that, for

some reason, matrin 3 phosphorylation is very hard to detect. This may be due to the high molecular weight of the matrin 3 protein, which may contribute to inefficient transfer but this is unlikely because the same assay has been used successfully to validate targets with very similar molecular weight. Matrin 3 might not be highly phosphorylated (as I observed for tensin, for example), although it has several tyrosine phosphorylation sites.

3.3. Final attempt- R390A/ SYF cells

In our final repeat, I incorporated several steps to be able to detect phosphorylation. These steps are described in the methods section and represented in **Appendix 1 Figure 4**. After I followed these steps, I could observe bands at the correct molecular weight for the first time in the anti-phosphotyrosine immunoblot after matrin 3 immunoprecipitation.

3.3.1. Matrin 3 loading control (R390A/ SYF cells)

The loading control (matrin 3 immunoprecipitation and matrin 3 immunoblot) is satisfactory **(Appendix 1 Figure 5)**. The amount of sample loaded for this matrin 3 blot and the anti-phosphotyrosine blot is exactly the same. I performed one immunoprecipitation with lysate coming from treated cells and another one with lysate from untreated cells. The sample from each immunoprecipitation was divided in two, regardless of the total volume resulting from the immunoprecipitation. One of the gels was transferred and blotted against matrin 3, and the other one was transferred and

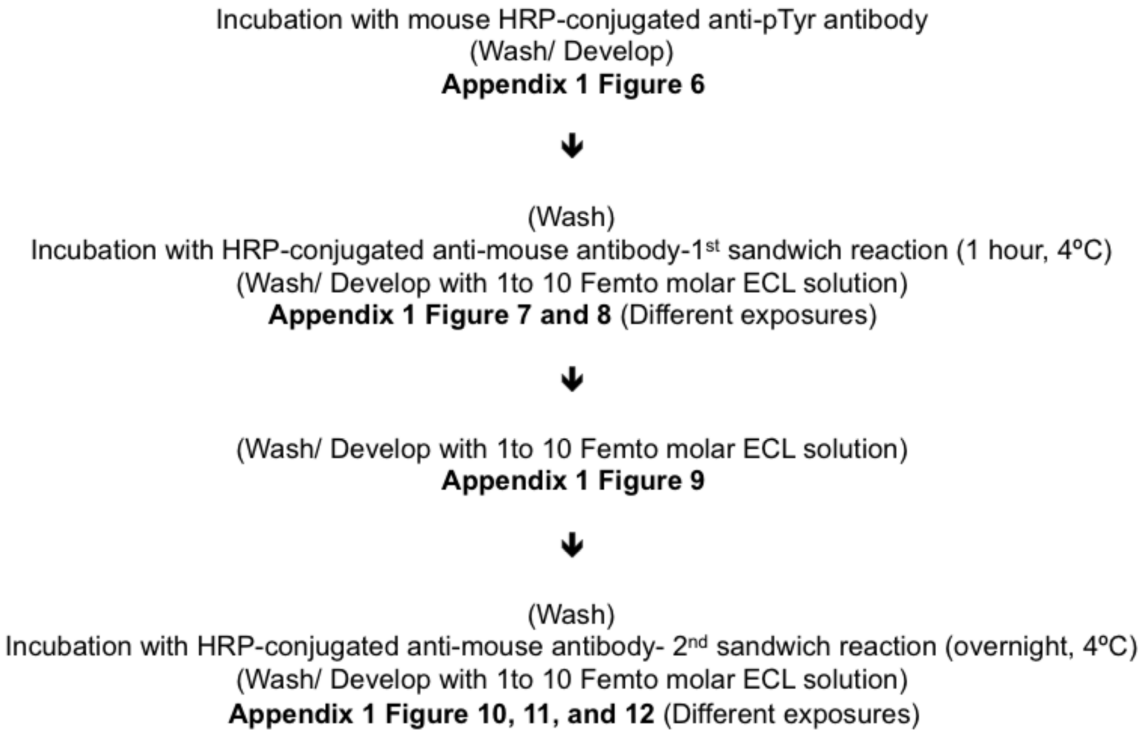

Appendix 1 Figure 4. Workflow of the process to obtained the different blots in the last attempt to detect matrin 3 phosphorylation

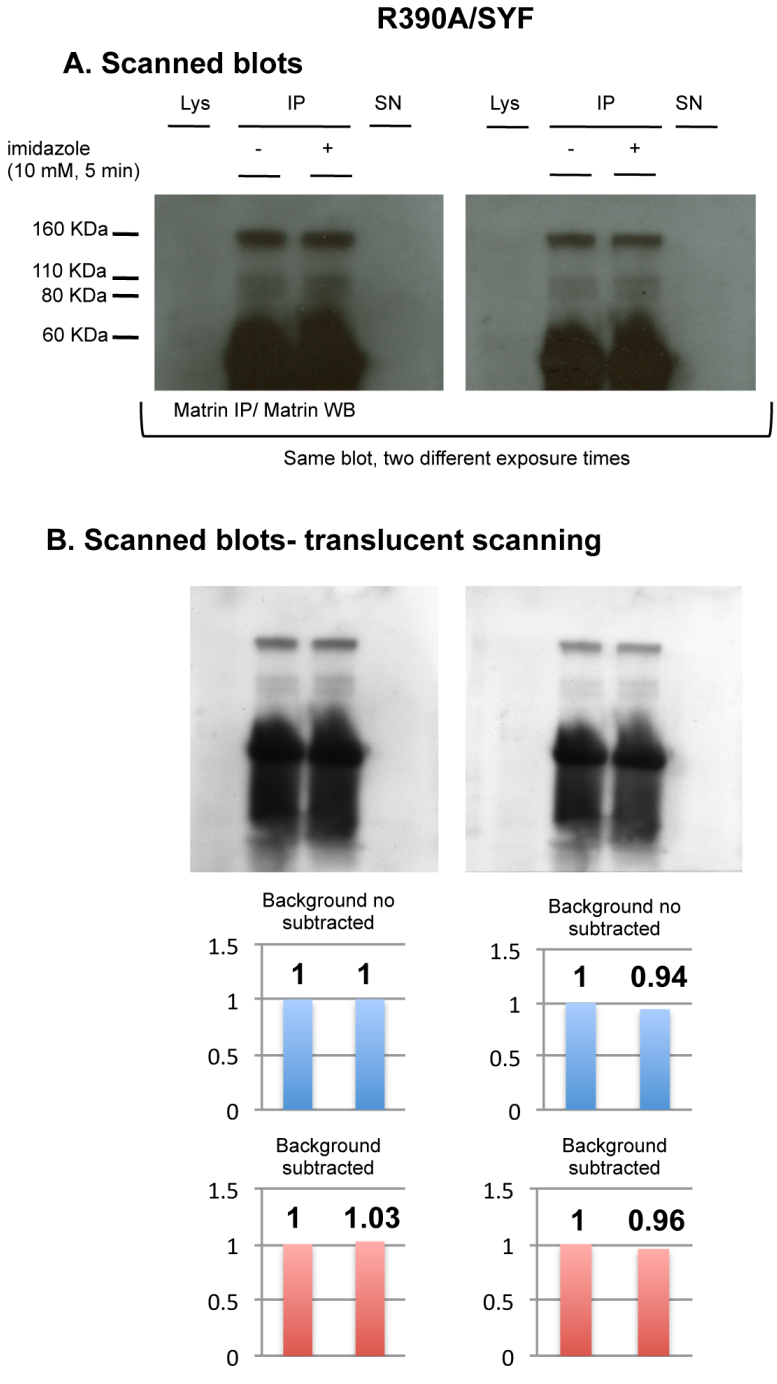

Appendix 1 Figure 5. Matrin 3 loading control of the final experimental repeat in the rescuable cell line R390A/SYF.

Immunoprecipitation- Western blot experiment to validate matrin 3 as a potential c-Src substrate. The untreated and the treated cells were lysed and immunoprecipitation was performed using matrin 3 antibody.

Western blot against matrin 3 was used as a loading control. A. Images and quantitations obtained by scanning the image. B. Images and quantitations obtained by translucent scanning. Two blots corresponding to two different exposure times are presented.

blotted against phosphotyrosine. I loaded exactly the same volume of samples for both the matrin 3 immunoblot and the phosphotyrosine immunoblot (35 μl for untreated cells and 39 μl for treated cells). Special attention was paid to the loading process for accuracy and equal loading for both blots. However, because the loading control and the experiment are on separate gels, it is theoretically possible that there could be a manual mistake in the loading of the gels. However, the careful process of loading makes this unlikely.

The matrin 3 loading control blot always reveals an upper more intense band around 160 kDa, a doublet around 110 kDa, and antibody chains around 55 kDa. We observed no change in intensity in the upper more intense band (if any, I think a very slight decrease in intensity may be observed by eye in the right blot corresponding to a shorter exposure time). The doublet seems a bit more intense in the treated R390A/SYF cells, but it is also true that the band is somewhat narrower in the treated R390/SYF cells, and this could account for/ justify the minimal increase in intensity in the doublet bands. Overall, I consider the loading control satisfactory. We quantitated the upper bands in the blots and obtained what we believe are representative values from the two different exposures from images obtained from translucent scanning (1/ 1 and 1/1.03, no background subtraction; 1/0.94 and 1/0.96, background subtraction), which confirm the satisfactory loading.

3.3.2. Anti-phosphotyrosine Western blot before the sandwich reaction

Before the sandwich reaction **(Appendix 1 Figure 6)**, the anti-phosphotyrosine immunoblot only showed bands in the lanes corresponding to the lysate and the supernatant, as we had observed in previous repeats. The image was obtained from scanning the blot.

3.3.3. Anti-phosphotyrosine Western blot after the first sandwich reaction

Blots shown in **Appendix 1 Figures 7-12** correspond to the same biological replicate, where the blot was subjected to different additional steps in a sequence that is described here **(Appendix 1 Figure 4)**. After the additional steps described in the methods, bands appeared in the lanes corresponding to the immunoprecipitated lysates. The bands in that blot appear at the correct molecular weight for matrin 3, based on where it was observed in the matrin 3 immunoblot **(Appendix 1 Figure 5)**. In addition, both the upper more intense band and the lower less intense doublet show in the blot, as opposed to our first attempt **(Appendix 1 Figure 3.A)** where the upper band was not detected.

Appendix 1 Figure 7 shows the appearance of the blot after the first sandwich reaction and the development of the blot as indicated in the methods. The bands corresponding to matrin 3 are indicated with white arrows. We will mostly consider the upper band, because the matrin 3 immunoblot had a more intense band at this molecular weight as compared to the lower band. We show figures obtained after scanning the blot,

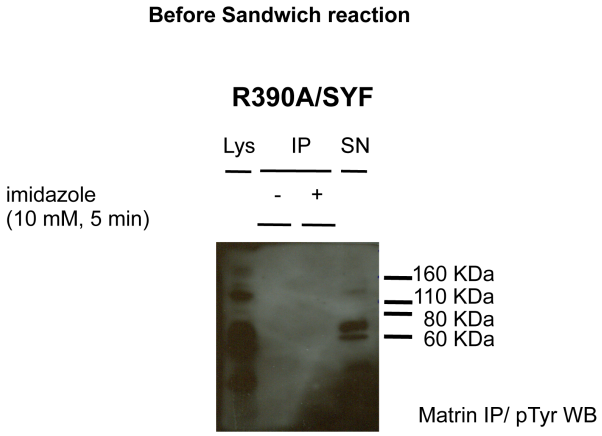

Appendix 1 Figure 6. IP-WB experiment to validate matrin 3 as a potential c-Src substrate. R390A/ SYF cells. Anti-phosphotyrosine Western blots before first sandwich reaction

Matrin 3 phosphorylation of the final experimental repeat in the rescuable cell line R390A/SYF. Immunoprecipitation- Western blot experiment to validate matrin 3 as a potential c-Src substrate. The untreated and the treated cells were lysed and immunoprecipitation was performed using matrin 3 antibody. Western blot against phosphotyrosine showed no signal of phosphorylated matrin 3. The image was scanned.

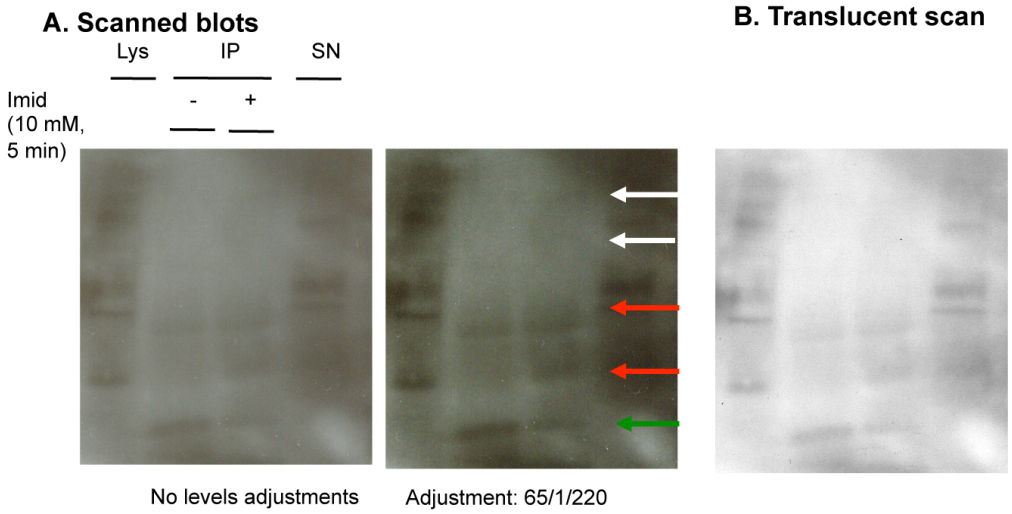

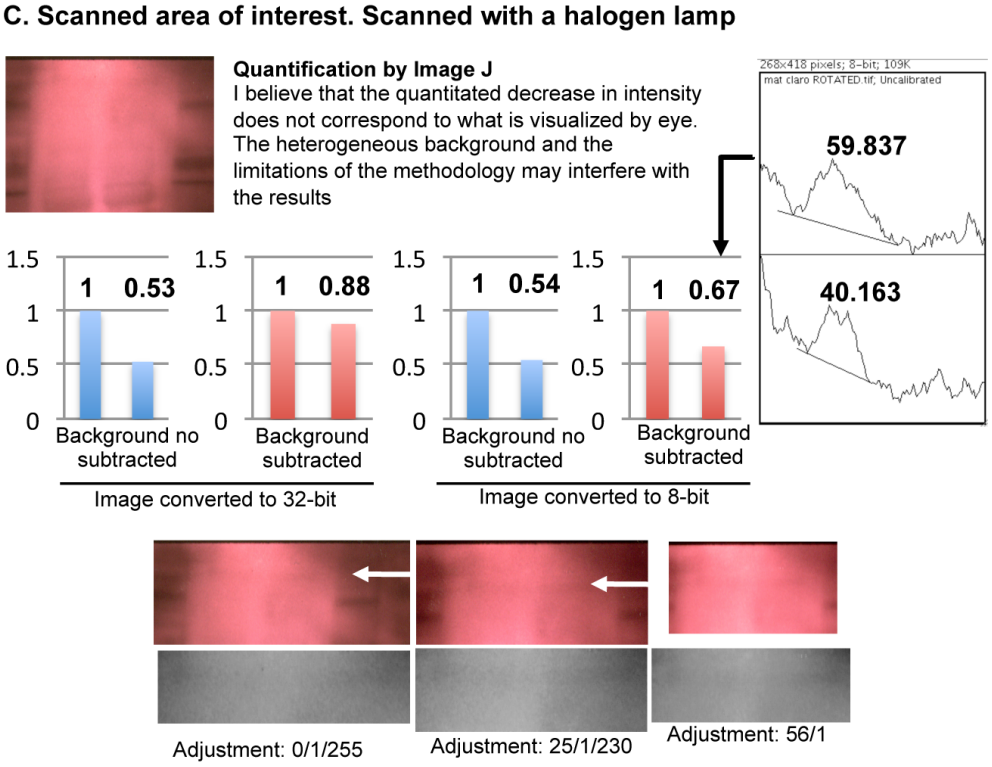

Specific concerns:

- Sandwich reaction does not increase the intensity of the bands in the Lys and SN lanes.
- Possibility of non-specific binding (2ary antibody)
- Appearance of bands showing and increase (red arrows) or a decrease (green arrows)
- Inconsistent behavior of bands in films obtained through the process
- High and heterogeneous background

Appendix 1 Figure 7.1. IP-WB experiment to validate matrin 3 as a potential c-Src substrate. R390A/ SYF cells. Anti-phosphotyrosine Western blots after the first sandwich reaction.

Matrin 3 phosphorylation of the final experimental repeat in the rescuable cell line R390A/SYF. Immunoprecipitation- Western blot experiment to validate matrin 3 as a potential c-Src substrate. The untreated and the treated cells were lysed and immunoprecipitation was performed using matrin 3 antibody. Western blot against phosphotyrosine after washing and performing a sandwich reaction. First exposure. **A.** Scans of the entire blot. The one in the left represents the intact scan and the one in the right the scan after the indicated adjustments in the levels. **B**. Image obtained by translucent scanning. **C.** The panel bellow shows a scan taken with the help of a lamp and the gray version of it after different adjustments in the levels. Quantitation of the bands corresponding to matrin 3 phosphorylation from the original image was attempted using different setting in Image J and results are shown. The arrows show bands of interest. White arrows indicate bands corresponding to matrin 3 phosphorylation. Red arrows indicate bands that show an increase in their intensity. Green arrows indicate bands that show a decrease in their intensity. Grey arrows indicate bands that do not change their intensity.

D. Representative picture taken with Cybershot camera and light box

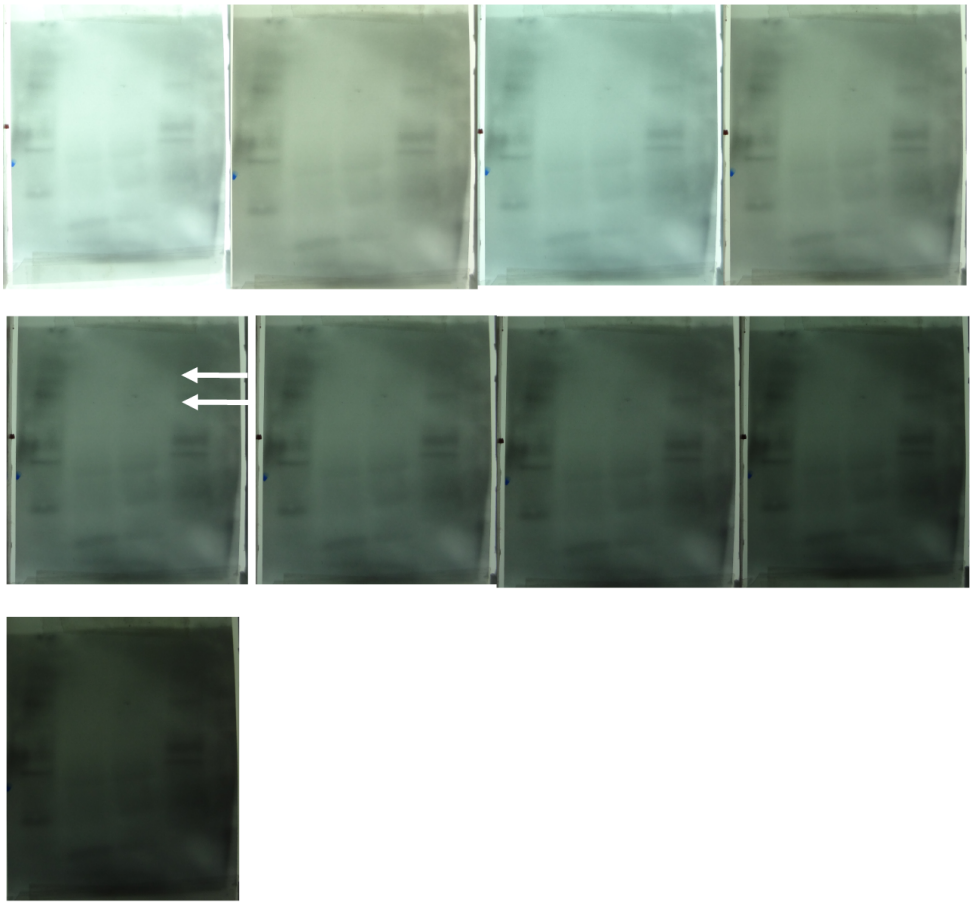

E. Representative pictures taken with imager and lamp

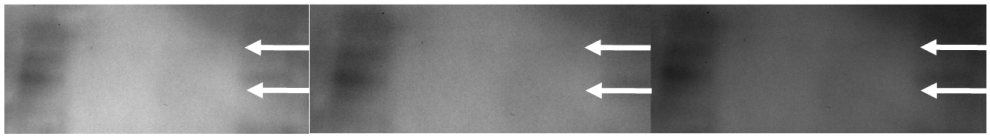

Appendix 1 Figure 7.2. IP-WB experiment to validate matrin 3 as a potential c-Src substrate. R390A/ SYF cells. Anti-phosphotyrosine Western blots after the first sandwich reaction (cont.)

Matrin 3 phosphorylation of the final experimental repeat in the rescuable cell line R390A/SYF. Immunoprecipitation- Western blot experiment to validate matrin 3 as a potential c-Src substrate. The untreated and the treated cells were lysed and immunoprecipitation was performed using matrin 3 antibody. Western blot against phosphotyrosine after washing and performing a sandwich reaction. First exposure. **D.** Representative pictures taken with a camera and the help of a light box. Different pictures correspond to

different adjustment in the brightness in the camera**. E.** Representative pictures bellow were taken with an imager and a lamp. Different pictures correspond to different adjustment in the light aperture**.**The arrows show bands of interest. White arrows indicate bands corresponding to matrin 3 phosphorylation.

scanning the blot with translucent scanning, scanning the area of interest with the help of a halogen lamp **(Appendix 1 Figure 7.1)**, taking a picture with the help of a light box, as well as representative pictures obtained with the imager, a UV lamp and a white light diffuser **(Appendix 1 Figure 7.2)**. Quantitation was attempted from the scanned image and the image obtained by translucent scanning but the low signal, and possibly the heterogeneous background, made this impossible.

Quantitation was performed from the image obtained scanning the area of interest with the help of a halogen lamp and the result is shown. However, due to the low signal and heterogeneous background we believe the quantitation is not representative of what can be observed by eye. A series of quantitation plots are shown and reveal that the characteristics of the blot are not optimal for quantitation.

Limitations:

One issue worth mentioning is that the sandwich reaction should lead to a stronger intensity of the bands. Indeed, I see new bands appearing in the immunoprecipitation lanes that did not appear before the sandwich reaction. However, the intensity of the bands that were present in the lysate and the supernatant lanes do not increase in intensity the same way the bands that appear in the immunoprecipitation lanes do for unknown reasons. We speculate that the fact that the phosphorylation signal in the lysate and supernatant may be already saturated may contribute to this observation.

Another concern is that multiple bands appear after the sandwich reaction. This could mean that the sandwich reaction may have led to non-specific binding of one of the antibodies used in the immunoblot to a contaminant protein of low abundance in the

samples. However, a sandwich reaction is a perfectly acceptable technique to increase the signal in a Western blot. Also, the conditions under which it was performed included a short incubation with the anti-mouse HRP-conjugated secondary antibody (4ºC for approximately one hour as I indicated in my notebook, but the exact period of time was not recorded) and very short exposure time (seconds to a few minutes). The short incubation period and exposure time should minimize the appearance of non-specific bands. A sandwich reaction may lead to reduced specificity and artifacts, but allowed us to visualize phosphorylation of matrin 3.

Also, in this particular blot, I see that some of the bands that appear below matrin 3 show an increase in intensity (red arrows) upon treatment of the cells with imidazole. The careful handling of the loading and the satisfactory loading control **(Appendix 1 Figure 5)** should be a good indicator of equal loading in the phosphotyrosine blot. However, the fact that this increase in intensity in some lower bands may be similar to a borderline possible increase that may be observed by eye in the band corresponding to matrin 3, suggests that there is a possibility of a human error in loading. This would mean that a possible increase in intensity in the band corresponding to matrin 3 could be a result of imprecise loading. However, there could be other explanations for this observation. Maybe the lower bands are proteins that are retained in the immunoprecipitation non-specifically and they increase their tyrosine phosphorylation level upon c-Src rescue. It is worth mentioning though that there are bands that show a decrease in intensity (green arrows), which would go against the argument of an overall imprecise loading favoring a possible stronger band of matrin 3 phosphorylation in the case of cells treated cells. Theoretically, there could still be a decrease even if there was

imprecise loading. c-Src rescue could lead to a decrease in phosphorylation of that protein that is pulled down non-specifically with matrin 3. This decrease could still be apparent even after having loaded more immunoprecipitated lysate from treated cells. However, the described measures taken for precise loading and the satisfactory loading control make the possibility of imprecise loading unlikely.

Also, these changes in intensity of the lower bands of the blot upon imidazole treatment are not consistent among all the blots obtained along the process followed in this experiment, as I will describe (and this is also the case of the bands corresponding to matrin 3 phosphorylation, which shows slightly different intensity changes in some blots). This raises the possibility that maybe some of the changes in the intensity of the bands may not be real in the worst case.

Another concern is that the blots are quite dirty and have a heterogeneous background and this may interfere with the evidence (bands) observed and the interpretation made. I used a high concentration of substrate for development of the film (1 to 10 femtomolar ECL or 1 to 2 femtomolar ECL) to increase the signal. These high concentrations of ECL can make the blots very dirty. This kind of background is expected but it can lead to a difficult process of washing and visualization of the bands. The bands corresponding to phosphorylated matrin 3 are quite faint, and thus signal-to-noise is a valid concern. If the resulting blot is not washed enough, it can lead to non-homogeneous background. Therefore, a possible apparent marginal increase in intensity or matrin 3 and/or some of the non-specific proteins may be a result of the heterogeneous background or be affected by it. This is hard or impossible to determine.

Taken together, we have lingering concerns that are very hard or impossible to

explain. We therefore wish to caution readers about the modest quality of the evidence this IP-WB experiment provided in the case of matrin 3.

Image acquisition:

The blot was scanned entirely first. It was also scanned by translucent scanning. The area of interest was scanned with the help of a halogen desk lamp. Results are shown in **Appendix 1 Figure 7.1**. The lamp was used to get a clearer image of the bands from a blot with high background. The lamp was carefully placed on top of the area of interest and we aimed to obtain a homogeneous illumination of the area of interest that was scanned. This did not seem to be a problem since the selected area was very small. However, this method was not specifically designed for this purpose. The levels were processed as indicated in the figure (approximate numbers). This type of illumination did not provide a very good image of the entire blot in some cases. For this reason, we took pictures of the entire blot with both a low-resolution camera and a Sony Cyber-shot camera (Appendix 1 Figure 7.2) on top of a light box. We also used an imager and a white light diffuser on top of the UV light to attempt homogenous illumination, although this may not be the optimal procedure either. All these images are shown in **Appendix 1 Figure 7.1 and Appendix 1 Figure 7.2**. The scanned images seem to have better quality than the ones taken with the cameras and the help of a light box and the translucent scanning is thought to provide the most homogeneous illumination that may be needed to visualize dark blots and is therefore a established way to illuminate and scan dark films.

Observations:

The bands are not clearly defined or sharp. They are also very faint. The background is strong and heterogeneous.

By eye, I believe I may see a borderline increase in intensity but I have to say this is very ambiguous: the left band (untreated cells) looks a bit more intense than the right band (treated cells) in the left part of the band, but the right band seems more solid and seems to have a more homogeneous intensity through the band. However, the observed heterogeneous background may affect either one or both bands. For example, there is a dark region bellow the right band and a diagonal clear band also close to the right band. However, the signal is so faint, it is hard to distinguish.

The blots were scanned and are shown here. We attempted quantifying the differences in intensity between both bands but it was not possible (area plots alsmot indistinguishable) in the original scans, the adjusted images or the scan obtained with translucent scanning.

When the film was scanned with a lamp, we attempted to measure the change in intensity again. The result is shown but we believe it is not representative of what can be observed by eye. This may be due to the heterogeneous background and the fact that Image J requires a large selected area to make the quantitations. As a result, we could not avoid including some areas that show heterogeneous background in our film that may affect the reading. Another reason could be the low signal in the blots. However, the area plots and the quantitation graphs are presented here to show the discrepancy between what can be observed by eye and what the quantitation indicates if these limitations are present.

Representative pictures made with the Cybershot Sony camera and a light box are also included and shown in Appendix 1 Figure 7.2. Representative pictures made with the imager are also included in Appendix 1 Figure 7.2. but quantitation was not possible.

3.3.4. Anti-phosphotyrosine Western blot after the first sandwich reaction. Second exposure.

The blot was then developed during a longer exposure time **(Appendix 1 Figure 8)** and the observations and concerns are very similar to the previous exposure **(Appendix 1 Figure 7)**. The bands are a bit stronger and the background is more apparent too.

Observations:

By eye, the observations are similar than with the previous blot but an increase is even less apparent or non existent. The left band (untreated) is sharper or better defined and more solid now. The right band seems a bit wider. If there is an increase, it is easier to detect this with the lower exposure. It is important to mention that the background is more visible, its heterogeneity more obvious, and its possible effect more apparent. A lighter diagonal stripe observed mostly in the right side may affect the bands, maybe the right one, but this is ambiguous and hard to determine. Bellow the right area there is a small darker area that could affect it. The background seems stronger but it is also strong in the top left side of the left band. Overall, the high and heterogeneous background makes it hard to make conclusions and quantitate the blot.

A. Translucent scan

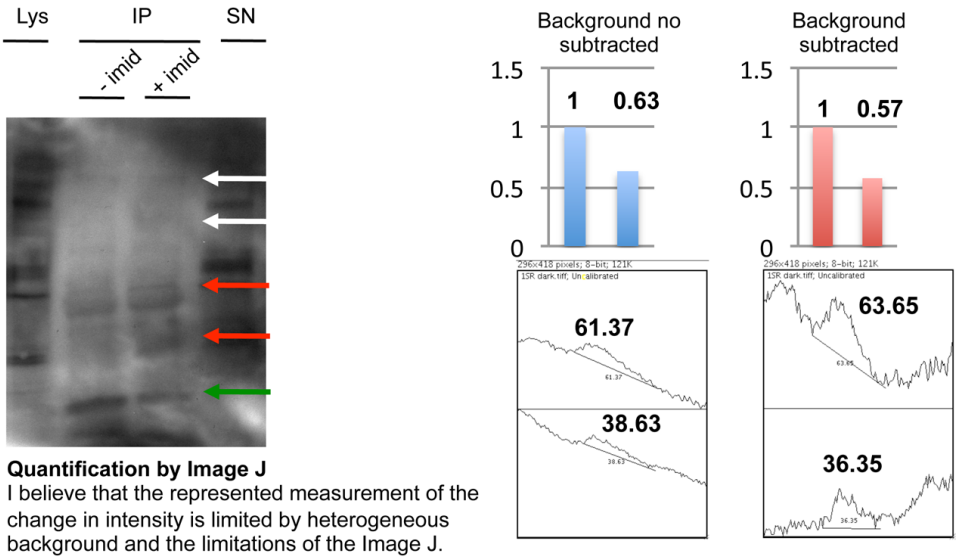

Quantification by Image J
I believe that the represented measurement of the change in intensity is limited by heterogeneous background and the limitations of the Image J.

B. Scanned area of interest. Scanned with a halogen lamp

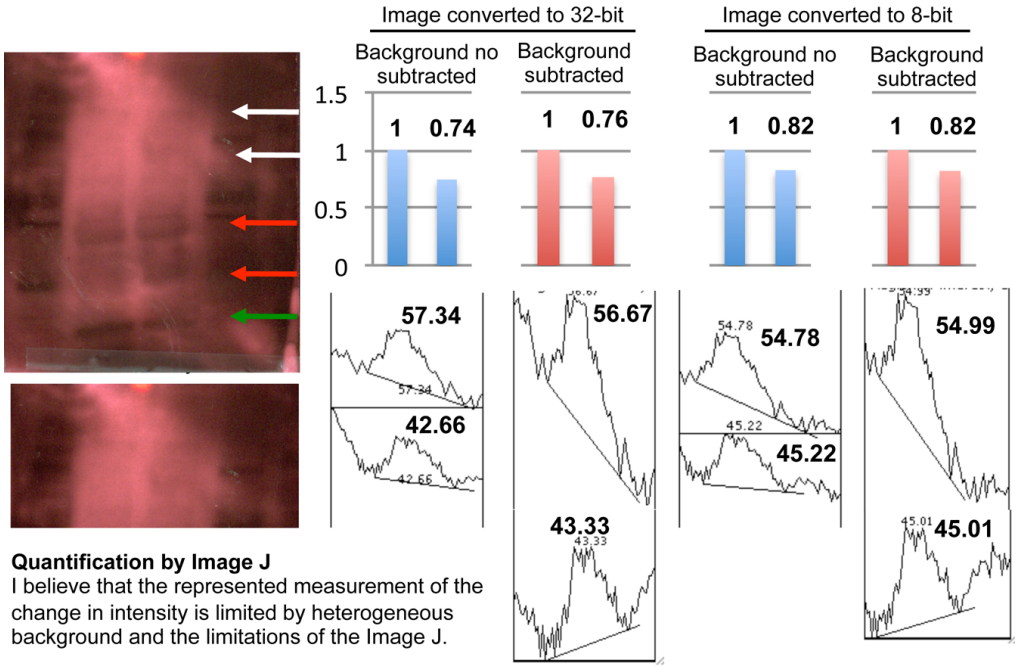

Quantification by Image J
I believe that the represented measurement of the change in intensity is limited by heterogeneous background and the limitations of the Image J.

Concerns:

- Sandwich reaction does not increase the intensity of the bands in the Lys and SN lanes
- Possibility of non-specific binding (2ary antibody)
- Appearance of bands showing and increase (red arrows) or a decrease (green arrows)
- Inconsistent behavior of bands in films obtained through the process
- High and heterogeneous background

Appendix 1 Figure 8.1. IP-WB experiment to validate matrin 3 as a potential c-Src substrate. R390A/ SYF cells. Anti-phosphotyrosine Western blots after the first sandwich reaction. Second exposure.

Matrin 3 phosphorylation of the final experimental repeat in the rescuable cell line R390A/SYF.

Immunoprecipitation- Western blot experiment to validate matrin 3 as a potential c-Src substrate. The untreated and the treated cells were lysed and immunoprecipitation was performed using matrin 3 antibody. Western blot against phosphotyrosine after washing and performing a sandwich reaction. Second exposure. **A.** Image obtained by translucent scanning. Quantitation of the bands corresponding to matrin 3 phosphorylation from the original image was attempted using different setting in Image J and results are shown. **B.** The panel bellow shows a scan taken with the help of a lamp and the gray version of it after different adjustments in the levels. Quantitation of the bands corresponding to matrin 3 phosphorylation from the original image was attempted using different setting in Image J and results are shown. The arrows show bands of interest. White arrows indicate bands corresponding to matrin 3 phosphorylation. Red arrows indicate bands that show an increase in their intensity. Green arrows indicate bands that show a decrease in their intensity. Grey arrows indicate bands that do not change their intensity.

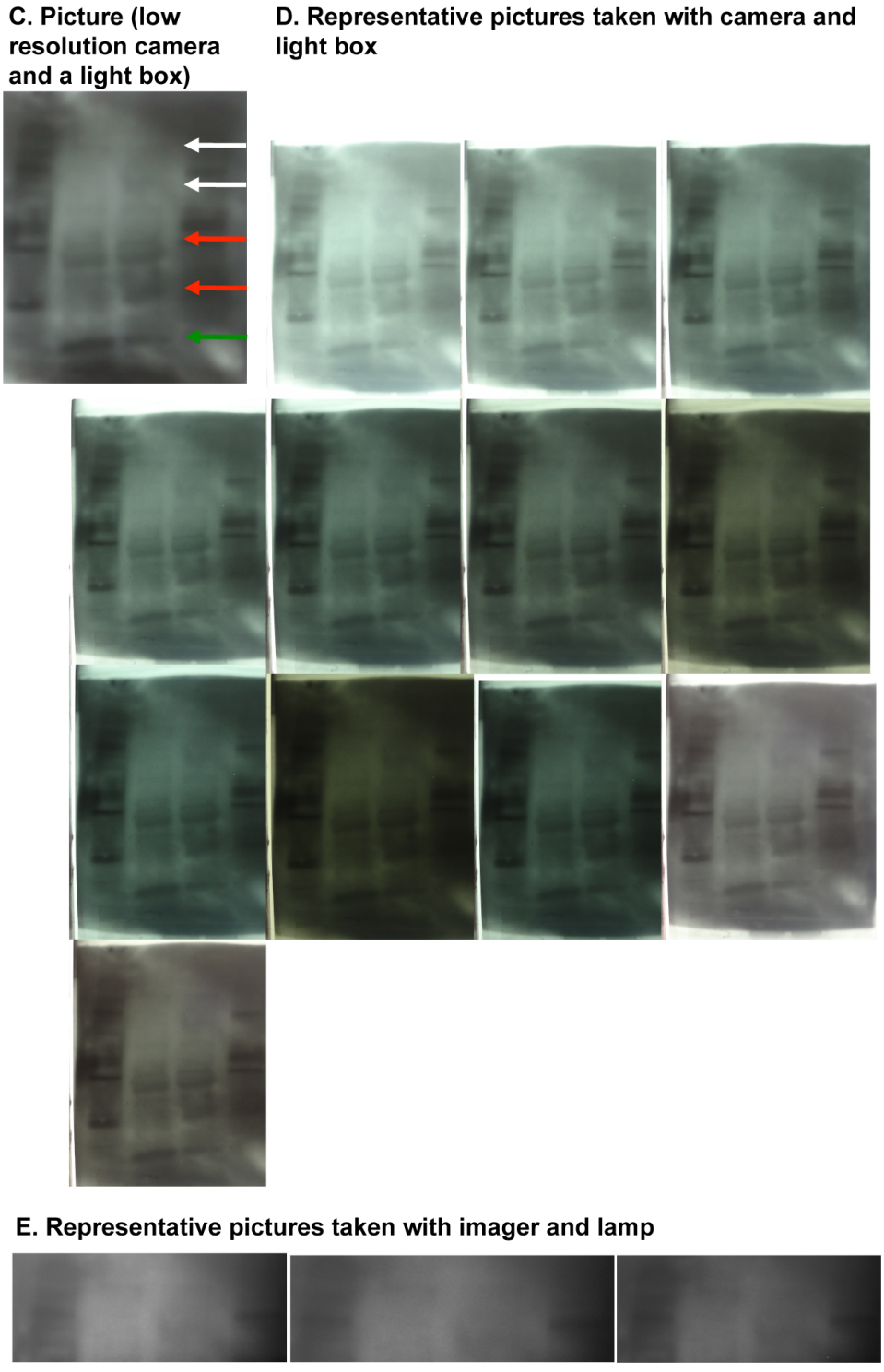

Appendix 1 Figure 8.2. IP-WB experiment to validate matrin 3 as a potential c-Src substrate. R390A/ SYF cells. Anti-phosphotyrosine Western blots after the first sandwich reaction. Second exposure (cont).

Matrin 3 phosphorylation of the final experimental repeat in the rescuable cell line R390A/SYF.

Immunoprecipitation- Western blot experiment to validate matrin 3 as a potential c-Src substrate. The untreated and the treated cells were lysed and immunoprecipitation was performed using matrin 3 antibody. Western blot against phosphotyrosine after washing and performing a sandwich reaction. **C.** Representative picture taken with a low-resolution camera and the help of a light box **D.** Representative pictures taken with a camera and the help of a light box. Different pictures correspond to different adjustment in the brightness in the camera**. E.** Representative pictures bellow were taken with an imager and a lamp. Different pictures correspond to different adjustment in the light aperture**.** The arrows show bands of interest. White arrows indicate bands corresponding to matrin 3 phosphorylation. Red arrows indicate bands that show an increase in their intensity. Green arrows indicate bands that show a decrease in their intensity. Grey arrows indicate bands that do not change their intensity.

blot was too dark to be visualized by scanning without the help of a lamp. The scanned images obtained with the help of a lamp are shown for both the entire blot and the region of interest. We attempted quantifying the differences in intensity between both bands. The results are shown (Scan with halogen lamp: Image converted to 32-bit: Background not subtracted: 1/0.74; Background subtracted-100 rolling ball radius: 1/0.76. Image converted to 8-bit: Background not subtracted: 1/0.82; Background subtracted-100 rolling ball radius: 1/0.82) but we believe the heterogeneous background and the fact that Image J requires a large selection surface (apparently to be able to take into consideration/ allow removin the effect of the background for the calculations) may limit it. In fact, we could not avoid including some areas that show heterogeneous background in our film that may affect the reading. We also attempted quantitation from the image obtained through translucent scanning. The value also does not show an increase (Translucent scan. Background not subtracted: 1/0.63; Background not subtracted-100 rolling ball radius: 1/0.57), but the same limitations for quantitation are present. I believe the result of this quantitations do not represent what can be observed by eye and therefore I don't think these quantitations are informative for this film.

A low-resolution photograph was taken of the blot on top of a light box with the purpose of being shown in Appendix 1 Figure 8.2. Representative pictures made with the Cybershot Sony camera and a light box are shown in Appendix 1 Figure 8.2. Representative pictures made with the imager are also included. We attempted to quantify the changes of intensity of these images that showed a tendency to decrease, but I believe the high background and its heterogeneous nature interfere with the quantification process.

Blots corresponding to Appendix 1 Figure 8 and Appendix 1 Figure 9 may have been inadvertently switched in my lab notebook, but the pattern of the background suggests that the order of the two blots is as the presented here.

3.3.5. Anti-phosphotyrosine Western blot after the first sandwich reaction. After washing and developing again.

The blot was then subjected to washing as indicated in the methods section, with the aim of cleaning up the background.

Limitations:

The resulting blot obtained after developing is shown in **Appendix 1 Figure 9.** As described for Appendix 1 Figure 7-8, several bands appear in the lanes corresponding to the immunoprecipitation, which were not present before the sandwich reaction (Appendix 1 Figure 5).

This blot is theoretically cleaner than the ones shown in Appendix 1 Figures 7-8. If washing reduces the background, the bands observed should theoretically be less affected by the heterogeneity of the background. It is therefore a concern that for this particular blot (obtained after washing to remove background and developing again), we did not observe an increase in the intensity of the band corresponding to matrin 3 upon c-Src chemical rescue. We observe that the signal does not change in intensity or that it even decreases very slightly (This is shown more clearly in some of the high-resolution

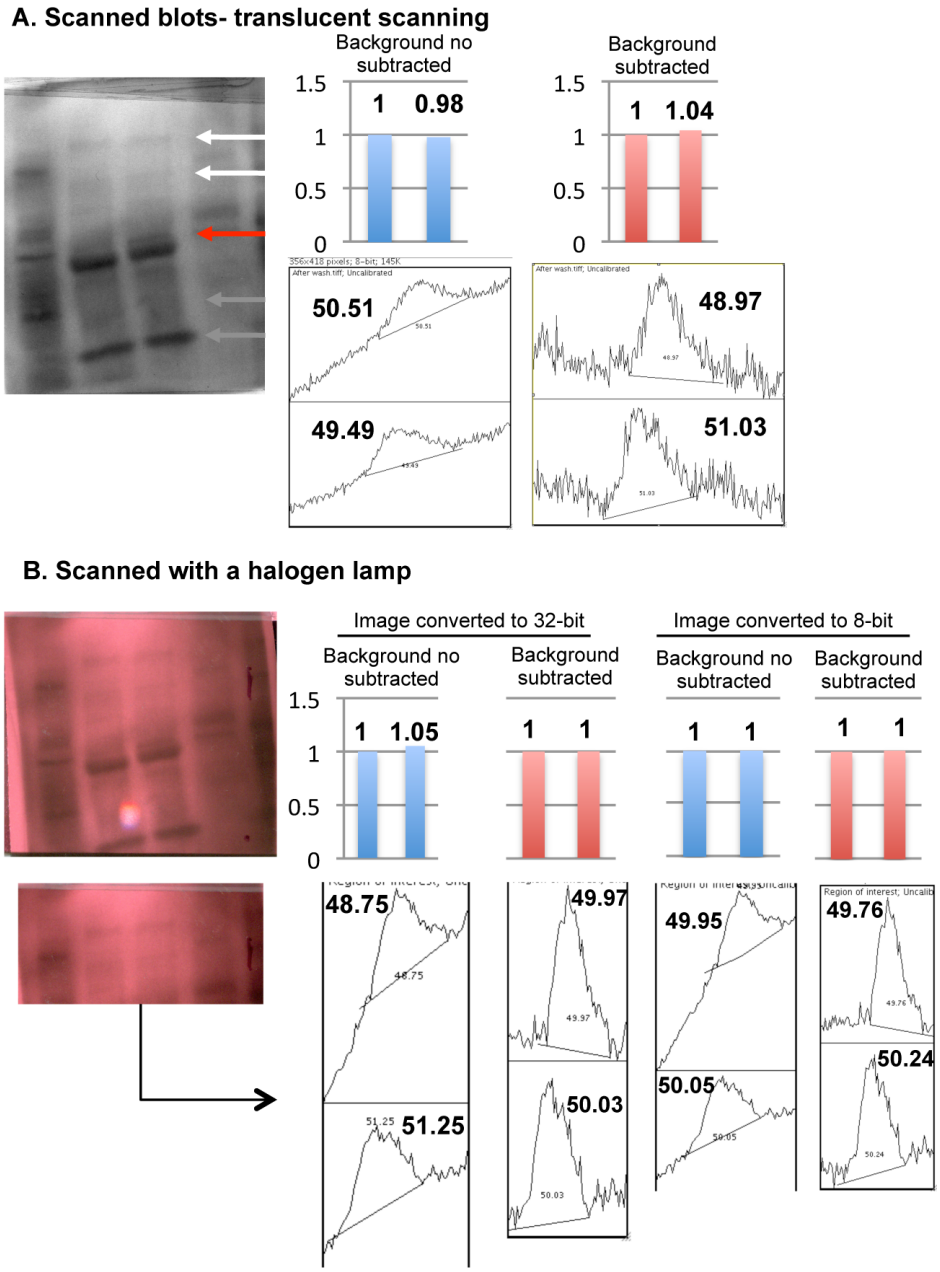

Concerns:

- Sandwich reaction does not increase the intensity of the bands in the Lys and SN lanes
- Possibility of non-specific binding (2ary antibody)
- Inconsistent behavior of bands in films obtained through the process
- High and heterogeneous background
- Top of the film is much clearer than the bottom part revealing uneven and/ or excessive washing

Appendix 1 Figure 9.1. IP-WB experiment to validate matrin 3 as a potential c-Src substrate. R390A/ SYF cells. Anti-phosphotyrosine Western blots after washing and redeveloping.

Matrin 3 phosphorylation of the final experimental repeat in the rescuable cell line R390A/SYF.

Immunoprecipitation- Western blot experiment to validate matrin 3 as a potential c-Src substrate. The

untreated and the treated cells were lysed and immunoprecipitation was performed using matrin 3 antibody. Western blot against phosphotyrosine after washing and performing a sandwich reaction, washing again and redeveloping. **A.** Image obtained by translucent scanning. Quantitation of the bands corresponding to matrin 3 phosphorylation from the original image was attempted using different setting in Image J and results are shown. **B.** The panel bellow shows a scan taken with the help of a lamp and the gray version of it after different adjustments in the levels. Quantitation of the bands corresponding to matrin 3 phosphorylation from the original image was attempted using different setting in Image J and results are shown. The arrows show bands of interest. White arrows indicate bands corresponding to matrin 3 phosphorylation. Red arrows indicate bands that show an increase in their intensity. Grey arrows indicate bands that do not change their intensity.

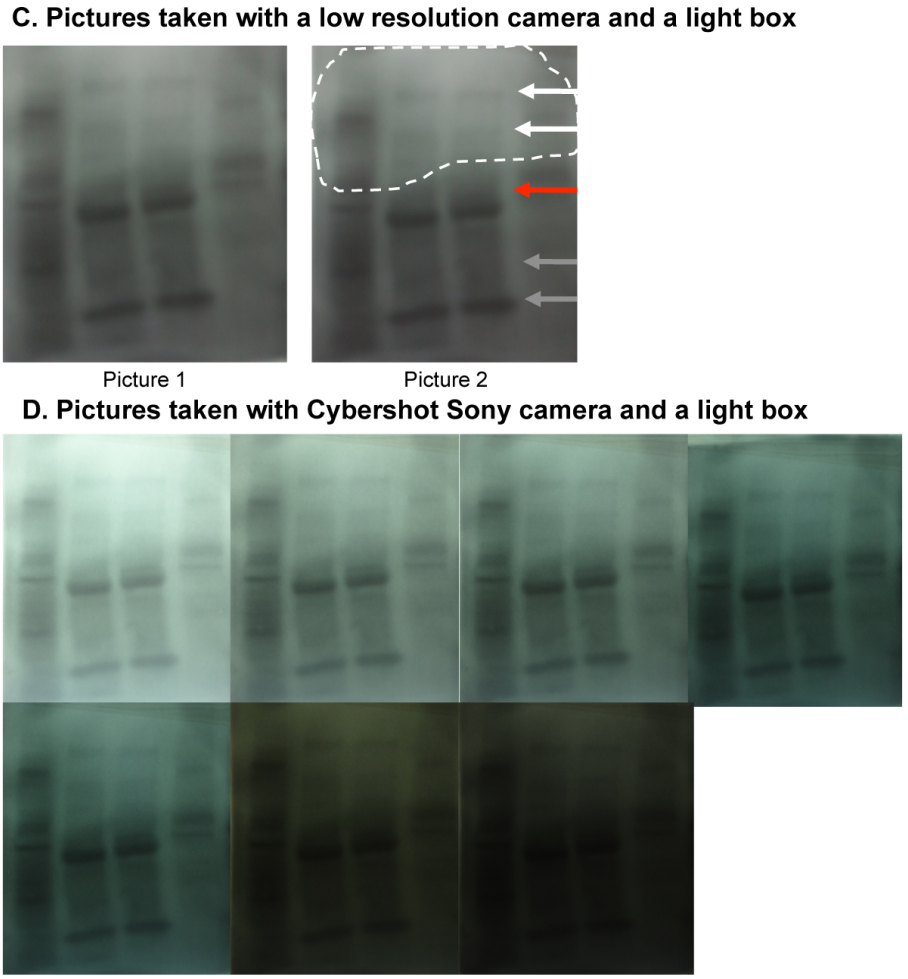

Appendix 1 Figure 9.2. IP-WB experiment to validate matrin 3 as a potential c-Src substrate. R390A/ SYF cells. Anti-phosphotyrosine Western blots after washing and redeveloping (cont).

Matrin 3 phosphorylation of the final experimental repeat in the rescuable cell line R390A/SYF. Immunoprecipitation- Western blot experiment to validate matrin 3 as a potential c-Src substrate. The untreated and the treated cells were lysed and immunoprecipitation was performed using matrin 3 antibody.

Western blot against phosphotyrosine after washing and performing a sandwich reaction, washing again and redeveloping. **C.** Representative picture taken with a low-resolution camera and the help of a light box **D.** Representative pictures taken with a camera and the help of a light box. Different pictures correspond to different adjustment in the brightness in the camera**. E.** Representative pictures bellow were taken with an imager and a lamp. Different pictures correspond to different adjustment in the light aperture**.** Quantitation of the bands corresponding to matrin 3 phosphorylation from the original image was attempted using and results are shown. The graphs with red columns indicate that the background has been subtracted (rolling ball radius: 50 pixels). The arrows show bands of interest. White arrows indicate bands corresponding to matrin 3 phosphorylation. Red arrows indicate bands that show an increase in their intensity. Green arrows indicate bands that show a decrease in their intensity. Grey arrows indicate bands that do not change their intensity.

pictures taken with the Cybershot Sony camera).

The blot background seems more homogeneous but the top part is much lighter/ clearer than the lower part, when comparing Appendix 1 Figure 9 with Appendix 1 Figure 7-8. I cannot explain why this is the case but it is a concern that this phenomenon may distort the real intensity of the bands making it difficult to interpret the results. In fact, some of the bands in the top part of the blot that show strong intensity in Appendix 1 Figures 7-8, are also strong in Appendix 1 Figure 9, whereas other show a much lower intensity suggesting that the background is not entirely homogeneous or that the reason that causes that the top of the film is much clearer may also have an effect in the intensity of the bands.

It is also important to consider that from comments obtained from colleagues, it is sometimes expected to observe different results when the blot has been washed and redeveloped, as compared to the initial development, and in this case it has been washed and developed twice (the first wash being after the initial incubation with HRP-conjugated anti-phosphotyrosine antibody and before sandwich reaction was attempted, the second this last wash). The washing also may have had an effect in partly removing the secondary antibody added in the first sandwich reaction.

It is also worth mentioning that one of the lower bands in the blot that showed an increase in Appendix 1 Figure 7-8, stills shows it in Appendix 1 Figure 9, but another of the lower bands that showed an increase in Appendix 1 Figure 7-8 does not show such a change now. Also, the bottom band, which showed a decrease in intensity in Appendix 1 Figure 7-8, does not show such a change in Appendix 1 Figure 9. This may indicate that either the increase in the bands observed in the previous blot was real and for some

reason does not show now or that it was a result of a heterogeneous background and now that this has been reduced the increase does not appear. If in the earlier exposure some bands seemed to show a change in intensity as a result of a heterogeneous background, this would explain why in this cleaner exposure no longer shows that change and this situation would be particularly worrisome. However, as mentioned, the appearance/ background of the blot obtained after washing is not optimal (very light on the top part as compared with the bottom of the blot) and conclusions are difficult to make. There is a possibility that there was excessive or uneven washing. Also, the change in pattern of the bands observed in the top part of the lysate lane shown in Appendix 1 Figure 7-8 compared with the one shown in Appendix 1 Figure 9 increases the suspicion that even the background of the top part of the film in Appendix 1 Figure 9 is not homogeneous.

It is true that in some occasions the lack of a visible increase may be due to a saturation of the signal, but the signal of the bands corresponding to phosphorylated matrin 3 in Appendix 1 Figure 9 does not seem saturated or at least, it is hard to tell given the fact that the top of the blot, for some reason, appears much clearer than the bottom.

It is therefore very hard to discern which of these increases are real due to the difficulty of using this assay for matrin-3 and the modest quality of the evidence.

Image acquisition:

The blot was too dark to be scanned without a lamp. For that reason, the entire film was also scanned by translucent scanning. The entire film and the area of interest were scanned with the help of a halogen desk lamp. Results are shown in **Appendix 1 Figure 9**. The lamp was used to get a clearer image of the bands from a blot with high

background. The lamp was carefully placed on top of the area of interest and we aimed to obtain a homogeneous illumination of the area of interest that was scanned. This did not seem to be a problem since the selected area was very small. The scanned images seem to have better quality than the ones taken with the cameras and the help of a light box (Appendix 1 Figure 9.1). In addition, pictures were taken with a low-resolution camera and a light box. Representative pictures made with the Cybershot Sony camera and a light box are shown. We also took pictures using imager and white light diffuser on top of the UV light. (Appendix 1 Figure 9.2).

Observations:

The bands are now defined and the background is clearer. This will facilitate the measurement of the changes in intensity since these are conditions that are necessary for correct measurement by ImageJ. However, the film is not completely homogeneous and the top part of the film is much clearer than the bottom. This is worrisome and we cannot explain why.

By eye, I believe I don't see a change in intensity in the bands. There may be a slight decrease in the intensity but I think the right band is slightly broader and this may account for the possible decrease.

Quantitation was also performed from the image obtained by translucent scanning and the result is similar (Translucent scan. Background not subtracted: 1/ 0.98; Background subtracted-50 rolling ball radius: 1/1.04). The film was scanned with a lamp. We attempted to measure the change in intensity in the blot that scanned the area of

interest with the help of a lamp, and we observed a minor change (Scan with halogen lamp: Image converted to 32-bit: Background not subtracted: 1/1.05; Background subtracted-50 rolling ball radius: 1/1. Image converted to 8-bit: Background not subtracted: 1/1; Background subtracted-50 rolling ball radius: 1/1). We believe the quality of the image obtained through scanning is the best within the ones shown. We believe the results from the quantitation are representative of the observation made by eye and this is probably due to the fact that this film seems to have the appropriate/ necessary characteristics for quantitation.

The pictures of the blots show a similar trend. We did not attempt to quantify them because we have better resolution images.

Representative pictures made with the imager are also included and quantitation was performed (Background subtracted-50 rolling ball radius: 1/0.92; 1/1.13; 1/15).

The overall results indicate that there is not a significant change in intensity between both bands.

3.3.6. Anti-phosphotyrosine Western blot after the second sandwich reaction. First exposure.

The blot was then subjected to a second sandwich reaction, with overnight incubation time (most likely an overnight reaction, although the exact incubation time was not recorded) as described in the methods.

Limitations:

Adding further steps to the process possibly led to an increased probability of observing non-specific bands.

Many of the lower bands are no longer visible since the signal was being lost in some areas in the left-top and in the mid-bottom part of the blot, that were very clear and interfered with the lower bands observed in previous blots. This shows that this final attempt is problematic, since the strong signal and the strong background may interfere with the visualization of the bands and the interpretation of the result, as happens here with the lower bands of the blot. The resulting blot is shown in **Appendix 1 Figure 10**.

We again observed that the sandwich reaction has probably led to an increase in the signal of the bands in the immunoprecipitation lanes, but not in the lanes corresponding to the lysate and the supernatant.

The signal is faint and the blot is dirty, although the background immediately around the bands seems more homogeneous than the blots shown in Appendix 1 Figure 7-8.

Image acquisition:

The blot was first scanned and the levels were modified as indicated. The blot was also scanned with translucent scanning (Appendix 1 Figure 10.1).

Representative pictures made with the Cybershot Sony camera and a light box are shown in Appendix 1 Figure 10.2. Pictures were taken with the imager and a lamp and representative pictures with different apertures are shown. In both cases, the signal was too low to allow quantification by Image J.

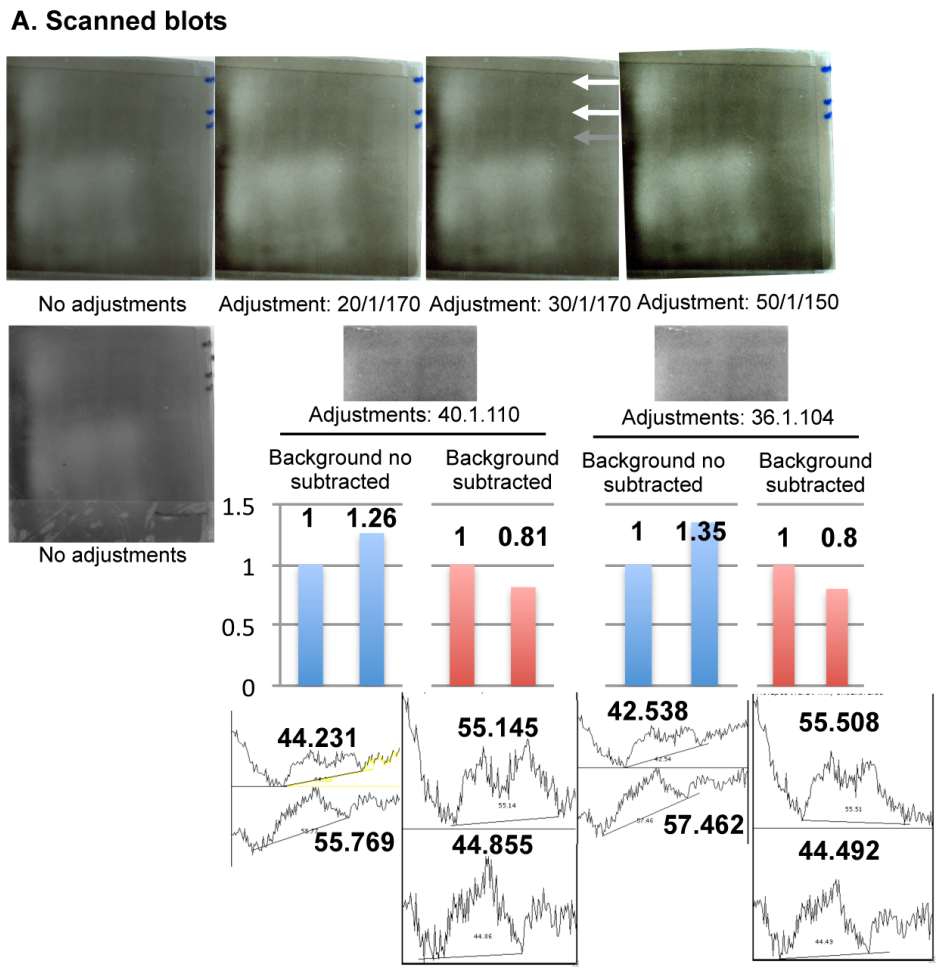

B. Scanned blot with translucent scanning

Concerns:

- The sandwich reaction does not increase the intensity of the bands in the lysate and supernatant lanes
- Increased possibility of non-specific binding (2nd sandwich reaction)
- High background
- Signal loss/ clear areas in blot may interfere with bands

Appendix 1 Figure 10.1. IP-WB experiment to validate matrin 3 as a potential c-Src substrate. R390A/ SYF cells. Anti-phosphotyrosine Western blots after second sandwich reaction. First exposure.

Matrin 3 phosphorylation of the final experimental repeat in the rescuable cell line R390A/SYF.

Immunoprecipitation- Western blot experiment to validate matrin 3 as a potential c-Src substrate. The untreated and the treated cells were lysed and immunoprecipitation was performed using matrin 3 antibody. Western blot against phosphotyrosine after washing and performing a sandwich reaction, washing again and redeveloping, and performing a second sandwich reaction. First exposure. **A.** Image obtained by scanning the film. The following films show the image resulting from adjusting the levels as indicated. Quantitation of the bands corresponding to matrin 3 phosphorylation from the original image was attempted using different setting in Image J and results are shown. **B.** Image obtained by translucent scanning

C. Representative pictures taken with a Cybershot camera and a light box

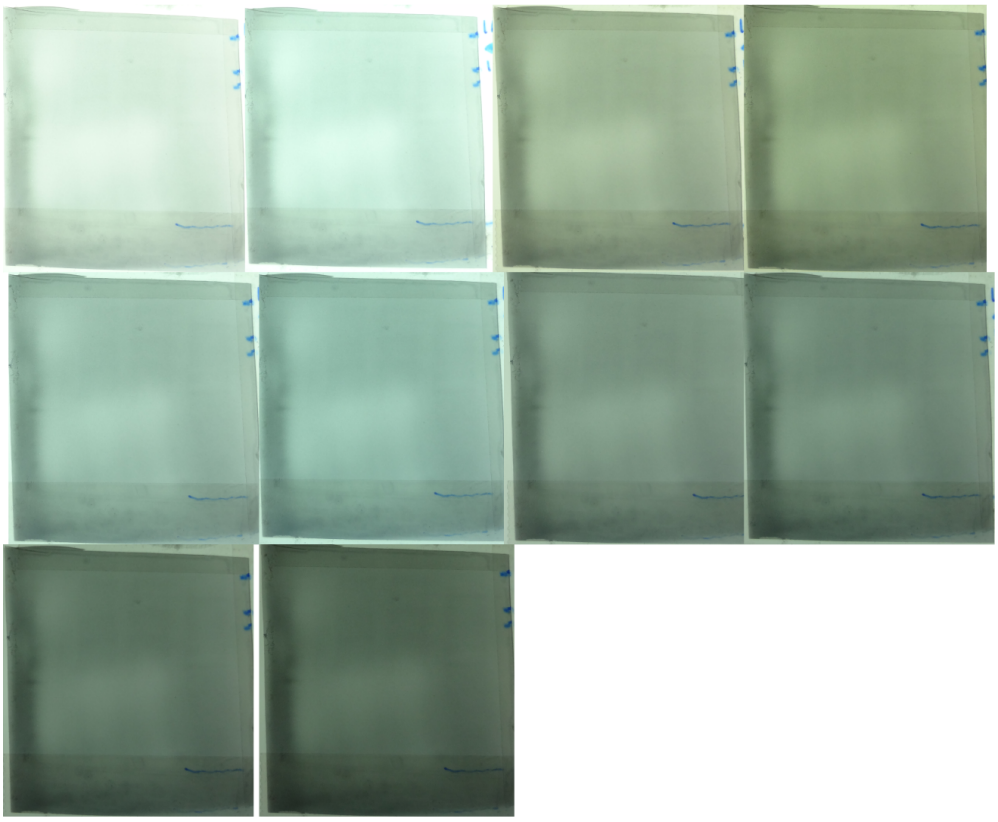

D. Representative pictures taken with imager and lamp

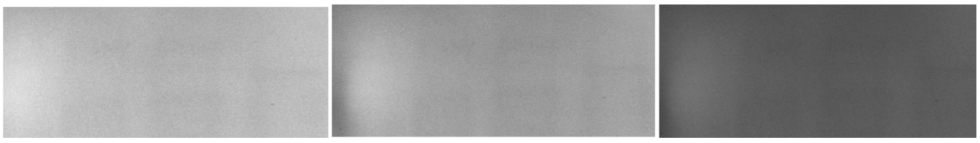

Appendix 1 Figure 10.2. IP-WB experiment to validate matrin 3 as a potential c-Src substrate. R390A/ SYF cells. Anti-phosphotyrosine Western blots after second sandwich reaction. First exposure (cont).

Matrin 3 phosphorylation of the final experimental repeat in the rescuable cell line R390A/SYF. Immunoprecipitation- Western blot experiment to validate matrin 3 as a potential c-Src substrate. The untreated and the treated cells were lysed and immunoprecipitation was performed using matrin 3 antibody. Western blot against phosphotyrosine after washing and performing a sandwich reaction, washing again and redeveloping, and performing a second sandwich reaction. First exposure. **C.** Representative pictures taken with a Cybershot camera and the help of a light box. Different pictures correspond to different

adjustment in the brightness in the camera. **E.** Representative pictures bellow were taken with an imager and a lamp. Different pictures correspond to different adjustment in the light aperture.

Observations:

As described, the blot is starting to become clearer in some areas of the blot and signal is being lost. One concern is that this may have an effect in the intensity of the band corresponding to phosphorylated matrin 3 from the untreated cells (left band). However, the area in the blot that is starting to clear is probably not large enough to have a major interference with the band although it may have a small effect. The only other band that is still visible (and is located below the two bands corresponding to matrin 3) does not seem to experience a change in intensity.

By eye, I believe there may be a potential borderline increase in the bands corresponding to matrin 3, (specially if the apparent larger area of the right band is taken into account) although this is ambiguous and may be limited by the eye perception.

The lightness of the signal made it impossible to make any quantitations by ImageJ with the intact images since the peak corresponding to the band was almost impossible to distinguish from the area plots. When the levels were adjusted to 40.1.110, we could visualize a peak but the quality of the area plots is not optimal (even more so after the background in subtracted) as can be seen in Appendix 1 Figure 10.1. The results are shown (Scan with halogen lamp: Background not subtracted: 1/1.26; Background subtracted-100 rolling ball radius: 1/0.81). We also performed quantitation after adjusting the levels to 36.1.104 and results are shown (Scan with halogen lamp: Background not subtracted: 1/1.35; Background subtracted-100 rolling ball radius: 1/0.8). We believe the heterogeneous background but mostly the lightness of the band may have limited the

quantitations. In fact, we could not avoid including some areas that show heterogeneous background in our film that may affect the reading. I believe the light intensity of the band makes it hard to quantitate this film. A slight increase may be slightly more representative to the observation by eye, but given the nature of the film (presence of background and low signal) this is hard to conclude.

There is a lower band in the gel, which seems to show no increase in intensity (very hard to determine), as was also shown in Appendix 1 Figure 9.

3.3.7. Anti-phosphotyrosine Western blot after the second sandwich reaction. Second exposure.

A different exposure was then obtained and shown in **Appendix 1 Figure 11**.

Limitations:

The background is very strong and the area where the background is getting clearer is larger than in **Appendix 1 Figure 10**. In fact, looking at the size of this clear area (which seems to increase with time), I believe this blot was maybe obtained after the one shown in **Appendix 1 Figure 12**.

One concern is that the background is very strong and, unlike the previous blot (Appendix 1 Figure 10), it looks a bit more heterogeneous (or the signal is getting stronger in the edges), for example, on top of the bands (top edge of the blot) where it is

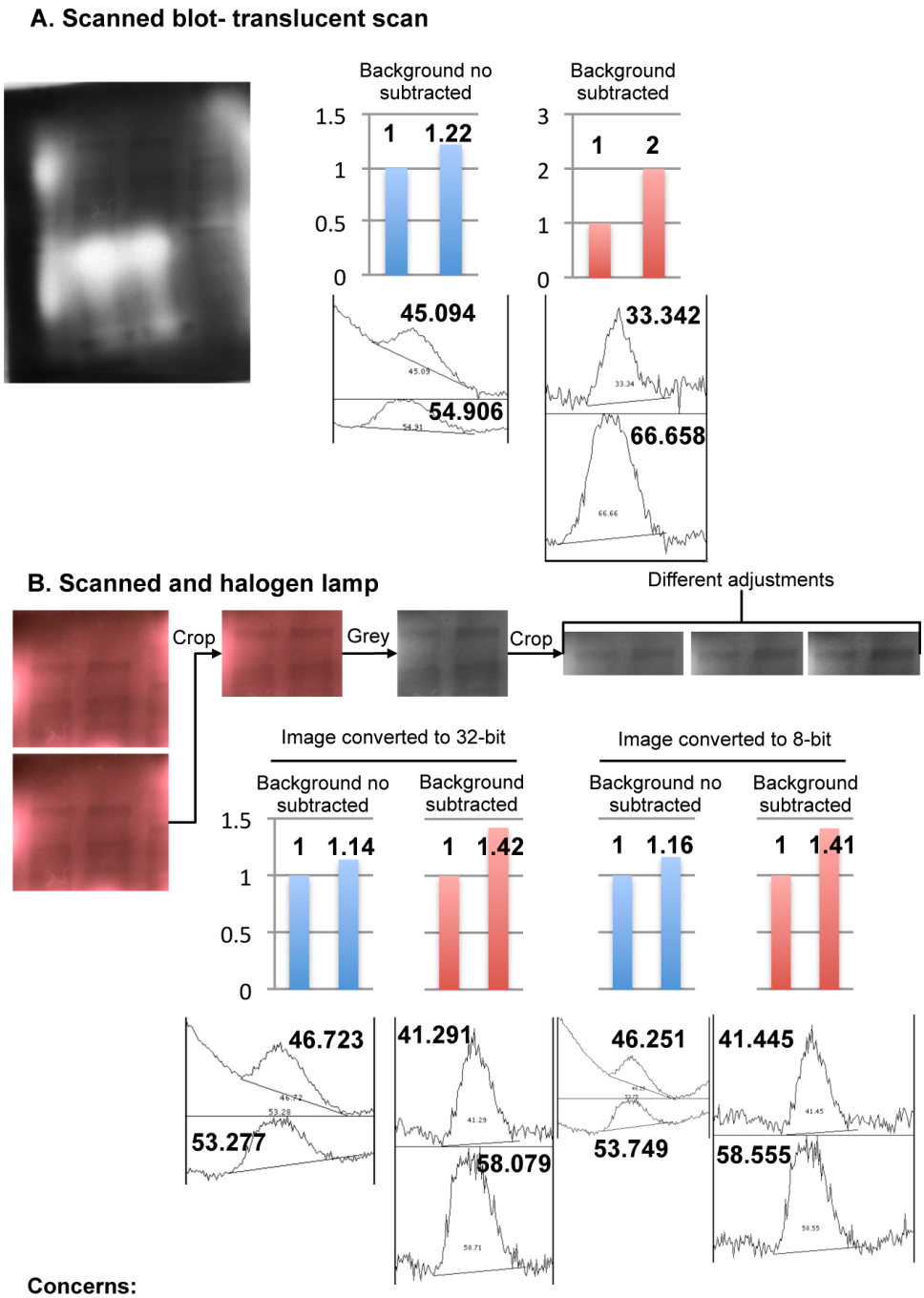

Concerns:

- The sandwich reaction does not increase the intensity of the bands in the lysate and supernatant lanes
- Increased possibility of non-specific binding (2nd sandwich reaction)
- High background
- Signal loss/ clear areas in blot may interfere with bands

Appendix 1 Figure 11.1. IP-WB experiment to validate matrin 3 as a potential c-Src substrate. R390A/ SYF cells. Anti-phosphotyrosine Western blots after second sandwich reaction. Second exposure.

Matrin 3 phosphorylation of the final experimental repeat in the rescuable cell line R390A/SYF. Immunoprecipitation- Western blot experiment to validate matrin 3 as a potential c-Src substrate. The untreated and the treated cells were lysed and immunoprecipitation was performed using matrin 3 antibody. Western blot against phosphotyrosine after washing and performing a sandwich reaction, washing again and redeveloping, and performing a second sandwich reaction.Second exposure. **A.** Image obtained by translucent scanning. Quantitation of the bands corresponding to matrin 3 phosphorylation from the original image was attempted using different setting in Image J and results are shown. **B.** The panel bellow shows a scan taken with the help of a lamp and the gray version of it after different adjustments in the levels. . The image was converted into greyscale and the levels adjusted to make the picture shown in Figure 28. Quantification of the bands corresponding to matrin 3 phosphorylation was performed from the image obtained by scanning with the help of a lamp and results are shown. Quantitation of the bands corresponding to matrin 3 phosphorylation from the original image was attempted using different setting in Image J and results are shown.

C. Picture taken with low resolution camera and light box

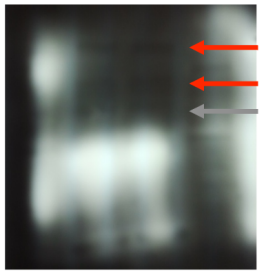

D. Representative pictures taken with a Cybershot camera and a light box

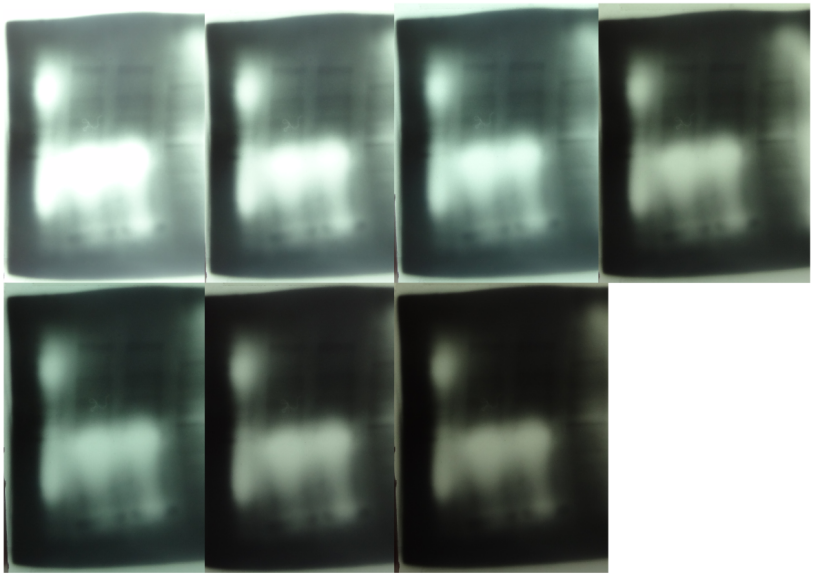

E. Representative pictures taken with imager and lamp

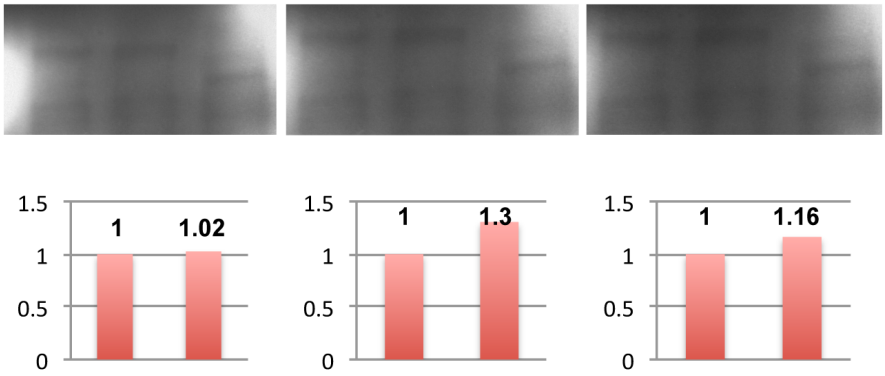

Appendix 1 Figure 11.2. IP-WB experiment to validate matrin 3 as a potential c-Src substrate. R390A/ SYF cells. Anti-phosphotyrosine Western blots after second sandwich reaction. Second exposure (cont).

Matrin 3 phosphorylation of the final experimental repeat in the rescuable cell line R390A/SYF. Immunoprecipitation- Western blot experiment to validate matrin 3 as a potential c-Src substrate. The untreated and the treated cells were lysed and immunoprecipitation was performed using matrin 3 antibody. Western blot against phosphotyrosine after washing and performing a sandwich reaction, washing again and redeveloping, and performing a second sandwich reaction. Second exposure. **C.** Representative picture taken with a low-resolution camera and the help of a light box **D.** Representative pictures taken with a camera and the help of a light box. Different pictures correspond to different adjustment in the brightness in the camera**. E.** Representative pictures bellow were taken with an imager and a lamp. Different pictures correspond to different adjustment in the light aperture**.** Quantitation of the bands corresponding to matrin 3 phosphorylation from the original image was attempted using and results are shown. The arrows show bands of interest. White arrows indicate bands corresponding to matrin 3 phosphorylation. Red arrows indicate bands that show an increase in their intensity. Green arrows indicate bands that show a decrease in their intensity. Grey arrows indicate bands that do not change their intensity.

darker than in the rest of the blot. However, except for the area that is getting clear at the left side of the left band, the background seems quite homogeneous in the area immediately around the matrin 3 bands.

Some of my main concerns about this blot are that the blot is being subjected to several additional steps (two sandwich reactions), which may lead to the appearance of artifacts but may also be of advantage in seeing weak bands.

Another concern, as described in Appendix 1 Figure 10, is that the blot looks clearer in certain areas, and this clearing may interfere with the intensity of the bands corresponding to phosphorylated matrin 3. Specifically, the band corresponding to the IP from untreated cells is near an area of the blot that is clearer. The lower intensity of the background and/or the band may be a result of, or may be partially affected by, the effects of this clearer area of the blot, which may make the intensity band itself appear weaker. It seems like the background around the left band is lighter and this may make the left band weaker in intensity too. It could also make it appear darker. This is hard or impossible to determine. The bigger the clearing the most likely it is that it affects the background. The background is more affected in the left part of the left band. However, even taking this last factor into account, it is possible that the increase is still apparent if we look at the right part of both bands. The right part of the left band is less likely to be affected by the clearing of the blot (loss of signal) and the clearing is therefore less likely to affect the intensity of the left band and the background around it.

I believe Image J would take into consideration the background for its calculations and in fact it is possible to subtract it as I have done for this Appendix. However, even if this is the case, this may only account for the graphic aspect of the

image, once it is obtain, but may not cover the fact that the clearing may affect the signal and/ or the background in a way we can not approach (maybe even related with the linearity of the signal in the film), even through ImageJ considerations of the background or even the visualization by eye.

Also, it is conceivable that the halogen lamp is somehow illuminating selectively in a way that has a much higher illuminating effect in the already clear background areas (left band) than in the darker ones. Maybe the illumination from the halogen lamp affects differently different backgrounds and even Image J cannot take this into account but we also have quantitation from images scanned by translucent scanning which is an optimal way to homogeneously illuminate the blots.

Image acquisition:

The film was scanned through translucent scanning. The blot was then scanned with a halogen lamp on top of the blot. The lamp only illuminated a small part of the blot and it was therefore located so that it could illuminate the region of interest and so that the light was homogeneously illuminating the selection of interest. I tried using a light diffuser but I believe it did not make a difference because the light seemed homogeneous in the selected area without the light diffuser. The selected area was scanned and converted into greyscale. The levels were adjusted to 20/1/220 (approximate numbers). In an attempt to be consistent, the exact same adjustments were done in the Western blot against phosphotyrosine with the D388N/SYF cells that will be described later. The approximate flow of the performed image processing is indicated in the figure. It may not

be exhaustive/ complete but is definitively representative. This blot was used to make the figure shown in Figure 28 and in the paper (Martinez-Ferrando, MCP, 2012).

The first picture shown was taken with a low-resolution camera and placing the film on top of a light box. Representative pictures made with the Cybershot Sony camera and a light box are shown in Appendix 1 Figure 11.2. We also took pictures using imager and white light diffuser on top of the UV light.

Observations:

The bands are very sharp and the background around them is relatively homogeneous and low facilitating the quantification. The only aspect that interferes with visualization is the clearing of the blot at the left of the band correspondent to untreated cells.

By eye, I believe a mild increase is observed in the intensity of the band corresponding to phosphorylated matrin 3. The clear area in the left side of the blot may have an effect but I believe that, even if we look at the right side of the bands, where the clearing is less prevalent (in the left band), the increase is still visible. In addition, the surface area of the right band (treated cells) seems to be equal or slightly greater than the one in the left (untreated cells).

Quantitation was performed from the image obtained by translucent scanning and the results are shown (Translucent scan. Background not subtracted: 1/ 1.22; Background subtracted-50 rolling ball radius: 1/2). The film was scanned with a lamp. We attempted to measure the change in intensity in the blot that scanned the area of interest with the help of a lamp, and we observed a minor change (Scan with halogen lamp: Image

converted to 32-bit: Background not subtracted: 1/1.14; Background subtracted-50 rolling ball radius: 1/1.42. Image converted to 8-bit: Background not subtracted: 1/16; Background subtracted-50 rolling ball radius: 1/1.41). We believe the quality of the image obtained through scanning is the best within the ones shown. We believe the results from the quantitation may representative of the observation made by eye and this is probably due to the fact that this fild seems to have better characteristics for quantitation than other films which did not lead to representative values when considering the observation made by eye.

I was recommended to subtract the background by an experience colleague and I have attempted to provide results before and after subtracting the background. The results are slightly different but the tendency is the same. The quantitation values were slightly different when the image was obtained by translucent scanning or by scanning with the help of a lamp. The type of illumination may explain part of this difference. It is hard to determine which is most appropriate. The lamp included in the imager was used with a light diffuser, but special care was put in the scanned images to illuminate the region of interest homogeneously. Also, we believe the resolution of the scanned images is superior to the rest. The process of translucent scanning is optimal both in resolution and in illumination homogeneity.

Although these are not the optimal images, quantitation was also performed from representative images obtained from the imager. After subtracting the background the values obtained are (1/1.02, 1/1.3, 1/1.16).

In any case, the tendency to increase seems consistent from the quantitation.

Since this is the film we used for the paper, we decided to further analyze the change in intensity of the bands by comparing it with the matrin 3 loading control. We compared images that were obtained exactly the same way (translucent scan) and processed the same way (either the background was not subtracted or it was with a rolling ball radius of 50 pixels). We compared the image for this exposure with the two films obtained through different exposures in the matrin 3 loading control (Appendix 1 Figure 6). Once we take into consideration the loading, the results show that the tendency to increase in signal is more apparent, based on the calculations and taking into account all the limitations described (**Appendix 1 Figure 11.3**).

MATRIN 1-dark

Background no subtracted

Sample	Condition	pTyr Area	Relative Area	matrin Area	Relative change	Normalized change
1	(-) imidazole	2353.409	1.00	15398.785	1.00	1.00
2	(+) imidazole	2865.489	1.22	15415.028	1.00	1.22

Background subtracted

Sample	Condition	pTyr Area	Relative Area	matrin Area	Relative change	Normalized change
1	(-) imidazole	5751.489	1.00	14331.238	1.00	1.00
2	(+) imidazole	11498.459	2.00	14700.238	1.03	1.95

MATRIN2-light

Background no subtracted

Sample	Condition	pTyr Area	Relative Area	matrin Area	Relative change	Normalized change
1	(-) imidazole	2353.409	1.00	16053.078	1.00	1.00
2	(+) imidazole	2865.489	1.22	15093.886	0.94	1.29

Background subtracted

Sample	Condition	pTyr Area	Relative Area	matrin Area	Relative change	Normalized change
1	(-) imidazole	5751.489	1.00	14423.359	1.00	1.00
2	(+) imidazole	11498.459	2.00	13823.116	0.96	2.09

Appendix 1 Figure 11.3. Change in phosphorylation of matrin 3 upon c-Src when using the quantitation from the image obtained from the translucent scan of the blot obtained after the second sandwich reaction (second exposure) and the translucent scans of the matrin 3 loading control.

3.3.8. Anti-phosphotyrosine Western blot after the second sandwich reaction. Third exposure.

An extra image of the blot was obtained with a different exposure time **(Appendix 1 Figure 12).**

Limitations:

The background is even stronger than in **Appendix 1 Figure 11.** It is also a bit heterogeneous in the edges. The clearing is less intense.

Image acquisition:

The blot was scanned by translucent scanning. In the figure, we show an example of how the halogen lamp was placed on top of the blot to help visualize the bands with a dark background. As noted before, this type of image seems to have better quality than the ones taken with the low-resolution camera by placing the film on top of a light box.

Pictures were taken with a low-resolution camera and placing the film on a light box. Representative pictures made with the Cybershot Sony camera and a light box are shown in Appendix 1 Figure 12.2. Representative pictures taken with the help of a lamp are also shown.

Observations:

The observations are similar from the ones made in Appendix 1 Figure 11, although the blot was dark and a quality scanned image was hard to obtain.

A. Scanned blots-translucent scan

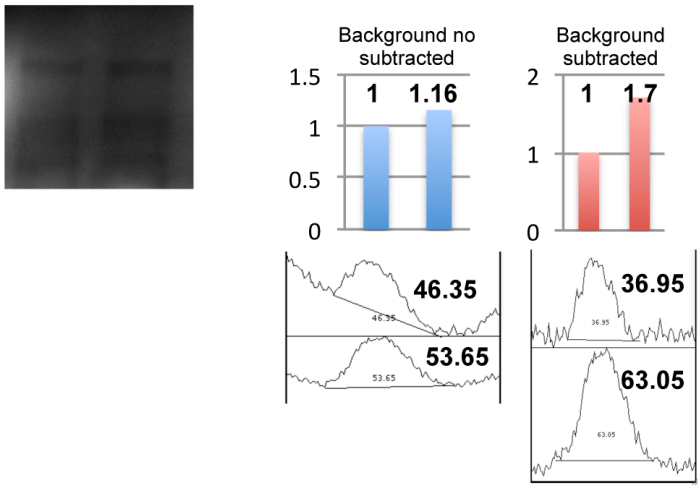

B. Scanned with a halogen lamp

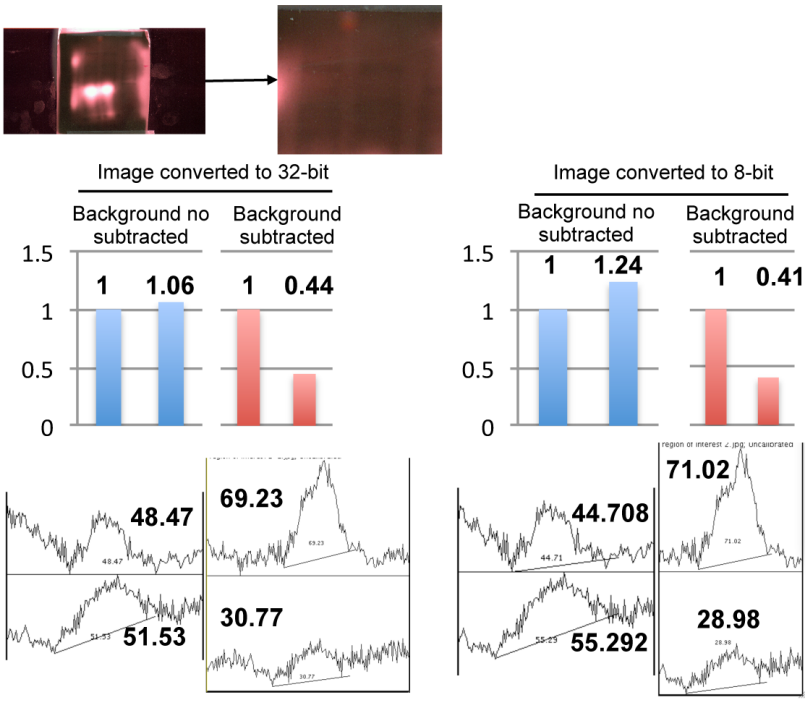

Concerns:

- The sandwich reaction does not increase the intensity of the bands in the lysate and supernatant lanes
- Increased possibility of non-specific binding (2nd sandwich reaction)
- High background
- Signal loss/ clear areas in blot may interfere with bands

Appendix 1 Figure 12.1. IP-WB experiment to validate matrin 3 as a potential c-Src substrate. R390A/ SYF cells. Anti-phosphotyrosine Western blots after second sandwich reaction. Third exposure.

Matrin 3 phosphorylation of the final experimental repeat in the rescuable cell line R390A/SYF. Immunoprecipitation- Western blot experiment to validate matrin 3 as a potential c-Src substrate. The untreated and the treated cells were lysed and immunoprecipitation was performed using matrin 3 antibody. Western blot against phosphotyrosine after washing and performing a sandwich reaction, washing again and redeveloping, and performing a second sandwich reaction. Third exposure. **A.** Image obtained by translucent scanning. Quantitation of the bands corresponding to matrin 3 phosphorylation from the original image was attempted using different setting in Image J and results are shown. **B.** The panel bellow shows a scan taken with the help of a lamp and the gray version of it after different adjustments in the levels. Quantification of the bands corresponding to matrin 3 phosphorylation was performed from the image obtained by scanning with the help of a lamp and results are shown.

C. Picture taken with a low resolution camera and a light box

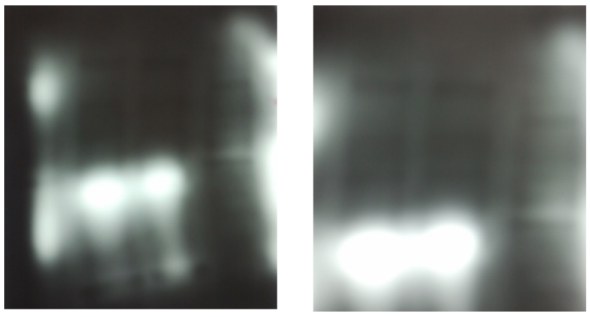

Two different pictures

D. Picture taken with a low resolution camera and a light box

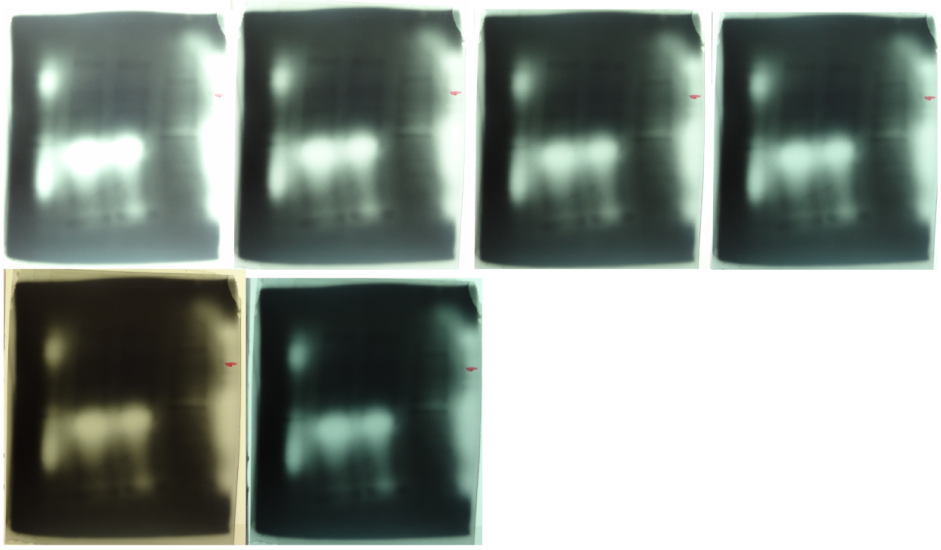

E. Representative pictures taken with imager and lamp

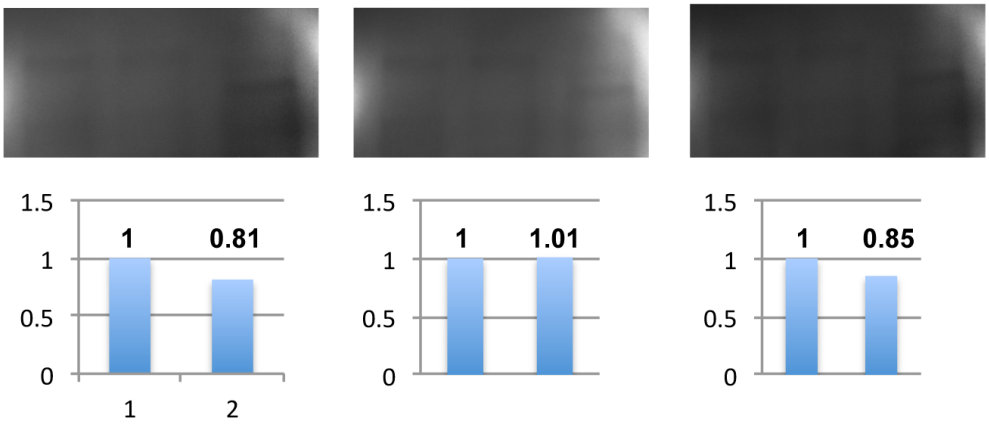

Appendix 1 Figure 12.2. IP-WB experiment to validate matrin 3 as a potential c-Src substrate. R390A/ SYF cells. Anti-phosphotyrosine Western blots after second sandwich reaction. Third exposure (cont).

Matrin 3 phosphorylation of the final experimental repeat in the rescuable cell line R390A/SYF. Immunoprecipitation- Western blot experiment to validate matrin 3 as a potential c-Src substrate. The untreated and the treated cells were lysed and immunoprecipitation was performed using matrin 3 antibody. Western blot against phosphotyrosine after washing and performing a sandwich reaction, washing again and redeveloping, and performing a second sandwich reaction. Third exposure. **C.** Representative pictures taken with a low-resolution camera and the help of a light box **D.** Representative pictures taken with a camera and the help of a light box. Different pictures correspond to different adjustment in the brightness in the camera**. E.** Representative pictures bellow were taken with an imager and a lamp. Different pictures correspond to different adjustment in the light aperture**.** Quantitation of the bands corresponding to matrin 3 phosphorylation from the original image was attempted using and results are shown (background not subtracted). The arrows show bands of interest. White arrows indicate bands corresponding to matrin 3 phosphorylation.

By eye, a very borderline increase can be observed again, with the darker band corresponding to rescue of c-Src. The effect of the clearing in the left side of the blot on the left band (untreated cells) seems to be smaller than in the previous blot but still apparent.

Quantitation was performed from the image obtained by translucent scanning and the results are shown (Translucent scan. Background not subtracted: 1/ 1.16; Background subtracted-50 rolling ball radius: 1/1.7). Both results show an increase but the ratios are different. We think that the film is darker than the one in Appendix 1 Figure 11.1 and therefore the background is interfering more with the quantitation process. The film was scanned with a lamp. We attempted to measure the change in intensity in the blot that scanned the area of interest with the help of a lamp (Scan with halogen lamp: Image converted to 32-bit: Background not subtracted: 1/1.06; Background subtracted-50 rolling ball radius: 1/0.44. Image converted to 8-bit: Background not subtracted: 1/1.24; Background subtracted-50 rolling ball radius: 1/0.41). We must warn, however, that the background was strong and not ideal for the calculations. There is a clear difference in the ratios obtained when the background was not subtracted (showing an increase) and when it was subtracted (showing a stron decrease). I believe this blot is not optimal for quantitation. When the background is subtracted the quality of the area plot dimisnihes and we chose the areas being the most conservative (in an attempt to avoid any bias). When the area plots look like the ones shown, it is easy to obtain a very diiferent result by chosing the area in a slighty different way. The area plot is just not smooth and this causes this effect. Since we were conservative, we ‘favored’ a decrease. Therefore, I don´t believe these values are representative of the observation by eye. The area plots

obtained from the quantitation of the image from the translucent scan are much smoother and, even having been conservative as can be observe in the figure, we obtained an increase.

Although these are not the optimal images, quantitation was also performed from representative images obtained from the imager. The appearance of the images obtained from the imager is quite different from the appearance if the images obtained with the scanner and the lamp and what can be observed by eye which suggest that maybe this type of illumination from the UV and the white light diffuser is not optimal. After subtracting the background the values obtained are (1/0.81, 1/1.01, 1/0.85). The results from the quantitation of the images from the imager are inconsistent maybe due to the effects of a non-optimal illumination or due to the high background of the darker images, which makes it hard to use Image J for this purpose. However, we are showing the results obtained to illustrate this hypothesis.

The type of illumination may explain part of the difference in quantifitation in the image obtained from the scanner with the help of a halogen lamp and the translucent scanning versus the one obtained from the imager. The lamp included in the imager was used with a light diffuser, but special care was put in the scanned images to illuminate the region of interest homogeneously. Also, we believe the resolution of the scanned images is superior to the rest. We also believe that both the resolution and the illumination homogeneity of the translucent scanning is optimal and it supports an increase.

We have only this biological replicate for the IP-WB to validate matrin 3's mass spectrometry evidence as a potential c-Src substrate in rescuable cells (R390A/ SYF).

3.4. Final attempt- D398N/ SYF cells. Anti-matrin 3 Western blot and anti-phosphotyrosine Western blot

The similar experiment was performed with the non-rescuable cell line D388N/ SYF. As in the case of tensin, we performed the control experiment (the one done with the non rescuable cell line) several times but we could visualize phosphorylation of the protein only once. The loading control is shown in **Appendix 1 Figure 13**.

In the matrin 3 Western blot, the intensity of the band corresponding to matrin 3 decreases slightly but it is also true that the band corresponding to the cells treated with imidazole is slightly broader. Also, when I verified the volume loaded in the gel used for the matrin 3 immunoblot (but not the anti-phosphotyrosine immunoblot), I made the observation that the sample corresponding to immunoprecipitated lysate from untreated cells had 10 μl more than the volume of the same sample added in the gel that was transferred and incubated against the phosphotyrosine antibody, so this may explain the higher intensity of the left band in the loading control immunoblot (but not in the anti-phosphotyrosine immunoblot).

Unlike the experiment with rescuable cells, the control using non-rescuable cells was performed with a different anti-phosphotyrosine antibody. For the non-rescuable control, the primary 4G10 anti-phosphotyrosine antibody was not HRP-conjugated, and was detected using an HRP-conjugated anti-mouse secondary antibody, without use of sandwich reaction. This may have been the reason why phosphorylation was visualized without the need of a sandwich reaction.

The blot was quite dark and was therefore scanned with a halogen lamp on top of the blot **(Appendix 1 Figure 13)**. The selected area was scanned, cropped, and converted into greyscale. The levels were adjusted to 20/1/220 (approximate numbers). Special attention was taken for making the same adjustments for this blot than those that were done in the Western blot against phosphotyrosine with the R390A/SYF cells that were described before. The approximate flow of image processing is indicated in the figure. This blot was used to make the figure shown in the paper.

By eye, the intensity of the signal does not seem to experience a significant increase, but there is high background which clearly darkens partly the right band in its right half. Quantification was performed from the images obtained after scanning the film with the help of a lamp. The quantitation made from the image obtained from the translucent scan showed an increase in intensity (1/1.39). Quantitation with background subtraction was not possible due to the quality of the area plots. We believe that this strong increase revealed in some quantitations from these images does not correspond to the observation made by eye. However, we are showing the results obtained to illustrate this hypothesis. Another quantitation (done trying to avoid the heterogeneous background more) showed a value of 1/1.13, which is more consistent with our observation by eye. As mentioned before we believe that the resolution of the scanner, the illumination provided by the translucent scanning and the methodology used for Image J quantitation make this quantitation one of the most reliable potentially. The variability observed is a result of the heterogeneity of the background and the low signal.

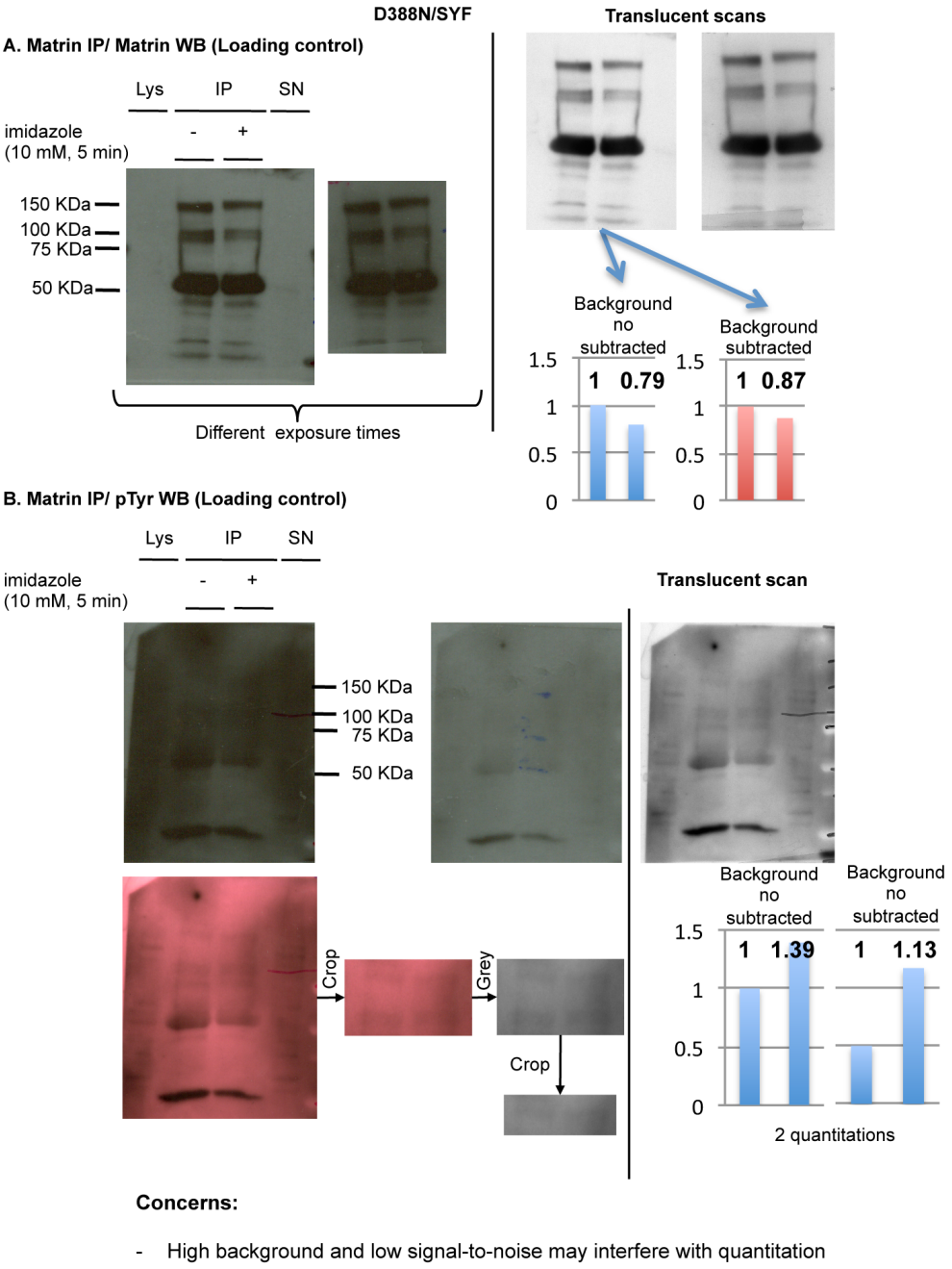

Appendix 1 Figure 13. Matrin 3 loading control of the final experimental repeat in the non-rescuable cell line D388N/SYF.

Immunoprecipitation- Western blot experiment to validate matrin 3 as a potential c-Src substrate. The untreated and the treated cells were lysed and immunoprecipitation was performed using matrin 3 antibody. A. Western blot against matrin 3 was used as a loading control. Two blots corresponding to two different exposure times are presented. Translucent scans of the films are also shown and quantitation is shown. B.

Western blot against phosphotyrosine antibody non-conjugated to HRP followed by incubation with secondary antibody showed weak signal of phosphorylated matrin 3. The top two pictures are scans of the entire blot obtained after developing during different exposure times. The bottom blot shows scan of the left blot taken with the help of a lamp. The image was converted into grey, cropped and different adjustments in the levels were made. This workflow represents the way the correspondent image in Figure 28 was acquired. A translucent scan was perfomed and the image is shown. Two different quantitations without subtraction of the background is shown.

Discussion

We have only one biological replicate for the immunoprecipitation-Western blot experiment (IP-WB) to validate matrin 3's mass spectrometry evidence as a potential c-Src downstream substrate both in rescuable cells (R390A/ SYF) and in non-rescuable cells (D388N/ SYF). In the one replicate performed in rescuable cells matrin 3 phosphorylation seems to show a marginal increase in some of the exposures from some of the blots obtained at different stages during the experimental process to which we subjected the blots for visualization of phosphorylation. This observation by eye was validated for 2 of the films obtained after the second sandwich reaction (Appendix 1 Figure 11 and 12) by quantitation, which seemed to favor the possibility of an increase when the image was obtained by translucent scanning. When the image was obtained with a scanner and the help of a halogen lamp there was one occasion when we observe a decrease instead of an increase (Appendix 1 Figure 12), but we believe this does not represent the observation made by eye and may be due to the limited quality of the blot for quantitation). We have lingering concerns about the evidence obtained in this experiment that are complex and hard to explain. We therefore wish to caution readers about the modest quality of the IP-WB evidence in the case of matrin 3. I would like to first summarize some of our observations as well as their caveats, which make us cautious about interpreting these data.

One concern is the possibility that the process of the sandwich reaction (a conventional and accepted technique used to amplify the signal in a Western blot) may lead to **non-specific binding or other artifacts.** Nevertheless, it was the only way we

were able to visualize matrin 3' phosphorylation. For the first sandwich reaction, we chose a short incubation period and exposure time in order to minimize the appearance of non-specific bands. The band correspondent to matrin 3 phosphorylation may have a borderline increase in intensity by eye in our initial blots (Appendix 1 Figure 7 and 8), especially in the lighter exposure, but the ambiguity of this observation, the heterogeneous background and the fact that the quantitation does not reveal an increase makes us question the increase itself. We must note, however, that the heterogeneous background would make any quantitation very difficult. Besides the bands at the molecular weight of matrin 3, several non-matrin 3 bands appeared in the immunoprecipitation lanes, which may correspond to proteins that were non-specifically pulled down with matrin 3 during the immunoprecipitation. The second sandwich reaction was performed for a longer period of time, making the possibility of non-specific binding (or other caveats) stronger. However, no obvious additional bands seemed to appear, although this is hard to tell due to the appearance of clear or lighter areas in some parts of the blot that prevents us from visualizing the bands in the lower part of the blot. The figure corresponding to matrin 3 validation for rescuable cells shown in Figure 28 results from imaging the blot obtained after the second sandwich reaction with the help of a halogen lamp.

Another concern is the possibility of a loading inconsistency due to a human error in loading. This was suggested as a result of the observation that some non-matrin 3 bands showed a slight increase in intensity upon imidazole treatment. If this increase was due to imprecise loading, a possible similar increase in the intensity of the band corresponding to matrin 3 phosphorylation could also be the result of imprecise loading

and the increase will be unreliable. However, the precise technique during the loading process, as well as a satisfactory even loading control should be good indicators of equal loading.

Another concern is the strong and **heterogeneous background** due to the sandwich reaction process and/or the high concentration of ECL substrate used (1 to 10 femtomolar or 1 to 2 femtomolar). A dark background from such a concentrated substrate solution is expected and is not a problem by itself, but makes the washing of the blots and the visualization of the bands very difficult. A heterogeneous background may interfere with our bands of interest and make the visualization and/or the quantitation of the difference in intensity difficult or impossible to determine. Interpretation of the results is hard to make and, in fact, a heterogenous background could be a conceivable explanation of an apparent increase in the intensity of matrin 3 and/or other non-matrin 3 bands. Nevertheless, it is possible that in the anti-phosphotyrosine immunoblot the non-matrin 3 bands that show an increase in intensity upon c-Src rescue could be proteins that also have an increase in phosphorylation after c-Src rescue, and therefore should not be considered evidence of uneven loading or contamination by high background. However, all such concerns that could question a possible increase in the intensity of the bands are challenged (but not completely overruled) by an **inconsistent behavior of bands other than matrin 3 in different blots developed at different stages of the process.** For example, one of the non-matrin 3 bands that increases in intensity upon c-Src rescue in some of the blots (Appendix 1 Figure 7 and 8), still shows an increase when the blot was washed and developed again (Appendix 1 Figure 9), while another band that also showed an initial increase does not show this increase when blot was washed and developed again

(Appendix 1 Figure 9). Another non-matrin 3 band, which initially shows a decrease in intensity (Appendix 1 Figure 7 and 8) shows no change in intensity upon c-Src rescue after washing and developing again (Appendix 1 Figure 9). We must also note that matrin 3 phosphorylation shows a borderline increase by eye in some blots obtained in this biological replicate (with reservations and limitations), but in one occasion (Appendix 1 Figure 9) matrin 3 phosphorylation showed no change or even a slight decrease in intensity upon c-Src rescue. In summary there is an inconsistency in the pattern of change of these bands and we cannot really explain this observation. This inconsistency challenges the possibility that possible increases in intensity of the bands may be caused by imprecise loading or strong background (darker in the right area, where the bands corresponding to the treated cells are). If imprecise loading was the only responsible factor for a possible increase in the intensity of the bands from treated cells, the tendency of the bands to increase, remain or decrease in intensity would remain the same after washing the blot, and the pattern of change between bands correspondent to untreated and treated cells will be constant among the blots. Also, one of the lower non-matrin 3 bands shows a decrease in its intensity upon treatment, contradicting the possibility of a higher load in the lane corresponding to treated cells. If darker background (darker in the right region of the blot where the bands corresponding to the treated cells are) was responsible for the detection of an increase in intensity of several bands, washing the blot and reducing the background would lead to a cleaner blot where the bands will be equally affected by the washing. This is not the case in our experiment, where some bands appear clearer after washing while others keep their intensity (Appendix 1 Figures 7 and 8 vs Appendix 1 Figure 9). However, it is also possible that the background was very

heterogeneous through the blot that affected different bands differently and washing led to an homogeneous background that will allow visualization of the real tendency of the band to decrease, maintain, or increase in intensity. This could be worrisome because it may suggest that some of the potential increases observed may not be real, but caused by heterogeneous background, since washing, further incubations, etc, lead to changes in their tendency to increase, maintain or decrease in intensity.

After developing the blot resulting from the first sandwich reaction, the blot was washed further and developed again, with the expectation of a reduced and more homogeneous background that facilitates visualization of the real tendency of the intensity of the bands. The bands showed no change in intensity both by eye and by the quantitations made (which makes sense since this blot seems more appropriate for quantitation by Image J). However, this brought another concern, since the top part of the blot was inexplicably much clearer than the bottom (Appendix 1 Figure 9), which makes it hard to determine if the pattern observed in this area of the blot is reliable. In the blot, matrin 3 phosphorylation showed no increase or even a slight decrease. This is obviously worrisome, although excessive or uneven washing, uneven background or other factors related to the clearer aspect of the top part of the blot might account for this.

An additional type of concern related to the blots obtained after the second sandwich reaction (Appendix Figures 10-12) is that **the areas of the blot that are getting clearer likely interfere with the matrin 3 control band** (no imidazole) and make it look a bit lighter (less intense) that what it really is. Some of this clearing/ fading occurs in an area of the blot near the band corresponding to untreated cell, and may contribute to the lighter intensity of this band as compared with the one showing matrin 3

phosphorylation after imidazole treatment. We hope that Image J, which is a very established way to quantitate blots and takes into account the background, and has been used in two different recommended ways, covers this issue during its calculations but we don´t have the certainty that the clearing may cause effects that ImageJ can not address.

Another issue I have mentioned through the text and worth discussing again here is the **methodology used for scanning the very dark films**: The way I initially scanned the films was using a desk halogen lamp illuminating the film and this may not be the most appropriate/ homogeneous way to illuminate the film in order to be able to scan it, although I was very careful in selecting the area of interest and applying homogenous illumination to it. The images shown in Figure 28 come from images taken following this methodology and adjusting the levels as indicated. It is encouraging to see that when the technique of translucent scanning, which has optimal resolution and homogeneous illumination, was used, the same tendency was revealed in the quantitations regarding the intensity changes in matrin 3's phosphorylation.

Another related issue is the **variability of the quality and sometimes even the appearance of the figures depending on the methodology used to capture them**. If the blots had a strong signal and a clear background I just scanned them with the help of a halogen lamp or by translucent scanning. If the blots were light and the signal weak, I scanned them, sometimes using a halogen lamp to obtain a clear image (less background), scanned them by translucent scanning, or I used an imager and a lamp. When the images were dark, I often had to use a halogen lamp to scan them and then I did scan them by translucent scanning. In order to get a picture of the whole film, I often used a low-resolution camera and a light box or an imager and a lamp. Sometimes the

images obtained through these last two methods showed slightly different appearances. This may be related to the different types of illumination (some may be more intense and/or homogeneous than others) and/or the quality or resolution that the instrument can obtain. In those cases, I tried emphasizing the appearance that corresponds to what I can observe by eye, but I was cautious to make strong conclusions because even this observation can be misleading (by factors such as heterogeneous background that is hard to identify or distinguish sometimes, vision limitation) or biased. In general, I also give more credibility to the images obtained in the approximate following order: scanning the blot by translucent scanning or by simple scanning, by scanning with the help of a halogen lamp, by taking pictures with a Cyber-shot Sony camera and a light box, by taking pictures with a low-resolution camera and a light box or by the imager and the UV lamp with the white light diffuser.

In fact, this leads to another concern, which is the **methodology used when trying to quantify the changes of intensity of the bands**. Since methodologies like the traditional use of Photoshop to subtract the background can be biased, I used Image J established method for Western blot quantitation, which takes the background into account. From my experience doing this and the information I have obtained online and through colleagues, I can say that this methodology works well when both the background is clear and homogeneous and the band intensity is strong enough. I tried applying this methodology to most of the films. However, I believe some of them did not meet the requirements for being measured through this methodology since they provide numbers indicating changes that are very different from what can be observed by eye. A reason for this may be the fact that the software needs a large selection area containing

the band and a large area of background to be able to take it into account it. However, in cases where the background on and/or around the band is heterogeneous, it was impossible to avoid including part of it in our selection and I think this affected the results. The eye is able to focus only in the region of interest but of course, it is not perfect since it can also miss a mildly heterogeneous background that is hard to identify or distinguish sometimes or can lead to biased interpretations. However, if the observation by eye seems more real than the numbers obtained in a non-optimal blot, I gave more credibility to the first one. However, the graphs are shown to illustrate this too. The methodology used to quantitate images from scanning the film with the help of a lamp or from translucent scanning showed the same tendency but values were relatively different. This may be due to the illumination technique or the difference in settings use in Image J. As I mentioned before, and this is just speculation, it is conceivable that the halogen lamp is somehow illuminating selectively in a way that has a much higher illuminating effect in the already clear background areas (left band) than in the darker ones. Maybe the illumination from the halogen lamp affects differently different backgrounds and even Image J cannot take this into account but we also have quantitation from images scanned by translucent scanning which is an optimal way to homogeneously illuminate the blots and they show the same tendency.

I usually preferred to choose images obtained through scanning since they have the higher resolution. I also used images obtained through the scanner and the halogen lamp. In fact, this was the methodology used to obtain the figures currently shown in the paper. I could sometimes observe a dissonance between the numbers obtained from images of the same film obtained through these two methodologies. The scanned images

have higher resolution. The halogen lamp may not be the optimal method to homogeneously illuminate the blot but I made a special effort to manually locate the lamp in a way that favored homogeneity. I also believed this illumination method is the one of the ones that created a clearer image of the film and I was not aware of the translucent scanning method initially. The pictures taken with the low resolution camera and the help of a light box probably had homogeneous localization but did not have good resolution so I did not use them to quantify the blots. I also took pictures with a better camera but I am not sure I was being consistent with the different blots since I did not have a set system to fix the camera so I also did not use these images to quantify the blots. The images obtained with the imager and the lamp, seem to have less resolution than the scanned versions and sometimes the images seem to have difference appearance than what can be observed by eye. I used a white light diffuser over a UV lamp that should make the illumination homogeneous but is not an established way so I lack information to judge how reliable this method is. Also, there was an extra factor with the images obtained through the imager, which is the aperture of the light. Representative pictures that were taken using different apertures are shown and sometimes the tendency of the band's intensity to increase, remain, or decrease upon c-Src rescue depends on the aperture used. **There was therefore variability in the numbers obtained depending on the methodology used to illuminate the blot and obtain the image.** This made the interpretations extremely hard to make, even when attempting to quantify. In general, I will trust more the quantitation if the blot meets the requirements for proper quantification, if the tendency is mostly consistent through the blots obtained through different methodologies, if I obtained the image through scanning, and if I believe it

reflects what can be observed by eye.

Finally, I would like to mention that **the loading control (IP and Western blot with matrin 3 antibody) performed with the non-rescuable cell lines (D388N/ SYF) shows a slight decrease in the total amount of matrin 3 (Appendix 1 Figure 13).** The bands corresponding to phosphorylated matrin 3 in the anti-phosphotyrosine Western blot shows no significant difference in intensity (Appendix 1 Figure 13) by eye and one of the most reliable images/ quantitation (done trying to avoid the heterogeneous background more) (not after quantitation of images obtained by Imager). I believe by eye one could observe a mild increase but there is clear heterogenous background interfering with the right band. I believe that the fact that the blot does not meet the requirements of background and signal intensity for proper quantification by Image J led to the significant decreased obtained through quantification. However, if we take into account the decrease in the loading control, we could consider there is an increase in matrin 3's phosphorylation too. However, I have mentioned the possible explanation of the decrease observed in the blot in Appendix 1 Figure 13, which may respond to a higher (10 ml) higher volume of sample loaded in the sample corresponding to the untreated cells. This extra volume was not loaded in the anti-phosphotyrosine Western blot (Appendix 1 Figure 13), and this probably will make the possibility of an increased phosphorylation of matrin 3 in non-rescuable cells more unlikely.

A final attempt was made to reproduce these results, but the reagents used were not fresh, and the loading controls and bad quality of the blot made it very difficult to make any conclusions.

After the first sandwich reaction to magnify signals due to phosphorylation, I

obtained two blots, using both a shorter and longer exposure. In the one obtained through the shorter exposure (Appendix 1 Figure 7) I believe I may see a borderline increase in phosphorylation after rescue, but this interpretation is ambiguous and difficult to determine because of the faintness of the bands that is not well defined and because of heterogeneous background that is mildly apparent but become more apparent after observing the longer exposure. Attempts at quantitation did not confirm such an increase. The only quantification that was possible led to numbers that actually reflect a decrease in intensity but I believe the heterogeneous background affected the methodology because the Area plots/ curves provided by Image J were not of appropriate quality. I would therefore not value this quantitation very much. The longer exposure is shown in Appendix 1 Figure 8. The observations made by eye are very similar than the ones for Appendix 1 Figure 7, but I believe it is harder to see because the left band is more defined and solid than in the previous exposure and the background is more apparent and heterogeneous, interfering with the clear visualization of the bands. At the same time, the right band seems wider. Again, the only quantitation that was possible (image obtained by scanning blot with the help of a halogen lamp and from translucent scanning) led to numbers that actually reflect no change or a marginal decrease in intensity but I believe the heterogeneous background affected the methodology.

After washing and redeveloping the blot, we obtained the blot shown in Appendix 1 Figure 9. The bands are now more defined and the background seems clearer and more homogeneous (facilitating quantitation), but it is actually not completely homogeneous. Also, the top part of the film is much clearer than the bottom, which may suggest excessive washing or other unknown artifact that may lead to a misleading interpretation.

By eye, I believe I don't see a change in intensity in the bands. There may be a slight decrease in the intensity but I think the right band is slightly broader and this may account for the possible decrease. After scanning the film with a lamp, we quantified and still did not observe a significant change in phosphorylation. After scanning the film by translucent scanning, we quantified and still did not observe a significant change in phosphorylation. The overall results indicate that there is not a significant change in intensity between both bands but the very different and much clearer top of the blot makes us take this observation also with reservations.

After performing the second sandwich reaction, the blot became clearer in some areas. For more information about the possible causes of this phenomenon please read this manual: http://www.piercenet.com/files/AN0011.pdf. One concern is that this may have an effect in the intensity of the band corresponding to phosphorylated matrin 3 from the untreated cells (left band). However, the area in the blot that is starting to clear is not large enough to really have a major interference with the band. In the first exposure (lighter one) I believe that, by eye, I may see a borderline and extremely mild increase in the bands corresponding to matrin 3 (especially if the apparent larger area of the right band is taken into account) although this is very ambiguous and I am not convinved by it. The lightness of the signal made it impossible to make any quantitations by Image J.

A different exposure is shown in Appendix 1 Figure 11. Here the bands are very sharp and the background around them is relatively homogeneous facilitating the quantification. By eye, a mild increase is observed in the intensity of the band corresponding to phosphorylated matrin 3. The clear area in the left side of the blot may have an effect in the left band intensity, which may appear weaker. However, even when

I take this into account, there may still be a marginal/ mild increase in the intensity of the band corresponding to phosphorylated matrin 3 upon s-Src rescue, especially if we look at the right side of both bands where the clearing is less prevalent, but this is hard to determine. In addition, the surface area of the right band (treated cells) seems to be equal or slightly greater than the one in the left (untreated cells). However, the quality of the blot makes it hard to make conclusions. Quantitation was performed from images obtained from scanning the blot with the help of a lamp and by translucent scanning. A mild increase is reflected in this calculation. The quantitation was also performed by ImageJ, from images obtained from the imager and a lamp. These images (except for the first film) also show an increase, although not so apparent. However, we consider the resolution and illumination technique of these images are not optimal and we give them less weight than the previous ones.

A third exposure was obtained and is shown in Appendix 1 Figure 12. The observations are similar from the ones made in Appendix 1 Figure 11, although the blot was dark and a quality scanned image was hard to obtain. By eye, a very borderline increase can be observed again, with the darker band corresponding to rescue of c-Src. We quantified the change in the intensity of the bands from the image obtained scanning the film with the help of a halogen band, and an increase in intensity is shown upon c-Src chemical rescue when we don´t subtract the background. A strong decrease shows through quantitation when we subtract the background but we believe this does not correspond with what can be visualized by eye and we think it is probably due to the nature of the blot which is darker than the one shown in Appendix 1 Figure 11.1, which leads to area plots for calculations that are not smooth and can lead to very different

outcomes than what we observe by eye. We also quantified the change in the intensity of the bands from the image obtained scanning the film by translucent scanning and an increase in intensity is shown upon c-Src chemical rescue. We must warn, however, that the background was strong and not ideal for the calculations due to the clearing in some areas of the blot. Also, the images obtained by the imager are very different and both their appearance and the quantitation resulting from them don't show an increase. Again, I think the amount/ homogeneity of illumination affects the appearance of the blot and the quantitation. Therefore, the methodology used affects the observations and both the resolution and illumination of this last methodology is not ideal so less weight was given to this quantitation values.

We performed this experiment to validate the mass spectrometry results that revealed matrin 3 as a potential downstream c-Src target. The experiment consistent of an immunoprecipitation with matrin 3 antibody, followed by Western blot with matrin 3 antibody (loading control) and anti-phosphotyrosine antibody (in order to detect the changes in matrin 3 phosphorylation upon c-Src chemical rescue). Our initial attempt seemed successful but we then realized of the presence of non-specific proteins that have probably been pulled down with matrin 3 in the immunoprecipitation. Among other reasons, thoroughly described above, some of these non-specific proteins are visualized at a molecular weight that is very similar to matrin 3, making the blot unreliable. The next attempts to replicate the experiment did no reveal any phosphorylated matrin 3, even though the immunoprecipitation worked satisfactorily, based on the anti-matrin 3 Western blots. If matrin 3 is not heavily phosphorylated, we would need a method to

strengthen the signal. For that reason we introduced the sandwich reaction to magnify the weak signal. After several attempts to visualize matrin 3 phosphorylation, we were encouraged when we observed what we believe is phosphorylation of matrin 3. We had to include additional steps to increase the signal in this kind of experiment. In principle, the conclusions from images obtained after the first sandwich reaction should be the most reliable since they were subjected to less manipulation. Taken into account our observations we could only talk about a possible borderline increase in intensity by eye (although not clear), with no change in intensity on quantitation. These observation (and its quantitation) is limited by the heterogeneous background and the problematic signal-to-noise so conclusions are hard to make. After washing and developing we should observe an even more reliable blot that shows no difference in intensity. However, we see no change in intensity (and even a marginal decrease) in the intensity of the bands corresponding to phosphorylated matrin 3 upon c-Src rescue. This interpretation is limited by the fact that top of the membrane is much brighter than the bottom and it that may or may be not homogenous. The fact that is so different from the bottom part of the film raises my concerns about the presence of excessive washing or other artifacts. The blots obtained after the second sandwich reaction had been subject to more processing, but nevertheless, these are the ones that revealed bands that were sharper and easier to visualize and quantitate. On average, and based on observation by eye and quantitation of scanned images with the help of the lamp and by translucent scanning (and if I don't heavily weight/ take too much into consideration the quantitation done after subtracting the background from the images obtained in the third exposure after the second sandwich reaction, after scanning the film with the help of a lamp (Appendix 1 Figure 12), nor the

quantitation from the images obtained from the imager, due to the reasons described above), it could be said that a marginal/ mild increase in the intensity of the band corresponding to imidazole- treated cells (rescued c-Src) was observed supporting the mass spectrometry results. The blot used for making the publication figure (Martinez-Ferrando et al. MCP 2012) was obtained from Appendix 1 Figure 11, after performing the second sandwich reaction. This blot reveals clear and sharp bands with relatively homogeneous background around them that facilitated quantitation. The quantitation values from both Appendix 1 Figures 11 and 12 (except for the quantitation done after subtracting the background from the images obtained in the third exposure after the second sandwich reaction, after scanning the film with the help of a lamp (Appendix 1 Figure 12), nor the quantitation from the images obtained from the imager), suggest a mild but discernible increase in phosphorylation of matrin 3 upon c-Src rescue. Quantitation by Image J takes into consideration the background and even in this case, the increase is revealed in the calculations. Apart from the level of processing this blot has been subjected to in order to magnify the signal, my other primary concern with the analysis of this blot is that the regions where the blot is clearing due to signal loss (maybe "ghost-banding") have an effect in the intensity of the left band and the background around it. This effect could impact the observation and the quantitation of the band, leading to a misleading conclusion. However, when the observed differences in local background are reduced using background correction in Image J, the quantitation of the bands still reveals a marginal to mild increase (except for the quantitation done after subtracting the background from the images obtained in the third exposure after the second sandwich reaction, after scanning the film with the help of a lamp (Appendix 1

Figure 12), nor the quantitation from the images obtained from the imager). It is true that the described concerns and the fact that I only have a biological replicate showing these results make the conclusion less solid and should be interpreted with caution.

In summary, and taking all these considerations into account, we believe that the immunoprecipitation and Western blot experiment done to validate the mass spectrometry results for matrin 3 has several lingering caveats and may not be the best assay to measure matrin 3 phosphorylation, given the technical difficulties to observe phosphorylation. Some of the blots showed no response, a mild response or a response that is hard to measure. Even though the experiment provided some evidence that supports the increase observed in mass spectrometry, each of the obtained blots has its own caveats that I have tried to explain here are clearly and thoroughly as possible. The second sandwich reaction showed a response that is measurable and has however provided modest evidence of a marginal increase in matrin 3 phosphorylation upon c-Src rescue (except for the quantitation done after subtracting the background from the images obtained in the third exposure after the second sandwich reaction, after scanning the film with the help of a lamp (Appendix 1 Figure 12), nor the quantitation from the images obtained from the imager), but the caveats and weakness at this stage of the experiment (mostly the level of processing and the clearing of the blot in the left side of the left band) remain and represent concerns about this result.

The complete set of data is presented here for full transparency. We must warn about the weak nature of this set of evidence that provides some evidence about a

possible marginal to mild increase in phosphorylation of matrin 3 upon c-Src rescue, but presents some lingering concerns and inconsistencies we can not explain, and does not contradict as a whole the results obtained in our SILAC experiment at the protein level.

It is evident that if one were to pursue this issue at a later time, additional techniques should be used, since standard Western Blot/IP approaches that were valid for other proteins are technically challenging in the case of matrin-3.

Probability Legend
over 95%
80% to 94%
50% to 79%
20% to 49%
0% to 19%

BioView:
Identified Proteins (57)
Including 0 Decoys

#	Visible?	Starred?		Accession Number	Molecular Weight	Protein Grouping Ambiguity	ProteinLevelData-SRcPTry_Fe...
1	☑		myosin-9 isoform 1 [Mus musculus]	gi|114326446	226 kDa		15
2	☑		focal adhesion kinase 1 isoform 1 [Mus musculus]	gi|194353972	119 kDa		8
3	☑		keratin, type I cytoskeletal 10 [Mus musculus]	gi|112983636	57 kDa		7
4	☑		ephrin type-A receptor 2 precursor [Mus musculus]	gi|32484983	109 kDa		7
5	☑		keratin, type I cytoskeletal 17 [Mus musculus]	gi|7106335	48 kDa		6
6	☑		rho guanine nucleotide exchange factor 7 isoform b [Mus musculus]	gi|165377089 (+1)	80 kDa		6
7	☑		actin, cytoplasmic 1 [Mus musculus]	gi|6671509 (+1)	42 kDa		5
8	☑		albumin precursor [Mus musculus]	gi|163310765	69 kDa		5
9	☑		tyrosine-protein kinase SgK269 [Mus musculus]	gi|157909795	191 kDa		5
10	☑		PREDICTED: similar to SH2/SH3 adaptor protein [Mus musculus]	gi|149233948 (+1)	43 kDa		5
11	☑		alpha-2-macroglobulin precursor [Mus musculus]	gi|110347469	166 kDa		4
12	☑		ARF GTPase-activating protein GIT1 [Mus musculus]	gi|51921285	85 kDa		4
13	☑		sorting nexin-18 [Mus musculus]	gi|91598596	68 kDa		4
14	☑		paxillin isoform beta [Mus musculus]	gi|114326502 (+1)	65 kDa		4
15	☑		breast cancer anti-estrogen resistance protein 1 [Mus musculus]	gi|40254593	94 kDa		3
16	☑		ARF GTPase-activating protein GIT2 isoform 3 [Mus musculus]	gi|116517295	76 kDa		3
17	☑		heat shock cognate 71 kDa protein [Mus musculus]	gi|31981690	71 kDa		3
18	☑		ATP-dependent RNA helicase DDX3X [Mus musculus]	gi|6753620	73 kDa		3
19	☑		mitogen-activated protein kinase 3 [Mus musculus]	gi|21489933	43 kDa		3
20	☑		complement C3 [Mus musculus]	gi|126518317	186 kDa		3
21	☑		keratin, type II cytoskeletal 5 [Mus musculus]	gi|20911031	62 kDa		2
22	☑		vimentin [Mus musculus]	gi|31982755	54 kDa		2
23	☑		elongation factor 1-alpha 1 [Mus musculus]	gi|126032329	50 kDa		2
24	☑		activated CDC42 kinase 1 isoform 1 [Mus musculus]	gi|158711692	117 kDa		2
25	☑		40S ribosomal protein S4, X isoform [Mus musculus]	gi|6677805	30 kDa		2
26	☑		neuronal proto-oncogene tyrosine-protein kinase Src isoform 2 [Mus ...	gi|70794809 (+1)	60 kDa		2
27	☑		probable ATP-dependent RNA helicase DDX5 [Mus musculus]	gi|83816893	69 kDa		2
28	☑		mitogen-activated protein kinase 1 [Mus musculus]	gi|6754632 (+1)	41 kDa		2
29	☑		murinoglobulin-1 precursor [Mus musculus]	gi|31982171	165 kDa		2
30	☑		keratin, type II cytoskeletal 6A [Mus musculus]	gi|54607171	59 kDa		2
31	☑		keratin, type II cytoskeletal 2 epidermal [Mus musculus]	gi|124487419	71 kDa		2
32	☑		elongation factor 2 [Mus musculus]	gi|33859482	95 kDa		2
33	☑		stress-70 protein, mitochondrial [Mus musculus]	gi|162461907	73 kDa		2
34	☑		non-catalytic region of tyrosine kinase adaptor protein 1 [Mus muscul...	gi|34328187	43 kDa		2
35	☑		DNA replication licensing factor MCM5 [Mus musculus]	gi|112293273	82 kDa		2
36	☑		PREDICTED: similar to Tubulin, beta 4 [Mus musculus]	gi|149253488 (+4)	50 kDa		2
37	☑		keratin, type II cytoskeletal 1 [Mus musculus]	gi|126116585	66 kDa		2
38	☑		LIM domain-containing protein 1 [Mus musculus]	gi|224994267	71 kDa		2
39	☑		phosphatidylinositol 3-kinase regulatory subunit alpha isoform 2 [Mus...	gi|117320524 (+1)	84 kDa		2
40	☑		ephrin type-B receptor 4 isoform b [Mus musculus]	gi|227330573 (+1)	109 kDa		1
41	☑		mitogen-activated protein kinase 14 isoform 1 [Mus musculus]	gi|10092590	41 kDa		1
42	☑		serpin B6 isoform b [Mus musculus]	gi|6678097	43 kDa		1
43	☑		protein-L-isoaspartate O-methyltransferase domain-containing prote...	gi|23956398	41 kDa		1
44	☑		myosin X [Mus musculus]	gi|130507685	237 kDa		1
45	☑		keratin, type I cuticular Ha1 [Mus musculus]	gi|145966692	47 kDa		1
46	☑		tensin-like C1 domain-containing phosphatase [Mus musculus]	gi|119372288	152 kDa		1
47	☑		tropomyosin alpha-1 chain isoform 3 [Mus musculus]	gi|31560030	33 kDa		1
48	☑		PREDICTED: hypothetical protein isoform 1 [Mus musculus]	gi|149266991	38 kDa		1
49	☑		keratin, type I cytoskeletal 42 [Mus musculus]	gi|154090941	50 kDa		1
50	☑		NCK-interacting protein with SH3 domain [Mus musculus]	gi|49258190	79 kDa		1
51	☑		heterogeneous nuclear ribonucleoprotein U [Mus musculus]	gi|160333923	88 kDa		1
52	☑		keratin, type I cytoskeletal 13 [Mus musculus]	gi|6754480	48 kDa		1
53	☑		PREDICTED: similar to Chain L, Structural Basis Of Antigen Mimicry In A...	gi|149255637 (+2)	26 kDa		1
54	☑	☆	F-actin-capping protein subunit alpha-2 [Mus musculus]	gi|6671672	33 kDa		1

Probability Legend
over 95%
80% to 94%
50% to 79%
20% to 49%
0% to 19%

#	Visible?	Starred?	BioView: Identified Proteins (57) Including 0 Decoys	Accession Number	Molecular Weight	Protein Grouping Ambiguity	ProteinLevelData-SRcPTry_Fe...
55	☑	☆	PREDICTED: hypothetical protein [Mus musculus]	gi|149251929 (+6)	33 kDa		1
56	☑	☆	DNA-dependent protein kinase catalytic subunit [Mus musculus]	gi|124517706	471 kDa		1
57	☑	☆	poly(rC)-binding protein 1 [Mus musculus]	gi|6754994	37 kDa	★	1

Appendix 1 Table 1. List of proteins identified with 95% confidence by Scaffold

Probability Legend
over 95%
80% to 94%
50% to 79%
20% to 49%
0% to 19%

BioView:
Identified Proteins (85)
Including 6 Decoys

#	Visible?	Starred?		Accession Number	Molecular Weight	Protein Grouping Ambiguity	ProteinLevelData-SRcPTry_Fe...
1	☑		keratin, type I cytoskeletal 10 [Mus musculus]	gi|112983636	57 kDa		9
2	☑		focal adhesion kinase 1 isoform 1 [Mus musculus]	gi|194353972	119 kDa		22
3	☑		myosin-9 isoform 1 [Mus musculus]	gi|114326446	226 kDa		21
4	☑		keratin, type II cytoskeletal 5 [Mus musculus]	gi|20911031	62 kDa		10
5	☑		keratin, type I cytoskeletal 17 [Mus musculus]	gi|7106335	48 kDa		7
6	☑		actin, cytoplasmic 1 [Mus musculus]	gi|6671509 (+1)	42 kDa		11
7	☑		rho guanine nucleotide exchange factor 7 isoform b [Mus musculus]	gi|165377089 (+1)	80 kDa		14
8	☑		keratin, type II cytoskeletal 1 [Mus musculus]	gi|126116585	66 kDa		2
9	☑		paxillin isoform beta [Mus musculus]	gi|114326502 (+1)	65 kDa		5
10	☑		albumin precursor [Mus musculus]	gi|163310765	69 kDa		8
11	☑		ephrin type-A receptor 2 precursor [Mus musculus]	gi|32484983	109 kDa		11
12	☑		alpha-2-macroglobulin precursor [Mus musculus]	gi|110347469	166 kDa		9
13	☑		ARF GTPase-activating protein GIT1 [Mus musculus]	gi|51921285	85 kDa		9
14	☑		activated CDC42 kinase 1 isoform 1 [Mus musculus]	gi|158711692	117 kDa		4
15	☑		keratin, type II cytoskeletal 2 epidermal [Mus musculus]	gi|124487419	71 kDa		3
16	☑		tyrosine-protein kinase SgK269 [Mus musculus]	gi|157909795	191 kDa		10
17	☑		PREDICTED: similar to SH2/SH3 adaptor protein [Mus musculus]	gi|149233948 (+1)	43 kDa		9
18	☑		sorting nexin-18 [Mus musculus]	gi|91598596	68 kDa		6
19	☑		PREDICTED: similar to Ig gamma-2b chain membrane isoform 1 [M...	gi|149263750	47 kDa		4
20	☑		breast cancer anti-estrogen resistance protein 1 [Mus musculus]	gi|40254593	94 kDa		7
21	☑		elongation factor 1-alpha 1 [Mus musculus]	gi|126032329	50 kDa		4
22	☑		PREDICTED: similar to Chain L, Structural Basis Of Antigen Mimicry ...	gi|149255637 (+2)	26 kDa		2
23	☑		ARF GTPase-activating protein GIT2 isoform 3 [Mus musculus]	gi|116517295	76 kDa		6
24	☑		ATP-dependent RNA helicase DDX3X [Mus musculus]	gi|6753620	73 kDa		5
25	☑		keratin, type II cytoskeletal 6A [Mus musculus]	gi|54607171	59 kDa		3
26	☑		PREDICTED: similar to Hist1h2bj protein [Mus musculus]	gi|149264032 (+16)	14 kDa		1
27	☑		mitogen-activated protein kinase 3 [Mus musculus]	gi|21489933	43 kDa		6
28	☑		mitogen-activated protein kinase 1 [Mus musculus]	gi|6754632 (+1)	41 kDa		3
29	☑		DNA-dependent protein kinase catalytic subunit [Mus musculus]	gi|124517706	471 kDa		1
30	☑		heat shock cognate 71 kDa protein [Mus musculus]	gi|31981690	71 kDa		6
31	☑		vimentin [Mus musculus]	gi|31982755	54 kDa		5
32	☑		probable ATP-dependent RNA helicase DDX5 [Mus musculus]	gi|83816893	69 kDa		3
33	☑		complement C3 [Mus musculus]	gi|126518317	186 kDa		5
34	☑		neuronal proto-oncogene tyrosine-protein kinase Src isoform 2 [M...	gi|70794809 (+1)	60 kDa		3
35	☑		heat shock 70 kDa protein 1B [Mus musculus]	gi|124339826 (+1)	70 kDa		3
36	☑		keratin, type I cuticular Ha1 [Mus musculus]	gi|145966692	47 kDa		3
37	☑		gi|163310753-R	gi|163310753-R	?		1
38	☑		40S ribosomal protein S4, X isoform [Mus musculus]	gi|6677805	30 kDa		4
39	☑		ephrin type-B receptor 4 isoform b [Mus musculus]	gi|227330573 (+1)	109 kDa		4
40	☑		mitogen-activated protein kinase 14 isoform 1 [Mus musculus]	gi|10092590	41 kDa		3
41	☑		protein-L-isoaspartate O-methyltransferase domain-containing pr...	gi|23956398	41 kDa		3
42	☑		tensin-like C1 domain-containing phosphatase [Mus musculus]	gi|119372288	152 kDa		2
43	☑		PREDICTED: similar to PTB-associated splicing factor [Mus musculus]	gi|149252953 (+1)	70 kDa		1
44	☑		keratin, type I cytoskeletal 42 [Mus musculus]	gi|154090941	50 kDa		2
45	☑		Rap guanine nucleotide exchange factor (GEF) 1 isoform 3 [Mus m...	gi|16905083 (+2)	122 kDa		3
46	☑		myosin X [Mus musculus]	gi|130507685	237 kDa		2
47	☑		intersectin-2 [Mus musculus]	gi|46560563	189 kDa		2
48	☑		NCK-interacting protein with SH3 domain [Mus musculus]	gi|49258190	79 kDa		2
49	☑		PREDICTED: hypothetical protein [Mus musculus]	gi|149251929 (+6)	33 kDa		2
50	☑		thyroid hormone receptor-associated protein 3 [Mus musculus]	gi|68533246	108 kDa		1
51	☑		tubulin alpha-1B chain [Mus musculus]	gi|34740335 (+8)	50 kDa		1
52	☑		serpin B6 isoform b [Mus musculus]	gi|6678097	43 kDa		4
53	☑		non-catalytic region of tyrosine kinase adaptor protein 1 [Mus mu...	gi|34328187	43 kDa		3
54	☑	☆	DNA replication licensing factor MCM5 [Mus musculus]	gi|112293273	82 kDa		3

Probability Legend
over 95%
80% to 94%
50% to 79%
20% to 49%
0% to 19%

#	Visible?	Starred?	BioView: Identified Proteins (85) Including 6 Decoys	Accession Number	Molecular Weight	Protein Grouping Ambiguity	ProteinLevelData-SRcPTry_Fe...
55	☑		PREDICTED: similar to Tubulin, beta 4 [Mus musculus]	gi|149253488 (+4)	50 kDa		2
56	☑		hypothetical protein LOC239796 [Mus musculus]	gi|86262157	56 kDa		1
57	☑		succinate dehydrogenase [ubiquinone] flavoprotein subunit, mitoc...	gi|54607098	73 kDa		2
58	☑		murinoglobulin-1 precursor [Mus musculus]	gi|31982171	165 kDa		3
59	☑		elongation factor 2 [Mus musculus]	gi|33859482	95 kDa		3
60	☑		stress-70 protein, mitochondrial [Mus musculus]	gi|162461907	73 kDa		2
61	☑		FCH and double SH3 domains protein 2 isoform 1 [Mus musculus]	gi|225579023 (+1)	87 kDa		3
62	☑		tropomyosin alpha-1 chain isoform 3 [Mus musculus]	gi|31560030	33 kDa		3
63	☑		PREDICTED: hypothetical protein isoform 1 [Mus musculus]	gi|149266991	38 kDa		3
64	☑		LIM domain-containing protein 1 [Mus musculus]	gi|224994267	71 kDa		2
65	☑		keratin, type I cytoskeletal 13 [Mus musculus]	gi|6754480	48 kDa		2
66	☑		ankyrin 3, epithelial isoform a [Mus musculus]	gi|116256491 (+8)	188 kDa		1
67	☑		fibronectin 1 precursor [Mus musculus]	gi|46849812	273 kDa		1
68	☑		phosphatidylinositol 3-kinase regulatory subunit alpha isoform 2 [...	gi|117320524 (+1)	84 kDa		2
69	☑		PREDICTED: similar to very large inducible GTPase 1 [Mus musculus]	gi|149257960	279 kDa		1
70	☑		F-actin-capping protein subunit alpha-2 [Mus musculus]	gi|6671672	33 kDa		2
71	☑		gi|124249105-R	gi|124249105-R	?		1
72	☑		gi|85861220-R	gi|85861220-R	?		1
73	☑		myosin-10 [Mus musculus]	gi|33598964	229 kDa		2
74	☑		ATP-binding cassette sub-family F member 2 [Mus musculus]	gi|23956078	72 kDa		1
75	☑		heterogeneous nuclear ribonucleoproteins C1/C2 isoform 1 [Mus ...	gi|8393544	34 kDa		1
76	☑		heterogeneous nuclear ribonucleoprotein U [Mus musculus]	gi|160333923	88 kDa		2
77	☑		bromodomain and WD repeat-containing protein 3 [Mus musculus]	gi|125490358	203 kDa		2
78	☑		SH3 and PX domain-containing protein 2A isoform 1 [Mus musculus]	gi|181336814	124 kDa		2
79	☑		actin-related protein 3 [Mus musculus]	gi|23956222 (+1)	47 kDa		1
80	☑		annexin A2 [Mus musculus]	gi|6996913	39 kDa		2
81	☑		poly(rC)-binding protein 1 [Mus musculus]	gi|6754994	37 kDa		1
82	☑		glycogen synthase kinase-3 beta [Mus musculus]	gi|9790077	47 kDa		1
83	☑		gi|224994231-R	gi|224994231-R	?		1
84	☑		gi|226823286-R	gi|226823286-R	?		1
85	☑		gi|225543509-R	gi|225543509-R	?		1

Appendix 1 Table 2. List of proteins identified with 85% confidence by Scaffold

REFERENCES

1. Jordan, J. D., Landau, E. M., and Iyengar, R. (2000) *Cell* **103**, 193-200

2. Peles, E., Schlessinger, J., and Grumet, M. (1998) *Trends in biochemical sciences* **23**, 121-124

3. Hehlgans, S., Haase, M., and Cordes, N. (2007) *Biochimica et biophysica acta* **1775**, 163-180

4. Delbridge, L. M., and O'Riordan, M. X. (2007) *Current opinion in immunology* **19**, 10-16

5. Shami, P. J., Moore, J. O., Gockerman, J. P., Hathorn, J. W., Misukonis, M. A., and Weinberg, J. B. (1995) *Leukemia research* **19**, 527-533

6. Walsh, C. T. (2006) *Posttranslational modifications of proteins: Expanding nature's inventory* Roberts and Co. Greenwood Village, CO

7. Faux, M. C., and Scott, J. D. (1996) *Cell* **85**, 9-12

8. Pawson, T. (1995) *Nature* **373**, 573-580

9. Sadowski, I., Stone, J. C., and Pawson, T. (1986) *Molecular and cellular biology* **6**, 4396-4408

10. Mayer, B. J., Hamaguchi, M., and Hanafusa, H. (1988) *Nature* **332**, 272-275

11. Songyang, Z., Shoelson, S. E., McGlade, J., Olivier, P., Pawson, T., Bustelo, X. R., Barbacid, M., Sabe, H., Hanafusa, H., Yi, T., and et al. (1994) *Molecular and cellular biology* **14**, 2777-2785

12. Filippakopoulos, P., Kofler, M., Hantschel, O., Gish, G. D., Grebien, F., Salah, E., Neudecker, P., Kay, L. E., Turk, B. E., Superti-Furga, G., Pawson, T., and Knapp, S. (2008) *Cell* **134**, 793-803

13. Moarefi, I., LaFevre-Bernt, M., Sicheri, F., Huse, M., Lee, C. H., Kuriyan, J., and Miller, W. T. (1997) *Nature* **385**, 650-653

14. Young, M. A., Gonfloni, S., Superti-Furga, G., Roux, B., and Kuriyan, J. (2001) *Cell* **105**, 115-126

15. Hubbard, S. R., and Till, J. H. (2000) *Annual review of biochemistry* **69**, 373-398

16. Scott, J. D., and Pawson, T. (2009) *Science* **326**, 1220-1224

17. Yaffe, M. B., Rittinger, K., Volinia, S., Caron, P. R., Aitken, A., Leffers, H., Gamblin, S. J., Smerdon, S. J., and Cantley, L. C. (1997) *Cell* **91**, 961-971

18. Yaffe, M. B., and Cantley, L. C. (1999) *Nature* **402**, 30-31

19. Ciechanover, A., Elias, S., Heller, H., Ferber, S., and Hershko, A. (1980) *The Journal of biological chemistry* **255**, 7525-7528

20. Hicke, L., Schubert, H. L., and Hill, C. P. (2005) *Nature reviews. Molecular cell biology* **6**, 610-621

21. Polo, S., Sigismund, S., Faretta, M., Guidi, M., Capua, M. R., Bossi, G., Chen, H., De Camilli, P., and Di Fiore, P. P. (2002) *Nature* **416**, 451-455

22. Basu, A., Rose, K. L., Zhang, J., Beavis, R. C., Ueberheide, B., Garcia, B. A., Chait, B., Zhao, Y., Hunt, D. F., Segal, E., Allis, C. D., and Hake, S. B. (2009) *Proceedings of the National Academy of Sciences of the United States of America* **106**, 13785-13790

23. Vogelstein, B., Lane, D., and Levine, A. J. (2000) *Nature* **408**, 307-310

24. Karin, M., Cao, Y., Greten, F. R., and Li, Z. W. (2002) *Nature reviews. Cancer* **2**, 301-310

25. Krause, D. S., and Van Etten, R. A. (2005) *The New England journal of medicine* **353**, 172-187

26. al-Obeidi, F. A., Wu, J. J., and Lam, K. S. (1998) *Biopolymers* **47**, 197-223

27. Heldin, C. H. (1995) *Cell* **80**, 213-223

28. Ullrich, A., and Schlessinger, J. (1990) *Cell* **61**, 203-212

29. Cary, L. A., Han, D. C., Polte, T. R., Hanks, S. K., and Guan, J. L. (1998) *The Journal of cell biology* **140**, 211-221

30. Klein, D. E., Nappi, V. M., Reeves, G. T., Shvartsman, S. Y., and Lemmon, M. A. (2004) *Nature* **430**, 1040-1044

31. Jaye, M., Schlessinger, J., and Dionne, C. A. (1992) *Biochimica et biophysica acta* **1135**, 185-199

32. Cochet, C., Gill, G. N., Meisenhelder, J., Cooper, J. A., and Hunter, T. (1984) *The Journal of biological chemistry* **259**, 2553-2558

33. Joazeiro, C. A., Wing, S. S., Huang, H., Leverson, J. D., Hunter, T., and Liu, Y. C. (1999) *Science* **286**, 309-312

34. Elchebly, M., Payette, P., Michaliszyn, E., Cromlish, W., Collins, S., Loy, A. L., Normandin, D., Cheng, A., Himms-Hagen, J., Chan, C. C., Ramachandran, C., Gresser, M. J., Tremblay, M. L., and Kennedy, B. P. (1999) *Science* **283**, 1544-1548

35. Stehelin, D., Fujita, D. J., Padgett, T., Varmus, H. E., and Bishop, J. M. (1977) *Virology* **76**, 675-684

36. Oppermann, H., Levinson, A. D., Varmus, H. E., Levintow, L., and Bishop, J. M. (1979) *Proceedings of the National Academy of Sciences of the United States of America* **76**, 1804-1808

37. Martin, G. S. (2004) *Oncogene* **23**, 7910-7917

38. Czernilofsky, A. P., Levinson, A. D., Varmus, H. E., Bishop, J. M., Tischer, E., and Goodman, H. M. (1980) *Nature* **287**, 198-203

39. Thomas, S. M., and Brugge, J. S. (1997) *Annual review of cell and developmental biology* **13**, 513-609

40. Buser, C. A., Sigal, C. T., Resh, M. D., and McLaughlin, S. (1994) *Biochemistry* **33**, 13093-13101

41. Sigal, C. T., Zhou, W., Buser, C. A., McLaughlin, S., and Resh, M. D. (1994) *Proceedings of the National Academy of Sciences of the United States of America* **91**, 12253-12257

42. Chackalaparampil, I., and Shalloway, D. (1988) *Cell* **52**, 801-810

43. Morgan, D. O., Kaplan, J. M., Bishop, J. M., and Varmus, H. E. (1989) *Cell* **57**, 775-786

44. Sicheri, F., and Kuriyan, J. (1997) *Current opinion in structural biology* **7**, 777-785

45. Courtneidge, S. A., Fumagalli, S., Koegl, M., Superti-Furga, G., and Twamley-Stein, G. M. (1993) *Dev Suppl*, 57-64

46. Ladbury, J. E., Lemmon, M. A., Zhou, M., Green, J., Botfield, M. C., and Schlessinger, J. (1995) *Proceedings of the National Academy of Sciences of the United States of America* **92**, 3199-3203

47. Xu, W., Doshi, A., Lei, M., Eck, M. J., and Harrison, S. C. (1999) *Molecular cell* **3**, 629-638

48. Parsons, J. T., and Weber, M. J. (1989) *Current topics in microbiology and immunology* **147**, 79-127

49. Chong, Y. P., Mulhern, T. D., and Cheng, H. C. (2005) *Growth Factors* **23**, 233-244

50. Xu, W., Harrison, S. C., and Eck, M. J. (1997) *Nature* **385**, 595-602

51. Yeatman, T. J. (2004) *Nature reviews. Cancer* **4**, 470-480

52. Bowman, T., Broome, M. A., Sinibaldi, D., Wharton, W., Pledger, W. J., Sedivy, J. M., Irby, R., Yeatman, T., Courtneidge, S. A., and Jove, R. (2001) *Proceedings of the National Academy of Sciences of the United States of America* **98**, 7319-7324

53. Niu, G., Wright, K. L., Huang, M., Song, L., Haura, E., Turkson, J., Zhang, S., Wang, T., Sinibaldi, D., Coppola, D., Heller, R., Ellis, L. M., Karras, J., Bromberg, J., Pardoll, D., Jove, R., and Yu, H. (2002) *Oncogene* **21**, 2000-2008

54. Kazansky, A. V., and Rosen, J. M. (2001) *Cell growth & differentiation : the molecular biology journal of the American Association for Cancer Research* **12**, 1-7

55. Assoian, R. K., and Klein, E. A. (2008) *Trends in cell biology* **18**, 347-352

56. Kumar, S., Maxwell, I. Z., Heisterkamp, A., Polte, T. R., Lele, T. P., Salanga, M., Mazur, E., and Ingber, D. E. (2006) *Biophysical journal* **90**, 3762-3773

57. Geiger, B., Spatz, J. P., and Bershadsky, A. D. (2009) *Nature reviews. Molecular cell biology* **10**, 21-33

58. Ichetovkin, I., Han, J., Pang, K. M., Knecht, D. A., and Condeelis, J. S. (2000) *Cell motility and the cytoskeleton* **45**, 293-306

59. Carlier, M. F., Laurent, V., Santolini, J., Melki, R., Didry, D., Xia, G. X., Hong, Y., Chua, N. H., and Pantaloni, D. (1997) *The Journal of cell biology* **136**, 1307-1322

60. Pawlak, G., and Helfman, D. M. (2002) *Molecular biology of the cell* **13**, 336-347

61. Carragher, N. O., Fincham, V. J., Riley, D., and Frame, M. C. (2001) *The Journal of biological chemistry* **276**, 4270-4275

62. Sakai, T., Jove, R., Fassler, R., and Mosher, D. F. (2001) *Proceedings of the National Academy of Sciences of the United States of America* **98**, 3808-3813

63. Datta, A., Huber, F., and Boettiger, D. (2002) *The Journal of biological chemistry* **277**, 3943-3949

64. Zou, J. X., Liu, Y., Pasquale, E. B., and Ruoslahti, E. (2002) *The Journal of biological chemistry* **277**, 1824-1827

65. Fujita, Y., Krause, G., Scheffner, M., Zechner, D., Leddy, H. E., Behrens, J., Sommer, T., and Birchmeier, W. (2002) *Nature cell biology* **4**, 222-231

66. Ozawa, M., and Ohkubo, T. (2001) *Journal of cell science* **114**, 503-512

67. Lampe, P. D., and Lau, A. F. (2004) *The international journal of biochemistry & cell biology* **36**, 1171-1186

68. Lampe, P. D., and Lau, A. F. (2000) *Archives of biochemistry and biophysics* **384**, 205-215

69. Maeda, S., Nakagawa, S., Suga, M., Yamashita, E., Oshima, A., Fujiyoshi, Y., and Tsukihara, T. (2009) *Nature* **458**, 597-602

70. Lin, R., Warn-Cramer, B. J., Kurata, W. E., and Lau, A. F. (2001) *The Journal of cell biology* **154**, 815-827

71. Van Lint, P., and Libert, C. (2007) *Journal of leukocyte biology* **82**, 1375-1381

72. Hauck, C. R., Hsia, D. A., and Schlaepfer, D. D. (2002) *IUBMB life* **53**, 115-119

73. Hsia, D. A., Mitra, S. K., Hauck, C. R., Streblow, D. N., Nelson, J. A., Ilic, D., Huang, S., Li, E., Nemerow, G. R., Leng, J., Spencer, K. S., Cheresh, D. A., and Schlaepfer, D. D. (2003) *The Journal of cell biology* **160**, 753-767

74. Frame, M. C. (2004) *Journal of cell science* **117**, 989-998

75. Roche, S., Fumagalli, S., and Courtneidge, S. A. (1995) *Science* **269**, 1567-1569

76. Frame, M. C. (2002) *Biochimica et biophysica acta* **1602**, 114-130

77. Irby, R. B., and Yeatman, T. J. (2000) *Oncogene* **19**, 5636-5642

78. Talamonti, M. S., Roh, M. S., Curley, S. A., and Gallick, G. E. (1993) *The Journal of clinical investigation* **91**, 53-60

79. Hynes, N. E. (2000) *Breast cancer research : BCR* **2**, 154-157

80. Wiener, J. R., Windham, T. C., Estrella, V. C., Parikh, N. U., Thall, P. F., Deavers, M. T., Bast, R. C., Mills, G. B., and Gallick, G. E. (2003) *Gynecologic oncology* **88**, 73-79

81. Jones, R. J., Avizienyte, E., Wyke, A. W., Owens, D. W., Brunton, V. G., and Frame, M. C. (2002) *British journal of cancer* **87**, 1128-1135

82. Brunton, V. G., Ozanne, B. W., Paraskeva, C., and Frame, M. C. (1997) *Oncogene* **14**, 283-293

83. Kaplan, J. M., Varmus, H. E., and Bishop, J. M. (1990) *Molecular and cellular biology* **10**, 1000-1009

84. Bjorge, J. D., Jakymiw, A., and Fujita, D. J. (2000) *Oncogene* **19**, 5620-5635

85. Timpson, P., Jones, G. E., Frame, M. C., and Brunton, V. G. (2001) *Current biology : CB* **11**, 1836-1846

86. Burns, C. M., Sakaguchi, K., Appella, E., and Ashwell, J. D. (1994) *The Journal of biological chemistry* **269**, 13594-13600

87. Jung, E. J., and Kim, C. W. (2002) *Experimental & molecular medicine* **34**, 476-480

88. Zheng, X. M., Wang, Y., and Pallen, C. J. (1992) *Nature* **359**, 336-339

89. Schaller, M. D., and Parsons, J. T. (1994) *Current opinion in cell biology* **6**, 705-710

90. Thomas, J. W., Ellis, B., Boerner, R. J., Knight, W. B., White, G. C., 2nd, and Schaller, M. D. (1998) *The Journal of biological chemistry* **273**, 577-583

91. DeMali, K. A., Godwin, S. L., Soltoff, S. P., and Kazlauskas, A. (1999) *Experimental cell research* **253**, 271-279

92. Landgren, E., Blume-Jensen, P., Courtneidge, S. A., and Claesson-Welsh, L. (1995) *Oncogene* **10**, 2027-2035

93. Muthuswamy, S. K., and Muller, W. J. (1994) *Advances in cancer research* **64**, 111-123

94. Tice, D. A., Biscardi, J. S., Nickles, A. L., and Parsons, S. J. (1999) *Proceedings of the National Academy of Sciences of the United States of America* **96**, 1415-1420

95. Brown, M. T., and Cooper, J. A. (1996) *Biochimica et biophysica acta* **1287**, 121-149

96. Schlaepfer, D. D., Hauck, C. R., and Sieg, D. J. (1999) *Progress in biophysics and molecular biology* **71**, 435-478

97. Schaller, M. D. (2001) *Biochimica et biophysica acta* **1540**, 1-21

98. Giancotti, F. G., and Ruoslahti, E. (1999) *Science* **285**, 1028-1032

99. Hanks, S. K., Ryzhova, L., Shin, N. Y., and Brabek, J. (2003) *Frontiers in bioscience : a journal and virtual library* **8**, d982-996

100. Fincham, V. J., and Frame, M. C. (1998) *The EMBO journal* **17**, 81-92

101. Webb, D. J., Donais, K., Whitmore, L. A., Thomas, S. M., Turner, C. E., Parsons, J. T., and Horwitz, A. F. (2004) *Nature cell biology* **6**, 154-161

102. Schaller, M. D., and Parsons, J. T. (1995) *Molecular and cellular biology* **15**, 2635-2645

103. Fincham, V. J., James, M., Frame, M. C., and Winder, S. J. (2000) *The EMBO journal* **19**, 2911-2923

104. Noritake, H., Miyamori, H., Goto, C., Seiki, M., and Sato, H. (1999) *Clinical & experimental metastasis* **17**, 105-110

105. Batzer, A. G., Rotin, D., Urena, J. M., Skolnik, E. Y., and Schlessinger, J. (1994) *Molecular and cellular biology* **14**, 5192-5201

106. Bar-Sagi, D., and Hall, A. (2000) *Cell* **103**, 227-238

107. Shields, J. M., Pruitt, K., McFall, A., Shaub, A., and Der, C. J. (2000) *Trends in cell biology* **10**, 147-154

108. Wellbrock, C., Karasarides, M., and Marais, R. (2004) *Nature reviews. Molecular cell biology* **5**, 875-885

109. Chen, H. C., Chan, P. C., Tang, M. J., Cheng, C. H., and Chang, T. J. (1998) *The Journal of biological chemistry* **273**, 25777-25782

110. King, A. J., Wireman, R. S., Hamilton, M., and Marshall, M. S. (2001) *FEBS letters* **497**, 6-14

111. Mason, C. S., Springer, C. J., Cooper, R. G., Superti-Furga, G., Marshall, C. J., and Marais, R. (1999) *The EMBO journal* **18**, 2137-2148

112. Tran, N. H., and Frost, J. A. (2003) *The Journal of biological chemistry* **278**, 11221-11226

113. Yip-Schneider, M. T., Miao, W., Lin, A., Barnard, D. S., Tzivion, G., and Marshall, M. S. (2000) *The Biochemical journal* **351**, 151-159

114. Weber, J. D., Raben, D. M., Phillips, P. J., and Baldassare, J. J. (1997) *The Biochemical journal* **326 (Pt 1)**, 61-68

115. Twamley-Stein, G. M., Pepperkok, R., Ansorge, W., and Courtneidge, S. A. (1993) *Proceedings of the National Academy of Sciences of the United States of America* **90**, 7696-7700

116. Barone, M. V., and Courtneidge, S. A. (1995) *Nature* **378**, 509-512

117. Luttrell, L. M., Hawes, B. E., van Biesen, T., Luttrell, D. K., Lansing, T. J., and Lefkowitz, R. J. (1996) *The Journal of biological chemistry* **271**, 19443-19450

118. Haefner, B., Baxter, R., Fincham, V. J., Downes, C. P., and Frame, M. C. (1995) *The Journal of biological chemistry* **270**, 7937-7943

119. Kim, M., Tezuka, T., Tanaka, K., and Yamamoto, T. (2004) *Oncogene* **23**, 1645-1655

120. Raabe, T., Riesgo-Escovar, J., Liu, X., Bausenwein, B. S., Deak, P., Maroy, P., and Hafen, E. (1996) *Cell* **85**, 911-920

121. Reynolds, A. B., Kanner, S. B., Wang, H. C., and Parsons, J. T. (1989) *Molecular and cellular biology* **9**, 3951-3958

122. Skolnik, E. Y., Margolis, B., Mohammadi, M., Lowenstein, E., Fischer, R., Drepps, A., Ullrich, A., and Schlessinger, J. (1991) *Cell* **65**, 83-90

123. Zhu, H., Klemic, J. F., Chang, S., Bertone, P., Casamayor, A., Klemic, K. G., Smith, D., Gerstein, M., Reed, M. A., and Snyder, M. (2000) *Nature genetics* **26**, 283-289

124. Parang, K., Kohn, J. A., Saldanha, S. A., and Cole, P. A. (2002) *FEBS letters* **520**, 156-160

125. Shah, K., Liu, Y., Deirmengian, C., and Shokat, K. M. (1997) *Proceedings of the National Academy of Sciences of the United States of America* **94**, 3565-3570

126. Zhang, H., Zha, X., Tan, Y., Hornbeck, P. V., Mastrangelo, A. J., Alessi, D. R., Polakiewicz, R. D., and Comb, M. J. (2002) *The Journal of biological chemistry* **277**, 39379-39387

127. Knowles, J. R. (1987) *Science* **236**, 1252-1258

128. Profy, A. T., and Schimmel, P. (1988) *Progress in nucleic acid research and molecular biology* **35**, 1-26

129. Hedstrom, L. (2002) *Chemical reviews* **102**, 4501-4524

130. Dodson, G., and Wlodawer, A. (1998) *Trends in biochemical sciences* **23**, 347-352

131. Carter, P., and Wells, J. A. (1987) *Science* **237**, 394-399

132. Craik, C. S., Roczniak, S., Largman, C., and Rutter, W. J. (1987) *Science* **237**, 909-913

133. Toney, M. D., and Kirsch, J. F. (1989) *Science* **243**, 1485-1488

134. Qiao, Y., Molina, H., Pandey, A., Zhang, J., and Cole, P. A. (2006) *Science* **311**, 1293-1297

135. Anderson, N. L., and Anderson, N. G. (1998) *Electrophoresis* **19**, 1853-1861

136. Blackstock, W. P., and Weir, M. P. (1999) *Trends in biotechnology* **17**, 121-127

137. James, P. (1997) *Quarterly reviews of biophysics* **30**, 279-331

138. Packer, N. H., MR, W. I., Golaz, O., Lawson, M. A., Gooley, A. A., Hochstrasser, D. F., Redmond, J. W., and Williams, K. L. (1996) *Biotechnology (N Y)* **14**, 66-70

139. Harrison, P. M., Kumar, A., Lang, N., Snyder, M., and Gerstein, M. (2002) *Nucleic acids research* **30**, 1083-1090

140. Kabuyama, Y., Resing, K. A., and Ahn, N. G. (2004) *Current opinion in genetics & development* **14**, 492-498

141. Rogers, S., Girolami, M., Kolch, W., Waters, K. M., Liu, T., Thrall, B., and Wiley, H. S. (2008) *Bioinformatics* **24**, 2894-2900

142. Dhingra, V., Gupta, M., Andacht, T., and Fu, Z. F. (2005) *International journal of pharmaceutics* **299**, 1-18

143. McDonald, W. H., and Yates, J. R., 3rd. (2003) *Current opinion in molecular therapeutics* **5**, 302-309

144. Li, J., Steen, H., and Gygi, S. P. (2003) *Molecular & cellular proteomics : MCP* **2**, 1198-1204

145. Link, A. J., Eng, J., Schieltz, D. M., Carmack, E., Mize, G. J., Morris, D. R., Garvik, B. M., and Yates, J. R., 3rd. (1999) *Nature biotechnology* **17**, 676-682

146. Gygi, S. P., Rist, B., Gerber, S. A., Turecek, F., Gelb, M. H., and Aebersold, R. (1999) *Nature biotechnology* **17**, 994-999

147. Perrot, M., Sagliocco, F., Mini, T., Monribot, C., Schneider, U., Shevchenko, A., Mann, M., Jeno, P., and Boucherie, H. (1999) *Electrophoresis* **20**, 2280-2298

148. Tonella, L., Hoogland, C., Binz, P. A., Appel, R. D., Hochstrasser, D. F., and Sanchez, J. C. (2001) *Proteomics* **1**, 409-423

149. Klose, J., Nock, C., Herrmann, M., Stuhler, K., Marcus, K., Bluggel, M., Krause, E., Schalkwyk, L. C., Rastan, S., Brown, S. D., Bussow, K., Himmelbauer, H., and Lehrach, H. (2002) *Nature genetics* **30**, 385-393

150. Peng, J., Elias, J. E., Thoreen, C. C., Licklider, L. J., and Gygi, S. P. (2003) *Journal of proteome research* **2**, 43-50

151. Lipton, M. S., Pasa-Tolic, L., Anderson, G. A., Anderson, D. J., Auberry, D. L., Battista, J. R., Daly, M. J., Fredrickson, J., Hixson, K. K., Kostandarithes, H., Masselon, C., Markillie, L. M., Moore, R. J., Romine, M. F., Shen, Y., Stritmatter, E., Tolic, N., Udseth, H. R., Venkateswaran, A., Wong, K. K., Zhao, R., and Smith, R. D. (2002) *Proceedings of the National Academy of Sciences of the United States of America* **99**, 11049-11054

152. Florens, L., Washburn, M. P., Raine, J. D., Anthony, R. M., Grainger, M., Haynes, J. D., Moch, J. K., Muster, N., Sacci, J. B., Tabb, D. L., Witney, A. A., Wolters, D., Wu, Y., Gardner, M. J., Holder, A. A., Sinden, R. E., Yates, J. R., and Carucci, D. J. (2002) *Nature* **419**, 520-526

153. Resing, K. A., Meyer-Arendt, K., Mendoza, A. M., Aveline-Wolf, L. D., Jonscher, K. R., Pierce, K. G., Old, W. M., Cheung, H. T., Russell, S., Wattawa, J. L., Goehle, G. R., Knight, R. D., and Ahn, N. G. (2004) *Analytical chemistry* **76**, 3556-3568

154. Wu, C. C., and Yates, J. R., 3rd. (2003) *Nature biotechnology* **21**, 262-267

155. Aebersold, R., and Mann, M. (2003) *Nature* **422**, 198-207

156. Goshe, M. B., and Smith, R. D. (2003) *Current opinion in biotechnology* **14**, 101-109

157. Ong, S. E., Foster, L. J., and Mann, M. (2003) *Methods* **29**, 124-130

158. Bondarenko, P. V., Chelius, D., and Shaler, T. A. (2002) *Analytical chemistry* **74**, 4741-4749

159. Wang, W., Zhou, H., Lin, H., Roy, S., Shaler, T. A., Hill, L. R., Norton, S., Kumar, P., Anderle, M., and Becker, C. H. (2003) *Analytical chemistry* **75**, 4818-4826

160. Gronborg, M., Kristiansen, T. Z., Stensballe, A., Andersen, J. S., Ohara, O., Mann, M., Jensen, O. N., and Pandey, A. (2002) *Molecular & cellular proteomics : MCP* **1**, 517-527

161. Posewitz, M. C., and Tempst, P. (1999) *Analytical chemistry* **71**, 2883-2892

162. Oda, Y., Nagasu, T., and Chait, B. T. (2001) *Nature biotechnology* **19**, 379-382

163. Zhou, H., Watts, J. D., and Aebersold, R. (2001) *Nature biotechnology* **19**, 375-378

164. Qian, W. J., Goshe, M. B., Camp, D. G., 2nd, Yu, L. R., Tang, K., and Smith, R. D. (2003) *Analytical chemistry* **75**, 5441-5450

165. Ghaemmaghami, S., Huh, W. K., Bower, K., Howson, R. W., Belle, A., Dephoure, N., O'Shea, E. K., and Weissman, J. S. (2003) *Nature* **425**, 737-741

166. Neet, K., and Hunter, T. (1995) *Molecular and cellular biology* **15**, 4908-4920

167. Lock, P., Abram, C. L., Gibson, T., and Courtneidge, S. A. (1998) *The EMBO journal* **17**, 4346-4357

168. Songyang, Z., Carraway, K. L., 3rd, Eck, M. J., Harrison, S. C., Feldman, R. A., Mohammadi, M., Schlessinger, J., Hubbard, S. R., Smith, D. P., Eng, C., and et al. (1995) *Nature* **373**, 536-539

169. Shah, K., and Shokat, K. M. (2002) *Chemistry & biology* **9**, 35-47

170. Liu, Y., Shah, K., Yang, F., Witucki, L., and Shokat, K. M. (1998) *Bioorganic & medicinal chemistry* **6**, 1219-1226

171. Liu, Y., Shah, K., Yang, F., Witucki, L., and Shokat, K. M. (1998) *Chemistry & biology* **5**, 91-101

172. Amanchy, R., Zhong, J., Molina, H., Chaerkady, R., Iwahori, A., Kalume, D. E., Gronborg, M., Joore, J., Cope, L., and Pandey, A. (2008) *Journal of proteome research* **7**, 3900-3910

173. Luo, W., Slebos, R. J., Hill, S., Li, M., Brabek, J., Amanchy, R., Chaerkady, R., Pandey, A., Ham, A. J., and Hanks, S. K. (2008) *Journal of proteome research* **7**, 3447-3460

174. Irby, R. B., Mao, W., Coppola, D., Kang, J., Loubeau, J. M., Trudeau, W., Karl, R., Fujita, D. J., Jove, R., and Yeatman, T. J. (1999) *Nature genetics* **21**, 187-190

175. Amanchy, R., Zhong, J., Hong, R., Kim, J. H., Gucek, M., Cole, R. N., Molina, H., and Pandey, A. (2009) *Molecular oncology* **3**, 439-450

176. Rush, J., Moritz, A., Lee, K. A., Guo, A., Goss, V. L., Spek, E. J., Zhang, H., Zha, X. M., Polakiewicz, R. D., and Comb, M. J. (2005) *Nature biotechnology* **23**, 94-101

177. Harsha, H. C., Molina, H., and Pandey, A. (2008) *Nature protocols* **3**, 505-516

178. Rappsilber, J., Mann, M., and Ishihama, Y. (2007) *Nature protocols* **2**, 1896-1906

179. Cox, J., Neuhauser, N., Michalski, A., Scheltema, R. A., Olsen, J. V., and Mann, M. (2011) *Journal of proteome research* **10**, 1794-1805

180. Perkins, D. N., Pappin, D. J., Creasy, D. M., and Cottrell, J. S. (1999) *Electrophoresis* **20**, 3551-3567

181. Eng, J. K. M., A. L.; Yates III, J. R. (1994) *Journal of the American Society for Mass Spectrometry* **5**, 976-989

182. Balgley, B. M., Laudeman, T., Yang, L., Song, T., and Lee, C. S. (2007) *Molecular & cellular proteomics : MCP* **6**, 1599-1608

183. Dennis, G., Jr., Sherman, B. T., Hosack, D. A., Yang, J., Gao, W., Lane, H. C., and Lempicki, R. A. (2003) *Genome biology* **4**, P3

184. Klinghoffer, R. A., Sachsenmaier, C., Cooper, J. A., and Soriano, P. (1999) *The EMBO journal* **18**, 2459-2471

185. Ong, S. E., and Mann, M. (2006) *Nature protocols* **1**, 2650-2660

186. Hornbeck, P. V., Chabra, I., Kornhauser, J. M., Skrzypek, E., and Zhang, B. (2004) *Proteomics* **4**, 1551-1561

187. Wei, J., Xu, G., Wu, M., Zhang, Y., Li, Q., Liu, P., Zhu, T., Song, A., Zhao, L., Han, Z., Chen, G., Wang, S., Meng, L., Zhou, J., Lu, Y., Wang, S., and Ma, D. (2008) *Anticancer research* **28**, 327-334

188. Cussac, D., Greenland, C., Roche, S., Bai, R. Y., Duyster, J., Morris, S. W., Delsol, G., Allouche, M., and Payrastre, B. (2004) *Blood* **103**, 1464-1471

189. Olsen, J. V., de Godoy, L. M., Li, G., Macek, B., Mortensen, P., Pesch, R., Makarov, A., Lange, O., Horning, S., and Mann, M. (2005) *Molecular & cellular proteomics : MCP* **4**, 2010-2021

190. Carragher, N. O., Westhoff, M. A., Fincham, V. J., Schaller, M. D., and Frame, M. C. (2003) *Current biology : CB* **13**, 1442-1450

191. Hynes, R. O. (1992) *Cell* **69**, 11-25

192. Lu, W., Strohecker, A., and Ou Jh, J. H. (2001) *The Journal of biological chemistry* **276**, 47993-47999

193. Zhang, Z., Shen, K., Lu, W., and Cole, P. A. (2003) *The Journal of biological chemistry* **278**, 4668-4674

194. Sastry, S. K., and Burridge, K. (2000) *Experimental cell research* **261**, 25-36

195. Jamora, C., and Fuchs, E. (2002) *Nature cell biology* **4**, E101-108

196. Burridge, K., and Chrzanowska-Wodnicka, M. (1996) *Annual review of cell and developmental biology* **12**, 463-518

197. Schwartz, M. A., Schaller, M. D., and Ginsberg, M. H. (1995) *Annual review of cell and developmental biology* **11**, 549-599

198. Howe, A., Aplin, A. E., Alahari, S. K., and Juliano, R. L. (1998) *Current opinion in cell biology* **10**, 220-231

199. Qian, X., Li, G., Vass, W. C., Papageorge, A., Walker, R. C., Asnaghi, L., Steinbach, P. J., Tosato, G., Hunter, K., and Lowy, D. R. (2009) *Cancer cell* **16**, 246-258

200. Mitra, S. K., Hanson, D. A., and Schlaepfer, D. D. (2005) *Nature reviews. Molecular cell biology* **6**, 56-68

201. Fujisawa, K., Madaule, P., Ishizaki, T., Watanabe, G., Bito, H., Saito, Y., Hall, A., and Narumiya, S. (1998) *The Journal of biological chemistry* **273**, 18943-18949

202. Chang, J. H., Gill, S., Settleman, J., and Parsons, S. J. (1995) *The Journal of cell biology* **130**, 355-368

203. Kai, M., Yasuda, S., Imai, S., Kanoh, H., and Sakane, F. (2007) *Biochimica et biophysica acta* **1773**, 1407-1415

204. Zrihan-Licht, S., Fu, Y., Settleman, J., Schinkmann, K., Shaw, L., Keydar, I., Avraham, S., and Avraham, H. (2000) *Oncogene* **19**, 1318-1328

205. Kiyokawa, E., Mochizuki, N., Kurata, T., and Matsuda, M. (1997) *Critical reviews in oncogenesis* **8**, 329-342

206. Ichiba, T., Hashimoto, Y., Nakaya, M., Kuraishi, Y., Tanaka, S., Kurata, T., Mochizuki, N., and Matsuda, M. (1999) *The Journal of biological chemistry* **274**, 14376-14381

207. Radha, V., Rajanna, A., and Swarup, G. (2004) *BMC cell biology* **5**, 31

208. Gotoh, T., Hattori, S., Nakamura, S., Kitayama, H., Noda, M., Takai, Y., Kaibuchi, K., Matsui, H., Hatase, O., Takahashi, H., and et al. (1995) *Molecular and cellular biology* **15**, 6746-6753

209. Xu, A. S., Ohba, Y., Vida, L., Labotka, R. J., and London, R. E. (2000) *Biochemical pharmacology* **60**, 917-922

210. Knudsen, B. S., Feller, S. M., and Hanafusa, H. (1994) *The Journal of biological chemistry* **269**, 32781-32787

211. Tanaka, S., Morishita, T., Hashimoto, Y., Hattori, S., Nakamura, S., Shibuya, M., Matuoka, K., Takenawa, T., Kurata, T., Nagashima, K., and et al. (1994) *Proceedings of the National Academy of Sciences of the United States of America* **91**, 3443-3447

212. Kirsch, K. H., Georgescu, M. M., and Hanafusa, H. (1998) *The Journal of biological chemistry* **273**, 25673-25679

213. Ohba, Y., Mochizuki, N., Matsuo, K., Yamashita, S., Nakaya, M., Hashimoto, Y., Hamaguchi, M., Kurata, T., Nagashima, K., and Matsuda, M. (2000) *Molecular and cellular biology* **20**, 6074-6083

214. Sakai, R., Iwamatsu, A., Hirano, N., Ogawa, S., Tanaka, T., Mano, H., Yazaki, Y., and Hirai, H. (1994) *The EMBO journal* **13**, 3748-3756

215. Nakamoto, T., Sakai, R., Ozawa, K., Yazaki, Y., and Hirai, H. (1996) *The Journal of biological chemistry* **271**, 8959-8965

216. Polte, T. R., and Hanks, S. K. (1995) *Proceedings of the National Academy of Sciences of the United States of America* **92**, 10678-10682

217. Matsuda, M., Tanaka, S., Nagata, S., Kojima, A., Kurata, T., and Shibuya, M. (1992) *Molecular and cellular biology* **12**, 3482-3489

218. Birge, R. B., Kalodimos, C., Inagaki, F., and Tanaka, S. (2009) *Cell communication and signaling : CCS* **7**, 13

219. Matsuda, M., Hashimoto, Y., Muroya, K., Hasegawa, H., Kurata, T., Tanaka, S., Nakamura, S., and Hattori, S. (1994) *Molecular and cellular biology* **14**, 5495-5500

220. Wang, B., Mysliwiec, T., Feller, S. M., Knudsen, B., Hanafusa, H., and Kruh, G. D. (1996) *Oncogene* **13**, 1379-1385

221. Feller, S. M., Knudsen, B., and Hanafusa, H. (1995) *Oncogene* **10**, 1465-1473

222. Ren, R., Ye, Z. S., and Baltimore, D. (1994) *Genes & development* **8**, 783-795

223. Feller, S. M., Knudsen, B., and Hanafusa, H. (1994) *The EMBO journal* **13**, 2341-2351

224. Bos, J. L. (1998) *The EMBO journal* **17**, 6776-6782

225. Kitayama, H., Sugimoto, Y., Matsuzaki, T., Ikawa, Y., and Noda, M. (1989) *Cell* **56**, 77-84

226. Cook, S. J., Rubinfeld, B., Albert, I., and McCormick, F. (1993) *The EMBO journal* **12**, 3475-3485

227. Frische, E. W., and Zwartkruis, F. J. (2010) *Developmental biology* **340**, 1-9

228. Gloerich, M., and Bos, J. L. (2011) *Trends in cell biology* **21**, 615-623

229. Medeiros, R. B., Dickey, D. M., Chung, H., Quale, A. C., Nagarajan, L. R., Billadeau, D. D., and Shimizu, Y. (2005) *Immunity* **23**, 213-226

230. Cabodi, S., del Pilar Camacho-Leal, M., Di Stefano, P., and Defilippi, P. (2010) *Nature reviews. Cancer* **10**, 858-870

231. Sakai, R., Nakamoto, T., Ozawa, K., Aizawa, S., and Hirai, H. (1997) *Oncogene* **14**, 1419-1426

232. Iwahara, T., Akagi, T., Fujitsuka, Y., and Hanafusa, H. (2004) *Proceedings of the National Academy of Sciences of the United States of America* **101**, 17693-17698

233. Akagi, T., Shishido, T., Murata, K., and Hanafusa, H. (2000) *Proceedings of the National Academy of Sciences of the United States of America* **97**, 7290-7295

234. Ichiba, T., Kuraishi, Y., Sakai, O., Nagata, S., Groffen, J., Kurata, T., Hattori, S., and Matsuda, M. (1997) *The Journal of biological chemistry* **272**, 22215-22220

235. Xing, L., Ge, C., Zeltser, R., Maskevitch, G., Mayer, B. J., and Alexandropoulos, K. (2000) *Molecular and cellular biology* **20**, 7363-7377

236. Buensuceso, C. S., and O'Toole, T. E. (2000) *The Journal of biological chemistry* **275**, 13118-13125

237. de Jong, R., van Wijk, A., Heisterkamp, N., and Groffen, J. (1998) *Oncogene* **17**, 2805-2810

238. Knudsen, B. S., Zheng, J., Feller, S. M., Mayer, J. P., Burrell, S. K., Cowburn, D., and Hanafusa, H. (1995) *The EMBO journal* **14**, 2191-2198

239. Zhu, T., Goh, E. L., LeRoith, D., and Lobie, P. E. (1998) *The Journal of biological chemistry* **273**, 33864-33875

240. Okada, S., and Pessin, J. E. (1997) *The Journal of biological chemistry* **272**, 28179-28182

241. Okada, S., Matsuda, M., Anafi, M., Pawson, T., and Pessin, J. E. (1998) *The EMBO journal* **17**, 2554-2565

242. Olayioye, M. A., Graus-Porta, D., Beerli, R. R., Rohrer, J., Gay, B., and Hynes, N. E. (1998) *Molecular and cellular biology* **18**, 5042-5051

243. Li, L., Okura, M., and Imamoto, A. (2002) *Molecular and cellular biology* **22**, 1203-1217

244. Ling, L., Zhu, T., and Lobie, P. E. (2003) *The Journal of biological chemistry* **278**, 27301-27311

245. Mochizuki, N., Yamashita, S., Kurokawa, K., Ohba, Y., Nagai, T., Miyawaki, A., and Matsuda, M. (2001) *Nature* **411**, 1065-1068

246. Zwartkruis, F. J., and Bos, J. L. (1999) *Experimental cell research* **253**, 157-165

247. Rosen, M. K., Yamazaki, T., Gish, G. D., Kay, C. M., Pawson, T., and Kay, L. E. (1995) *Nature* **374**, 477-479

248. Bos, J. L. (2005) *Current opinion in cell biology* **17**, 123-128

249. Kooistra, M. R., Dube, N., and Bos, J. L. (2007) *Journal of cell science* **120**, 17-22

250. Waters, S. B., Holt, K. H., Ross, S. E., Syu, L. J., Guan, K. L., Saltiel, A. R., Koretzky, G. A., and Pessin, J. E. (1995) *The Journal of biological chemistry* **270**, 20883-20886

251. Langlois, W. J., Sasaoka, T., Saltiel, A. R., and Olefsky, J. M. (1995) *The Journal of biological chemistry* **270**, 25320-25323

252. Hashimoto, Y., Katayama, H., Kiyokawa, E., Ota, S., Kurata, T., Gotoh, N., Otsuka, N., Shibata, M., and Matsuda, M. (1998) *The Journal of biological chemistry* **273**, 17186-17191

253. Tanis, K. Q., Veach, D., Duewel, H. S., Bornmann, W. G., and Koleske, A. J. (2003) *Molecular and cellular biology* **23**, 3884-3896

254. Liu, F., Hill, D. E., and Chernoff, J. (1996) *The Journal of biological chemistry* **271**, 31290-31295

255. Songyang, Z., Shoelson, S. E., Chaudhuri, M., Gish, G., Pawson, T., Haser, W. G., King, F., Roberts, T., Ratnofsky, S., Lechleider, R. J., and et al. (1993) *Cell* **72**, 767-778

256. Birge, R. B., Fajardo, J. E., Reichman, C., Shoelson, S. E., Songyang, Z., Cantley, L. C., and Hanafusa, H. (1993) *Molecular and cellular biology* **13**, 4648-4656

257. Schaller, M. D., and Schaefer, E. M. (2001) *The Biochemical journal* **360**, 57-66

258. Bouton, A. H., Riggins, R. B., and Bruce-Staskal, P. J. (2001) *Oncogene* **20**, 6448-6458

CURRICULUM VITAE

Isabel Martínez Ferrando
Department of Pharmacology and Molecular Sciences
Johns Hopkins University School of Medicine
725 N. Wolfe Street, Hunterian 316, Baltimore, MD 21205
(443) 939-4839 (cell) (410) 614-0322
mmarti65@gmail.com

EDUCATION

Ph.D. candidate 08*/2004 - present*
Department of Pharmacology and Molecular Sciences
The Johns Hopkins University School of Medicine – Baltimore, MD

M.Sc. in Plant Biochemistry *01/2002-12/2002*
Department of Biotechnology
Escuela Técnica Superior de Ingenieros de Montes
Universidad Politécnica de Madrid – Madrid, Spain
(Advanced Technical School of Environmental Engineering.
Polytechnic University of Madrid – Madrid, Spain)

B.S. in Environmental/Biological Engineering, magna cum laude *09/1996 –12/2002*
Escuela Técnica Superior de Ingenieros de Montes
Universidad Politécnica de Madrid – Madrid, Spain
(Advanced Technical School of Environmental Engineering.
Polytechnic University of Madrid – Madrid, Spain)

RESEARCH EXPERIENCE

Ph.D. Thesis, **Laboratory of Philip A. Cole** 01*/2006 – present*
The Johns Hopkins University School of Medicine – Department of Pharmacology and Molecular Sciences
Summary of work: Engineering and utilizing molecular tools to:

- Optimize the chemical rescue technique for the tyrosine kinase c-Src *in vivo* in order to specifically activate the kinase.
- Combine c-Src chemical rescue with a quantitative phosphoproteomic approach involving SILAC (Stable Isotope Labeling with Amino acids in Cell culture) and LC-MS/MS with the goal of discovering potential new c-Src proteins substrates and phosphorylation sites.
- Elucidate the role of c-Src mediated phosphorylation of the newly discovered targets involved in cell adhesion, motility and invasion (Vimentin, C3G).
- Dissect the mechanism of activation of C3G in a spatiotemporal manner attempting to connect the distinct events that are known to occur in the Crk-C3G-Rap1 pathway.

Rotation, Laboratory of Craig Townsend *09/2004 12/2004*
Active site mutagenesis of ß Lactam Synthetase.

Rotation, Laboratory of Jun Liu *01/2005 - 04/2005*
Target identification and mechanisms of action of the anticancer natural product OSW-1.

Rotation, Laboratory of Robert Siliciano *05/2005 - 07/2005*
Design of an artificial model of HIV infected latent T- cell. Search for alternative pathways of T cell activation independent from NFkB.

Research Trainee *05/2003 – 09/2003*
Cell Biology and Biophysics Unit
European Molecular Biology Laboratory (EMBL) – Heidelberg, Germany

- Explore the possible *Drosophila melanogaster* proteins homologous to vertebrate TPX2, a microtubule-associated protein required for mitotic spindle assembly.
- Use *Drosophila melanogaster* genetics to understand the role of Ran and TPX2 during mitosis.

Research internship *02/2003 – 05/2003*
Natural Products Research Center (CIPRONA)- Pharmacy Department
Universidad de Costa Rica – San José, Costa Rica
Search for bioactive compounds against Chagas from *Quassia Amara* ('Hombre Grande'): extraction, isolation, identification of active compounds and essays to test its biological activity and toxicity.

M.Sc. Thesis in Plant Biochemistry *01/2002 – 12/2002*
Laboratory of Luis Gomez Fernandez
Department of Biotechnology
Escuela Técnica Superior de Ingenieros de Montes
Universidad Politécnica de Madrid – Madrid, Spain
Antifungal proteins of long- lived woody plant species of forest interest: Molecular and genetic analysis of osmotins in the sweet chestnut (*Castanea sativa* Mil).

SKILLS

Molecular cloning. Two-hybrid screening. Analytical chemistry. Mammalian cell culture. Western blotting. Immuno-precipitation and co-immunoprecipitation. Quantitative proteomics (SILAC). Mass spectrometry. Bioinformatics and data analysis (Maxquant, Proteome Discoverer, Ingenuity systems, DAVID software). Subcellular fractionation. Immunohistochemistry. Live cell and immuno-fluorescence imaging, epifluorescence and confocal microscopy. FRET.

PUBLICATIONS

Martinez-Ferrando I, Chaerkady R, Zhong J, Molina H, Kishore H, Herbst K, Dancy BM, Katju V, Bose R, Zhang J, Pandey A, Cole PA. Identification of Targets of c-Src Tyrosine Kinase by Chemical Complementation and Phosphoproteomics (Accepted. Molecular and Cellular Proteomics. 2012 Apr 12. Epub ahead of print)

Ramirez-Correa GA, **Martinez-Ferrando I**, Hart G, Murphy A. Detection of *O*-GlcNAc modifications on cardiac myofilament proteins (Manuscript in revision. Submitted to Methods in Molecular Biology)

Martinez-Ferrando I. Chemical approached for cell signaling modulation (Manuscript in preparation. Invited by Investigacion y Ciencia, Spanish version of Scientific American)

Huang R, **Martinez-Ferrando I** Cole PA. Enhanced interrogation: Emerging strategies for cell signaling inhibition *Nat Struct Mol Biol.* 2010 Jun;17(6):646-9. Review.

CONFERENCES AND PRESENTATIONS

Technology Centers for Networks and Pathways "Special K" Meeting, Johns Hopkins School of Medicine – Baltimore, MD. September, 2011.
Oral presentation: Identification of targets of c-Src tyrosine kinase by chemical complementation and phosphoproteomics

American Association for the Advancement of Science (AAAs) annual meeting – Washington, DC. February 17-21, 2011
Poster presentation: Exploring the role of c-Src in the cell: Identification of Targets of c-Src Tyrosine Kinase by Chemical Complementation and Phosphoproteomics.

American Society of Biochemistry and Molecular Biology annual meeting – Washington, DC. April 9-13, 2011.
Poster presentation: Exploring the role of c-Src in the cell adhesion. Implications of c-Src activation on the Crk-C3G-Rap1 pathway.

Chemical Insights into Biological Processes, National Cancer Institute – Frederick, MD. August 2010

Phosphorylation and G-protein mediated signaling networks, Gordon Research Conference – Biddeford, ME. June 6-11, 2010.
Poster presentation: The role of c-Src in the cell adhesion.

Chemical Insights into Biological Processes, National Cancer Institute – Frederick, MD. August 2008

HONORS AND AWARDS

Scheinberg Travel Award towards expenses for ASBMB meeting	*2011*
La Caixa Foundation (Barcelona, Spain) Award and Scholarship for graduate funding.	*2008*
Fulbright-IIE Scholarship Graduate Award and Scholarship for full graduate funding.	*2004-2006*
European Molecular Biology Laboratory Traineeship (Full funding for traineeship period)	*2003*
Universidad Politécnica de Madrid Scholarship for summer research	*2000*
Universidad Politécnica de Madrid Scholarship for summer research	*1999*
Award for best cumulative score in the last 4 years of High School and scholarship for highest score in the admission exam to university (Jesus Maestro High School)	*1996*

TEACHING EXPERIENCE

National Aquarium volunteer and instructor	*2009*
Spanish and Math instructor for Latino Outreach	*2008*
United States Botanical Garden volunteer and instructor	*2007*

Universidad Politécnica de Madrid. Engineering School:

Teaching Assistant, Algebra	*1997 - 1999*
Teaching Assistant, Calculus	*1998 - 1999*
Teaching Assistant, Biochemistry	*1997*

MEMBERSHIPS

American Association for the Advancement of Science (AAAs)
American Society of Biochemistry and Molecular Biology
Association of Women in Science (AWIS)
National Capital Area Chapter of the Fulbright Association
Spanish Fulbright Association Alumni